Report Title:	Low Cost, High Capacity Regenerable Sorbent for Carbon Dioxide Capture from Existing Coal-fired Power Plants
Type of Report:	Final Technical Report
Reporting period Start Date:	October 1, 2011
Reporting period End Date:	September 30, 2015
Principal Authors:	Dr. Gokhan Alptekin Dr. Ambalavanan Jayaraman Dr. Steven Dietz
Date report was Issued:	March 3, 2016
DOE Award Number:	DE-FE0007580
Name and Address of Submitting Organization:	TDA Research, Inc. 12345 W. 52nd Avenue Wheat Ridge, CO 80033-1916 (303) 422-7819

Disclaimer

Abstract

In this project TDA Research, Inc (TDA) has developed a new post combustion carbon capture technology based on a vacuum swing adsorption system that uses a steam purge and demonstrated its technical feasibility and economic viability in laboratory-scale tests and tests in actual coal derived flue gas. TDA uses an advanced physical adsorbent to selectively remove CO_2 from the flue gas. The sorbent exhibits a much higher affinity for CO_2 than N_2, H_2O or O_2, enabling effective CO_2 separation from the flue gas. We also carried out a detailed process design and analysis of the new system as part of both sub-critical and super-critical pulverized coal fired power plants. The new technology uses a low cost, high capacity adsorbent that selectively removes CO_2 in the presence of moisture at the flue gas temperature without a need for significant cooling of the flue gas or moisture removal. The sorbent is based on a TDA proprietary mesoporous carbon that consists of surface functionalized groups that remove CO_2 via physical adsorption. The high surface area and favorable porosity of the sorbent also provides a unique platform to introduce additional functionality, such as active groups to remove trace metals (e.g., Hg, As).

In collaboration with the Advanced Power and Energy Program of the University of California, Irvine (UCI), TDA developed system simulation models using Aspen Plus^{TM} simulation software to assess the economic viability of TDA's VSA-based post-combustion carbon capture technology. The levelized cost of electricity including the TS&M costs for CO_2 is calculated as \$116.71/MWh and \$113.76/MWh for TDA system integrated with sub-critical and super-critical pulverized coal fired power plants; much lower than the \$153.03/MWhand \$147.44/MWh calculated for the corresponding amine based systems. The cost of CO_2 captured for TDA's VSA based system is \$38.90 and \$39.71 per tonne compared to \$65.46 and \$66.56 per tonne for amine based system on 2011 \$ basis, providing 40% lower cost of CO_2 captured. In this analysis we have used a sorbent life of 4 years. If a longer sorbent life can be maintained (which is not unreasonable for fixed bed commercial PSA systems), this would lower the cost of CO_2 captured by \$0.05 per tonne (e.g., to \$38.85 and \$39.66 per tonne at 5 years sorbent replacement).

These system analysis results suggest that TDA's VSA-based post-combustion capture technology can substantially improve the power plant's thermal performance while achieving near zero emissions, including greater than 90% carbon capture. The higher net plant efficiency and lower capital and operating costs results in a substantial reduction in the cost of carbon capture and cost of electricity for the power plant equipped with TDA's technology.

List of Contributors

TDA Research, Inc.
12345 W. 52nd Avenue
Wheat Ridge, CO 80033-1916
(303) 422-7819

Dr. Gökhan O. Alptekin
Dr. Ambalavanan Jayaraman
Dr. Steve Dietz
Sarah Devoss
David Gribble

Gas Technology Institute
1700 S Mount Prospect Road
Des Plaines, IL 60018
(847) 768-0558
Dr. Chakravarthy Sishtla

University of California, Irvine
CA 92697-3550
(949) 824-7302 ext. 11345
Dr. Ashok Rao

Table of Contents

1. Executive Summary

Fossil fuel combustion is increasing the atmospheric concentration of CO_2 and causing concerns over global warming (IEA, 2014). The electric power generation industry is one of the largest CO_2 emitters; roughly one third of the U.S. carbon emissions come from power plants (Azar, 1997). Therefore, it is imperative to find cost-effective ways to recover CO_2 from the flue gases of existing plants, since the existing fleet of pulverized coal power plants (which account for most of the U.S. and world's generating capacity) will be with us for decades.

The methods for post-combustion flue gas CO_2 separation from existing power plants include chemical and physical solvent processes, chemical absorption and physical adsorption using solid sorbents, CO_2 selective membranes and cryogenic separation. Chemical absorption using aqueous solutions of alkanolamines such as monoethanolamine (MEA) is accepted as the baseline CO_2 separation method. However, amine absorption has large capital and operating costs. Large amounts of heat are needed to dissociate the CO_2-amine complex via steam stripping during the regeneration step, resulting in very high energy consumption (Nsakala et al., 2001). The liquid phase contactors and circulation systems are also complex and expensive. A recent DOE/NETL study showed that conventional amine scrubbing to capture and purify CO_2 from flue gas for sequestration could nearly double the cost of electricity and reduces the plant's output by 30% (Haslbeck et al., 2013).

Chemical absorbents also suffer from the same efficiency penalty because of the large heat input required to break a chemical bond to regenerate the sorbent. Physical adsorbents that bind the CO_2 through a weaker interaction may help to reduce the regeneration energy input, however, the commercially available adsorbents have a number of drawbacks, including low capacity at the desired operating temperature and interference from water vapor and flue gas contaminants.

In this project, TDA Research, Inc. (TDA) developed a low cost, high capacity CO_2 adsorbent and demonstrated its technical and economic viability for post-combustion CO_2 capture for existing (and new) pulverized coal-fired power plants. TDA's sorbent uses a mesoporous carbon support structure grafted with Lewis base functionalized groups that remove CO_2 via physical adsorption. The relatively strong Lewis acid-base interaction enables effective operation of the sorbent at high flue gas temperatures (60-150°C range). However, because the Lewis base adsorption sites and the CO_2 do not form a true covalent bond, the heat required to regenerate our sorbent is only 5.2 kcal per mol of CO_2, which is much lower than that for either chemical absorbents (e.g., 29.9 kcal/mol CO_2 for sodium carbonate) or amine-based solvents (e.g., 14.2 kcal/mol CO_2 for monoethanolamine). The heat of desorption of CO_2 from our sorbent is more comparable to that of the physical absorption solvents such as Selexol (4.0 kcal/mol). We optimized the CO_2 sorbent formulation and scaled-up its production and produced the sorbent used in the field tests.

In this project, we investigated two process design options for the flue gas – CO_2 sorbent contactor: fixed-bed and moving-bed VSA systems. Both cases uses a steam sweep under mild vacuum to regenerate sorbent and recover the CO_2 as mixed CO_2/steam stream, condensing the steam recovering the CO_2 as a high purity product. Although our original work in post combustion CO_2 recovery was based on the moving-bed design (and we successfully built and demonstrated its technical viability in a proof-of-concept prototype unit in this project), we then switched to much simpler fixed-bed system that is now the heart of our process. We have a unique reactor design that allowed us to reduce the pressure drop through the fixed-bed system, one of the key limitations that has previously prevented the use of the fixed-bed reactors in flue gas carbon capture systems.

In a related SBIR Phase II project (DE-SC-0006239), we further improved our CO_2 sorbent, optimizing its chemical composition and physical properties and scaling-up its production using high throughput equipment. We improved the bulk density (and hence the volumetric capacity) of the carbon sorbent and its production yield significantly. Figure 1 shows the comparison of the baseline (density =0.28 kg/L) against the improved (density = 0.46 kg/L) sorbent. We demonstrated the sorbent performance in a fixed bed system and tested the sorbent's durability through 34,000+ adsorption/regeneration cycles. We also built a 4-bed vacuum swing adsorption system to demonstrate the VSA cycle operation under coal derived flue gas. We showed that the system can achieve 90+ CO_2 capture with 90+ CO_2 purity (Figure 2).

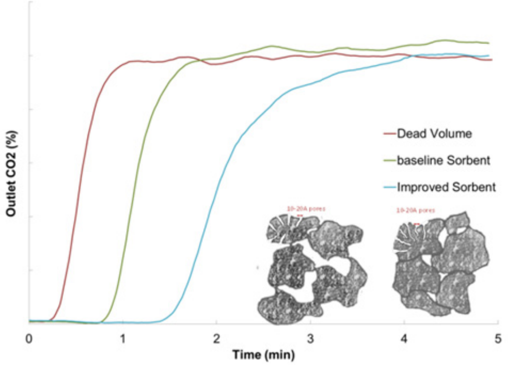

Figure 1. CO_2 breakthrough from fixed bed adsorption tests CO_2 = 10%, H_2O = 2% by vol. in N_2 (simulated flue gas).

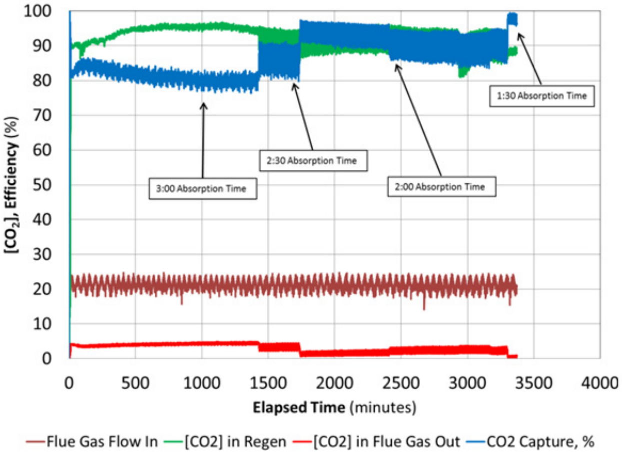

Figure 2. Results with fixed bed prototype unit at a flue gas flow rate of 1.0 scfm, CO_2 = 13.2%, P_{ads}=14 psia.

This 4-bed VSA system was demonstrated as part of this DOE sponsored project (DE-FE-0007580), where we carried out tests at the site of our partner, the Gas Technology Institute (GTI), using coal and natural gas derived flue gas for total 1,033 hours (9,795 cycles) while maintaining stable performance. Figure 3 shows the picture of TDA's moving bed and fixed bed (4-bed VSA) systems installed at GTI, next to the coal furnace. Figure 4 shows the typical system performance under coal derived flue gas in the presence of NO_x and SO_x.

Figure 3. Picture of TDA's moving bed and fixed bed prototype units installed at GTI.

In collaboration with the Advanced Power and Energy Program of the University of California, Irvine (UCI), we completed the process design using Aspen Plus™ simulation software. The analysis provided a thorough comparison against a current state-of-the-art amine based CO_2 capture system integrated with both sub-critical and super-critical coal-fired power plants. In the simulation work, UCI strictly followed the guidelines and assumptions established by DOE/NETL for assessing the economic viability of competing CO_2 capture technologies. First, the accuracy of the Aspen Model was verified by checking the simulation results against the DOE/NETL analysis

(Case 10 and Case 12 in the updated DOE/NETL report DOE/NETL-2010/1397 Rev. 2a). The results of the UCI's Aspen model simulating the amines based CO_2 capture case was found in close agreement with the DOE/NETL results (Table 1).

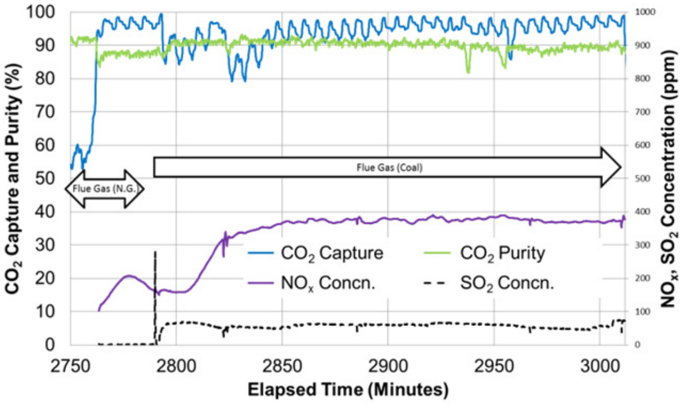

Figure 4. Results with fixed bed prototype unit at a flue gas flow rate of 1.0 scfm (wet basis), CO_2 = 13.2%, P_{ads}=14 psia under natural gas (start-up) and coal (steady state) derived flue gases .

The analysis explored several design options; the moving bed system, axial flow "stacked" fixed beds with external manifolds, radial flow fixed beds with internal manifolds, using LP steam from steam turbine cycle for purge and LP steam generated from CO_2 compression. We decided to use the steam generated from CO_2 compression to eliminate any changes to the ST cycle. In this final summary we incorporated the lower steam consumption of Steam: CO_2 ratio of 0.44 in the steam purge step. This ratio was demonstrated in our tests at GTI using coal derived flue gas and also used a VSA cycle time of 4.5 min and desorption pressure of 4.5 psia. TDA's post combustion CO_2 capture system integrated with a sub-critical and super-critical pulverized coal fired power plant achieves a net plant efficiency of 31.55% and 33.81% on HHV basis; these are significantly higher than that can be achieved by amines based CO_2 capture system (26.2% and 28.4%). The water consumption in the plant on a net kW basis is also lower for TDA's process (29.7 and 26.8 m^3/min for TDA Case 10 and case 12 vs 42.5 and 38.1 m^3/min for amines Case 10 and Case 12), preserving a valuable resource). The capital expense for the plant was estimated following the DOE/NETL cost guidelines (e.g. higher contingencies were applied for unproven technologies such as the VSA unit). The total capital cost for the sub-critical and super-critical coal fired plants integrated with TDA's process is estimated as \$2,583/kW_e and \$2,613/kW_e, respectively. These capital costs are 28.2% and 26.7% lower than those of the corresponding amine based cases.

Table 1. Comparison of TDA's VSA based CO_2 capture system against amine based CO_2 capture system integrated with a super-critical power plant (550 MW_e net plant output).

Power plant Type	**Sub-critical PC Plant**		**Supercritical PC Plant**	
CO_2 Capture Technology	**Amines**	**TDA- VSA**	**Amines**	**TDA - VSA**
Case ID	**Case 10 DOE**	**Case 10 TDA**	**Case 12 DOE**	**Case 12 TDA**
Gross Power Generated, kWe	672,700	669,778	662,800	661,828
Auxiliary Load, kWe	122,740	119,778	112,830	111,828
Net Power, kWe	549,960	550,000	549,970	550,000
Net Plant Efficiency, % HHV	**26.20**	**31.55**	**28.40**	**33.81**
Coal Feed Rate, kg/h	278,956	231,261	256,652	215,810
Total Plant Cost, \$/kWe	3,596	2,583	3,563	2,613
COE without CO_2 TS&M, \$/MWh	142.22	107.86	137.45	105.99
COE with CO_2 TS&M, \$/MWh	**153.03**	**116.71**	**147.44**	**113.76**
Cost of CO_2 Captured, \$/tonne	**65.46**	**38.90**	**66.56**	**39.71**

The levelized cost of electricity including the TS&M costs for CO_2 is calculated as $116.71/MWh and $113.76/MWh for TDA system integrated with sub-critical and super-critical pulverized coal fired power plants; much lower than the $153.03/MWhand $147.44/MWh calculated for the corresponding amine based systems. The cost of CO_2 captured for TDA's VSA based system is $38.90 and $39.71 per tonne compared to $65.46 and $66.56 per tonne for amine based system on 2011 $ basis, providing 40% lower cost of CO_2 captured. In this analysis we have used a sorbent life of 4 years. If a longer sorbent life can be maintained (which is not unreasonable for fixed bed commercial PSA systems), this would bring the cost of CO_2 captured lower by $0.05 per tonne (e.g., $38.85 and $39.66 per tonne at 5 years sorbent replacement).

These system analysis results suggest that TDA's VSA-based post-combustion capture technology can substantially improve the power plant's thermal performance while achieving near zero emissions, including greater than 90% carbon capture. The higher net plant efficiency and lower capital and operating costs results in a substantial reduction in the cost of carbon capture and cost of electricity for the power plant equipped with TDA's technology.

As part of this DOE funded program, an Environmental, Health & Safety Assessment was performed by our partner Babcock & Wilcox (B&W) on the pulverized coal-fired power plant utilizing the TDA solid-sorbent process and all system waste streams. The toxicological, ecological, and regulatory compliance for each waste stream was evaluated and discussed. IN their analysis, B&W concluded that there are no additional EH&S concerns with the TDA solid-sorbent over a current pulverized coal-fired power plant.

2. Introduction

TDA Research, Inc (TDA) is developing a low cost, high capacity CO_2 adsorbent and demonstrating its technical and economic viability for post-combustion CO_2 capture for existing pulverized coal-fired power plants. TDA uses an advanced physical adsorbent to selectively remove CO_2 from the flue gas. The sorbent exhibits a much higher affinity for CO_2 than N_2, H_2O or O_2, enabling effective CO_2 separation from the flue gas. The sorbent binds CO_2 more strongly than common adsorbents, providing the chemical potential needed to remove the CO_2. However, because CO_2 does not form a true covalent bond with the surface sites, the regeneration can be carried out with only a very small energy input. The heat input to regenerate our sorbent is only 4.9 kcal per mol of CO_2, which is much lower than that for chemical absorbents (e.g., 29.9 kcal/mol CO_2 for sodium carbonate) or amine-based solvents (e.g., 14.2 kcal/mol CO_2 for mono-ethanolamine).

The physical adsorbent was previously developed by TDA with DOE funding (Contract No. DE-FE-0000469) for pre-combustion CO_2 capture, and its stable sorbent capacity has been demonstrated for over 10,000 cycles with simulated coal-derived synthesis gas. A process analysis carried out by University of California, Irvine showed that the net plant efficiency for an Integrated Gasification Combined Cycle (IGCC) plant using our sorbent is about 2% points higher than an IGCC plant equipped with Selexol to capture CO_2. We have successfully completed field demonstrations at the National Carbon Capture Center (Southern- Wilsonville, AL) in 2011 and at the Wabash River IGCC plant (Terra Haute, IN) and demonstrated our sorbent's ability to remove CO_2 from air blown and oxygen blown gasifier streams, respectively. We also showed that our sorbent could successfully separate CO_2/CH_4 and remove CO_2 from biogas (in a privately funded project by a leading supplier of was water treatment facilities, we are designing a pilot-scale unit) and for multi-contaminant control from refinery flue gas to remove CO_2 along with mercury and arsenic impurities (EPA Contract No. EP-D-11-047).

We also proved the sorbent's efficacy in removing CO_2 from coal flue gas under conditions simulating the environment downstream of a wet flue gas desulfurization unit. We showed stable CO_2 capacity for over 220 cycles with no sign of degradation. The presence of acid gases such as SO_2 and NOx (80 and 200 ppmv, respectively) and water vapor up to 15% vol. caused no adverse effect on the CO_2 capacity. The regeneration of the sorbent and the recovery of CO_2 and its pressurization can then be achieved by several approaches, including temperature swing and vacuum swing. Our preliminary analysis showed that the proposed CO_2 capture process using our sorbent will reduce plant efficiency only by 7.76% (as opposed to a 30% reduction by the amine scrubbers) while providing 90% capture.

In this project, we took this technology originally developed for use with IGCCs and adapted it for use with pulverized coal fired power plants. TDA Research worked with Babcock & Wilcox (B&W), MeadWestvaco Corporation (MWV), the University of California, Irvine (UCI), the Gas Technology Institute (GTI) and the Illinois Clean Coal Institute (ICCI) to advance the technology by improving the material capabilities and the process design, and carried out an evaluation with a fully-equipped prototype unit using coal flue gas to demonstrate the technical viability of the concept. All our results fed into a techno-economic analysis using Aspen Plus^{TM} software to estimate the impact of the CO_2 capture system on the plant efficiency and cost of electricity (all analyses are consistent with DOE/NETL's Cost Estimation Guidelines).

2.1 TDA's CO_2 Capture System

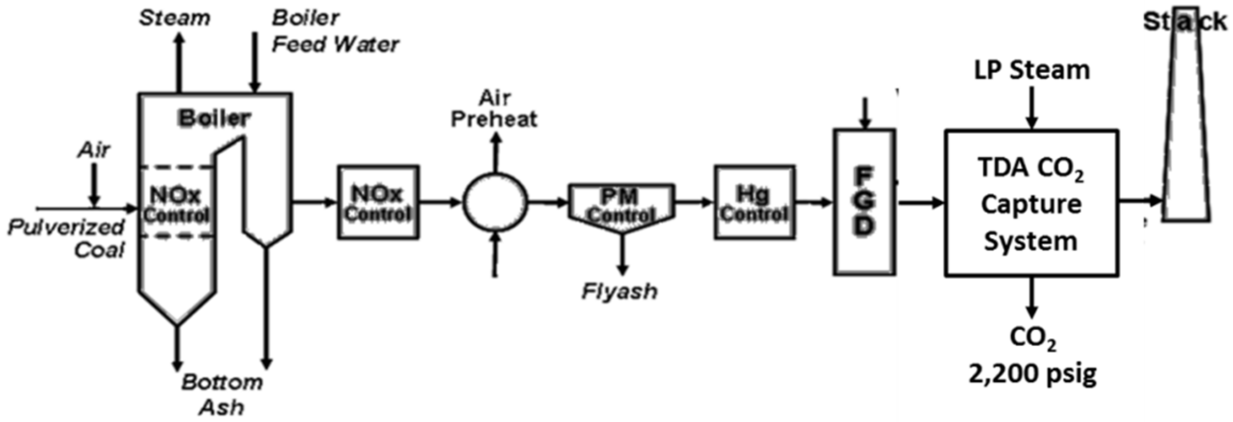

Figure 5. TDA's CO_2 Capture System integrated with a power plant.

In this project, we investigated two process design options for the flue gas – CO_2 sorbent contactor: fixed-bed and moving-bed VSA systems. Both cases uses a steam sweep under mild vacuum to regenerate sorbent and recover the CO_2 as mixed CO_2/steam stream, condensing the steam recovering the CO_2 as a high purity product. Although our original work in post combustion CO_2 recovery was based on the moving-bed design (and we successfully built and demonstrated its technical viability in a proof-of-concept prototype unit in this project), we then switched to much simpler fixed-bed system that is now the heart of our process. We have a unique reactor design that allowed reducing the pressure drop through the fixed-bed system, one of the key limitations that prevented the use of the fixed-bed reactors in flue gas carbon capture systems.

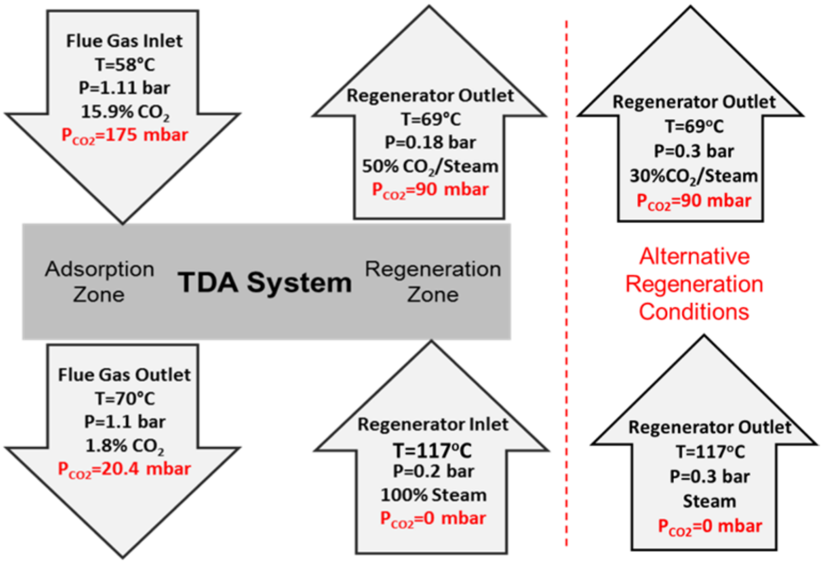

Figure 6. Gas flows around TDA system.

Regardless of the gas-solid contactor design, the CO_2 capture system is placed downstream of the FGD unit (Figure 5), where the gas is cooled to 57°C. After further cooling, removal of some water and re-heating (which are all necessary to prevent water condensation in the system), the gas enters the bed at 58°C. The system consists of multiple beds (we envision 8 beds) to house the sorbent; one or more beds will be on-line at all times adsorbing CO_2 from the flue gas to ensure we achieve greater than 90% carbon capture, while the other bed(s) are regenerating and/or going through pressure transitions.

The flue gas stream is introduced from the top of the sorbent beds at near ambient pressure (1.12 bar); the sorbent selectively removes CO_2 and the mildly exothermic CO_2 adsorption increases the bed temperature to 70°C. Once the sorbent is saturated with CO_2 (i.e., as sorbent reached its working capacity), the bed is isolated (using a series of valves) for regeneration. The bed first goes through a series of pressure equalizations to reduce the bed pressure to 0.2 bar (or alternatively to 0.3 bar). A superheated steam flow at 70°C and 0.2 bar sweeps across the bed to recover the released CO_2. The steam sweep is used to facilitate the CO_2 release at low CO_2 partial pressure, thereby ensuring a high removal efficiency during adsorption.

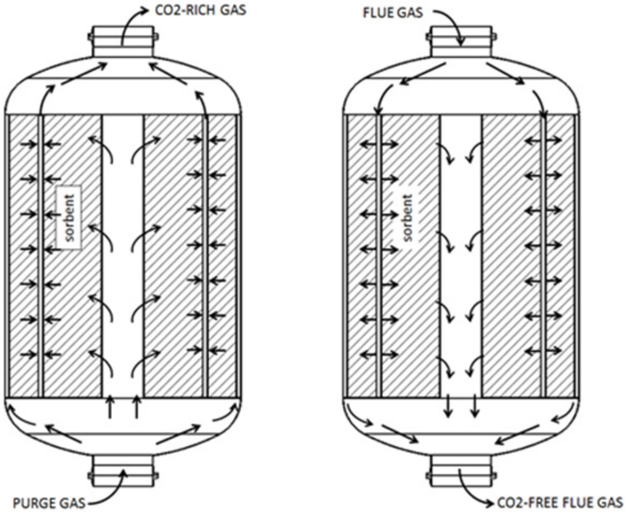

Figure 7. Radial flow full scale sorbent reactors in regeneration (left) and CO_2 adsorption (right).

Even though the fixed-bed contactors represent the simplest design and the least expensive housing option, the use of such reactors has been limited due to the potentially high pressure drop generated by these systems. Even in the rapidly cycling beds, because of the very large amounts of CO_2 to be removed, a significant inventory of sorbent must be placed into the flow path. Unfortunately, the conventional “pancake” reactor design (with very large diameter low depth beds with low aspect ratios) common for fixed-bed reactors used in similar applications will not be practical due to their large footprint and flow distribution issues. In our system, we use radially outflow reactors to house the sorbent. The reactor will resemble a traditional fixed-bed reactor, while the proper internal manifolds enable gas distribution in the radial direction allowing the flue gas to pass over a relatively thin bed of sorbent presented across the height of the reactor. The flue gas is introduced into the reactor via a common supply line from the top of the bed and is distributed into the two internal manifolds (as indicated by the arrows in Figure 7). The CO_2 free flue gas is collected in separate internal exhaust manifolds which then merges into a single exhaust line and leaves the reactor at the top of the reactor.

During the regeneration, pressure equalization of the beds moderates the sorbent pressure to 8.5 psia. A vacuum pump is used for further depressurization. The low pressure steam will be introduced at the bottom of the bed through the exhaust (three) manifolds where the CO_2 free flue gas has been removed. The steam also sweeps across the bed in the radial direction, but in the counter direction of the flue gas flow; the adsorbed CO_2 comes off from the surface and recovered, generating a 50% vol. CO_2/steam mixture (dry basis CO_2 purity of 95+%) at 0.18 bar at the regenerator exit after accounting for the pressure drop through the bed (the balance being ~50% vol. H_2O with some N_2 and O_2 impurities from the flue gas trapped within the sorbent pores). This off-gas from the regenerator is then compressed in a two-stage compressor to raise its pressure to 1.24 bar. The compression also raises the stream temperature to 182°C. We use this heat of compression to raise the low pressure steam (0.2 bar) used as the regenerator sweep gas. The low pressure steam is raised in two boilers following the compressors, providing 61°C saturated steam for the regeneration process. As the regeneration off-gas (mainly consisting of the released CO_2 and steam) goes through the compression and cooling steps, the water condenses and is recovered to feed back into the cycle. Following the two compressors in the regenerator, a product stream of 68.7% CO_2/steam mixture is produced at 77°C. The CO_2 is further concentrated and compressed in the compression/purification train.

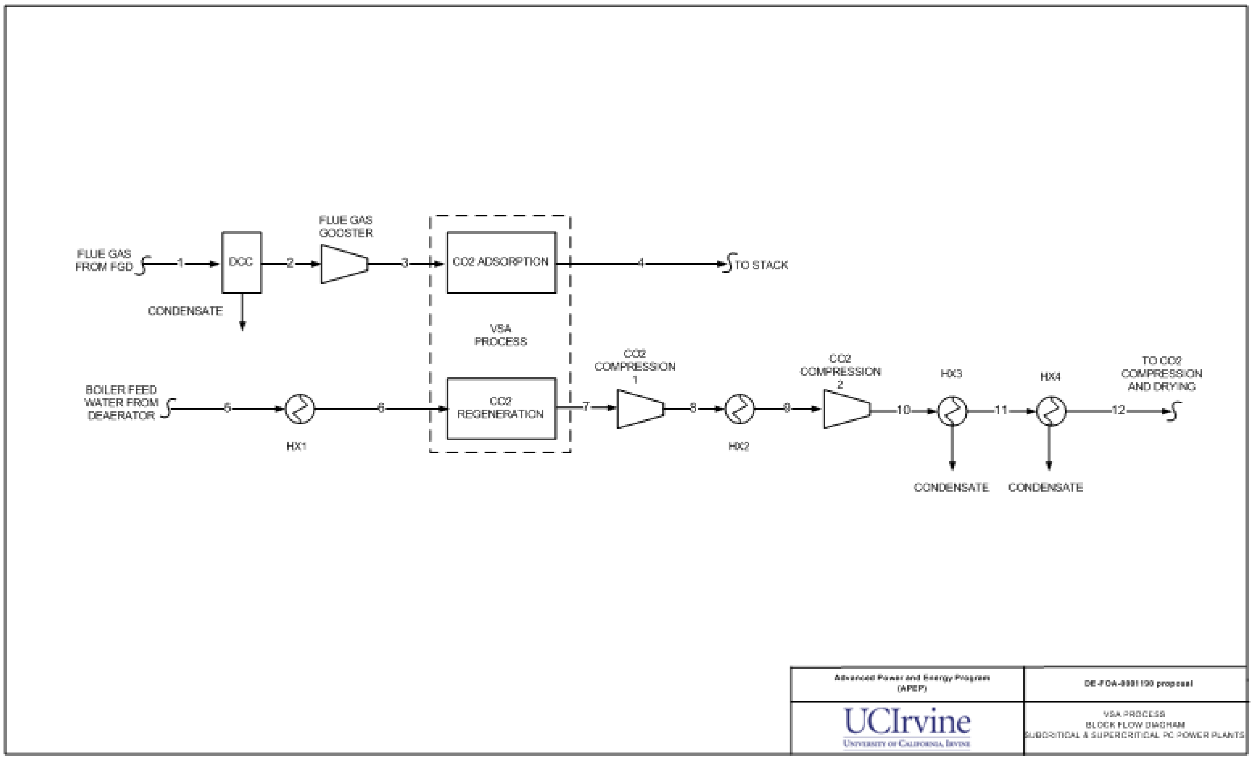

Figure 8. PFD around TDAs VSA based post combustion CO_2 capture system.

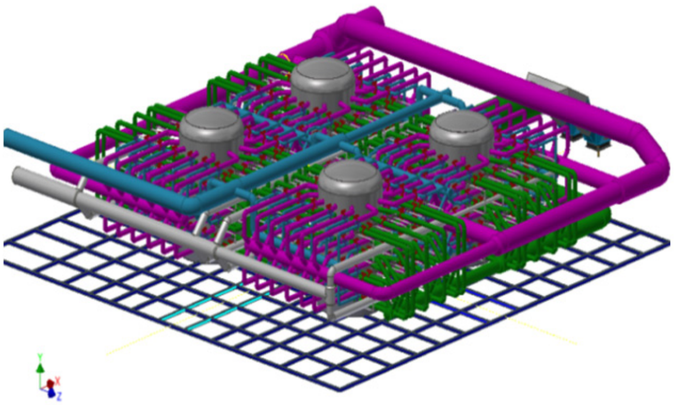

Figure 9. Stacked beds with external manifolds prepared by B&W.

Because the flue gas and the steam are at similar pressures and temperature, the transition from adsorption to regeneration (and vice versa) is very rapid, eliminating the need for multiple beds. We believe that 8 beds will be sufficient to all the transitions in a rapid cycling vacuum/concentration swing system. Based on the 2,326,545 lb/hr flue gas flow rate (the flow rate for AEP's 550MW Conesville #5 power plant), we expect only a 0.2 psid pressure drop across the bed.

Another unique advantage of the design is in the reduction in the number of flow selection valves to distribute the gases into the reactors. Combining all supply lines to the reactors into a single manifold (and distributing the gases internally in the reactor) requires only 1 valve per supply line per bed instead of 4 providing a 4X reduction in the number of valves for the operation of the system which was used in our early designs. In the initial fixed bed design carried out by B&W the gas flows during the adsorption and regeneration were distributed into "stacked" beds using external manifolds (Figure 9). This stacked bed design required 16 valves that had contributed to 25% of the overall costs. The radial outflow design represents a significant modification, substantially reducing the number of these valves per bed and hence the overall cost.

Figure 10. A commercial Round Louvre Valve.

We envision the valves used in our process to be similar to the Louvre Lock Valves that are available off-the-shelf and can be purchased at competitive costs (as little or no further design work is needed). Figure 10 shows a picture of the Louvre Damper Valves (DN 5600 mm with NICROFLEX sealing, rating T=400^{o}C, P_{diff}= 90 mbar) supplied to a DeNOx plant at the STEAG power station Herne, Germany. These valves are already designed to treat the desired gas volumes at the operating conditions of interest for similar application. We anticipate a straight forward integration into our system, providing substantial cost savings.

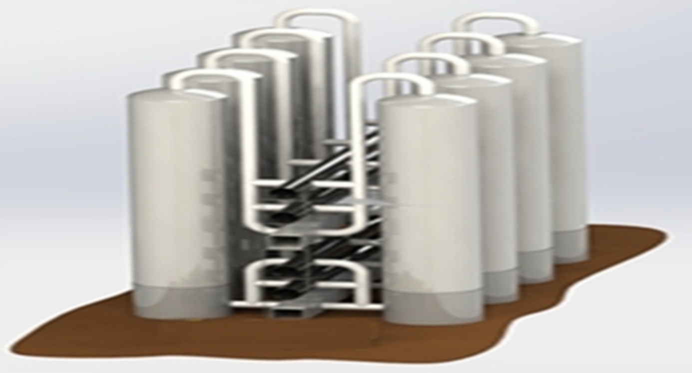

Figure 11. Full scale system.

Like every CO_2 capture process, TDA's system also includes a section that compresses, intercools, recompresses and refrigerates the CO_2 for purification; finally recovering the liquid CO_2 so that it can be pumped to 2200 psig for sequestration. The CO_2 compression, condensation and purification train used in our process will be similar to that described by Ramezan (2007).

2.1 Preliminary Technology Feasibility Study

We carried out a preliminary technology feasibility study of TDA's CO_2 capture process for existing coal-fired power plants following the guidelines provided in the U.S. DOE funding opportunity announcement DE-FOA-000403, Attachment 3. We provided the results from the preliminary technology feasibility study in a report to DOE. In this preliminary feasibility study, we considered a moving bed system with vacuum swing regeneration, in the full project we looked at other bed configurations and regeneration options and concluded that radial flow fixed beds are the best option using our low cost, high capacity CO_2 sorbents for post combustion CO_2 capture.

2.1.1 Assumptions Used in the Feasibility Study

We used the assumptions and methodology put forth in the DOE FOA.

System Boundaries:

1) Flue gas entering capture system from existing flue-gas desulfurization system (FGD), through high-pressure, high-purity CO_2 stream crossing plant fence
2) Parasitic electricity from PC plant generators
3) Low-pressure (LP) steam at steam turbine extraction conditions
4) Cooling and process water services
5) Waste streams generated in the CO_2 capture and compression systems should be identified and any special treatment requirements included

Process Design Assumptions:

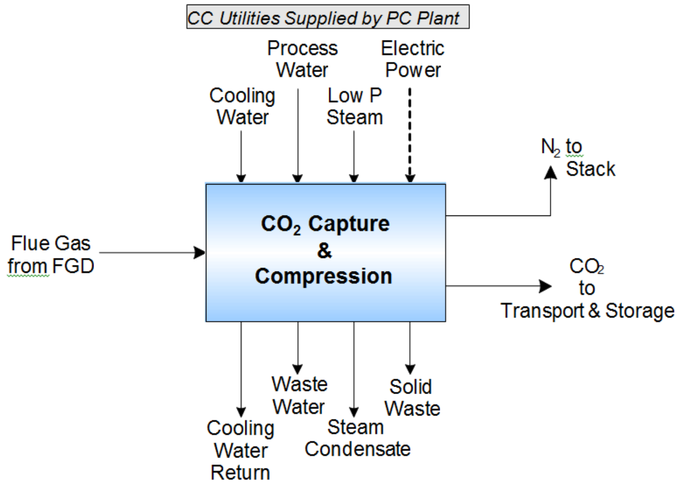

Figure 12. System boundaries.

1) Composition of flue gas leaving FGD (wet basis):		vol%
	CO_2	13.17
	H_2O	17.25
	N_2	66.44
	O_2	2.34
	Ar	0.80
		ppmv
	SOx	42
	NOx	74
2) Flowrate of flue gas leaving FGD (based on 550 MW net PC plant):		5,118,399 lb/hr
3) Pressure and temperature of flue gas leaving FGD:		14.7 psia 135°F
4) Conditions for LP steam available from power plant:		167.7 psia 743.3°F
5) Conditions for cooling water:		feed – 60°F return – 80°F min. approach – 30 F°
6) CO_2 Removal from flue gas:		greater than 90%
7) CO_2 Purity:		greater than 95 vol%
8) CO_2 Delivery pressure and temperature:		2,215 psia 124°F
9) Electric Power equivalence of LP Steam:		0.0911 kWh/lb

Economic Analysis Assumptions:

1) Levelized-Cost of Electricity without CO_2 capture:	64 mills/kWh
2) Levelized-Cost of Steam without CO_2 capture:	\$5.83 / 1,000 lbs
3) Levelized-Cost of Cooling Water:	\$0.12 / 1,000 gal
4) Levelized-Cost of Process Make-Up Water:	\$0.07 / 1,000 lb
5) Levelized-Cost of Wastewater Treatment:	\$0.21 / lb
6) Levelized-Cost of Solid-Waste Disposal:	\$17.87 / ton
7) Levelized-Cost of Toxic-Waste Disposal:	\$89.36 / ton
8) Levelized-Cost of CO_2 Transport, Storage & Monitoring:	\$4.05 / ton CO_2
9) Plant On-Stream Factor:	310.25 days/yr
10) Retrofit Factor:	1.0
11) Plant Location:	generic plant site, U.S. Midwest
12) Dollar-Year Reporting Basis:	2007
13) Total Fixed O&M Levelized-Costs	\$995 / calendar day
14) Levelized Maintenance-Material Costs (as percentage of initial equipment and materials costs)	2%
15) Capital Charge Factor: (based on 20-year levelized cost of electricity, LCOE)	17.5%/yr

2.1.2 Preliminary Feasibility Study Results

For use in this preliminary feasibility study, we carried out an initial process design analysis to determine the power requirements, capital and operating costs, and finally the CO_2 capture costs for our system. We carried out the preliminary analysis based on the mass and energy balances of AEP's Conesville Unit#5 (Ramezan 2007). We assumed a nominal working capacity of 3.0% wt. CO_2 for our sorbent as measured in bench-scale tests.

A summary of the energy requirements are given in Table 2. The major power requirements are in steam compression for regeneration and the compression of the CO_2 to 2200 psig. The net plant power output is estimated to be reduced to 430,550 kW (a loss of 119,450 kW in power output) with CO_2 capture. In comparison, the output is reduced to 178,853 kW in the baseline CO_2 capture case with amines described in DOE/NETL-401/110907 (DOE 2007), so our sorbent will have potential to reduce the cost of CO_2 capture. The net plant power out is reduced by 7.76% for TDA's CO_2 capture system compared to 11.9% loss for an amine system.

We also estimated the cost of CO_2 capture on the major process equipment cost and operating expenses. We estimate that the cost of CO_2 capture and cost of CO_2 avoided as \$33.4/ton and \$38.7/ton, respectively (much lower than those estimated for the amine scrubbers for the same application \$45/ton and \$68/ton, respectively). We recognize that these are preliminary numbers that need to be refined during the project based on the results from the more thorough sorbent evaluations and performance characterization. A more complete final technology feasibility report including detailed design and cost analysis along with the assumptions used will be provided at the end of the project.

Table 2. Power requirements for TDA system.

Compress to (psia)	kW_e
7.5	25,642
18	21,477
48.5	14,282
133	12,679
365	12,370
912	10,994
2230	10,694
Compressor total	108,137
Butane Refrigerator	8,905
Belt Elevators	2,065
Total	119,450

	kW_e	net eff. (%)
Plant power output without CO_2 capture	550,000	35.74
Plant power output with TDA's CO_2 capture system	430,550	27.97
Efficiency points lost (12,197 Btu/kWh)		7.76

Table 3. Cost of CO_2 capture with TDA system.

Annual Sorbent Replacement (tons/yr)	1,276
Process Make-Up Water (kg/h)	4,331
Wastewater Treatment (kg/h)	1,732
Solid Waste for Disposal (tons/yr)	1,068
Cooling Water Requirement (m^3/h)	5,234
Grass Roots Capital	$ 132,138,618
Annualized Cost of Capital (17.50%)	$ 23,124,258
General O&M (2%)	$ 2,642,772
Annual Sorbent Replacement	$ 11,600,000
Levelized-Cost of Process Make-Up Water	$ 4,966
Levelized-Cost of Wastewater Treatment	$ 5,959,743
Levelized-Cost of Solid-Waste Disposal	$ 19,092
Levelized-Cost of Cooling Water	$ 1,454,997
Cost of Replacement Power ($0.0640/kWh)	$ 56,923,181
Annual Cost	$ 101,729,010

Cost of CO_2 Captured (3,144,248 tonne/yr)	$	32.35	$/tonne CO_2
(3,466,533 tons/yr)	$	29.35	$/ton CO_2
Cost of CO_2 Sequestration	$	4.05	$/ton CO_2
CO_2 Capture & Sequestration	$	33.40	$/ton CO_2
CO_2 emitted by makeup power		836,520	tons/yr
CO_2 avoided		2,630,013	tons/yr
Cost of CO_2 avoided	$	38.68	$/ton CO_2

Calculated Output from Feasibility Study:

1) Parasitic power losses for 550 MW net plant, due to the addition of CO_2 capture and compression: {power loss due to capture auxiliaries} + {power loss due to compression requirements}+{equivalent power loss due to LP steam required for capture}

   {total parasitic power losses due to capture & compression} = 119.45 MW_e

2) Estimated levelized-cost of electric power and steam with CO_2 capture and compression:

   {cost of electric power in mills/kWh} = 0.3073×{total power loss in MWe} + 64.0 = 100.71

   {cost of steam in $/1,000 lb} = 0.0280×{total power loss in MWe} + 5.83 = 9.18

3) Itemized cost of all installed equipment and materials used in the CO_2 capture and compression process

Table 4. Itemized cost of installed equipment.

Cost of Regenerator Vacuum vessels		$ 17,613,410
Cost of Absorber		$ 3,002,286
Cost of Sorbent		$ 11,600,000
Compressors		$ 23,154,295
Motors		$ 1,699,186
Heat Exchangers		$ 413,440
Butane Refrigerator		$ 3,335,873
Belt Conveyors		$ 784,597
Installed Cost		$ 61,603,085
Auxiliary facilities	30%	$ 18,480,926
Sub total		$ 80,084,011
Contingency & Fee	32%	$ 25,626,884
Subtotal		$ 105,710,895
Risk Factor for new Technology	25%	$ 26,427,724
Grass Roots Capital		$ 132,138,618
Annualized Cost of Capital	17.50%	$ 23,124,258
General O&M	2%	$ 2,642,772
Annual sorbent replacement		$ 11,600,000

4) Cost of CO_2 Capture:

   {cost of all materials and utilities consumed in the CO_2 system}
   {cost of treating or disposing of any effluent streams from the system, including transport, storage and monitoring of CO_2}
   {cost of maintenance and materials}
   {fixed O&M Costs}
   \+ {capital charge for CO_2 capture system}
   {total cost of capturing CO_2}

   The cost per ton of CO_2 is obtained by dividing this cost by the tons of CO_2 captured.

   Cost of CO_2 capture ($/ton CO_2) = $33.40 (see Table 3 for details)

5) Percentage decrease in PC plant efficiency:

{total lost power due to CO_2 capture} = 7.76% (see Table 2 for details)
{heat content of coal feed (HHV)}

3. Project Objectives

The project tasks were divided into three budget periods (BPs). Our BP1 goals were to optimize the chemical and physical properties of the sorbent, and then carry out bench-scale evaluations, which include parametric tests to identify the optimum operating conditions for the sorbent, and complete a detailed design for the CO_2 capture process in collaboration with UCI and B&W. In BP2, the objectives were to scale-up sorbent production using high throughput equipment and low-cost raw materials and estimate the large-volume production cost of the sorbent. The other objectives in BP2 were to demonstrate the long life and durability of the sorbent (running over 5,000 cycles) and to design all critical system components, particularly the gas-solid contactors used in the adsorption and regeneration processes in collaboration with B&W. Finally, the process simulation will be revised based on the results of the multiple-cycle experiments. A sensitivity analysis will be carried out to improve the process design. In BP3, TDA will build a skid-mounted prototype unit that is capable of demonstrating the sorbent's operation throughout the full-cycle. We will run the prototype unit using actual coal flue gas to fully assess and demonstrate technical viability of the process. We will work with GTI to demonstrate the operation of the unit and optimize its operation using the flue gas generated by a pilot-scale coal combustor. Based on the field test results and the reactor and sorbent cost estimates, we will complete an economic evaluation to accurately estimate the cost of removal of CO_2 based on DOE/NETL's Cost Estimation Guidelines. We will also complete an Environmental, Health and Safety (EHS) assessment.

This report covers work carried out in all three budget periods.

3.1 Work Plan

The proposed R&D effort was divided into 14 Tasks. In Task 1 that runs the entire three years of the project we carried out all the project management tasks as per the Project Management Plan (PMP). We provide DOE with quarterly progress reports and project spending updates.

Budget Period 1 Tasks

In Task 2, we optimized the sorbent composition and production. In Task 3, we evaluated the sorbent at bench-scale under representative conditions. In Task 4, in collaboration with UCI and B&W we carried out detailed process design and simulations using Aspen-Plus^{TM} software and performed necessary material and energy balances. The design of the CO_2 process was reviewed with our partners (B&W and GTI) to ensure that it can be easily integrated to existing coal fired power plants and also to the test facility at GTI that was to be used for the demonstration tests. A preliminary technology feasibility study as outlined in Attachment 3 of solicitation (DE-FOA-0000403) was completed

Budget Period 2 Tasks

In Task 5, we scaled-up the sorbent production using scalable production equipment and carried out a detailed cost analysis. In Task 6, we carried out long–term cycling experiments through a minimum of 5,000 cycles in a relevant environment to evaluate the impact on the sorbent performance and life. In Task 7 with input from TDA, B&W completed the design of the sorbent reactors. B&W provided us with process flow and instrumentation diagrams and 3-dimensional layouts of the proposed reactors. In Task 8, we completed the design of the prototype test unit that will be evaluated at GTI's Des Plains, IL facility. In Task 9, TDA in collaboration with UCI and B&W worked together to update the process design and cost analysis based on BP2 results.

Budget Period 3 Tasks

In Task 10, we produced the sorbent needed for the prototype unit tests. In Task 11, we fabricated the prototype test unit while GTI completed the updates/changes to their pilot scale coal combustion facility. In Task 12, we worked with GTI to install the prototype test unit at their pilot-scale test site and carried out evaluations with flue gas generated from a pilot-scale coal combustor. In Task 13, based on the results of the prototype unit test campaigns, we carried out a final system analysis to determine the cost of the CO_2 capture system, and the cost of electricity for an integrated system in a commercial coal-fired power plant. The data was compared against the currently available CO_2 capture technology and a final technology feasibility study was completed following the guidelines provided in Attachment 3 of the solicitation (DE-FOA-0000403). We evaluated the results of the final systems and economic analysis to determine the commercial viability of the process and the scale-up potential for future pilot scale test campaigns. In task 14, in collaboration with our partners we performed a preliminary EH&S assessment associated with TDA’s process. The EH&S risk assessment was conducted following all industrial guidelines (and guidelines provided in Attachment 4 of the solicitation DE-FOA-0000403).

4. Results

4.1 Task 1. Project Management and Planning

The project commenced on October 1, 2011 and updated the PMP based on inputs from the DOE project manager and submitted it to DOE (Milestone# 1-1) on December 9, 2011. The Principal Investigator attended a kick-off meeting held at NETL's facility in Pittsburgh, PA on December 2, 2011 (Milestone# 1-2). A project outline, including company overview and project approach, was presented to the DOE technical staff and other interested parties, including other research groups within the overall project scope. Table 5 summarizes all the milestones along with their completion dates.

Table 5. Project Milestone Log.

Mile-stone #	Budget Period	Task/ Subtask No.	Milestone Description	Planned Comple-tion	Actual Comple-tion	Verification Method
			Project Start Date	10/1/2011		
1-1	1	1.1	Updated Project Management Plan (PMP) & Complete Initial Technical and Economic Feasibility Study	11/1/2011	12/9/2011	PMP file & Feasibility Report
1-2	1	1.1	Year 1: Kickoff meeting at NETL (Milestone review meeting with DOE)	1/2/2012	12/2/2011	Presentation file
1-3	1	2	Complete Sorbent Optimization	4/30/2012	4/30/2012	Results update
1-4	1	3	Complete Sorbent Evaluations	8/30/2012	8/30/2012	Results update
1-5	1	4	Complete Process design and Modeling	3/31/2013	3/31/2013	Results update
1-6	1	1.1	Year 1: Annual Review Meeting-NETL	9/28/2012	9/16/2012	Presentation file
			Go/No go Decision Point	9/28/2012		
2-1	2	5	Complete Sorbent Scale-up	6/28/2013	6/28/2013	Results update
2-2	2	7	Complete Design of Sorbent Reactors	6/28/2013	6/28/2013	Results update
2-3	2	8	Complete Design of the Prototype Unit	7/31/2013	7/31/2013	Results update
2-4	2	6	Complete Long-term Sorbent Cycles	9/30/2013	9/30/2013	Results update
2-5	2	9	Complete Process Optimization and Design	12/31/2013	12/9/2013	Results update
2-6	2	1.2	Year 2: Annual Review Meeting-NETL	12/31/2013	1/8/2014	Presentation file
			Go/No go Decision Point	12/31/2013		
3-1	3	10	Complete Sorbent Production for Prototype Unit	3/31/2014	3/31/2014	Presentation file
3-2	3	11	Complete Fabrication of the Prototype Test Unit	4/30/2014	3/27/2014	Results update
3-3	3	12	Complete Field Tests	8/31/2015	6/30/2015	Results update
3-4	3	13	Complete System Analysis and Process Economic Evaluation	8/31/2015	9/18/2015	Results update
3-5	3	14	Complete Preliminary EH&S Assessment	12/31/2014	12/31/2014	Results update
3-6	3	1.3	Year 3: Annual Review Meeting-NETL & Final Report	9/30/2015		Presentation file & Final Report

4.1.1 DOE Peer Review Comments

In the second quarter of FY 2013, we participated in the DOE peer review program conducted by AIChE. The response to the action items from that review meeting are provided in this section. Table 6 summarizes the FY13 Carbon Capture Peer review Milestones.

Table 6. FY13Carbon Capture Peer Review Milestones Log.

Award Number	Milestone Title	Description	Estimated Finish Date	Actual Finish Date	Status
FE0007580	FY14Q4 - Carbon Capture Peer Review (FY13) - R1	R1: Literature review of research on moving bed reactors should be conducted.	9/30/2014	7/31/2014	Completed – reported on 10/31/2014
FE0007580	FY15Q1 - Carbon Capture Peer Review (FY13) - R2	R2: Address the question of co-adsorption of nitrogen.	6/30/2015	4/30/2015	Completed – reported on 4/30/2015
FE0007580	FY14Q4 - Carbon Capture Peer Review (FY13) - R3	R3: Detail is missing on cost and risk information.	9/30/2014	8/31/2014	Completed – reported on 10/31/2014
FE0007580	FY15Q1 - Carbon Capture Peer Review (FY13) - R4	R4: Conduct a full-cost economic analysis.	9/30/2015	9/18/2015	Completed to be reported on 10/30/2015
FE0007580	FY15Q1 - Carbon Capture Peer Review (FY13) - R5	R5: Detail design considerations and establish a viable process scheme.	9/30/2015	9/18/2015	Completed to be reported on 10/30/2015
FE0007580	FY14Q4 - Carbon Capture Peer Review (FY13) - R6	R6: Set preliminary minimum targets.	9/30/2014	7/31/2014	Completed – reported on 10/31/2014
FE0007580	FY14Q4 - Carbon Capture Peer Review (FY13) - A1	A1: Establish a better list of target values to monitor the progress of the project.	9/30/2014	9/30/2014	Completed – reported on 10/31/2014

Review Panel Recommendation 1 (R1)
R1: Literature review of research on moving bed reactors should be considered
"Previous NETL-sponsored projects related to chemical looping technology and moving bed reactors should be reviewed."

> We completed the DOE Peer Review Panel Recommendation 1 (R1) on July 31, 2014, i.e., a detailed literature review of prior research on circulating fluidized and moving bed reactors was completed and few of the literature are included in the references section. A more detailed report is provided as an attachment (Attachment 1) to the final report.

Review Panel Recommendation 2 (R2)

R2: Address the question of co-adsorption of nitrogen

"The project team needs to address the co-adsorption of nitrogen (N_2) and determine if it is an issue. If so, a plan is needed to determine how it will be addressed."

We completed the DOE Peer Review Panel Recommendation 2 (R2) on March 30, 2015, TDA explored the use of multiple VSA cycle designs to reduce the amount of nitrogen that gets desorbed with the CO_2 during regeneration, and improve the CO_2 desorption product purity to greater than 95% needed for the sequestration and storage application. These design included steps such as pressure equalization, co-current blowdown and co-current CO_2 purge in the VSA cycle sequence. These were evaluated at TDA using simulated flue gas and we observed that a simple co-current blowdown to 6 psia before counter current desorption and steam purge increased the CO_2 desorption product purity to 95+%. Figure 13 shows a summary of the test results with the fixed bed system over 375 cycles where we changed the adsorption step time and used a co-current blowdown step to 6 psia before the counter current blowdown and steam purge. We observed that the desorption CO_2 product purity was in excess of 95%. This shows that co-adsorption of nitrogen in the sorbent bed could be mitigated and the CO_2 desorption product purity can be improved to greater than 95% by using co-current blowdown. This addresses DOE Peer Review Panel Recommendation 2 (R2). This was also demonstrated with the real coal derived flue gas .The results are presented in Section 4.12.3.

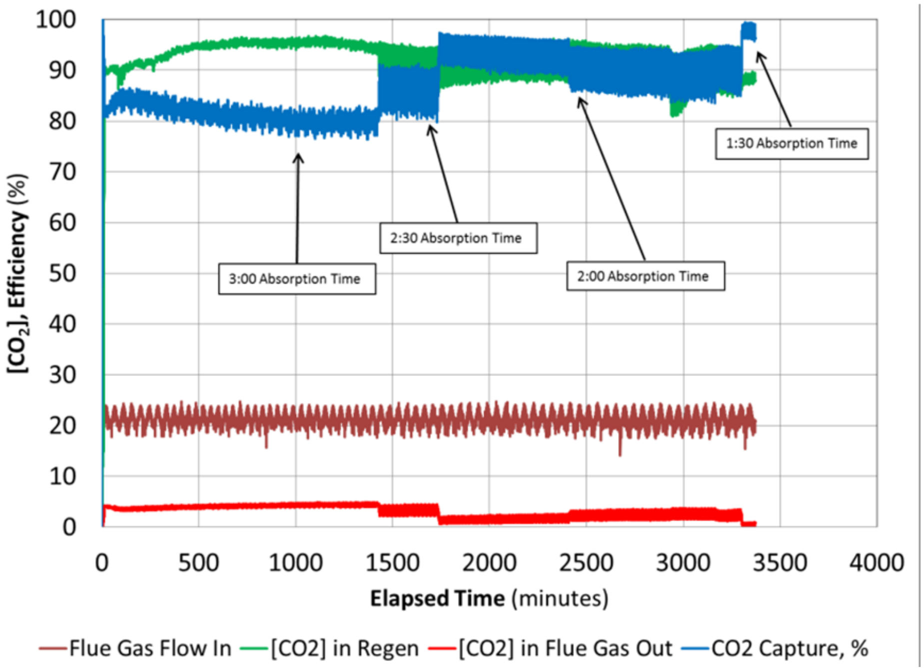

Figure 13. Results with fixed bed prototype unit at a flue gas flow rate of 1.0 scfm, CO_2 = 13.2%, P_{ads}=14 psia.

Review Panel Recommendation 3 (R3)

R3: Detail is missing on cost and risk information

"The team should present both efficiency and cost data, and keep both estimates up-to-date. The updates should reflect…"

We completed the DOE Peer Review Panel Recommendation 3 (R3) on August 31, 2014, i.e., we updated the risk information in the PMP to include the impact of contaminants in the flue gas on sorbent performance and cost of CO_2 capture, the cost information was updated at the end of the project based on the sorbent performance under real coal-derived flue gas in the tests at GTI. The updated cost analysis is completed and is reported in detail in Section 4.13.

Review Panel Recommendation 4 (R4)

R4: Conduct a full-cost economic analysis

"A full-cost economic analysis should be conducted with fixed bed vacuum swing adsorption (VSA) using a combination of shorter beds and shorter bed cycle times."

The updated full-cost economic analysis of TDA's Vacuum Swing Adsorption (VSA) based post combustion CO_2 capture system integrated with both a sub-critical and super-critical pulverized coal fired power plant have been completed in collaboration with our partner University of California Irvine (UCI) on 9/182015. The detailed results are reported in Section 4.13. A brief summary is provided below.

In collaboration with the Advanced Power and Energy Program of the UCI, TDA completed the process design using Aspen Plus^{TM} simulation software. The analysis provided a thorough comparison against a current state-of-the-art amine based CO_2 capture system integrated with both sub-critical and super-critical coal-fired power plants. In the simulation work, UCI strictly followed the guidelines and assumptions established by DOE/NETL for assessing the economic viability of competing CO_2 capture technologies. First, the accuracy of the Aspen Model was verified by checking the simulation results against the DOE/NETL analysis (Case 10 and Case 12 in the updated DOE/NETL report DOE/NETL-2010/1397 Rev. 2a). The results of the UCI's Aspen model simulating the amines based CO_2 capture case was found in close agreement with the DOE/NETL results (Table 7).

The analysis explored several design options; the moving bed system, axial flow "stacked" fixed beds with external manifolds, radial flow fixed beds with internal manifolds, using LP steam from steam turbine cycle for purge and LP steam generated from CO_2 compression. We decided to use the steam generated from CO_2 compression to eliminate any changes to the ST cycle. In this final summary we incorporated the lower steam consumption of Steam: CO_2 ratio of 0.44 in the steam purge step as shown in our tests at GTI using coal derived flue gas and also used a VSA cycle time of 4.5 min and desorption pressure of 4.5 psia. TDA's post combustion CO_2 capture system integrated with a sub-critical and

Table 7. Comparison of TDA's VSA based CO_2 capture system against amine based CO_2 capture system integrated with a super-critical power plant (550 MW_e net plant output).

Power plant Type	**Sub-critical PC Plant**		**Supercritical PC Plant**	
CO_2 Capture Technology	**Amines**	**TDA- VSA**	**Amines**	**TDA - VSA**
Case ID	**Case 10 DOE**	**Case 10 TDA**	**Case 12 DOE**	**Case 12 TDA**
Gross Power Generated, kWe	672,700	669,778	662,800	661,828
Auxiliary Load, kWe	122,740	119,778	112,830	111,828
Net Power, kWe	549,960	550,000	549,970	550,000
Net Plant Efficiency, % HHV	**26.20**	**31.55**	**28.40**	**33.81**
Coal Feed Rate, kg/h	278,956	231,261	256,652	215,810
Total Plant Cost, $/kWe	3,596	2,583	3,563	2,613
COE without CO_2 TS&M, $/MWh	142.22	107.86	137.45	105.99
COE with CO_2 TS&M, $/MWh	**153.03**	**116.71**	**147.44**	**113.76**
Cost of CO_2 Captured, $/tonne	**65.46**	**38.90**	**66.56**	**39.71**

super-critical pulverized coal fired power plant achieves a net plant efficiency of 31.55% and 33.81% on HHV basis; these are significantly higher than that can be achieved by amines based CO_2 capture system (26.2% and 28.4%). The water consumption in the plant on a net kW basis is also lower for TDA's process (29.7 and 26.8 m^3/min for TDA Case 10 and case 12 vs 42.5 and 38.1 m^3/min for amines Case 10 and Case 12), preserving a valuable resource). The capital expense for the plant was estimated following the DOE/NETL cost guidelines (e.g. higher contingencies were applied for unproven technologies such as the VSA unit). The total cost for the sub-critical and super-critical coal fired plants integrated with TDA's process is estimated as \$2,583/kW_e and \$2,613/kW_e, respectively. These are 28.2% and 26.7% lower than those of the corresponding amine based cases.

Review Panel Recommendation 5 (R5)
<u>R5: Detailed Design considerations and establish a viable process scheme</u>
"A process scheme that is practical and viable needs to be defined, at least at a high level…"

> The panel recommendations were addressed in the BP2 in collaboration B&W. Evaluation of different process design schemes suggested in the DOE review are complete and a viable process scheme has been established, which was then used in the full-cost economic analysis (9/18/2015). The VSA process scheme is described in detail below.

The DOE review panel recommended looking at different process design schemes, which we addressed in the BP2 in collaboration B&W, where we considered moving bed and fixed bed design options. The fixed bed option was found to be a cheaper and much simpler system to operate. In the BP3 we also looked to further optimize the fixed bed design scheme, considering a radial flow fixed bed design to minimize the complexity involved in stacking pancake style fixed beds. The flow diagram and VSA sequence of the 8 bed system are shown in Figure 14 and Figure 15.

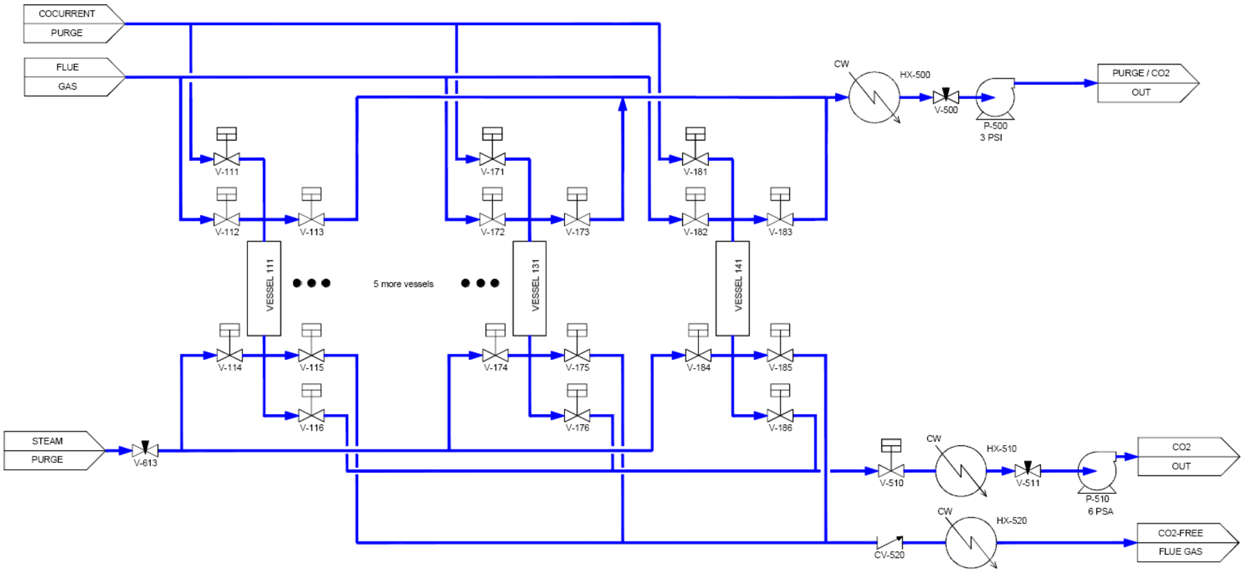

Figure 14. Flow diagram of the 8 bed PSA system.

The full size system is sized to process flue gas output from a coal fired power plant producing net power of 550 MW_e. It consists of two 8-bed assemblies. In this design, half the beds are adsorbing CO_2 while the other beds are in various regeneration steps. Thus the flow through each bed is approximately 132,000 SCFM (Table 8). To maintain an average gas velocity of about 0.15 m/s through the bed, each reactor consist of two concentric radial sorbent beds as shown in Figure 16.

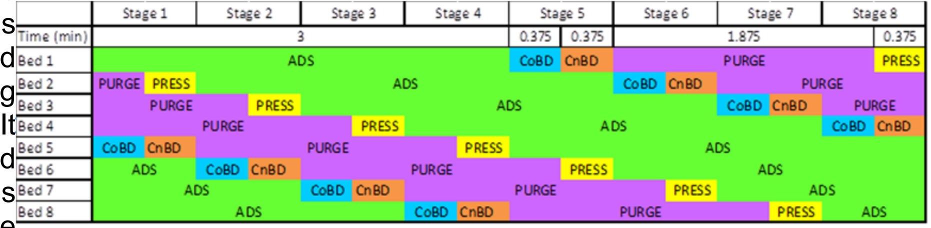

	Stage 1		Stage 2		Stage 3		Stage 4		Stage 5		Stage 6		Stage 7		Stage 8	
Time (min)	3								0.375	0.375	1.875					0.375
Bed 1	ADS								CoBD	CnBD	PURGE					PRESS
Bed 2	PURGE	PRESS	ADS								CoBD	CnBD	PURGE			
Bed 3	PURGE			PRESS	ADS								CoBD	CnBD	PURGE	
Bed 4	PURGE					PRESS	ADS								CoBD	CnBD
Bed 5	CoBD	CnBD	PURGE					PRESS	ADS							
Bed 6	ADS		CoBD	CnBD	PURGE					PRESS	ADS					
Bed 7	ADS				CoBD	CnBD	PURGE					PRESS	ADS			
Bed 8	ADS						CoBD	CnBD	PURGE					PRESS	ADS	

Figure 15. 8-bed VSA cycle sequence.

Table 8. Full scale VSA bed sizing based on 6 min full cycle time and bulk density of 0.28 kg/L

Basis:	550 MW_e
Fluegas flow	1,057,633 scfm
CO_2 flow	559,811 kg/hr
No. of. Beds	8
Total Sorbent	3,651 m^3
Total Cycle Time	6.0 min
Bed Volume	456 m^3
Vessel Diameter	24.3 ft
Vessel Height	48.5 ft
Inner bed thickness	7.9 ft
Outer bed thickness	4.6 ft
Inner Bed Volume	246 m^3
Outer Bed Volume	212 m^3
L/D	2.0
GHSV	984 h^{-1}

Each vessel is 24 ft in diameter and 48.5 ft tall and contains 456 m^3 of sorbent split in two concentric rings with an annulus between them (Figure 17). The thickness of the outer ring is 28" and the thickness of the inner ring of sorbent is 52". This leads to an average superficial gas velocity of 0.16 m/s through the inner bed and 0.1 m/s through the outer bed. During adsorption, flue gas enters the top of the vessel and enters the annulus between the two rings of sorbent. The gas then passes through both sets of sorbent and is collected in the central pipe and the outer wall (Figure 16). These flows are combined at the bottom where the CO_2-free flue gas exits the system. During regeneration, the purge gas enters the bottom and flows through the beds in reverse. The CO_2 is desorbed from the beds and the CO_2 laden purge gas (steam) exits the top of the vessel. The steam is condensed and the CO_2 rich stream is passed on for further processing.

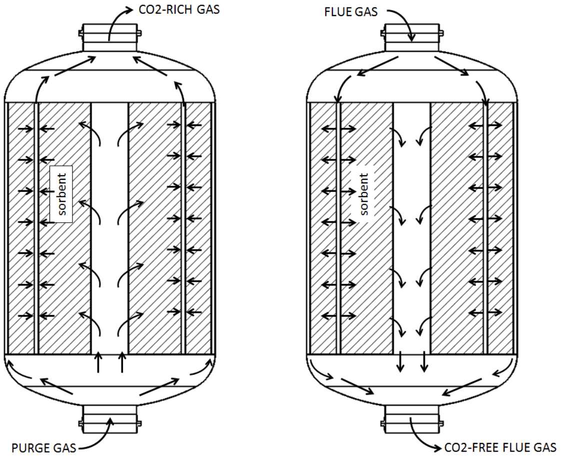

Figure 16. Dual radial flow configuration of full-size system.

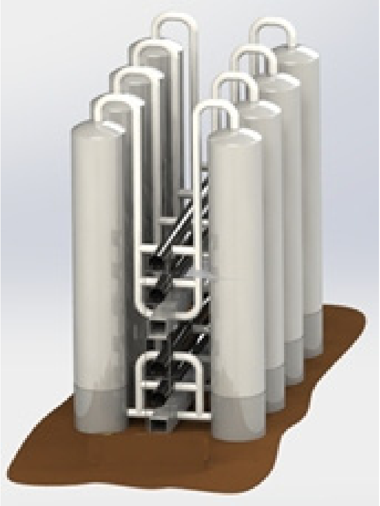

Figure 17. 550 MWe full scale 8-bed VSA system.

Review Panel Recommendation 6 (R6)

R6: Set Preliminary minimum targets

"Preliminary minimum targets for crush strength and attrition rate should be set for the type of process envisioned. Given the early stage of this project, it is recommended that the team use smaller, but practical, applications of similar processes elsewhere to select these targets."

> We completed the DOE Peer Review Panel Recommendation 6 (R6) on July 31, 2014, i.e., we have identified the preliminary minimum targets for crush strength and attrition rate. We have set the target crush strength to be at 1.5 lbf/mm based on those for commercial carbons. We have used Fluid Catalytic Cracking (FCC) catalysts as a basis to set the minimum attrition rate to be less than four times that of the FCC catalysts.

Review Panel Action Item 1 (A1)

A1: Establish a better list of target values to monitor the progress of the project

"The team has generated a significant amount of data in a fixed bed reactor and now needs to reevaluate the process to establish a better list of target values. This will enable better monitoring of project progress."

> We completed the Review Panel Action Item 1 (A1) on September 30, 2014, i.e., We re-established a list of target values to monitor the progress of the project. The target values identified were:
>
> Bulk packing density for sorbent of 0.3 kg/L (min.)
> CO_2 working capacity of at least 3 % wt.
> CO_2 capture of 90+% and CO_2 purity of 95+%

4.2 Task 2. Sorbent Optimization

Sorbent Preparation:

We optimized our sorbent formulation by preparing more than 20 different formulations. In these samples we changed the modifiers and pore formers used (to generate the desired pore size), i.e., the source of the surface active groups and the amount of promoters. We also controlled the pore size and surface area of our sorbents by changing the firing temperature and its duration. After making the sorbents, we measured their BET surface area and pore volume in our Micromeritics Gemini surface area analyzer (Figure 18). Table 9 shows the summary of the BET surface area and pore volume for selected preparations.

Figure 18. Micromeritics Gemini Unit.

Isotherm Measurement: TDA has an automated constant volume apparatus (CVA) for adsorption isotherm measurements from vacuum to pressures up to 1.8 atm. We used this apparatus to measure the adsorption isotherms at various temperatures and CO_2 partial pressures of interest. The CVA allows us to measure single component gas-solid equilibrium and kinetics (adsorption characteristics). The constant volume adsorption process is a static measurement technique where the pressure change due to adsorption in a closed constant volume system is measured with a pressure transducer. The adsorbed amount is calculated by making a material balance using any standard thermodynamic equation of state such as the "ideal gas law". Figure 19 is a picture of the constant volume apparatus. The set up consists of two cylindrical chambers or cells (dose and sample (test) cells) of known volume connected by a pneumatic ON/OFF valve. A few grams of the adsorbent (about 2-5 g) are placed in the sample cell. The feed gas from the gas cylinder is then filled into the dose cell through the mass flow controller to a pre-set pressure at which point the gas inlet valve (#V-1) is closed. Then the ON/OFF valve (#V-2) between the two cells is opened to provide a step change in the pressure of the sample cell. The size of the step depends on the time of opening of the valve and the initial difference in pressure (ΔP) between the two sides. This valve can be left open until equilibration of the pressures between the two sides to operate in pressure equalization mode. The pressure change after opening the valve is monitored by the data logging computer to generate the adsorption equilibrium and kinetics data.

Table 9. Summary of the BET surface area and pore volume for selected samples prepared as part of this DOE PRDA project (DE-FE-0007580).

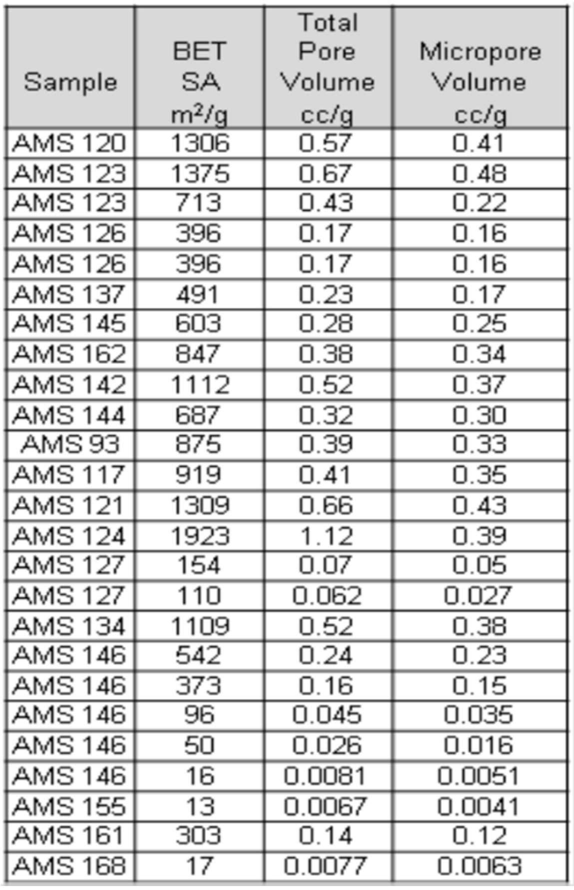

Sample	BET SA m²/g	Total Pore Volume cc/g	Micropore Volume cc/g
AMS 120	1306	0.57	0.41
AMS 123	1375	0.67	0.48
AMS 123	713	0.43	0.22
AMS 126	396	0.17	0.16
AMS 126	396	0.17	0.16
AMS 137	491	0.23	0.17
AMS 145	603	0.28	0.25
AMS 162	847	0.38	0.34
AMS 142	1112	0.52	0.37
AMS 144	687	0.32	0.30
AMS 93	875	0.39	0.33
AMS 117	919	0.41	0.35
AMS 121	1309	0.66	0.43
AMS 124	1923	1.12	0.39
AMS 127	154	0.07	0.05
AMS 127	110	0.062	0.027
AMS 134	1109	0.52	0.38
AMS 146	542	0.24	0.23
AMS 146	373	0.16	0.15
AMS 146	96	0.045	0.035
AMS 146	50	0.026	0.016
AMS 146	16	0.0081	0.0051
AMS 155	13	0.0067	0.0041
AMS 161	303	0.14	0.12
AMS 168	17	0.0077	0.0063

We measured adsorption isotherms at various temperatures and CO_2 partial pressures. In these screening tests, we used 22 and 60°C as the primary temperatures of interest. We then expanded these tests to N_2 and O_2 adsorption over the sorbent samples. In general all samples showed a reasonably high CO_2/N_2 and CO_2/O_2 selectivity. The adsorption kinetics are fast and the CO_2 uptake is rapid, indicating a high diffusion rate of 1.3×10^{-3} (D/r_c^2, 1/s). However, at very low surface areas i.e., < 10 m^2/g the rate of diffusion is too slow. A summary of CO_2 adsorption capacity at a CO_2 partial pressure of 0.15 atm along with the time taken to adsorb ½ of the CO_2 ($t_{1/2}$) are provided in Table 10.

Figure 19. Picture of TDA's constant volume apparatus.

Table 10. Summary of adsorption capacity and uptake rates from CVA measurements for selected samples prepared in this DOE PRDA project (DE-FE-0007580).

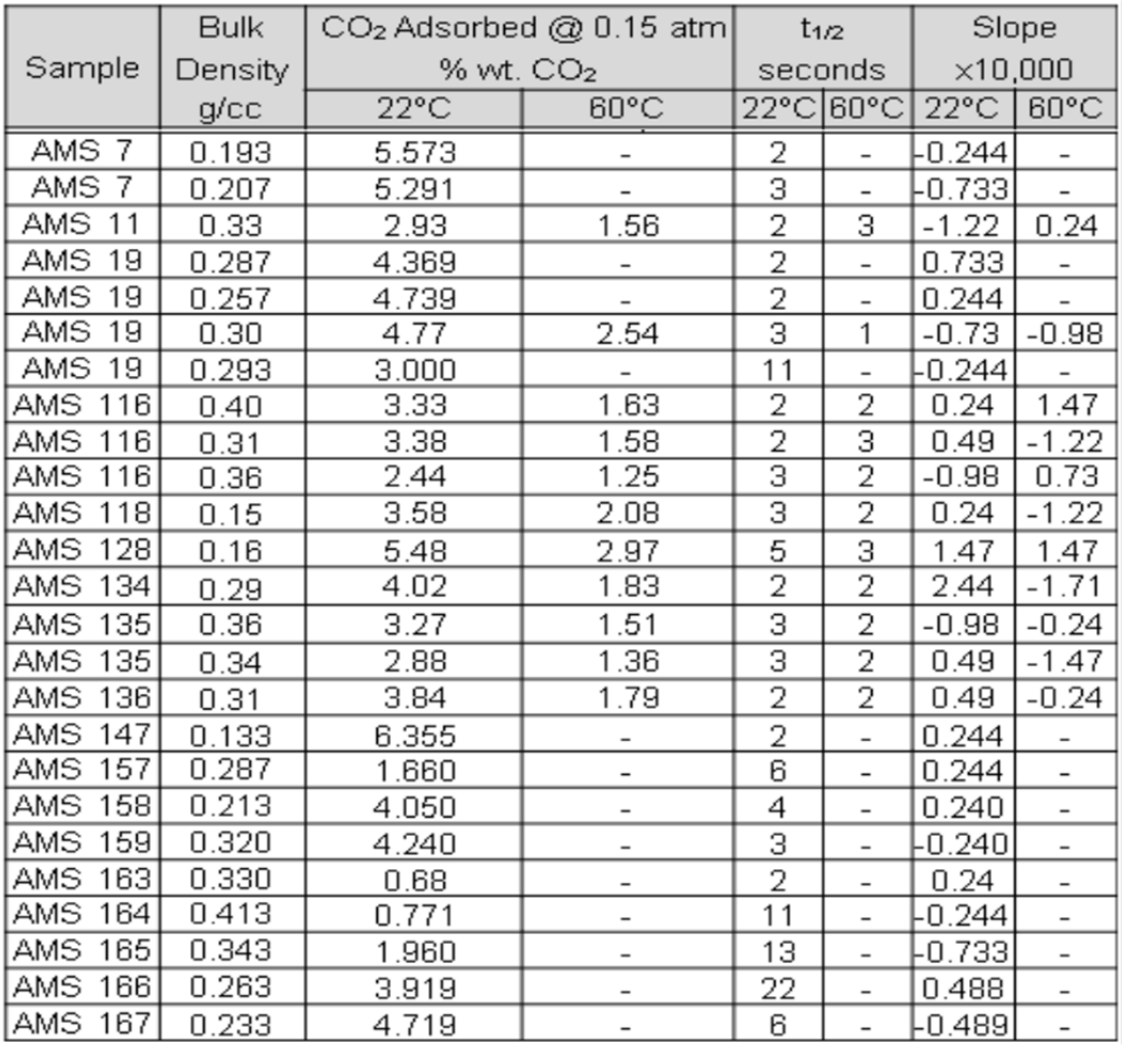

Sample	Bulk Density g/cc	CO_2 Adsorbed @ 0.15 atm % wt. CO_2 22°C	60°C	$t_{1/2}$ seconds 22°C	60°C	Slope ×10,000 22°C	60°C
AMS 7	0.193	5.573	-	2	-	-0.244	-
AMS 7	0.207	5.291	-	3	-	-0.733	-
AMS 11	0.33	2.93	1.56	2	3	-1.22	0.24
AMS 19	0.287	4.369	-	2	-	0.733	-
AMS 19	0.257	4.739	-	2	-	0.244	-
AMS 19	0.30	4.77	2.54	3	1	-0.73	-0.98
AMS 19	0.293	3.000	-	11	-	-0.244	-
AMS 116	0.40	3.33	1.63	2	2	0.24	1.47
AMS 116	0.31	3.38	1.58	2	3	0.49	-1.22
AMS 116	0.36	2.44	1.25	3	2	-0.98	0.73
AMS 118	0.15	3.58	2.08	3	2	0.24	-1.22
AMS 128	0.16	5.48	2.97	5	3	1.47	1.47
AMS 134	0.29	4.02	1.83	2	2	2.44	-1.71
AMS 135	0.36	3.27	1.51	3	2	-0.98	-0.24
AMS 135	0.34	2.88	1.36	3	2	0.49	-1.47
AMS 136	0.31	3.84	1.79	2	2	0.49	-0.24
AMS 147	0.133	6.355	-	2	-	0.244	-
AMS 157	0.287	1.660	-	6	-	0.244	-
AMS 158	0.213	4.050	-	4	-	0.240	-
AMS 159	0.320	4.240	-	3	-	-0.240	-
AMS 163	0.330	0.68	-	2	-	0.24	-
AMS 164	0.413	0.771	-	11	-	-0.244	-
AMS 165	0.343	1.960	-	13	-	-0.733	-
AMS 166	0.263	3.919	-	22	-	0.488	-
AMS 167	0.233	4.719	-	6	-	-0.489	-

Impact of Surface Area: We also optimized the surface area of the sorbent. We observed that keeping the sorbent formulation the same and changing the activation temperature and/or duration resulted in a sorbent sample with different pore size and/or chemical composition. Figure 20 shows the impact of surface area on our baseline sorbent formulation. The optimum surface area for this sample was around 400-450 m^2/g.

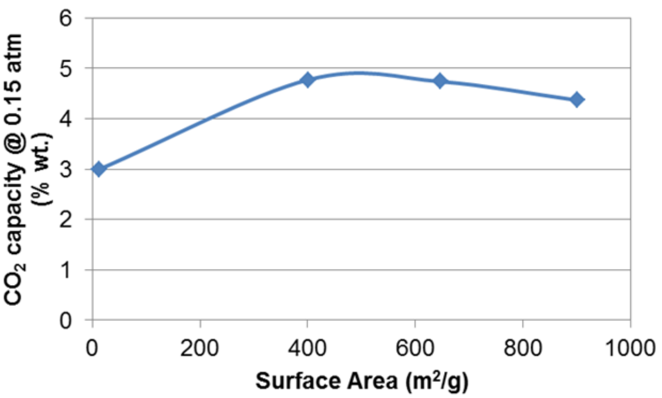

Figure 20. Impact of surface area on CO_2 adsorption capacity at 22°C and 0.15 atm for baseline sorbent.

Selectivity to CO_2:

We measured the adsorption isotherms using a constant volume apparatus. Figure 21 compares the CO_2, and N_2 adsorption capacity of our sorbent at 22°C. As expected from a physical adsorbent at 22°C, the CO_2 capacity increased from 6.4% wt. (lb CO_2 removed per lb of sorbent at CO_2 partial pressure of 0.15 atm) to 15.6% wt. (at a CO_2 partial pressure of 1 atm). The N_2 capacities at the same temperature were 1.4% and 2.2% wt. respectively, suggesting a reasonably high CO_2 selectivity and therefore the ability to separate CO_2 from N_2, the major flue gas component. Figure 22 shows the adsorption isotherms of CO_2 and N_2 at 22°C and 60°C. We also observed that the adsorption kinetics are fast and the CO_2 uptake is rapid, indicating high diffusion rates of 1.3 x 10^{-3} (D/r_c^2, 1/s). We fitted the adsorption data to a Langmuir-Freundlich isotherm model. The fitted model parameters are summarized in Table 11.

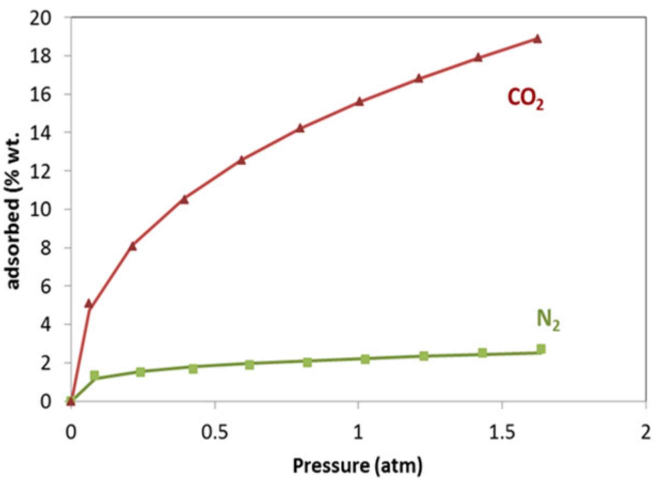

Figure 21. Adsorption isotherms on TDA's CO_2 sorbent at 22°C.

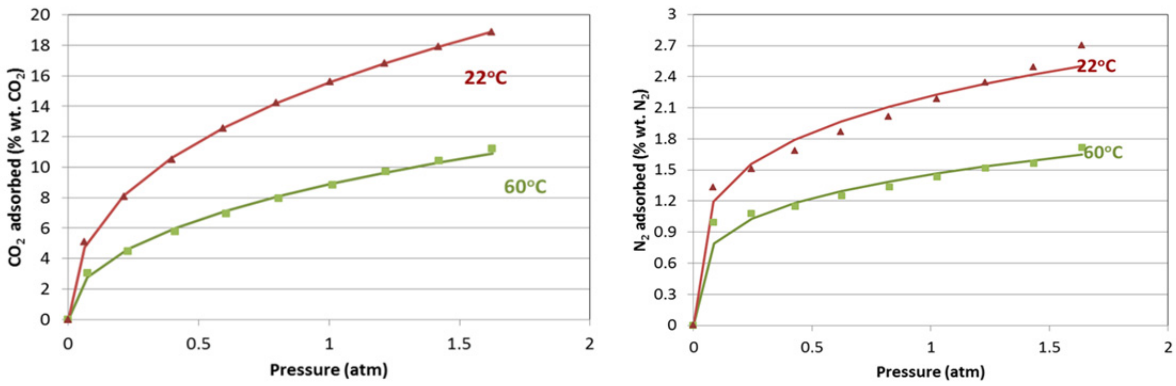

Figure 22. CO_2 and N_2 adsorption isotherms on TDA's sorbent at 22°C and 60°C.

Table 11. Langmuir-Freundlich isotherm model parameters.

$$q = \frac{q_s B P^n}{1 + B P^n} \qquad q_s = k_1 e^{k_2/T} \qquad B = k_3 e^{k_4/T}$$

	k_1	k_2	k_3	k_4	n	$-\Delta H$ (kcal/mol)
CO_2	28.0	1.63E-08	6.11E-04	1613.4	0.46	3.87
N_2	317.0	6.43E+02	6.37E-05	439.6	0.25	1.53

Using the isotherm data, we also carried out iso-steric calculations to estimate the heat of adsorption of CO_2 onto the sorbent media. We calculated a heat of adsorption of 3.9 kcal/mol for CO_2 which indicates a relatively low energy interaction, which in turn will require relatively small energy input to regenerate the sorbent. We also calculated the heat of adsorption of N_2 as 1.5 kcal/mol. This lower adsorption energy suggests that the sorbents affinity to CO_2 is much greater than that for N_2.

4.3 Task 3. Sorbent Evaluation

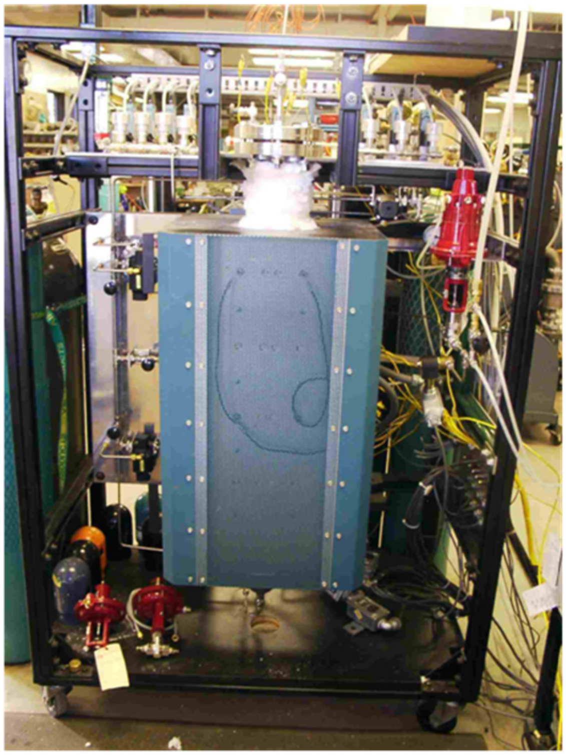

Figure 23. Test apparatus.

<u>Test Apparatus:</u> We modified an existing testing apparatus to evaluate the sorbent's performance in a bench-scale flow system under representative conditions (Figure 23). The apparatus was built at TDA for the specific purpose of measuring the activity of sorbents (with minimal dead volume in the reactor ullage space and in the manifolds). In this system, the desired gas mixtures were directed into a fixed-bed micro-reactor that houses granules or pellets of the sorbent. All gas flows are controlled with electronic mass flow controllers. A Waters pump is used to introduce water. After mixing in a manifold, the feed gas mixture is then directed into the reactor. A valve system allows the gases to bypass the reactor and flow directly to the analytical system for accurate measurement of the feed gas composition. In typical tests, the sorbent reactor is loaded with 100 mL of 4-20 mesh sorbent. The reactor has three thermocouple ports to monitor the sorbent bed temperature. A back pressure regulator is used to control the adsorption pressure (as needed). After exiting the reactor, the CO_2 content of the stream are monitored by an on-line NOVA Multi-gas Analyzer and Vaisala CO_2 and humidity probes. Continuous analysis of CO_2 allows us to monitor breakthrough gas concentrations and to measure a total CO_2 adsorption capacity.

The apparatus is fully automated using a LabVIEW control system and can run without an operator for long periods of time, including overnight. The LabVIEW system controls the test conditions, logs the analytical data, and also safely shut down the apparatus in case of a malfunction. We used 15% CO_2 on a dry basis for the bench-scale evaluations (water content was 2.4% by vol.).

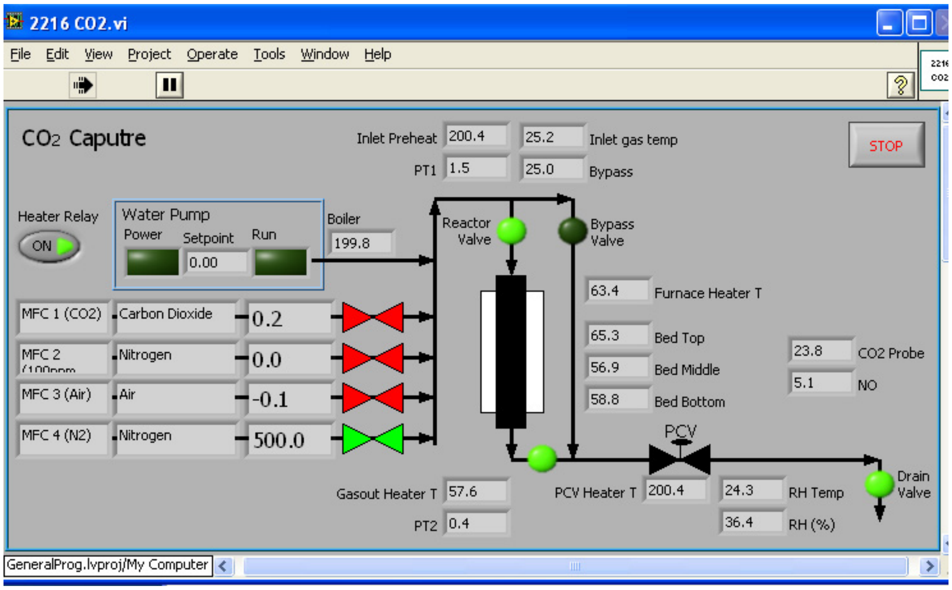

Figure 24. LabVIEW screen shot of the test apparatus.

4.3.1 Parametric Tests

Following the initial screening tests of the selected sorbents we investigated the impact of important operating parameters on the CO_2 capacity. These parametric tests also provided valuable information that we used to identify the optimum operating conditions.

Effect of Temperature

We evaluated the impact of adsorption temperature on the CO_2 capacity of the sorbent. As expected, the capacity decreases with increasing temperature (Figure 25).

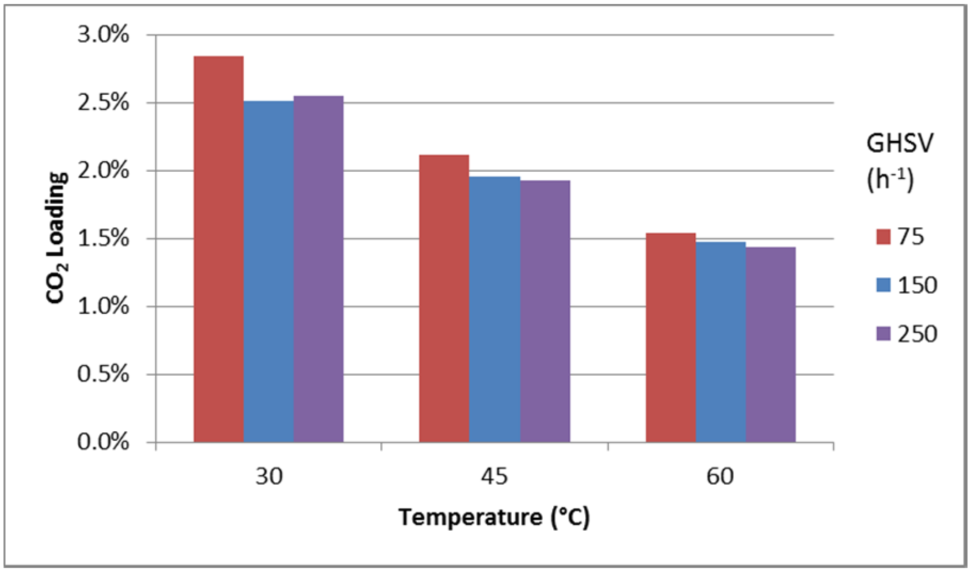

Figure 25. Effect of adsorption temperature at different GHSV. CO_2 = 15% by vol., dry simulated flue gas.

<u>Effect of Space Velocity</u>

Figure 25 shows the effect of the space velocity. As expected, lower space velocity resulted in slightly higher capacities. At higher adsorption temperatures the impact of the space velocity is lower. Although it is desirable to adsorb and regenerate the sorbent quickly (i.e., at higher space velocity) to achieve a higher sorbent utilization and minimize the amount of sorbent inventory that must be in place to complete the cycle, the use of high volumes of gas to support the regeneration process is not feasible since it increases the consumption of steam (a steam sweep is planned to recover the CO_2, because after condensation a high purity CO_2 stream can be recovered for pipeline transportation to the site of use or sequestration). We took this trade-off into account in selecting the regeneration gas flow rate in our process design.

<u>Impact of Moisture</u>

We ran several experiments in our flow apparatus with dry and wet flue gas to assess the impact of moisture. At 30°C, introduction of 2.4% vol. of water into the flue gas reduced the CO_2 capacity of the sorbent from 2.85% wt. to 2.45% wt. (Figure 26). This decline in capacity was not permanent; as the water is eliminated from the flue gas the capacity was recovered. We also observed that the sorbent maintained a stable capacity under cycling in the presence of moisture.

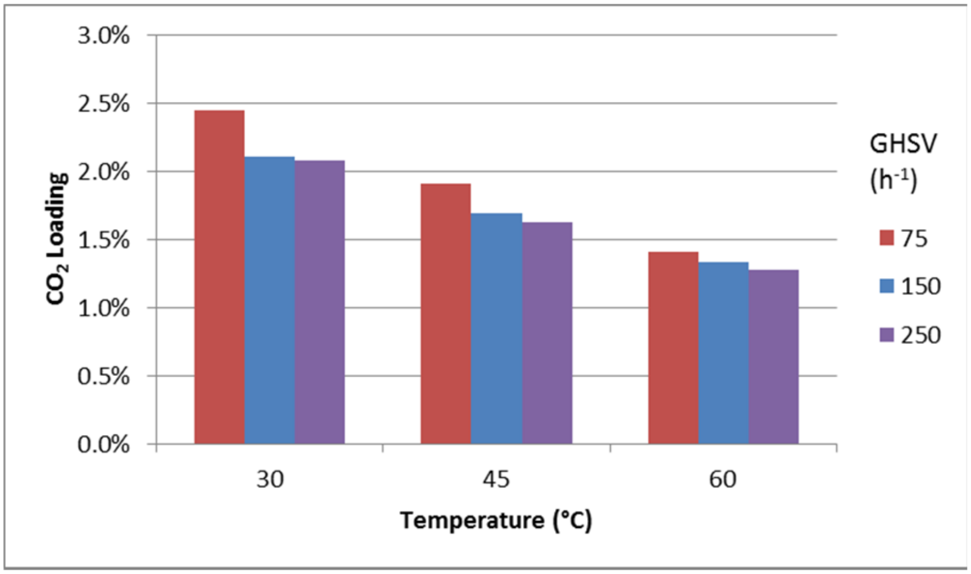

Figure 26. Impact of the presence of moisture (2.4% H_2O).

4.3.2 Vacuum Swing Adsorption Cycles

We carried out vacuum swing adsorption (VSA) cycle tests in our two-bed VSA system. Figure 28 shows the Process and Instrumentation Diagram for the system. The system consists of two sorbent beds whose volume can be adjusted using a spring loaded screens from 100-500 mL each. The two beds cycle between adsorption with feed gas flowing through the bed and desorption in counter current direction with the bed under vacuum using the automated solenoid valves (V-4104 and V-4105). The system has a vacuum pump (P-4201, Edwards Model No. RV3) and a needle valve (V-4201) to get the beds to vacuum during desorption. Check valves (V-4106 and V-4107) at the exit side of the reactors prevent product gas from back flowing into the reactors. An adjustable orifice (O-4101) is used to control the countercurrent product purge flow. The system can undergo rapid adsorption-desorption cycles and the product flow and concentration will be measured using a flowmeter (FT-4101, Porter Model No. 111) and a 0-20% Vaisala CO_2 probe (O2E-4101). There are Omega thermocouples, pressure transducers and Vaisala humidity sensors to measure the temperature, pressure and humidity of the inlet and outlet gas to the beds. Each of the reactors also has a thermocouple and pressure transducer to log the pressure and temperature in the sorbent beds as it undergoes adsorption-desorption cycles. The air flow into the system is controlled using a mass flow controllers (FTC-4101, FTC-4102, or FTC-4103, Porter Model No. 251 and Model No. 201). Pressure will vary up to 26 psia in the system, controlled using a downstream needle valve on the product line (not shown in the P&ID). An HPLC pump will deliver water at up to 1.5 ml/minute for humidification of the gas stream. All system lines are stainless steel to prevent any degassing under vacuum. Electronic control is via a National Instruments LabVIEW system. LabVIEW directly controls the flow of feed gas mixture into the system through the mass flow controllers FTC-4101, FTC-4102, or FTC-4103. Additionally, LabVIEW utilizes a PID algorithm to regulate the pump flow rate and maintain the desired humidity level in the system. Temperature and pressure will be measured and recorded directly by the LabVIEW control system. The safety monitoring, startup, shutdown procedures and sensor measurements are automated in LabVIEW using sequencers allowing for unattended operation. Figure 27 shows a picture of the test setup.

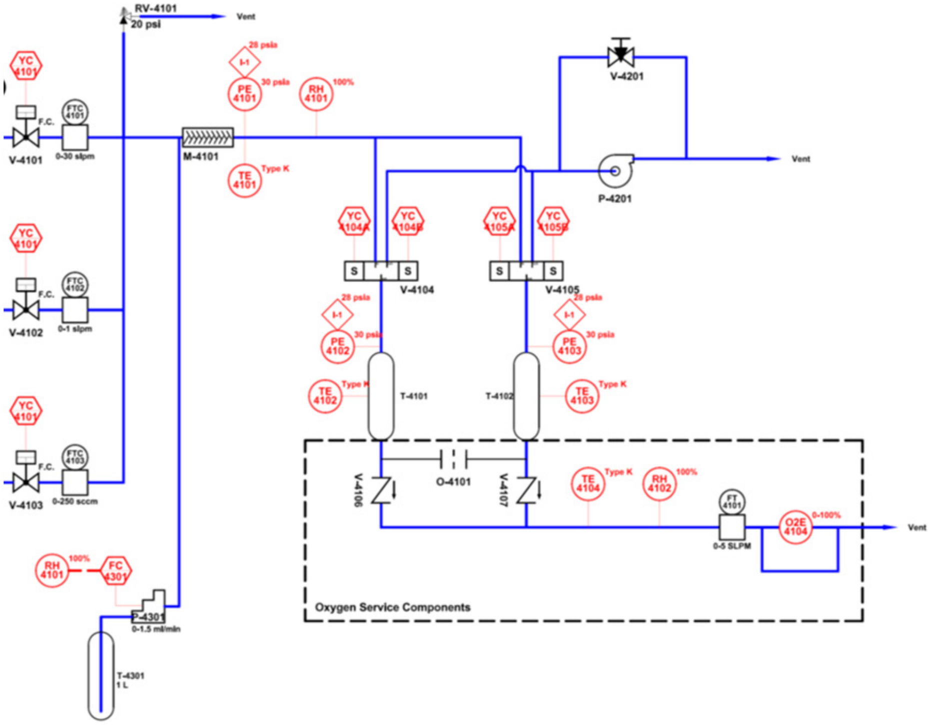

Figure 28. P&ID of TDA's two bed VSA cycle test system.

We carried out multiple vacuum swing adsorption cycles with our sorbent in the two-bed VSA system. We loaded about 250 mL sorbent into each of the reactor. We initially carried out VSA cycles using simulated flue gas (15% CO_2 in nitrogen) without purge and at a desorption pressure of 0.1 psia. The Sorbent achieved a stable capacity of 3.2% wt. CO_2 with more than 95% CO_2 removal. We introduced moisture into the flue gas stream resulting in a wet flue gas stream that contained 9,000 ppmv H_2O to saturated amounts at 22^{o}C. We slowly increased the desorption pressure to 3 psia in 1 psia increments, at the same time we also introduced some product nitrogen purge during desorption to simulate the steam purge that will be used in the actual VSA process. The sorbent achieved more than 1.8% wt. CO_2 capacity while capturing more than 90% CO_2 when desorbing at 3 psia. The sorbent also maintained its performance over 560 vacuum swing cycles. Figure 29 shows the summary of the vacuum swing cycling

Figure 27. Picture of TDA's two bed VSA cycle test system.

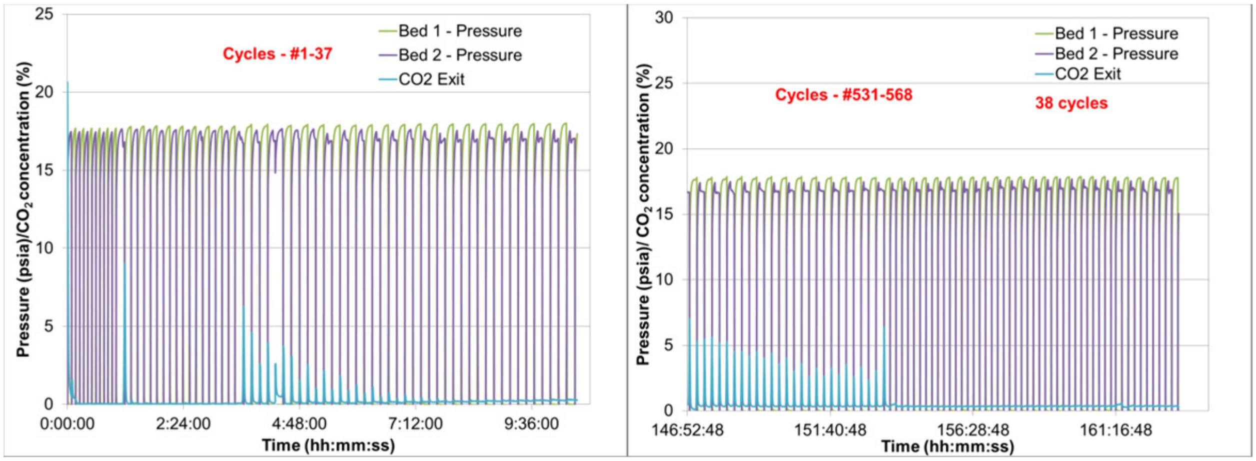

Figure 29. Vacuum swing cycling test results with TDA sorbent (AMS-19) in a two bed VSA system carried out as part of DOE PRDA project (DE-FE-0007580) showing the data from the initial and final few cycles. T = 22°C; half-cycle time = 4-15 min; adsorption pressure = 17.3 psia; desorption pressure = 0.1-3 psia; Purge/Feed ratio = 0-0.35; CO_2 capacity = up to 3.2% wt. CO_2; CO_2 removal > 90%; GHSV = 150 – 297 h^{-1}; Simulated flue gas containing 15% CO_2 in N_2, H_2O = 0-2.7% by vol., Purge gas = N_2 product.

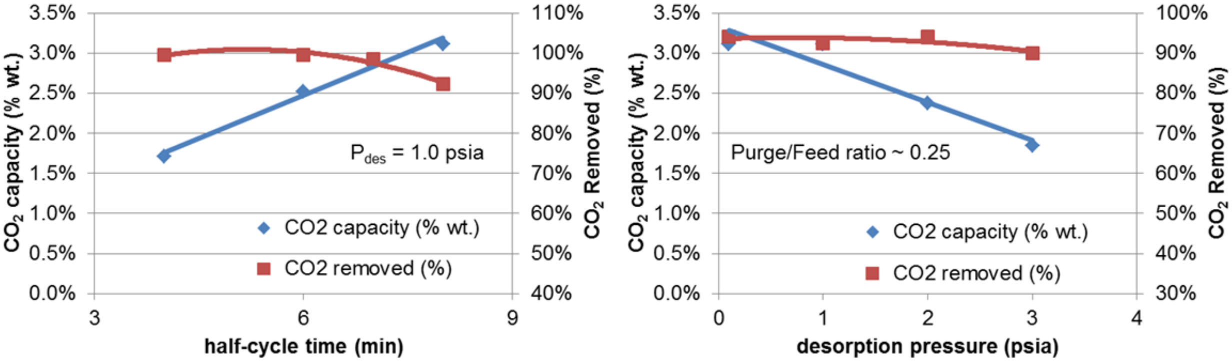

Figure 30. Impact of cycle time and desorption pressure on the CO_2 capacity and removal efficiency for TDA sorbent(AMS-19).

results showing the sorbent performance over 560 cycles. Figure 30 shows the impact of the cycle time and desorption pressure on CO_2 capacity and removal efficiency.

4.4 Task 4. Process Design and Modeling

In this task we (UCI in collaboration with TDA) first completed the modeling of the TDA's CO_2 capture system based on our low cost high capacity CO_2 sorbent integrated with a pulverized coal (PC) fired power plant in Aspen Plus^{TM}. Hence as part of this task we first optimized the design of our CO_2 capture process i.e., we explored various process options such as cooling of flue gas to sub ambient temperatures, regenerations using vacuum swing and/or thermal swing.

4.4.1 Flue gas Conditioning

Temperature and Vacuum Swing with Hydrogen Heat Pump Heat Source – flue gas at 7°C
In this process scheme we cooled the flue gas to 7°C using an ammonia refrigeration loop and the sorbent bed during adsorption is at 24°C and the regenerations are carried out at 89°C under vacuum (0.33 atm) with the sorbent being heated and cooled using H_2 heat pump. The parasitic energy loss for this process scheme is 27.91% compared to 23.2% for the amines.

Temperature and Vacuum Swing with Ammonia Heat Pump Heat Source – flue gas at 7°C
In this process scheme we cooled the flue gas to 7°C using an ammonia refrigeration loop and the sorbent bed during adsorption is at 24°C and the regenerations are carried out at 89°C under vacuum (0.33 atm) with the sorbent being heated and cooled using NH_3 heat pump. The parasitic energy loss for this process scheme is 21.9% compared to 23.2% for the amines.

Isothermal Vacuum Swing with Ammonia Cooling – flue gas at 7°C
In this process scheme we cooled the flue gas to 7°C using an ammonia refrigeration loop and the sorbent bed during adsorption is at 24°C and the regenerations are carried out at 30°C (i.e., heat from adsorption) under vacuum (0.33 atm). The working capacity of the sorbent is 5.6% wt. CO_2. The parasitic energy loss for this process scheme is 21.8% compared to 23.2% for the amines.

Isothermal Staged Vacuum Swing with Ammonia Cooling – flue gas at 7°C
In this process scheme we cooled the flue gas to 7°C using an ammonia refrigeration loop and the sorbent bed during adsorption is at 24°C and the regenerations are carried out at 30°C (i.e., heat from adsorption) under vacuum (0.33 atm). The vacuum is achieved using a staged vacuum pump. The parasitic energy loss for this process scheme is 18.8% compared to 23.2% for the amines. We can expect similar benefits in the temperature swing cases though they will still have a higher energy penalty compared to isothermal process.

Temperature and Vacuum Swing with Extraction Steam Heat Source – flue gas at 58°C
In this process scheme we did not cool the flue gas and the sorbent bed during adsorption is at 68°C and the regenerations are carried out at 120°C under staged vacuum (0.15 atm) with the sorbent being heated and cooled using extracted steam from steam cycle. The parasitic energy loss for this process scheme is 24.8% compared to 23.2% for the amines.

Isothermal Staged Vacuum Swing with Ammonia Cooling – flue gas at 20°C
In this process scheme we cooled the flue gas to 20°C using an ammonia refrigeration loop and the sorbent bed during adsorption is at 24°C and the regenerations are carried out at 30°C (i.e., heat from adsorption) under vacuum (0.023 atm). The working capacity of the sorbent is 2.1% wt. CO_2. The vacuum is achieved using a staged vacuum pump. The parasitic energy loss for this process scheme is 18.1% compared to 23.2% for the amines.

Isothermal Staged Vacuum Swing with Iso-butane Heat pump – flue gas at 70°C
In this process scheme we did not cool the flue gas and the sorbent bed is maintained at 70°C during adsorption and regeneration using an isobutene heat pump. The regenerations are carried out at 70°C under vacuum (0.2 atm). The vacuum is achieved using a staged vacuum pump. The working capacity of the sorbent is 1.4% wt. CO_2. The parasitic energy loss for this process scheme is 15.9% compared to 23.2% for the amines.

This analysis shows that even though we can improve the working capacity of the sorbent by cooling the flue gas during adsorption or by heating the sorbent bed during regeneration, the parasitic energy loss associated with cooling flue gas and/or heating the sorbent bed is large and the best process scheme is when the sorbent bed is maintained under isothermal conditions using heat exchange for e.g., using an iso-butane heat pump to maintain the sorbent bed at 70°C (slightly above the flue gas temperature) and using a vacuum of 0.2 atm. This scheme has significantly lower parasitic energy loss than that of amines. Hence, we chose this scheme for the detailed process modeling analysis that was carried out by UCI in AspenPlus^{TM}.

4.4.2 Process Modeling Results – Budget Period 1

UCI first completed the modeling of the coal fired power plant with amines based post combustion CO_2 capture system. Aspen Plus^{TM} was utilized in developing a steady state thermodynamic model of a Subcritical PC fired power plant with CO_2 capture described in DOE/NETL Report - 2010/1397, “Cost and Performance Baseline for Fossil Energy Plants - Volume 1: Bituminous Coal and Natural Gas to Electricity,” Revision 2, November 2010. The nominal net output is maintained at 550 MW at a net plant thermal efficiency of 26.2 percent (HHV basis) while utilizing Illinois No. 6 bituminous coal. The plant includes wet FGD system producing gypsum and a baghouse for particulate removal. The amine CO_2 capture facility, including CO_2 compression, accounts for approximately 58% of the auxiliary plant load. The cooling water system (pumps and cooling tower fans) accounts for over 13% of the auxiliary load, largely due to the high cooling water demand of the amines based CO_2 capture facility. Details of this plant may be found in the Case 10 of the DOE study. Next, the model was modified by replacing the amines based CO_2 capture system with TDA’s CO_2 capture system while keeping the net power output at 550 MW_e. Altogether, three options for Subcritical PC plants were evaluated: no-CO_2-capture option, AMINE-CO_2-capture option and VSA-CO_2-capture option. All three cases (or baseline cases) were developed in Aspen Simulation.

- Case 9 (No-CO_2 capture) and Case 10_AMINE well match the performance data provided in DOE report. All stream data (pressures and temperatures) and equipment data (powers) were well matched with data from DOE report. These two cases are used as baseline subcritical PC plant without CO_2 capture and subcritical PC plant with AMINE CO_2 capture.
- A VSA CO_2 capture process was developed in Aspen Plus based on updated data provided by TDA. This process is specifically designed for post-combustion CO_2 capture system, and a butane heat pump loop is designed for heat rejection and absorption of solid absorbents.
- Case 10A_VSA and Case 10B_VSA are subcritical PC plants with VSA CO_2 capture, developed by replacing AMINE CO_2 capture option with TDA’s VSA CO_2 capture option. Case10A_VSA at a net efficiency of 29.6% has the same higher LP steam turbine efficiency as Case 9 while Case10B_VSA at a net efficiency of 29.2% has the same lower LP steam turbine efficiency as the AMINE case. The AMINE case has a relatively smaller steam turbine and thus the lower steam turbine efficiency is justified for that case but for the VSA case, since no steam is extracted from the steam cycle, the higher efficiency is justifiable. Thus, it is recommended that Case10A_VSA should be considered as representative of the VSA based case.
- TDA’s VSA option shows a significantly higher net thermal efficiency over the AMINE option, 29.6% (or even 29.2%) vs. 26.2%.
- The butane heat pump loop consumes a large amount of power (11.66 MW); 6% of total power consumption. Other design options will be investigated as part of Task 9.

Table 12. Summary of results from UCI's Aspen modeling of TDA's post combustion CO_2 capture process.

	Case 9 (No-CO_2 Capture, DOE Report Data)	Case 9 (No-CO_2 Capture, Aspen)	Case 10 AMINE (DOE Report Data)	Case 10 AMINE (Aspen)	Case 10A VSA (Aspen) with LP ST same eff as Case 9	Case 10B VSA (Aspen) with LP ST same eff as Case 10 AMINE
GROSS POWER GENERATED (AT GENERATOR TERMINALS), KWE						
STEAM TURBINE POWER	582600	582600	672700	672700	814185	805977
AUXILIARY LOAD SUMMARY, KWE						
FEED HANDLING	4370	4370	6090	6090	6090	6090
ASH HANDLING	570	570	800	800	800	800
PRIMARY AIR FANS	1400	1400	1960	1960	1960	1960
FORCED DRAFT FANS	1780	1780	2500	2500	2500	2500
ID FANS	7540	7540	12080	12080	12080	12080
SCR POWER	50	50	70	70	70	70
BAGHOUSE POWER	70	70	100	100	100	100
FGD POWRE	3180	3175	4470	4466	4466	4465
CO2 REMOVAL POWER	--	--	22400	22084	--	--
SORBENT CONVEYING POWER	--	--	--	--	9147	9147
CO2 COMPRESSION POWER	--	--	48790	48791	133406	133406
SCELLANEOUS BALANCE OF PLANT	2000	2000	2000	2000	2000	2000
STEAM TURBINE AUXILIARIES	400	400	400	400	484	479
CONDENSATE PUMPS	890	890	700	700	1253	1253
CIRCULATING WATER PUMPS	5250	5250	11190	11190	9647	9647
GROUND WATER PUMPS	530	530	1020	1020	926	926
COOLING TOWER	2720	2229	5820	5649	4983	4983
TRANSFORMER LOSSES	1830	1830	2350	2350	2844	2816
TOTAL AUXILIARIES, KWE	32580	32084	122740	122250	192756	192721
NET POWER, KWE	550020	550516	549960	550451	621430	613256
% NET PLANT EFFICIENCY, % HHV	36.8	36.81	26.2	26.18	29.56	29.17
NET HEAT RATE						
KJ/KWH	9788	9779	13764	13752	12181	12343
BTU/KWH	9277	9268	13046	13034	11545	11699
CONDENSER COOLING DUTY						
10^6 KJ/H	2566	2515	2034	2034	3623	3623
10^6 BTU/H	2432	2384	1928	1927	3434	3434
CONSUMABLES						
AS-RECEIVED FEED						
KG/H	198391	198392	278956	278957	278957	278957
LB/H	437378	437378	614994	614994	614994	614994
LIMESTONE SORBENT FEED						
KG/H	19691	19944	28404	28831	28831	28831
LB/H	43410	43969	62618	63561	63561	63561
CO_2 SORBENT FEED						
SORBENT MAKEUP KG/H	--	--	--	--	182.78	182.78
SORBENT MAKEUP LB/H	--	--	--	--	402.96	402.96
SORBENT CIRCULATION KG/H	--	--	--	--	41958347	41958347
SORBENT CIRCULATION LB/H	--	--	--	--	92502211	92502211
FINES REMOVAL KG/H	--	--	--	--	182.78	182.78
FINES REMOVAL LB/H	--	--	--	--	402.96	402.96
THERMAL INPUT						
KWT HHV	1495379	1495381	2102643	2102644	2102644	2102644
RAW WATER USAGE						
M^3/MIN	22.3	24.76	42.5	42.44	38.5	38.5
GPM	5896	6541.678	11224	11212	10172	10171
CARBON CAPTURED, %	0	0	90	90	90	90

4.5 Task 5. Sorbent Scale-up

The process for making the sorbent consists of two-three thermal steps (Figure 31). In the first step the raw materials are heated in trays at 220°C in air to convert them into a char. The more critical step is the carbonization of the char into the product sorbent. In this step, the char is heated under a flow of nitrogen up to 900°C this may be followed by a higher surface area to further increase the surface area.

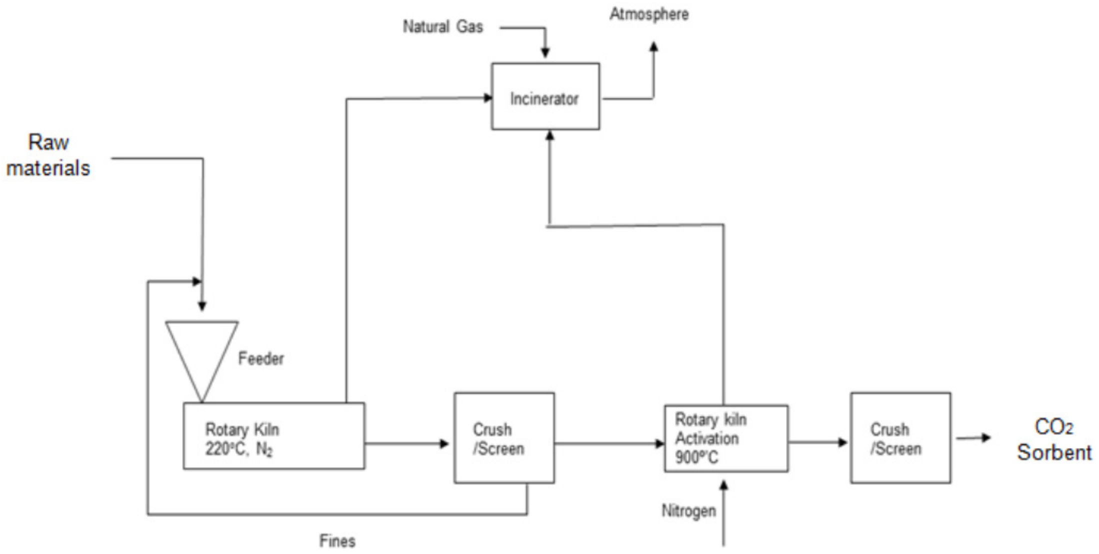

Figure 31. Simplified process flow diagram illustrating the CO_2 sorbent production process.

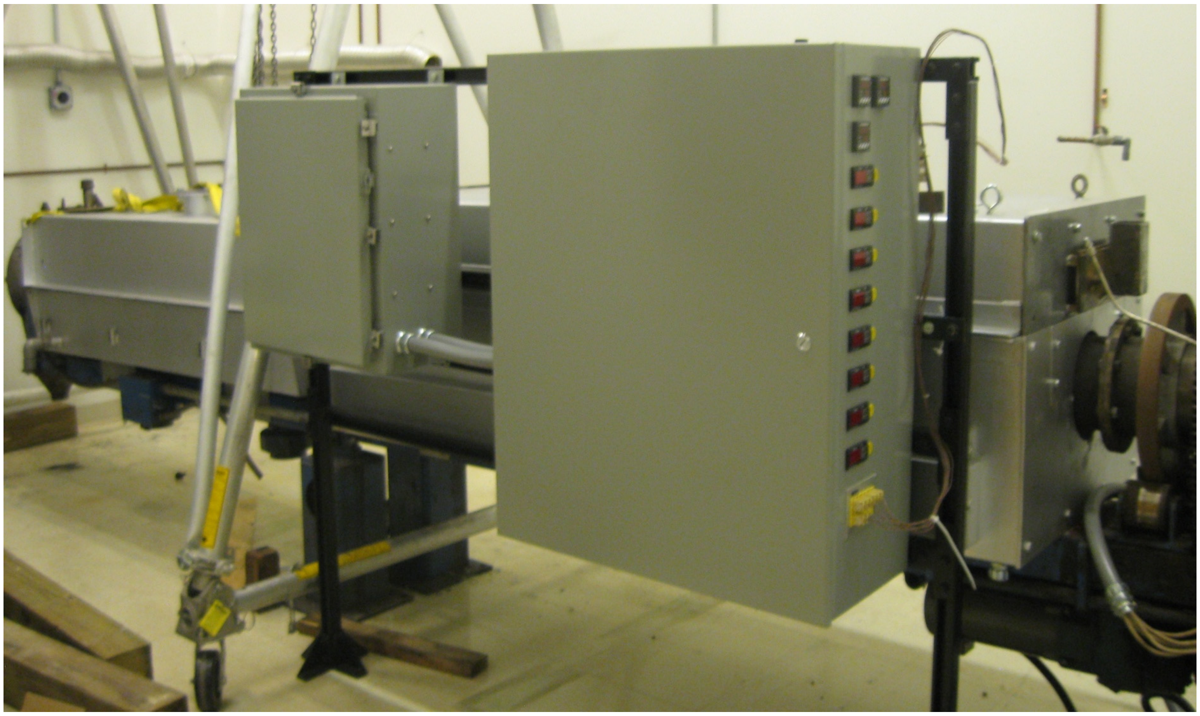

Figure 32. TDA's 7" rotary kiln.

Our initial samples for this project were made as granular carbon in ceramic trays using a 3” diameter Lindberg tube furnace and our sample sizes were limited to <50 g. We then scaled up production of the carbon to multi-kilogram quantities (up to 5 L per day), using our 7” continuous rotary kiln from Bartlett and Snow (Figure 32). This continuous rotary kiln was installed in our 27,000 sq. ft. Table Mountain facility located in Golden, CO as part of a DOE ARRA Phase II project (DE-SC0003582) to scale-up production of our ultracapacitors carbons. The rotary kiln is electrically heated and has a 7” Inconel tube that can be heated up to 1100°C. The carbon precursor is fed into the kiln using a single screw feeder as shown in Figure 33. It has a computer control system using Labview software. . This permits continuous operation (24 h/day) without direct supervision. It has all the safety features needed to operate in safely and an afterburner to process the off gases in an environmentally sound manner. Figure 34 shows the exhaust gas treatment section on the kiln exhaust. We used this pilot plant in this project to rapidly scale-up production of the CO_2 sorbents. The crush strengths of the samples were increased more than 3 folds compared to samples produced with bench-scale equipment, and the sorbent production was optimized to produce both 1/16” pellets and 1/8” pellets. This was accomplished by forming the pellets prior to carburization, which also improved the sorbent yield. These sorbents were then evaluated in bench-scale test system, a TDA universal testing apparatus located in the East Wheat Ridge building, to validate their performance. Figure 35 shows the impact of the temperature on the scaled-up sorbent. The sorbents achieved 1.5% wt. breakthrough (at 2% vol. CO_2 in the exit gas) capacity and 5.3% wt. saturation capacity (at 15.8% vol. CO_2 in the exit). These scaled up sorbents had a bulk density of 0.28 kg/L.

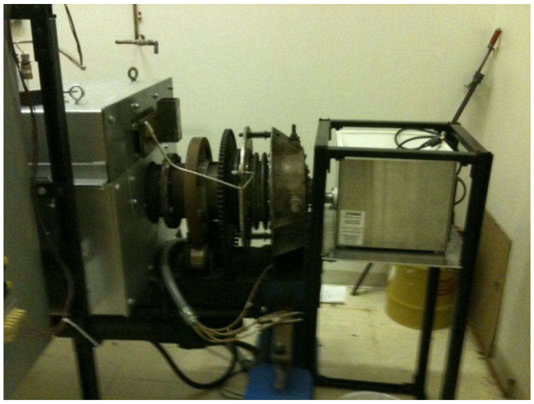

Figure 33. Screw feeder for rotary kiln.

Figure 34. Exhaust gas treatment.

In 2015, as part of another funded project (DE-SC0006239), where we worked on further improvements to the post combustion CO_2 sorbents that were initially developed and scaled-up in this project, we were able to further increase the density of the carbon sorbent to 0.45-0.5 g/cc by carrying out high pressure extrusion of the green pellets. The improved bulk density resulted in higher volumetric CO_2 adsorption capacity and increased sorbent yield during production. Figure 36 shows the comparison of the baseline (scaled up sorbent from 2013-14, bulk density =0.28 kg/L) against the improved (scaled-up sorbent from 2015, bulk density = 0.46 kg/L) sorbent. The improved sorbents from 2015 achieved more than 2x higher volumetric loading both at breakthrough and saturation.

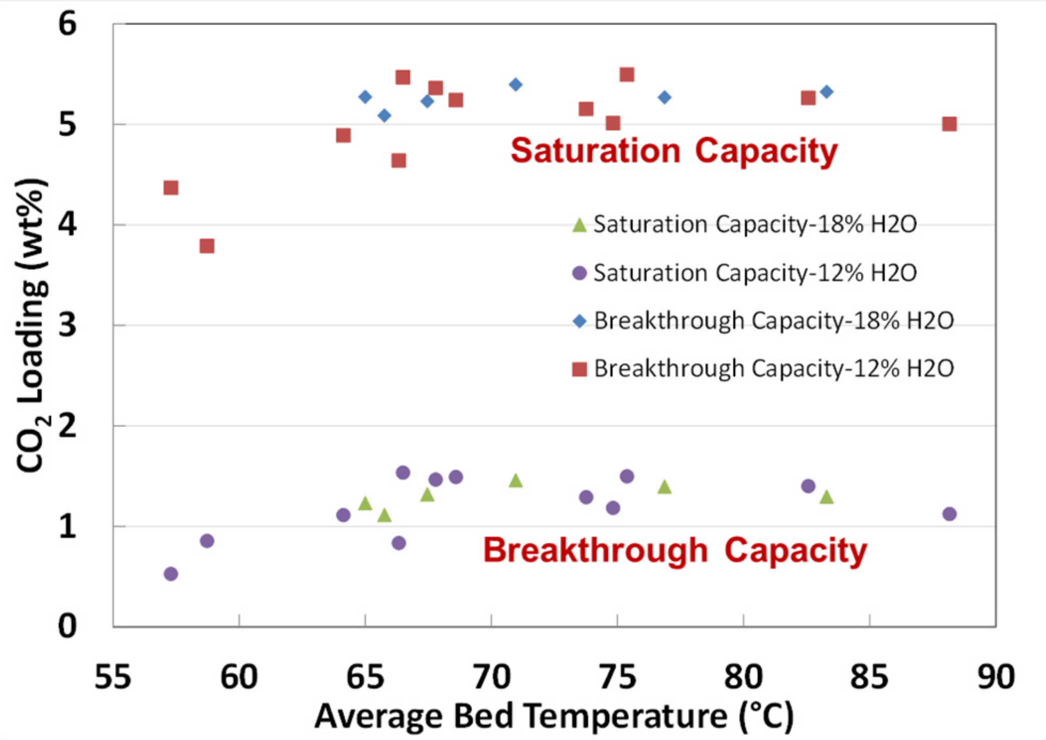

Figure 35. Impact of temperature on CO_2 breakthrough and saturation capacity at different temperatures. T=68°C, P=16 psia, GHSV= 2,000h^{-1}, 16% CO_2, 12-18% H_2O, simulated flue gas.

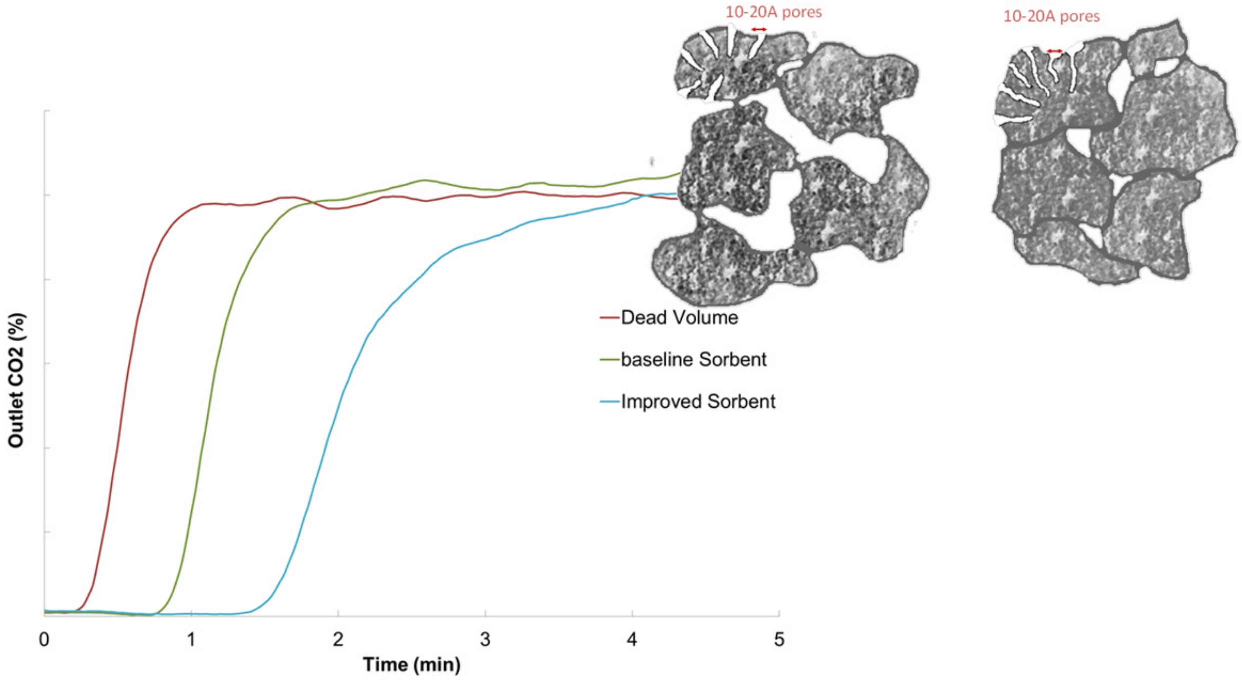

Figure 36. CO_2 breakthrough from fixed bed adsorption tests CO_2 = 10%, H_2O = 2% by vol. in N_2 (simulated flue gas).

4.6 Task 6. Long-term Sorbent Cycling

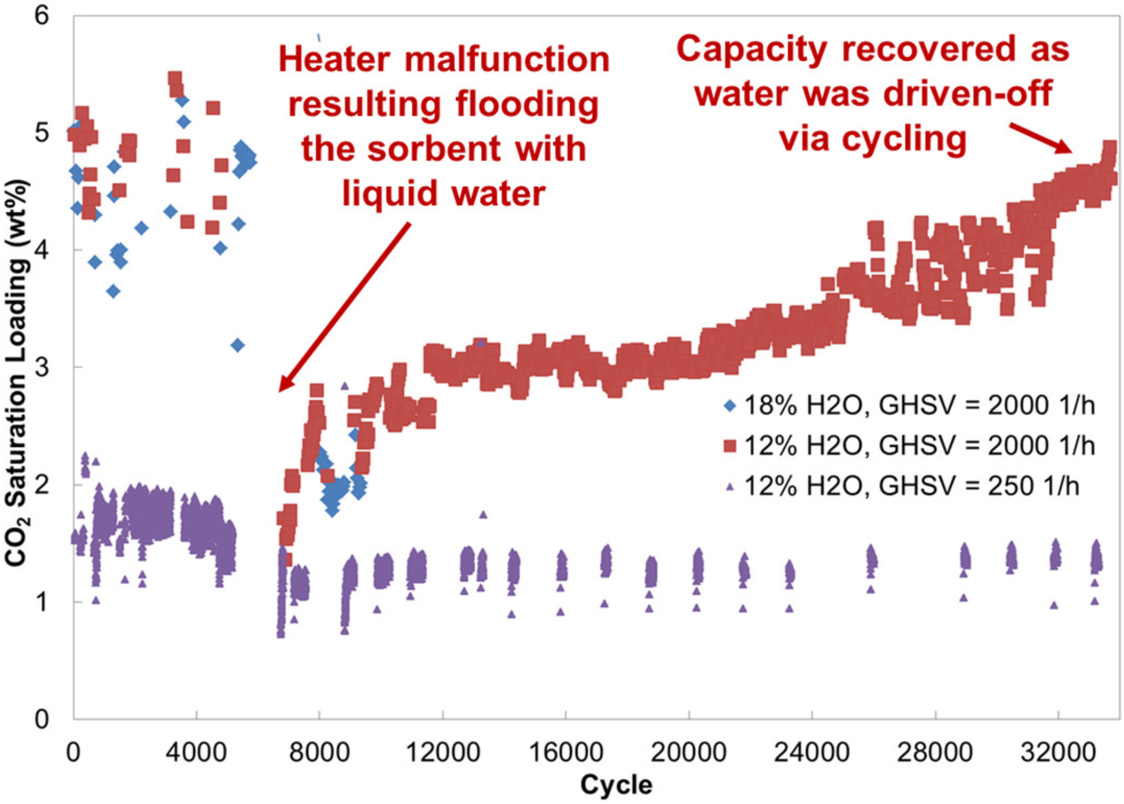

Figure 37. CO_2 Saturation loading, multiple cycle evaluation. T = 58-70°C, P_{ads}= 14-18 psia, P_{des}= 3 psia, GHSV= 250/2,000 h^{-1} CO_2 = 15%, H_2O = 12-18% by vol. in simulated flue gas.

We carried out long-term vacuum swing adsorption (VSA) cycling experiments under representative conditions using simulated flue gas. We had proposed running at least 5,000 cycles, and successfully completed over 34,000 cycles. The first 5,000 cycles were carried out as part this DOE contract (DE-FE-0007580). With funding from another DOE sponsored SBIR Phase II project (DE-SC0006239) we extended the cycling tests to 34,000 cycles which is approximately 1/10th of the minimum expected life for the sorbent at 3 years and 4.5 min full cycle time. In these tests we changed the various parameters such as the adsorption temperature, space velocity and water levels. We observed a typical working capacity of 3-4% wt. CO_2 while adsorbing CO_2 at 65°C and regenerating at the same temperature under vacuum swing. The sorbent has high CO_2 selectivity in the presence of up to 15%vol. moisture. Between 5,000 and 6,000 cycles the heaters in the experimental system malfunctioned, which flooded the sorbent bed with liquid water. We used this process upset to verify if the liquid water can be driven off via simple vacuum swing cycling. The sorbent recovered following this major upset and achieved a stable working capacity over the 34,000+ cycles as shown in Figure 37

4.7 Task 7. Design of Moving Bed Reactors

B&W in collaboration with TDA carried out the detailed design of the sorbent reactors for TDA's Vacuum swing adsorption system (Milestone 2-2). We looked at both moving bed and the fixed bed options. The system consists of 4 parallel trains of adsorption/desorption reactors that undergoes VSA cycles in the case of moving bed system. In the case of the fixed bed system we have 4 reactors in total that undergo vacuum swing cycles. The P&ID for the moving bed and fixed bed reactor systems are shown in Figure 38 and Figure 39, respectively. Each of the reactor designs have their own merits and challenges for e.g., in the case of moving beds the adsorption reactors need not be rated for vacuum while it would have the challenge of circulating a large quantity of the sorbent. In the fixed bed all the reactors need to be rated for

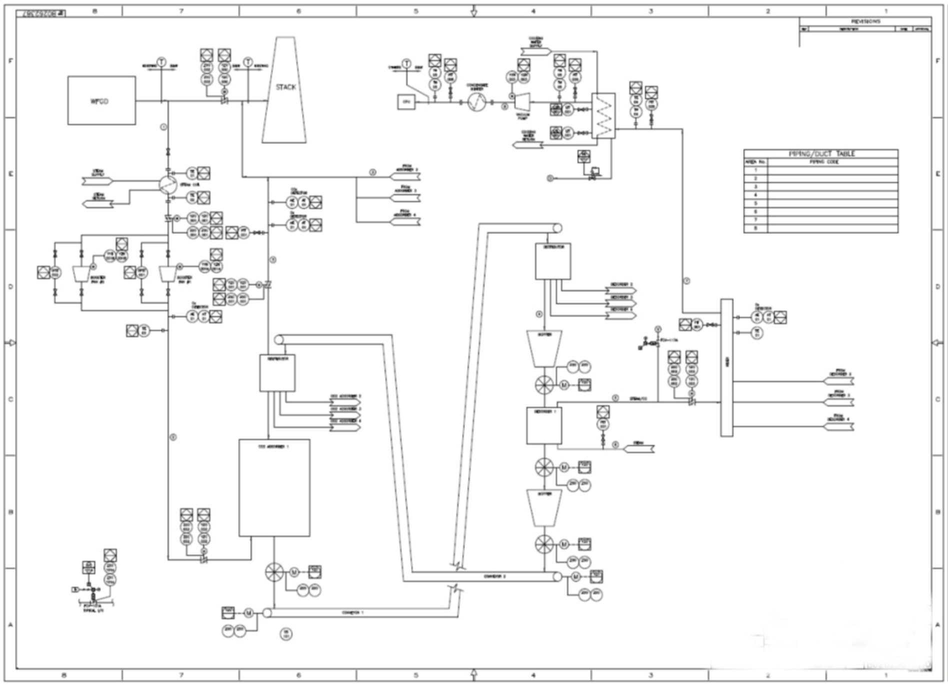

Figure 38. P&ID of single train of moving bed reactor system for TDA's CO_2 capture process.

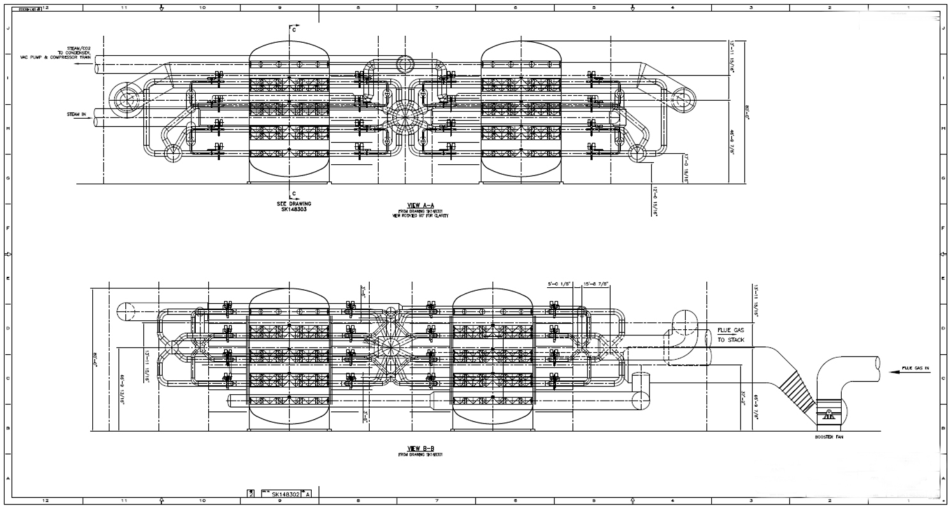

Figure 39. P&ID of single train of fixed bed reactor system for TDA's CO_2 capture process.

vacuum and also would involve complex valve schematic. Figure 40 and Figure 41 shows the 3-D layout of the moving bed design and fixed bed design, respectively. In Task 9, we assessed the relative merits of the two designs.

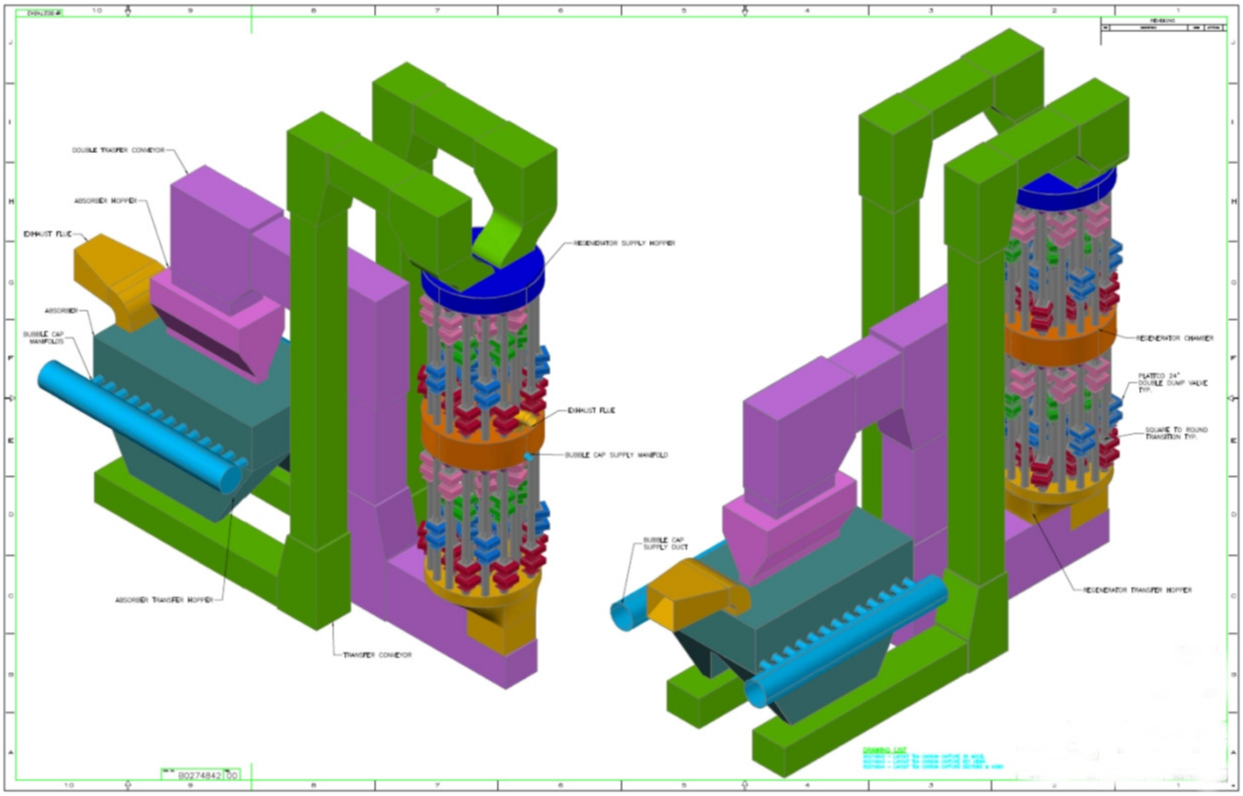

Figure 40. 3-D layout of single train of moving bed system for TDA’s CO_2 capture process.

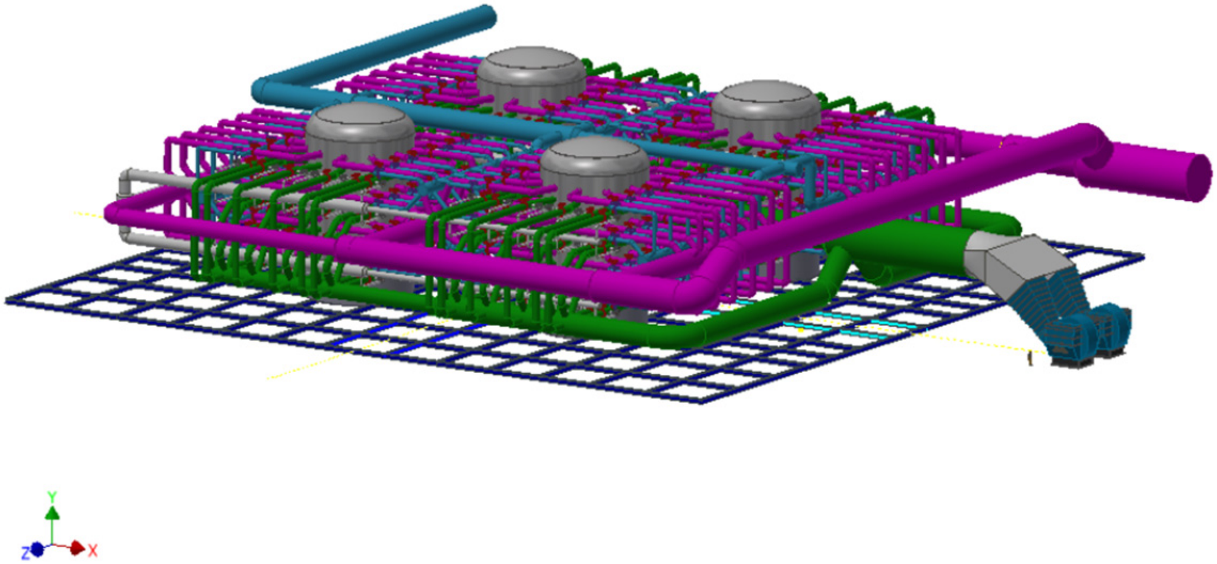

Figure 41. 3-D layout of 4-fixed bed VSA system for TDA’s CO_2 capture process.

4.7.1 TDA's CO_2 Capture System

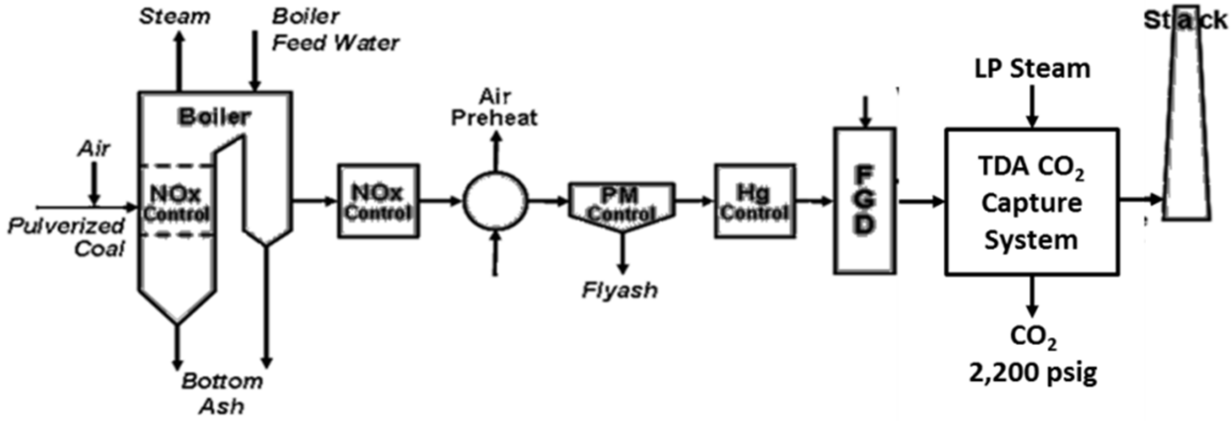

Figure 42. TDA's CO_2 Capture System integrated with a power plant.

In this project, we investigated two process design options for the Flue gas - CO_2 sorbent contactor: fixed-bed and moving-bed VSA systems. Both cases uses a steam sweep under mild vacuum to regenerate sorbent and recover the CO_2 as mixed CO_2/steam stream, condensing the steam recovering the CO_2 as a high purity product. Although our original work in post combustion CO_2 recovery was based on the moving-bed design (and we successfully built and demonstrated its technical viability in a proof-of-concept prototype unit in this project), we then switched to much simpler fixed-bed system that is now the heart of our process. We have a unique reactor design that allowed reducing the pressure drop through the fixed-bed system, one of the key limitations that prevented the use of the fixed-bed reactors in flue gas carbon capture systems.

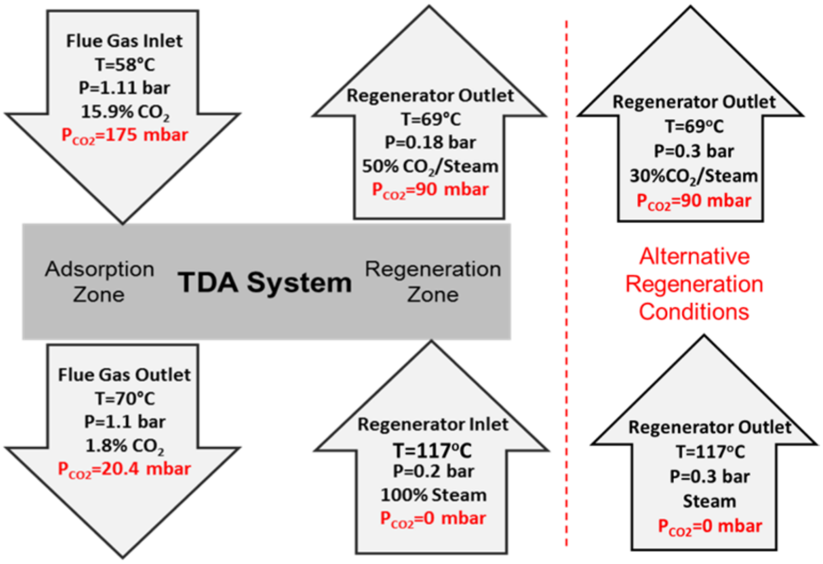

Figure 43. Gas flows around TDA system.

Regardless of the gas-solid contactor design, the CO_2 capture system is placed downstream of the FGD unit (Figure 5), where the gas is cooled to 57°C. After further cooling, removal of some water and re-heating (which are all necessary to prevent water condensation in the system), the gas enters the bed at 58°C. The system consists of multiple beds (we envision 8 beds) to house the sorbent; one or more beds will be on-line at all times adsorbing CO_2 from the flue gas to ensure we achieve greater than 90% carbon capture, while the other bed(s) are regenerating and/or going through pressure transitions.

The flue gas stream is introduced from the top of the sorbent beds at near ambient pressure (1.12 bar); the sorbent selectively removes CO_2 and the mildly exothermic CO_2 adsorption increases the bed temperature to 70^{o}C. Once the sorbent is saturated with CO_2 (i.e., as sorbent reached its working capacity), the bed is isolated (using a series of valves) for regeneration. The bed first goes through a series of pressure equalizations to reduce the bed pressure to 0.2 bar (or alternatively to 0.3 bar). A superheated steam flow at 70^{o}C and 0.2 bar sweeps across the bed to recover the released CO_2. The steam sweep is used to facilitate the CO_2 release at low CO_2 partial pressure, thereby ensuring a high removal efficiency during adsorption.

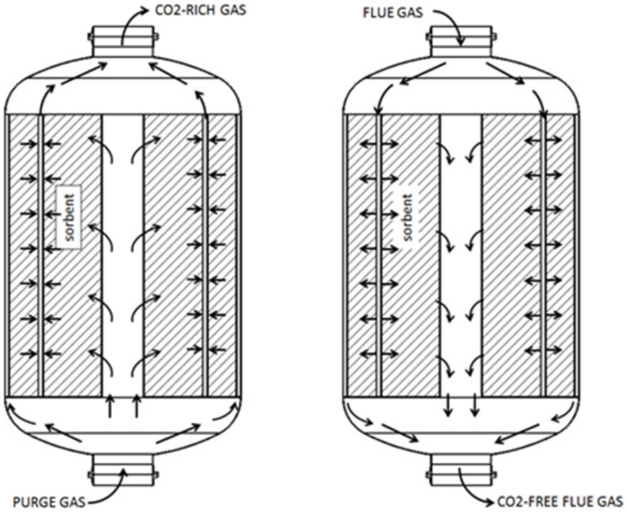

Figure 44. Radial flow full scale sorbent reactors in regeneration (left) and CO_2 adsorption (right).

Even though the fixed-bed contactors represent the simplest design and the least expensive housing option, the use of such reactors has been limited due to the potentially high pressure drop generated by these systems. Even in the rapidly cycling beds, because of the very large amounts of CO_2 to be removed, a significant inventory of sorbent must be placed into the flow path. Unfortunately, the conventional “pancake” reactor design (with very large diameter low depth beds with low aspect ratios) common for fixed-bed reactors used in similar applications will not be practical due to their large footprint and flow distribution issues. In our system, we use radially outflow reactors to house the sorbent. The reactor will resemble a traditional fixed-bed reactor, while the proper internal manifolds enable gas distribution in the radial direction allowing the flue gas to pass over a relatively thin bed of sorbent presented across the height of the reactor. The flue gas is introduced into the reactor via a common supply line from the top of the bed and is distributed into the two internal manifolds (as indicated by the arrows in Figure 44). The CO_2 free flue gas is collected in separate internal exhaust manifolds which then merges into a single exhaust line and leaves the reactor at the top of the reactor.

During the regeneration, pressure equalization of the beds moderates the sorbent pressure to 8.5 psia. A vacuum pump is used for further depressurization. The low pressure steam will be introduced at the bottom of the bed through the exhaust (three) manifolds where the CO_2 free flue gas has been removed. The steam also sweeps across the bed in the radial direction, but in the counter direction of the flue gas flow; the adsorbed CO_2 comes off from the surface and recovered, generating a 50% vol. CO_2/steam mixture (dry basis CO_2 purity of 95+%) at 0.18 bar at the regenerator exit after accounting for the pressure drop through the bed (the balance being ~50% vol. H_2O with some N_2 and O_2 impurities from the flue gas trapped within the sorbent pores). This off-gas from the regenerator is then compressed in a two-stage compressor to raise its pressure to 1.24 bar. The compression also raises the stream temperature to 182°C. We use this heat of compression to raise the low pressure steam (0.2 bar) used as the regenerator sweep gas. The low pressure steam is raised in two boilers following the compressors, providing 61°C saturated steam for the regeneration process. As the regeneration off-gas (mainly consisting of the released CO_2 and steam) goes through the compression and cooling steps, the water condenses and is recovered to feed back into the cycle. Following the two compressors in the regenerator, a product stream of 68.7% CO_2/steam mixture is produced at 77°C. The CO_2 is further concentrated and compressed in the compression/purification train.

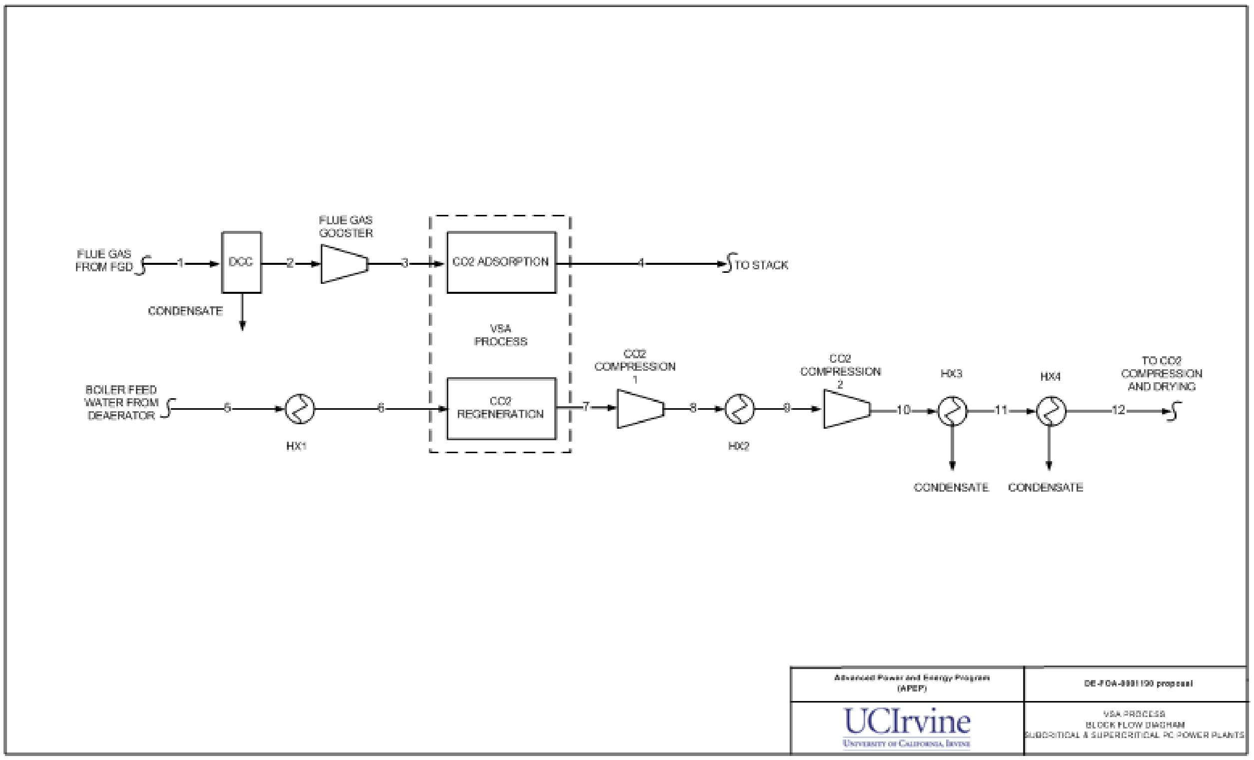

Figure 45. PFD around TDAs VSA based post combustion CO_2 capture system.

Because the flue gas and the steam are at similar pressures and temperature, the transition from adsorption to regeneration (and vice versa) is very rapid, eliminating the need for multiple beds. We believe that 8 beds will be sufficient to all the transitions in a rapid cycling vacuum/concentration swing system. Based on the 2,326,545 lb/hr flue gas flow rate (the flow rate for AEP's 550MW Conesville #5 power plant), we expect only a 0.2 psid pressure drop across the bed.

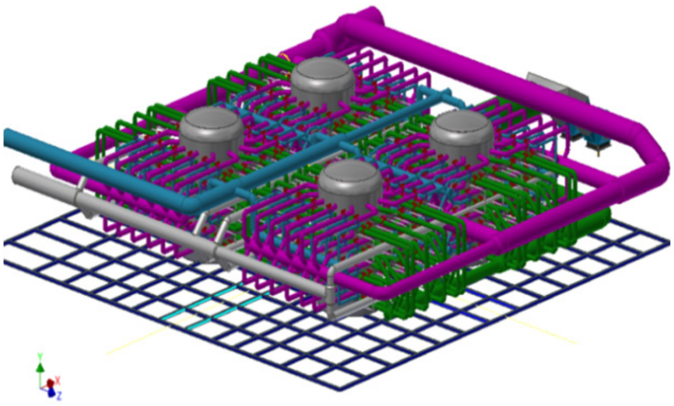

Figure 46. Stacked beds with external manifolds prepared by B&W.

Another unique advantage of the design is in the reduction in the number of flow selection valves to distribute the gases into the reactors. Combining all supply lines to the reactors into a single manifold (and distributing the gases internally in the reactor) requires only 1 valve per supply line per bed instead of 4 providing a 4X reduction in the number of valves for the operation of the system which was used in our early designs. In the initial fixed bed design carried out by B&W the gas flows during the adsorption and regeneration were distributed into "stacked" beds using external manifolds (Figure 9). This stacked bed design required 16 valves that had contributed to 25% of the overall costs. The radial outflow design represents a significant modification, substantially reducing the number of these valves per bed and hence the overall cost.

Figure 47. A commercial Round Louvre Valve.

We envision the valves used in our process to be similar to the Louvre Lock Valves that are available off-the-shelf and can be purchased at competitive costs (as little or no further design work is needed). Figure 10 shows a picture of the Louvre Damper Valves (DN 5600 mm with NICROFLEX sealing, rating T=400^{o}C, P_{diff}= 90 mbar) supplied to a DeNOx plant at the STEAG power station Herne, Germany. These valves are already designed to treat the desired gas volumes at the operating conditions of interest for similar application. We anticipate a straight forward integration into our system, providing substantial cost savings.

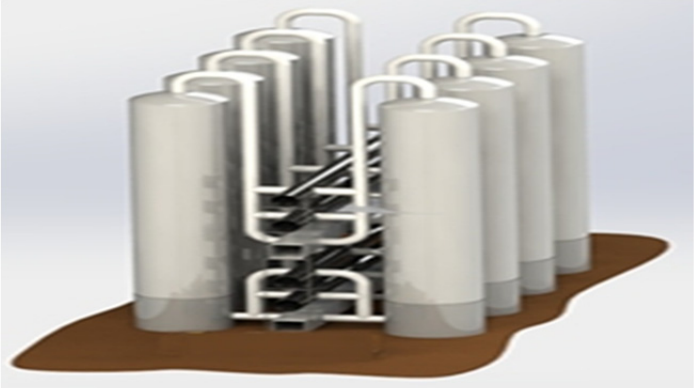

Figure 48. Full scale system.

Like every CO_2 capture process, TDA's system also includes a section that compresses, intercools, recompresses and refrigerates the CO_2 for purification; finally recovering the liquid CO_2 so that it can be pumped to 2200 psig for sequestration. The CO_2 compression, condensation and purification train used in our process will be similar to that described by Ramezan (2007).

4.8 Task 8. Design of Prototype Test Unit

Figure 49. Clear adsorption reactors with lock hopper inlets

In order to design the prototype moving bed reactors, we needed information on the flow characteristics of the sorbent material in a moving bed system. Hence, we first designed and fabricated a cold flow system using clear reactors to do the flow visualizations before finalizing the design for the prototype moving bed reactor system.

4.8.1 Cold Flow Visualization System

The clear adsorber was fabricated from polycarbonate material, allowing visual observation of the adsorbent flowing through the vessel. The flow characteristics will determine final design configuration. Figure 49, shows the completed, full size (bench-scale/prototype size) clear adsorption reactor in two views. The regenerator reactor is under construction; however will be identical to the adsorption reactor shown. The reactor size and configuration was initially determined through accepted engineering design practices and peer review then conceived through Solid Works. Figure 50, shows the initial drawing of the adsorption reactor in the final and full round configuration.

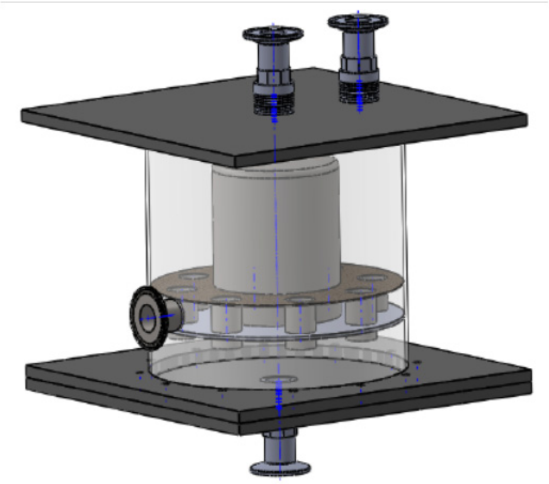

Figure 50. Solid Works drawing of adsorption/regeneration reactor in the full round configuration

Figure 51. CO_2 sorbent flowing through clear mini reactor

During this report period, the CO_2 adsorption material was tested in a mini clear flow reactor at the TDA Table Mountain site, room 222. The material chosen was manufactured by our chemical manufacturing team. The material was activated in the high temperature rotary furnace in room 628. The batch maintains a consistent classified size of 0.0624” (.1588cm). Figure 51, is a snapshot of the movie taken of the test, demonstrating the flow characteristics of the CO_2 material. The flow test generated positive results and the full size, half reactor was built to model the flow characteristics in the moving bed systems.

We also purchased and installed an elevator for moving the sorbent from the regenerator to the adsorbed. Our existing moving bed system uses pneumatic conveying of the sorbent material, and our calculations show that a screw elevation system will consume less energy and result in lower attrition rates for our sorbent. The rest of the apparatus was constructed in our TDA shop at the Wheat Ridge facility and then transported to the Table Mountain facility for commissioning and testing. The elevator is 15’2.5” high from base to top. All six sides have foam on the outside as insulation to inhibit heat transfer from within (Figure 52). The metal plates are designed for protection of the apparatus and operator alike. The

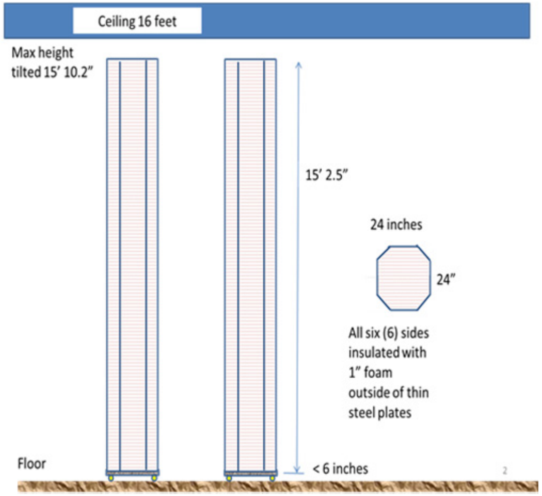

Figure 52. Containment plan for elevator and reactor system.

Figure 53. Solid Works rendering of the Adsorption, regeneration, and the purge reactors along with the lock hoppers.

motor for the elevator is Class1, Division 2, and all of the valves on the apparatus are pneumatic. The electronics cabinet, vacuum pump and all other electrical components will be placed inside a Class 1 Div 2 rated cabinet for placement on the industrial site. The clear full size, half reactor design as shown in Figure 53, shows, from top to bottom, the adsorber, three lock hoppers for continuous material flow while pressure equalization occurs for the regeneration reactor, followed by three lock hoppers for continuous material flow while pressure equalization occurs. The final reactor is a supplemental purge reactor we think will be needed to ensure the regenerated material is dry and CO_2 free before going into the elevator for recirculation to the top of the reactor.

TDA completed the design of the prototype unit, which was reviewed and accepted by GTI. Foot print of the prototype unit was determined by TDA to be 6 ft x 6 ft x 16 ft high (Figure 54). Figure 55 shows the cross-section of the prototype reactor adsorber/regenerator. The prototype unit was designed to handle up to 2.3 ACFM flue gas flow and a sorbent circulation flow rate of up to 8 ft^3/h.

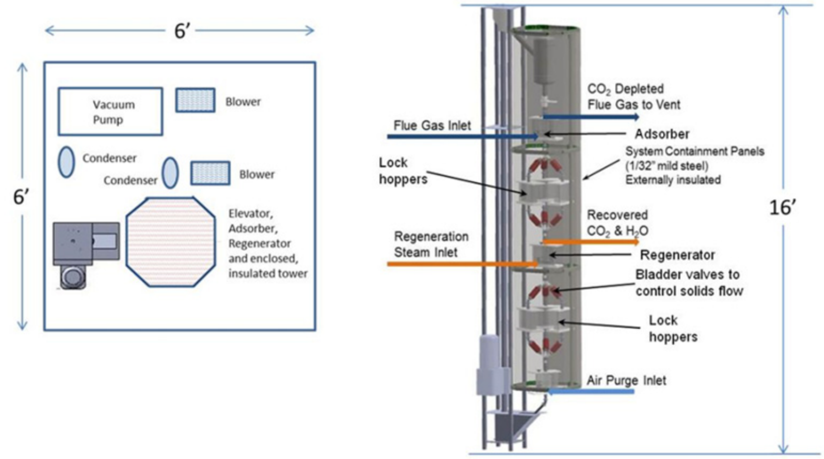

Figure 54. Foot Print of the TDA's Prototype Test Unit.

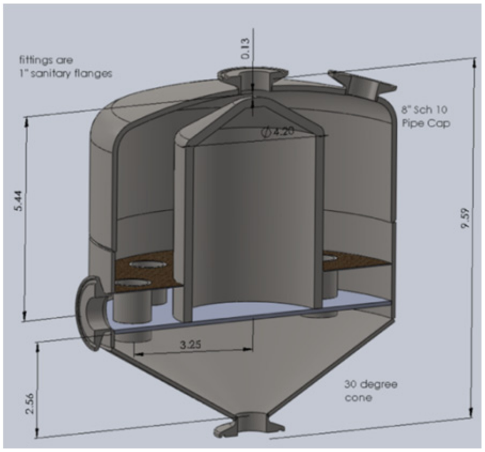

Figure 55. 3-D cross-section of the prototype absorber/regenerator.

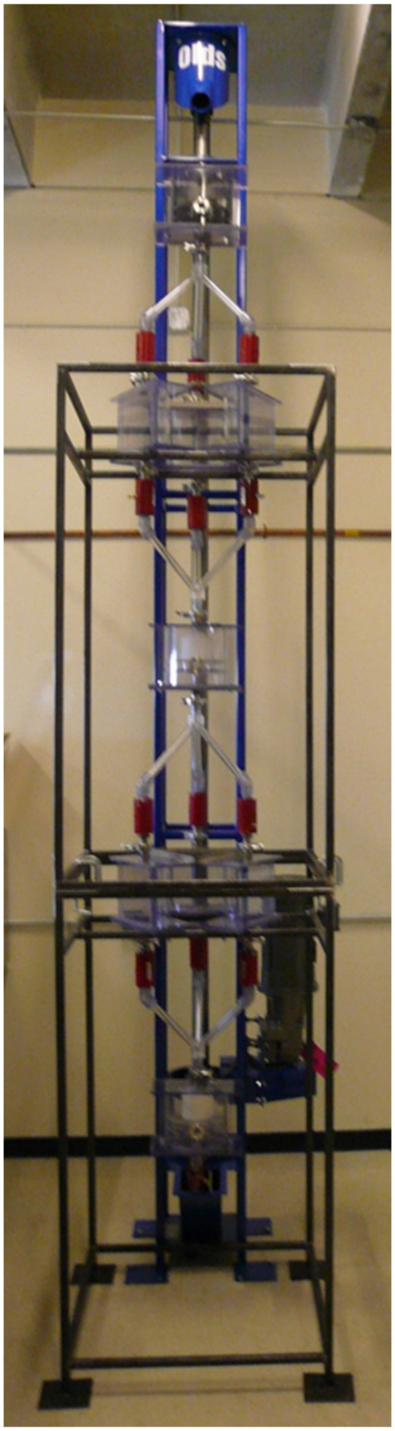

Figure 56. Picture of cold flow visualization moving bed system fabricated by TDA.

We have fabricated a cold flow visualization unit (Figure 56) which is a replica of the prototype unit design with plastic components instead of the stainless steel parts. Results from the cold flow visualization unit indicated that there are no sorbent hold ups in the moving bed system and the solid circulation rates were optimized. TDA had a site visit to GTI (demonstration site host in April 2013), key personnel from GTI visited TDA in August 2013, and we conducted a review of the prototype design and a detailed hazard analysis on the prototype test unit was completed.

4.9 Task 9. Process Optimization and Design

In collaboration with B&W and UCI we carried out the process optimization and design. A commercial concept plant for carbon capture using the TDA solid sorbent process was designed by B&W. Multiple designs were considered such as fixed bed vs. moving bed. Initially, B&W carried out the detailed design of the fixed bed reactor configuration as it showed the potential to provide a lower capital cost alternative to other designs considered. In this design, B&W used the working capacity of 1.4 % wt. for CO_2 adsorption sorbent based on the bench-scale evaluation from initial phase of budget period 1. The flue gas flow rate to the CO_2 reactor system is 5.12 million lbs/hr at a temperature of 135°F and 40 in H_2O (gauge). Flue gas flows through the sorbent beds in the adsorption cycle where 90% of the CO_2 is captured and the regeneration is accomplished with steam under a vacuum pressure of 3 psia. Later B&W carried out a detailed design of the moving bed design configuration based on the improved sorbent working capacities (4 % wt. CO_2) achieved in the budget period 2. The improvements on sorbent capacity are significant enough to warrant the evaluation of the alternative design and costing which uses a moving bed system. Therefore, B&W carried out detailed design and cost analysis for both the moving bed and fixed bed design options. The cost of TDA's CO_2 capture process for the fixed bed design option (for a working capacity of 1.4% wt. CO_2) and moving bed design option (for a working capacity of 4% wt. CO_2) are estimated to be $372.1 million and $425 million, respectively. The use of off-the-shelf components generated redundancy and increased cost. When the fixed bed design was revised to a working capacity of 4% wt. CO_2 the cost of the system was reduced to $276 million on $2011 basis. While for a similar sized amine based CO_2 capture system would cost $549.4 million, which is almost 2x times the cost of the VSA based system operating on TDA's mesoporous CO_2 capture sorbent.

In the Budget Period 2 UCI updated the Aspen Model to use the same configuration for the amine and the PSA cases, which consisted of a direct contact cooler (DCC) followed by a blower followed by the CO_2 removal step (amine or TDA's CO_2 Capture system) to overcome the pressure drop across the absorber and to cool the gas down to the required temperature for CO_2 capture. The pressure rise across the blower will compensate for the ΔP across the upstream DCC which is estimated to be 32 millibar (based on UCI's previous work) and the downstream absorber, which is calculated to be 100 millibar (Jansen et al. 2007) for amine system (Case 10a) and for the TDA system B&W has calculated the pressure drop to be 87.5 millibar for the fixed bed option (Case 11 & 11a) and 75 millibar (Case 12) for the moving bed option. UCI also carried out a sensitivity case to determine the improvements that can be made if the pressure drop across the fixed bed system can be reduced to 50 millibar (Case 11b). The revised net plant efficiency for the amine case and TDA's system taking into account the pressure drop through the system is provided in Table 13. The cost basis is on $2007 basis, which was later updated to $2011 basis in the budget Period 3.

Table 13. Summary of budget period 2 results from UCI's Aspen modeling of TDA's post combustion CO_2 capture process.

CASE NO.	UNITs	9	9	10	10a	11	11a	11aa	11b	12
CASE DEVELOPED BY		DoE	UCI	DoE	UCI	UCI	UCI	UCI	UCI	UCI
CO_2 CAPTURE TECHNOLOGY		**No CO_2 Capture**	**No CO_2 Capture**	**Amine**	**Amine**	**VSA**	**VSA-Fixed Bed**	**VSA-Fixed Bed**	**VSA-Fixed Bed**	**VSA-Moving Bed**
CASE DESCRIPTION		As reported in DoE report	Verification of methodology	As reported in DoE report	Booster fan added for higher ΔP	Fixed bed system	Butane loop for heat exchange and LP purge steam generation	No Butane loop and LP steam for purge from Steam turbine cycle	Higher capacity fixed bed system with lower ΔP	Butane loop for heat exchange and LP purge steam generation
VSA HEAT OPTION		N/A	N/A	N/A	Butane loop	Butane loop	Butane loop	LP Steam & Cooling water	Butane loop	Butane loop
CARBON CAPTURED	%	0	0	90	90	90	90	90	90	90
GROSS POWER GENERATED (AT GENERATOR TERMINALS), KWe										
STEAM TURBINE POWER	**kWe**	**582,600**	**580,395**	**672,700**	**669,880**	**806,985**	**806,985**	**798,903**	**806,985**	**806,985**
TOTAL AUXILIARY CONSUMPTION	kWe	32,580	32,859	122,740	140,501	189,759	189,759	178,065	186,533	195,637
AUXILIARY LOAD SUMMARY										
FLUE GAS BOOSTER	kWe	0	0	0	11,690	10,677	10,677	10,677	7,551	9,647
CO2 REMOVAL UNIT	kWe	0	0	22,400	22,084	11,661	11,661	0	11661	18,596
CO2 COMPRESSION	kWe	0	0	48,790	54,882	115,675	115,675	115,675	115,675	115,675
PUMPING & COOLING TOWER	kWe	9,390	9,681	18,730	19,041	18,380	18,380	18,382		18,354
OTHER LOADS	kWe	23,190	23,176	32,820	32,804	33,365	33,365	33,332		33,365
NET POWER OUTPUT	**kWe**	**550,020**	**547,536**	**549,960**	**529,379**	**617,226**	**617,226**	**620,837**	**620,451**	**611,348**
% NET PLANT EFFICIENCY, HHV	**%**	**36.8**	**36.62**	**26.2**	**25.18**	**29.36**	**29.36**	**29.53**	**29.51**	**29.08**
CONSUMABLES										
AS-RECEIVED COAL FEED	KG/H	198,391	198,392	278,956	278,957	278,957	278,957	278,957	278,957	278,957
LIMESTONE SORBENT FEED	KG/H	19,691	19,944	28,404	28,831	28,831	28,831	28,831	28,831	28,831
CO2 SORBENT INITIAL FEED	KG	0	0	0	0	6,068,145	2,123,851	2,123,851	2,123,851	4,442,749
RAW WATER USAGE	GPM	5,896	6,153	11,224	10,759	10,036	10,036	10,037	10,005	10,027
Net power, MW		**550.02**	**547.54**	**549.96**	**529.38**	**617.23**	**617.23**	**620.84**	**620.45**	**611.35**
Capacity factor (CF), %		85	85	85	85	85	85	85	85	85
Total plant cost (TPC), $		892,433,000	892,762,698	1,618,357,000	1,653,521,816	1,673,178,555	1,654,271,376	1,639,786,042	1,654,165,943	1,732,257,957
Total plant cost (TPC), $/kWe		**1,623**	**1,630**	**2,943**	**3,124**	**2,711**	**2,680**	**2,641**	**2,666**	**2,833**
Initial catalyst & chemicals cost, $		0	0	2,712,000	2,673,187	24,496,311	8,638,361	8,586,597	8,638,361	17,961,441
Total overnight cost (TOC), $		1,098,124,000	1,099,501,766	1,985,432,000	2,029,584,945	2,080,766,174	2,038,150,311	2,020,608,218	2,038,018,655	2,143,947,190
Cost of electricity (COE) w/o TS&M, $/MWh		**59.4**	**60.5**	**103.8**	**111.1**	**101**	**96.8**	**95.6**	**96.3**	**103**
Cost of electricity (COE), $/MWh		**59.4**	**60.5**	**109.6**	**117.9**	**106.9**	**102.6**	**101.4**	**102.1**	**108.9**
CO_2 in flue gas, ST/h		**576.8**	**576.8**	**730.0**	**730.0**	**730.0**	**730.0**	**730.0**	**730.0**	**730.0**
Cost of CO_2 Capture, $/ST		-	-	42.02	47.14	44.63	40.59	39.69	40.33	46.06
Cost of CO_2 Capture, $/tonne		-	-	46.32	51.96	49.19	44.74	43.75	44.45	50.77
Cost of CO_2 Avoided, $/ST		-	-	53.18	61.98	50.32	45.77	44.50	45.24	52.44
Cost of CO_2 Avoided, $/tonne		-	-	58.63	68.32	55.47	50.45	49.05	49.87	57.81

Using the cost estimates provided by B&W, UCI carried out a detailed economic analysis of the CO_2 capture system and the results are summarized in Table 13. TDA's VSA with Fixed-bed Option with LP steam purge, where the LP steam is generated in the CO_2 compression stages and the LP steam stream withdrawn from the ST is used to maintain isothermal operation o fthe sorbent beds, provided the lowest 1st year COE (including TS&M) of $101.4/MWh compared to $117.9/MWh for amine scrubbers. We also calculated the cost of electricity (COE) and the cost of CO_2 capture based on the basis for technology feasibility study provided in the DOE solicitation (DE-FOA-0000403). The fixed bed options both with and without using butane loop for LP steam generation provided a lower cost of CO_2 capture ($40.73 and $40.40 per ton, respectively) compared to the moving bed option ($50.85 per ton). The cost of CO_2 capture for TDA's fixed bed option is 21.2% lower than the amine based system. Hence, in BP3, we included testing a 4-bed VSA system under real coal derived flue gas at GTI (field tests) also as part of the work plan for BP3. This 4-bed system was fabricated at no-cost to this project and the design, fabrication and initial testing at TDA were all sponsored by a DOE funded SBIR Phase II project (DE-SC0006239).

Table 14. Techno-economic analysis of TDA's CO_2 Capture System in comparison against amine based system.

Technology Feasibility Study $2011 basis 550 MW net sub-crtitical pulverized coal-fired power plant	**Amine Based System**	**TDA Moving Bed System (Butane loop for LP Steam)**	**TDA Fixed Bed System (Butane loop for LP Steam)**	**TDA Fixed Bed System (No Butane loop for LP Steam)**
1) Parasitic Power Losses				
Power loss due to capture auxiliaries, MW	28.5	68.4	64.1	55.7
Power loss due to compression requirements, MW	39.7	39.7	39.7	39.7
Equivalent power loss due to LP steam requirement, MW	105.7	6.6	6.6	12.4
Total Paraistic power loss, MW	**173.9**	**114.6**	**110.4**	**107.8**
2) Estimated Levelized cost of electricity and steam				
Cost of Electricity, mills/kWh	**117.44**	**99.23**	**97.92**	**97.12**
Cost of Steam, $/1,000 lb	**10.67**	**9.01**	**8.89**	**8.82**
3) Itemized Cost of CO_2 Capture & Compression Equipment				
Cost of Equipment - CO_2 Capture Process	$356,336,564	$424,967,621	$276,751,323	$276,751,323
Cost of Initial Sorbent Loaded	$1,932,839	$12,986,959	$6,245,938	$6,245,938
Cost of CO_2 Compression System	$40,270,662	$40,270,662	$40,270,662	$40,270,662
Total Installed Equipment Cost	$398,540,065	$478,225,242	$323,267,923	$323,267,923
$/kWe	**$1,058.57**	**$1,089.44**	**$736.43**	**$736.43**
4) Cost of CO_2 Capture				
$/ton CO_2	**$51.26**	**$50.85**	**$40.73**	**$40.40**
$/tonne CO_2	**$56.50**	**$56.06**	**$44.89**	**$44.53**
5) Percentage decrease in PC plant efficiency	**11.4%**	**7.5%**	**7.3%**	**7.1%**
Total lost power due to CO_2 capture, MW	173.9	114.6	110.4	107.8
Heat content of coal feed (HHV), MW	1520.3	1520.3	1520.3	1520.3

4.10 Task 10. Sorbent Production for Prototype

Our initial samples for this project were made as granular carbon in ceramic trays using a 3" diameter Lindberg tube furnace, and our sample sizes were limited to <50 g. We have since scaled up production of the carbon to multi-kilogram quantities (up to 5 L per day), using our 7" continuous rotary Bartlett and Snow kiln (Figure 32). The rotary kiln is electrically heated and has a 7" Inconel tube that can be heated up to 1100°C. The carbon precursor is fed into the kiln using a single screw feeder as shown in Figure 33. It has a computer control system running on Labview software. It has all the safety features needed to operate safely, and an afterburner to process the off gases in an environmentally sound manner. We used this pilot plant to produce 50 L of sorbent needed for the prototype test unit. The bulk density of these sorbents used in the field tests was ~ 0.28 kg/L. Later in 2015, we had improved the sorbent bulk density and the volumetric loading of CO_2 as shown in the Figure 36 in the Section 4.5 (Task 5. Sorbent Production Scale-up).

Figure 57. TDA's 7" rotary kiln used to produce the sorbent used in the prototype unit field tests.

4.11 Task 11. Fabrication of the Prototype Test Unit

4.11.1 Moving Bed Test Unit

The fabrication of the prototype unit that can handle up to 2.3 ACFM flue gas flow and a sorbent circulation rate of up to 8 ft^3/h was done at TDA. Figure 58 shows picture of the prototype unit during fabrication with the steel reactors and lock hoppers. Figure 59 shows the close-up picture of the adsorber (left), regenerator (middle) and lock hoppers (right).

Figure 58. Picture of prototype moving bed system fabricated by TDA.

We have also completed the shakedown tests with the unit (i.e., carried out leak tests and preliminary sorbent flow circulations and CO_2 breakthrough tests under isolated bed conditions). The results from the breakthrough tests in isolated bed mode under ambient conditions are provided in Figure 60. The sorbent showed greater than 90% CO_2 capture for about 10 minutes confirming the CO_2 removal capability for the sorbent produced for the prototype test unit. We then carried out CO_2 removal tests with the prototype unit under moving bed conditions. We observed that the sorbent flow is not continuous and there is back-up in the inlet sections of the adsorber and the regenerator. It was determined that this was due to the shape of the reactor internals, which had a rounded top instead of a cone, the result was sorbent buildup that blocked the inlet tubing. We are now changing the reactor internals. Figure 61 shows the reactor internals, the old rounded unit on the left and the new conical unit on the right under fabrication.

Prior to commencing field tests with the prototype moving bed system, we are carrying out in-house tests using simulated flue gas to optimize the operation of the moving bed system.

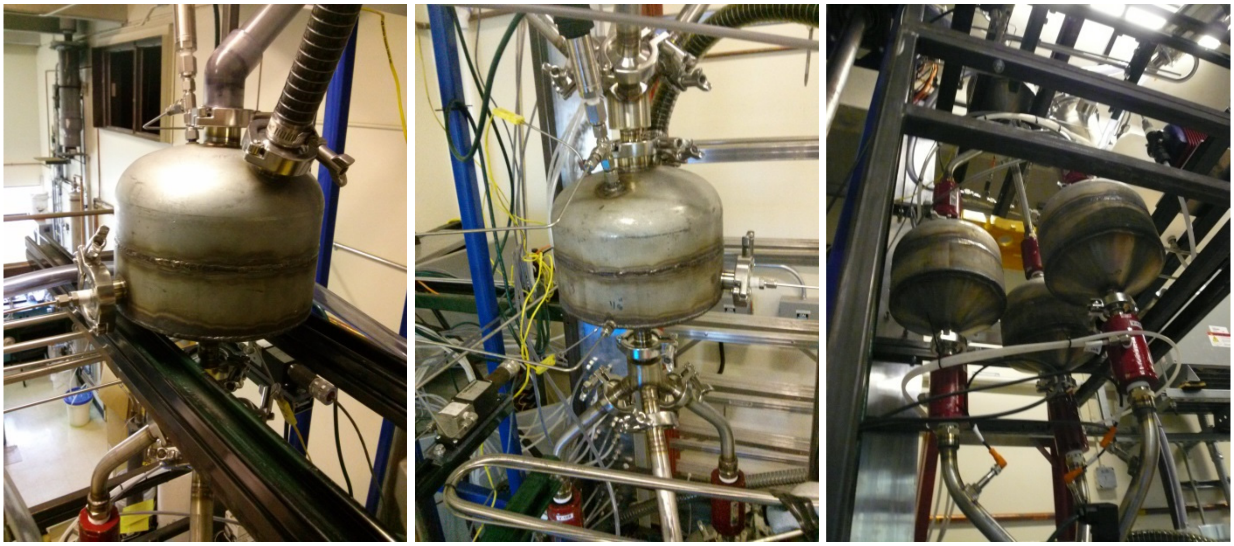

Figure 59. Pictures of the adsorber (left), regenerator (middle) and lock hoppers (right).

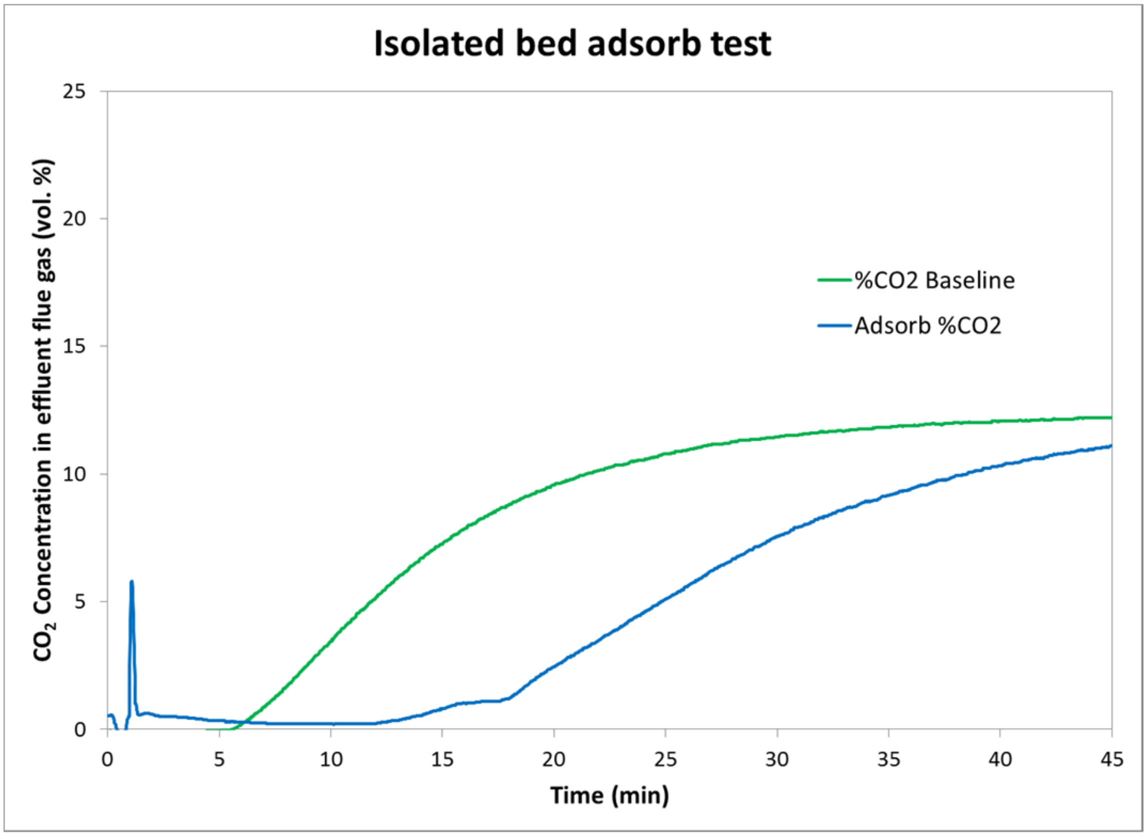

Figure 60. CO_2 breakthrough for blank adsorber and the sorbent loaded isolated adsorber under ambient conditions flue gas flow = 3.3 slpm

Figure 61. Reactor internals rounded top – old (left) and conical top – new (right).

4.11.2 Fixed Bed Test Unit

In a related DOE funded SBIR Phase II project (DE-SC0006239), we designed and built a four bed VSA system (Figure 62, Figure 63 and Figure 64), which was also tested at GTI as part of this project (DE-FE-0007580), since the process economic analysis showed that fixed beds would be a cheaper and more efficient option than moving bed contactors. We built and tested this fixed bed rig in house before the system was sent out for field tests. The design, fabrication and initial testing at TDA of this 4-bed VSA system (fixed bed test unit) were all sponsored by a DOE funded SBIR Phase II project (DE-SC0006239). The results from the design, fabrication and initial testing of the 4-bed VSA system are included here only for reference. The system was designed for 1-2 scfm of gas (the anticipated inlet gas was 13.17% CO_2, 17.25% H_2O, 66.44% N_2, 2.34% O_2 with 42 ppm SO_x and 74 ppm NO_x). We planned for a bed capacity of 2% wt. CO_2 which would result in a bed volume of 6.8L (based on the 2 scfm flow and the anticipated CO_2 loading. The beds are each 0.83 meters long, resulting in an L/D of 8.1. The system used a Sage flow meter to measure the gas flow on both the inlet and the outlets. The CO_2 concentrations were measures similarly using Visalia CO_2 meters. A Reimer steam generator was used to produce the steam for regeneration. An Agilent scroll vacuum pump is used to provide the decreased pressure needed for regeneration. The system was programmed with a LabView control system. The LabVIEW system controls the test conditions, logs the analytical data, and also safely shut down the apparatus. It gives us a second safety monitoring system (along with the mechanical safeties). For this testing system the LabView programing was enormously beneficial for automating the complicated 4-bed cycle sequences.

For the initial in-house shakedown testing the gas was provided using cylinders and was metered into the rig using a separate rig, built to provide gases to rigs without inlet manifolds. For the on-site testing, the post-combustion gas was provided directly from the gasifier and metered into the rig using a Badger valve and a flow-meter.

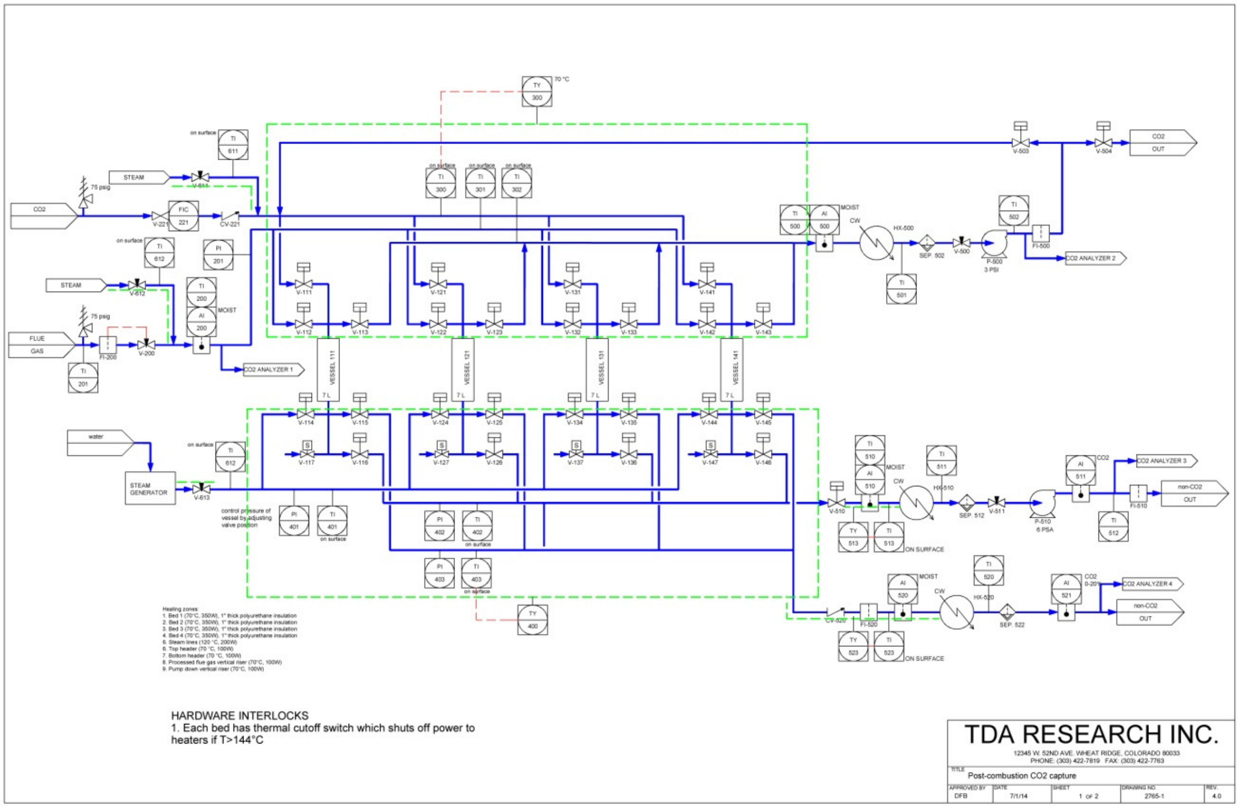

Figure 62. PID for the four bed system.

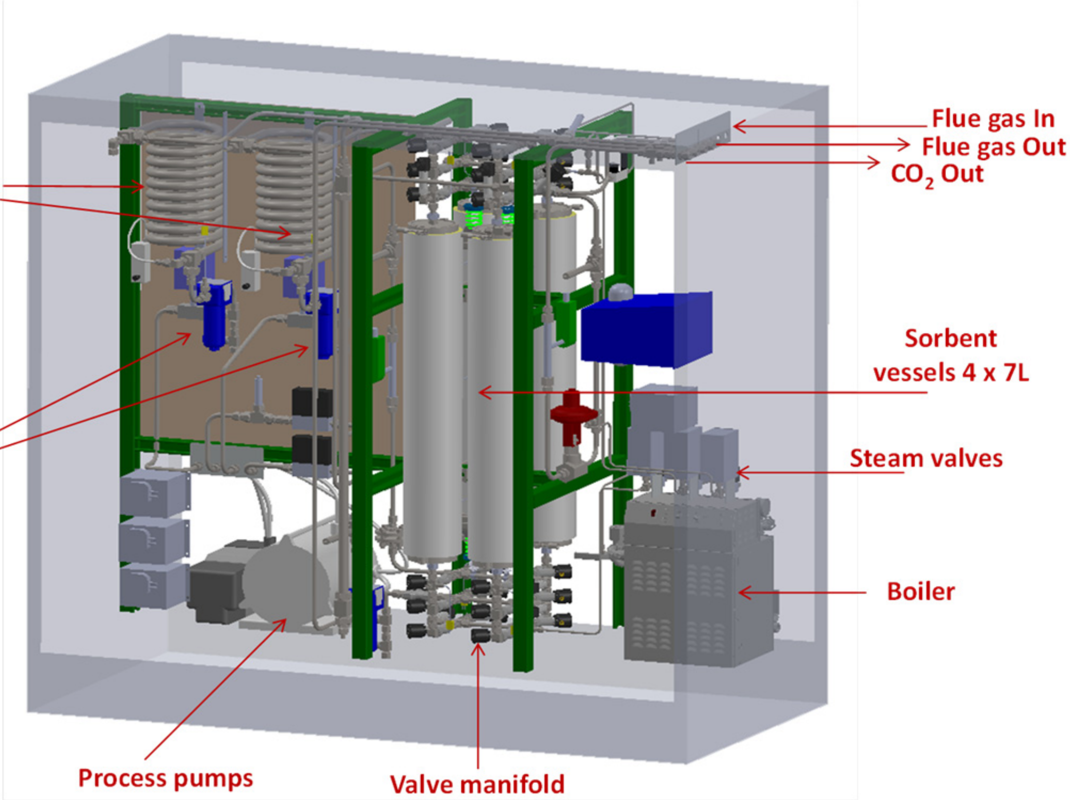

Figure 63. 3-D layout of the 4-bed VSA system.

Figure 64. Pictures of the completed system.

VSA Cycles

The system employs an 8 step cycle sequence to remove the CO$_2$ from the gas streams. In this scheme each bed is online and adsorbing for a fourth of the time. In the remaining time it is used to re-pressurize the newly regenerated bed, depressurized and regenerated under steam. After the regeneration, it is brought up to pressure (using the bed that has just completed the adsorption step), and the pressurized to system pressure in final preparation for adsorption.

The exact 4-Bed PSA Cycle is as follows (graphically in Table 15):

Step 1	Adsorption at 16 psia (ADS)
Step 2	Pressure Equalization to 9.5 psia (EQ1)
Step 3	Co-current Blowdown to 6 psia (CoBD)
Step 4	Co-current CO$_2$ purge at 6 psia (C-Purge)
Step 5	Blowdown to 3 psia (BD)
Step 6	Steam Purge at 3 psia (Purge)
Step 7	Pressure Equalization to 9.5 psia (EQ2)
Step 8	Pressurization with Product N$_2$ to 16 psia (Press)

Table 15. Summary of the VSA cycle.

	Stage 1			Stage 2			Stage 3			Stage 4		
Time (min)	3			1	2		1	2		1	2	
Bed 1	ADS			EQ1	CoBD	C-Purge	BD	PURGE		EQ2	PRESS	
Bed 2	EQ2	PRESS		ADS			EQ1	CoBD	C-Purge	BD	PURGE	
Bed 3	BD	PURGE		EQ2	PRESS		ADS			EQ1	CoBD	C-Purge
Bed 4	EQ1	CoBD	C-Purge	BD	PURGE		EQ2	PRESS		ADS		

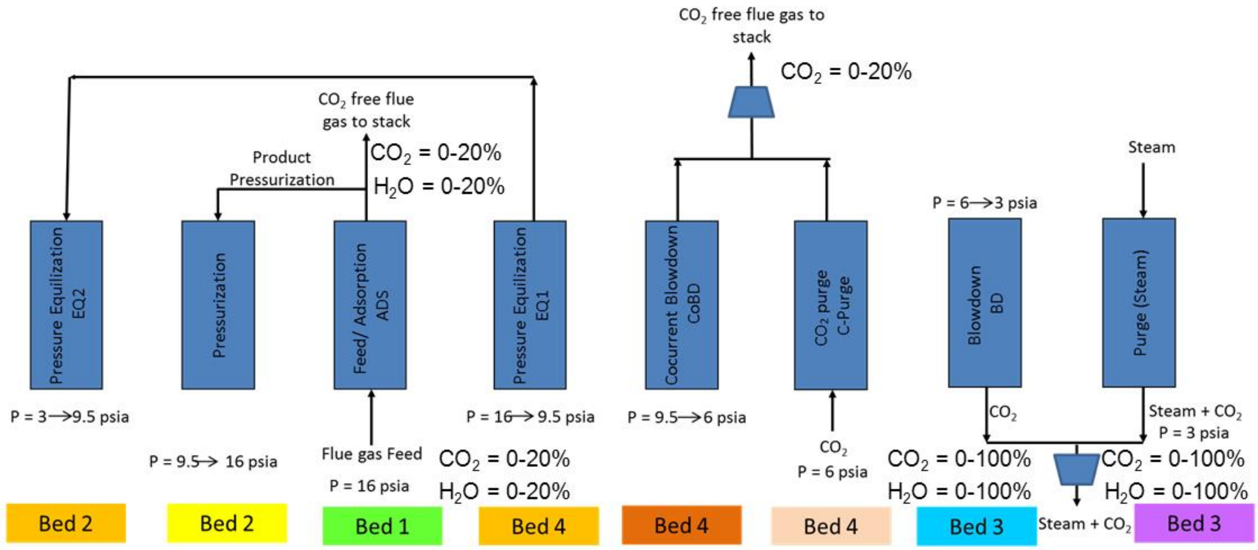

Figure 65. VSA cycle scheme in Stage 1

The scheme is further shown in Figure 65 which schematically represents the Stage 1 given in Table 15. Bed 1 (in green) remains on the flue gas feed stream throughout the testing; the majority of the CO_2 free outlet gas goes to the stack. Bed 2 begins the step at 3 psi, having just been regenerated. It is first brought to 9.5 psia in the pressure equilibration step with Bed 4 and then is brought to pressure using the CO_2 free outlet gas from Bed 1. Bed 3 is regenerated in this step, first being drawn down to 3 psia using the pump and then purged with steam at the lower pressure. Bed 4, having just completed adsorption in the previous step is first drawn down to 9.5 psia by equalizing with Bed 2 then is brought down to 6 psia with the Co-current blowdown and is then purged with CO_2 (recovered from the flue gas) in preparation for regeneration. We first purge with CO_2 to ensure that the gas recovered has above 90% CO_2 to be recovered for further use. Initially we intended each stage to last about 3 minutes, but we ultimately found shorter cycle times time to be beneficial.

Shakedown Testing

Before sending the rig out for testing at GTI, we first tested the rig at TDA. We used bottled gases to supply gas flow, simulating the stream with N_2 and CO_2. The gas was metered into the system using different system. This separate rig was built for metering and mixing gases to be sent to another system. The flow in was measured both at this separate rig and at the inlet of the four-bed system. In these shakedown tests we tested the full functionality of the system. First we started with dry simulated flue gas at room temperature and then added in other functionalities such as higher temperature, use of steam purge etc. A typical pressure cycle from Bed 1 during these tests is shown in Figure 66 with the different stages labeled.

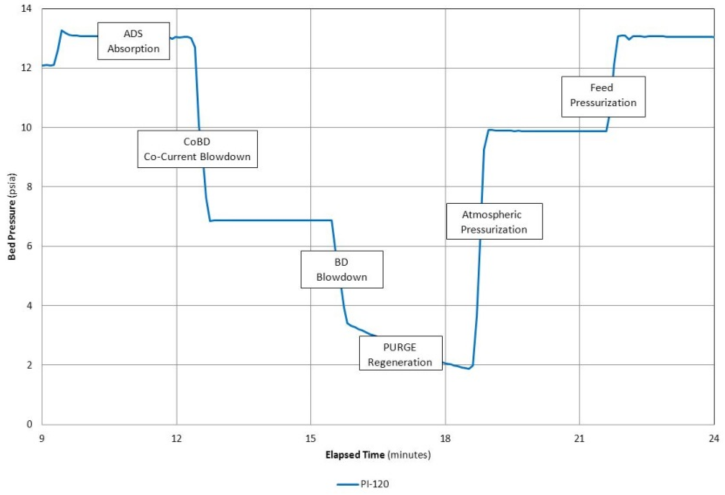

Figure 66. Bed 1 Pressures at the different VSA stages.

4.12 Task 12. Field Tests

In this task, in collaboration with the GTI, TDA evaluated the efficacy of the sorbent system in two prototype test units, allowing us to evaluate sorbent performance and cycle efficiency in both fixed-bed and moving-bed reactors. The two units were first tested at TDA using simulated flue gas before the field tests at GTI under coal derived flue gas. The two units were installed at GTI combustion Laboratory facility in the week of March 23, 2015. Figure 67 shows the block flow diagram (BFD) of GTI's coal burning furnace system, which GTI installed by converting one of their natural gas furnace under the State of Illinois funding as cost share through Illinois Clean Coal institute (ICCI). A slip stream of the flue gas that is getting generated is withdrawn and sent through the gas conditioning and cleanup to reduce the temperature and match the flue gas composition of the downstream of wet flue gas scrubber. Figure 68 shows the two units installed at GTI along with the pilot coal fired combustor with feeder and the associated gas cleanup subsystems used to generate coal-derived flue gas for prototype unit tests. In the tests at GTI Illinois #6 coal was burned in the combustor and a slipstream of the flue gas generated was sent through heat exchangers and gas cleanup sub systems to reduce the SO_x from 2,700 ppm to 22 ppm and the CO_2 concentration in the flue gas was 15.2% (on dry basis). This sulfur laden flue gas was sent to TDA's prototype unit for CO_2 capture.

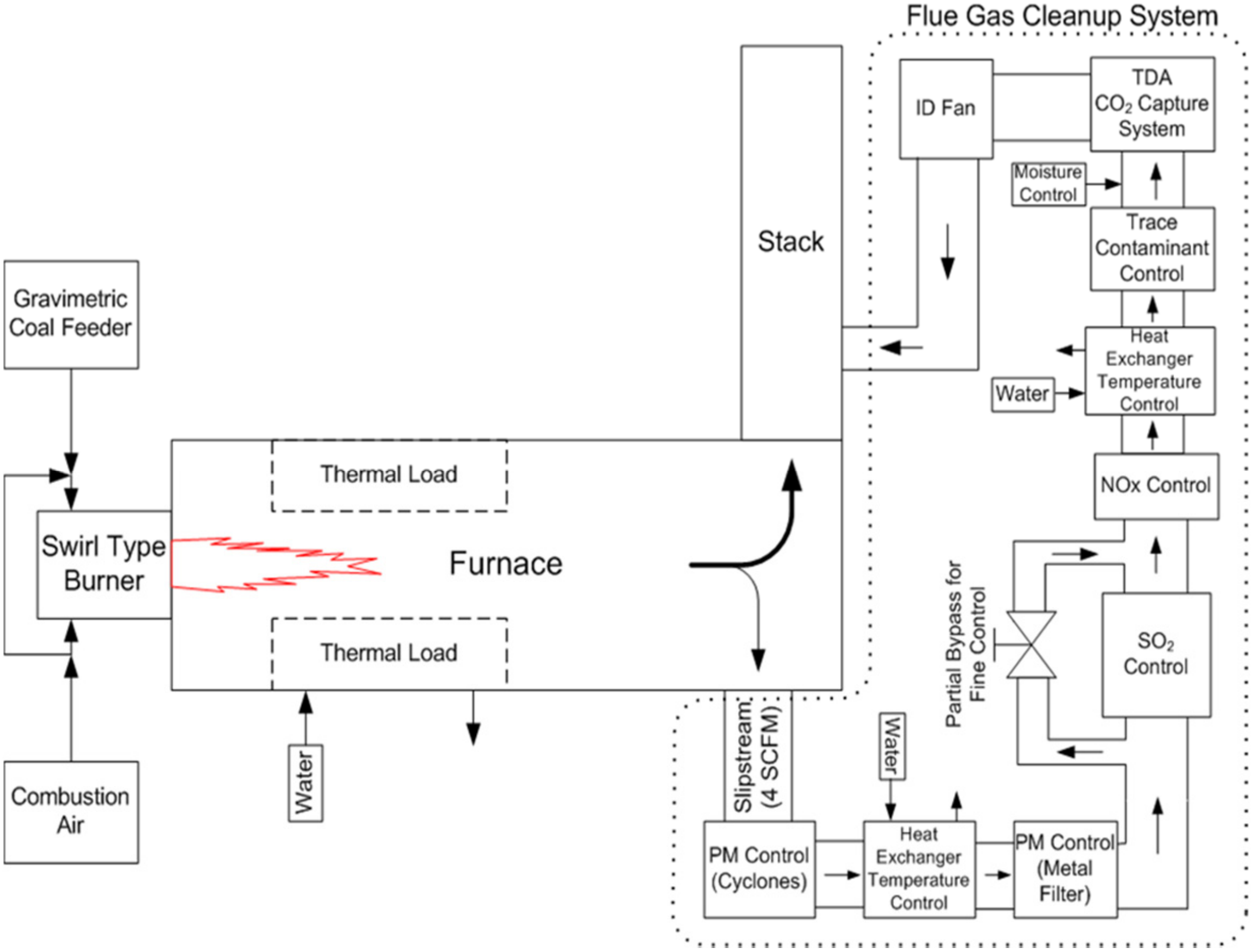

Figure 67. Block flow diagram (BFD) of GTI's coal burning furnace system, which GTI installed by converting one of their natural gas furnace under the State of Illinois funding as cost share through Illinois Clean Coal institute (ICCI).

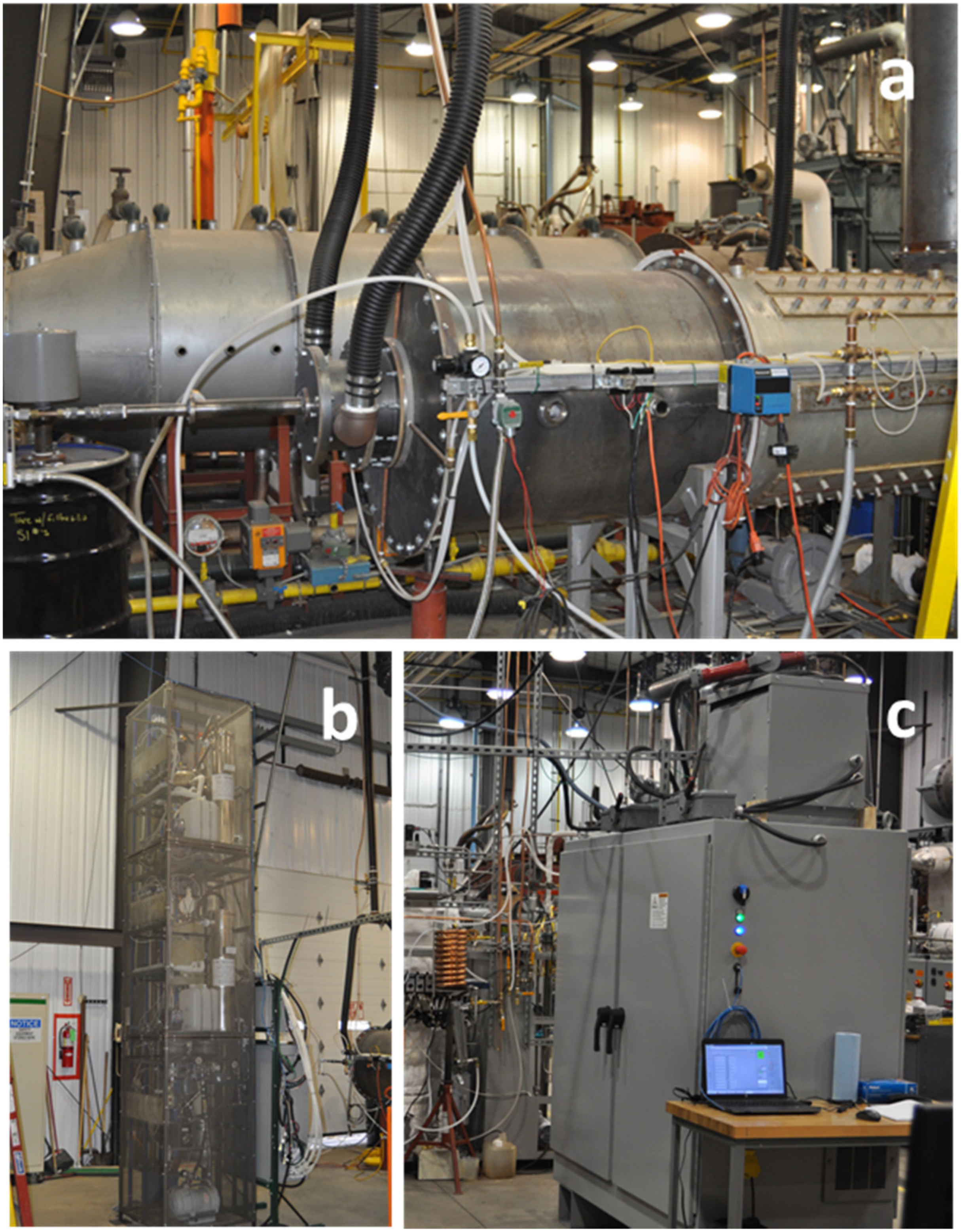

Figure 68. (a) GTI's pilot coal combustor used to generate coal-derived flue gas; (b) TDA's Moving bed prototype installed at GTI's combustion lab, (c) TDA's 4-bed VSA system installed at GTI's lab.

4.12.1 Removal of Contaminants in the flue gas at GTI

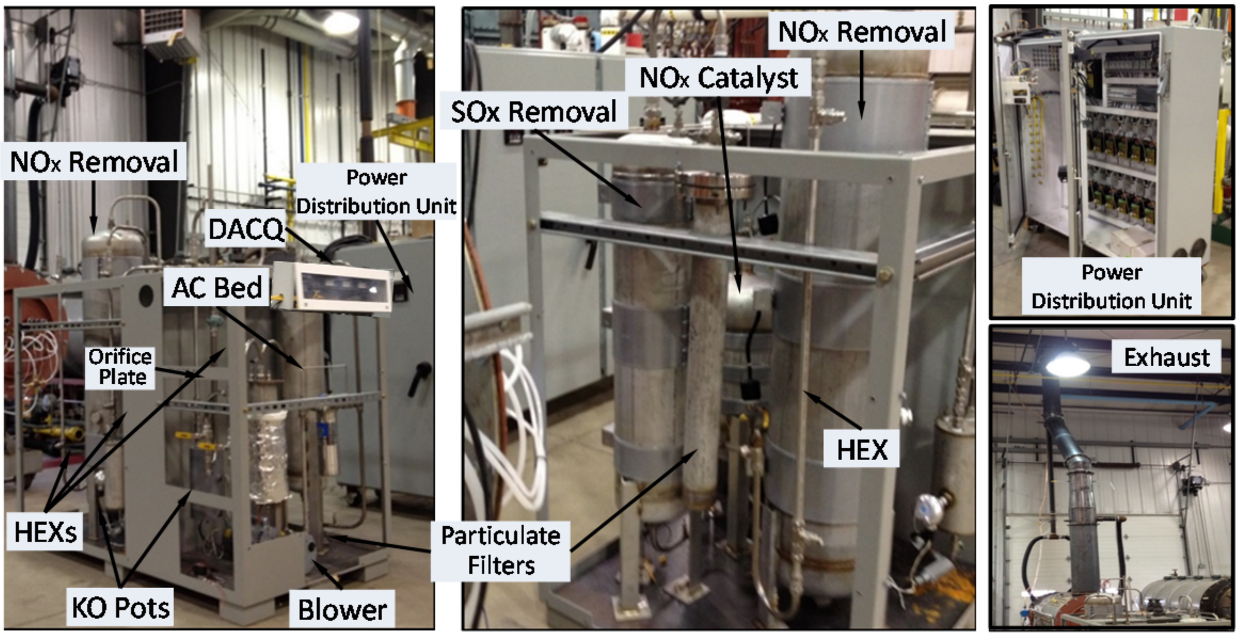

Figure 69. Pictures of the gas cleanup skid installed by GTI showing the NOx catalyst, NOx adsorber for NOx removal and SOx adsorber for removal of SOx fabricated under the State of Illinois funding as cost share through Illinois Clean Coal institute (ICCI).

In collaboration with TDA, GTI carried out the process and system design for the flue gas cleanup skid. NO_x andSO_2 control will be accomplished by materials provided by TDA. These were materials previously developed by TDA for NO_x and SO_2 removal under Small Business Innovation Research (SBIR) program. We used SulfaTrap^{TM}-SO for SO_2 scrubbing to sub ppmv concentration followed by a NO oxidation catalyst and a NO_2 scrubbing sorbent for NOx control at sub ppmv concentration. GTI had installed by-pass lines with needle valve to split the slipstream flue gas flow such that the exit NOx and SO2 concentration in the flue gas can be adjusted to simulate those expected downstream of a wet flue gas desulfurization (FGD) scrubber in the full-scale pulverized coal fired power plant.

However, when the NO_2 scrubbing sorbent was loaded into the reactor vessel and brought up in temperature it off-gassed heavily due to incomplete activation during preparation and the vapors condensed in the narrow channels of the heat exchanger used to cool the flue gas. This resulted in a blockage in the heat exchanger and prevented gas flow to TDA skids. TDA's sorbent has been tested at bench-scale under simulated flue gas containing up to 800 ppm NOx and 300 ppm SO2 without any loss in performance. Hence, we ended up by passing the NO_x removal portion of the gas cleanup skid in our tests at GTI

4.12.2 Moving Bed System Evaluations

Figure 70. Picture of prototype moving bed system built by TDA.

TDA's moving bed prototype unit can handle up to 2.3 ACFM flue gas flow and a sorbent circulation flow rate of up to 8 ft^3/h. Figure 58 shows picture of the prototype unit with steel reactors and lock hoppers. Figure 71 shows the test results from the moving-bed reactor. The sorbent in this unit is gravimetrically fed into the adsorption and regeneration reactors from a storage silo located at the top of the rig. A screw elevator was used to move the sorbent from a collection bin located at the bottom of the adsorption reactor and lifted back to the top storage bin. As shown in Figure 71, under the optimum solid recirculation rates (98.4 g/min), it was possible to achieve 94+% CO_2 removal efficiency. Figure 60 shows adsorption and regeneration pressure being 12.2 psia (ambient pressure in TDA facilities located in Golden, CO) and the regeneration pressure being between 3.5 to 4 psia. We also showed the sorbent maintained its integrity under the harsh operating conditions of the moving-bed reactor. After getting rid of the sharp edges and rough surfaces of the sorbent particles (after re-circulating the material for 100 cycles) the overall sorbent loss was maintained at less than 0.01% per hr of testing (6 full cycles). It should be noted that the operation with the small-scale screw extruder was much harder on the material than the mechanical stress generated by a belt conveyor selected for the actual full scale design. At GTI, we maximized the testing of the fixed bed system (the system of preference from our cost analysis) under coal-derived flue gas and the moving bed system was only operated briefly. Also, the availability of coal-derived flue gas was limited to the coal-furnace operation during regular business hours including start-up and shutdown.

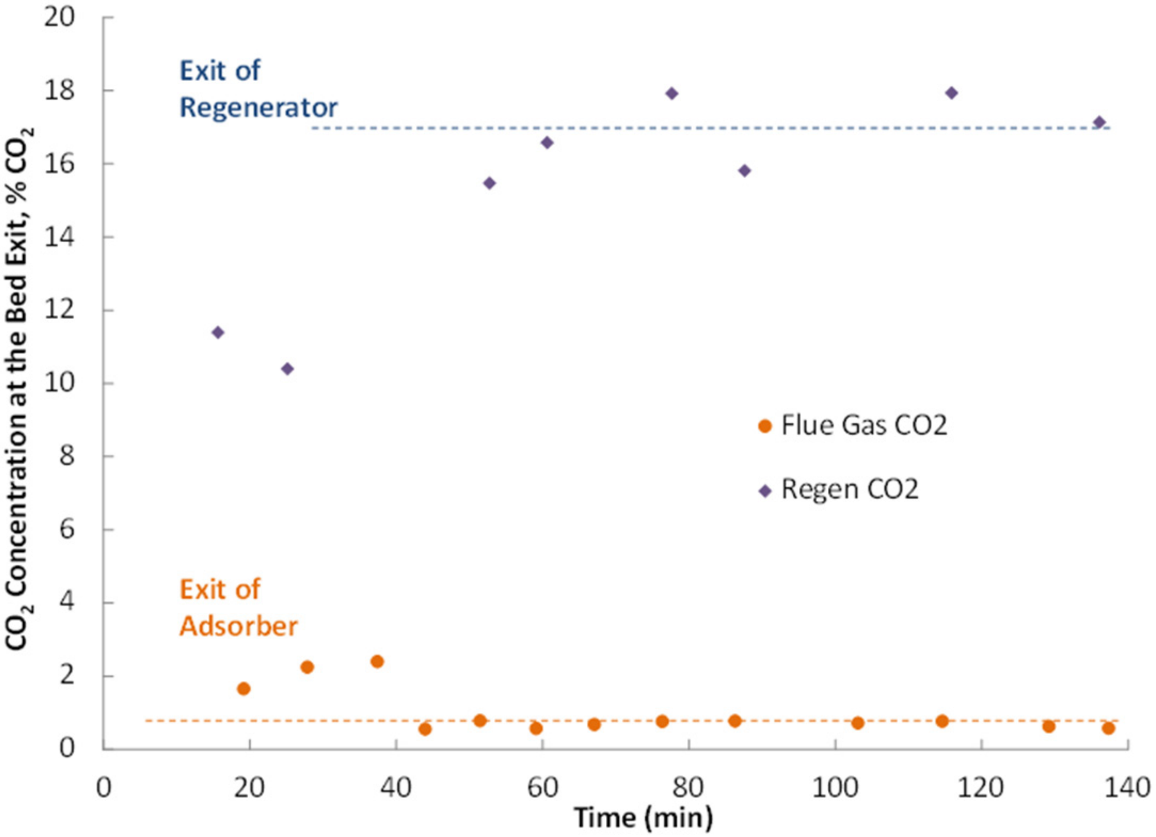

Figure 71. Representative results with moving bed unit. Flow rate of 1.4 scfm, CO_2 = 13.2%, P_{ads}=12.2 psia, P_{des}=3.5-4 psia, sorbent circulation rate of 98.3 g/min.

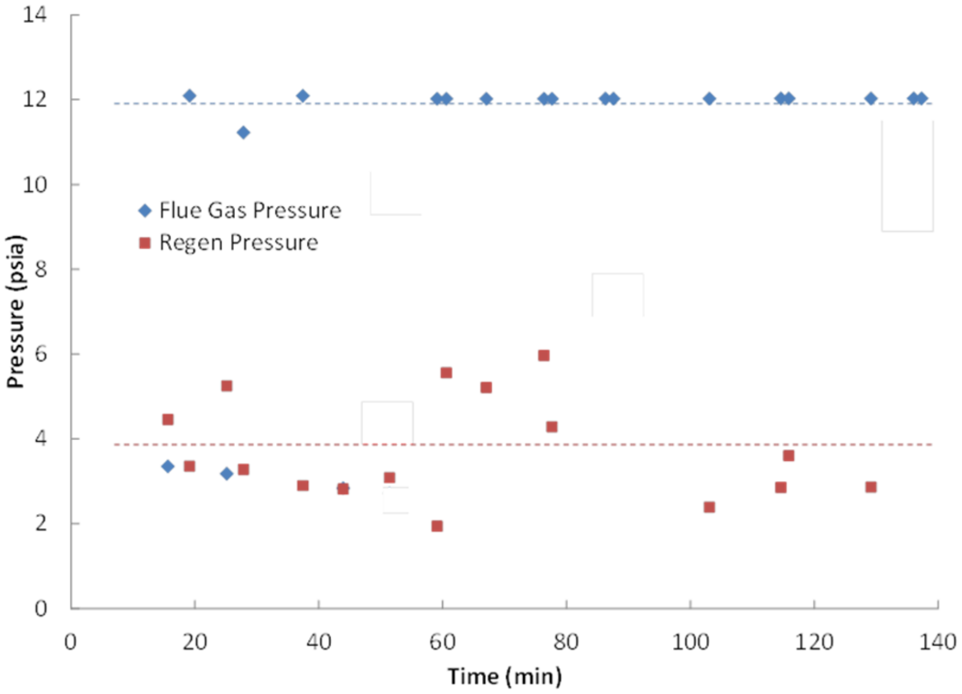

Figure 72. Flue gas and regeneration pressure as a function of time during vacuum swing cycles in the moving bed.

4.12.3 Fixed Bed System Evaluations

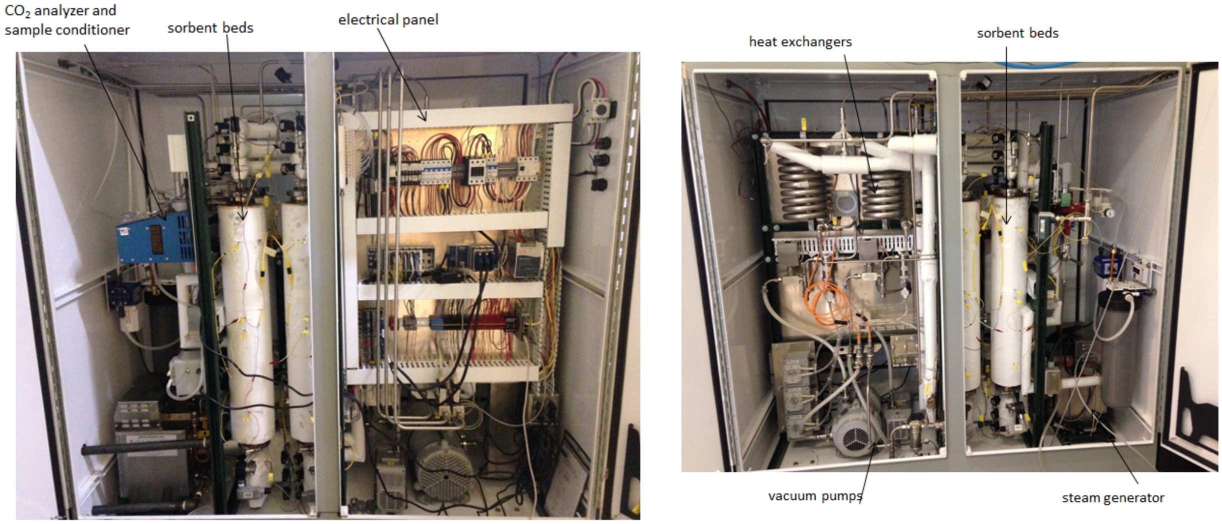

Figure 73. Pictures of the 4-bed VSA built by TDA.

We initially carried out tests with the fixed bed VSA system at TDA as part of the DOE sponsored SBIR Phase II project (DE-SC0006239) using simulated flue gas mixtures to optimize the VSA cycle scheme. Figure 73 shows the picture of the 4-bed VSA system built by TDA. The system is fully automated and can be controlled via a computer graphical user interface (see Figure 74). In the initial diagnostic VSA cycle tests we started with ambient temperatures VSA cycles with nitrogen purge using simulated flue gas containing 13%CO_2 in N_2. Figure 75 shows the pressure change (vacuum swing) in the 4-beds and outlet flue gas CO_2 concentration for the first cycle, the CO_2 leakage is high and it goes down to below 0.2% i.e., more than 98% CO_2 capture as the system reaches steady state as seen in Figure 76, which shows the same traces for cycle #4 with the cycle steps labeled and the duration of each step provided in the graphic.

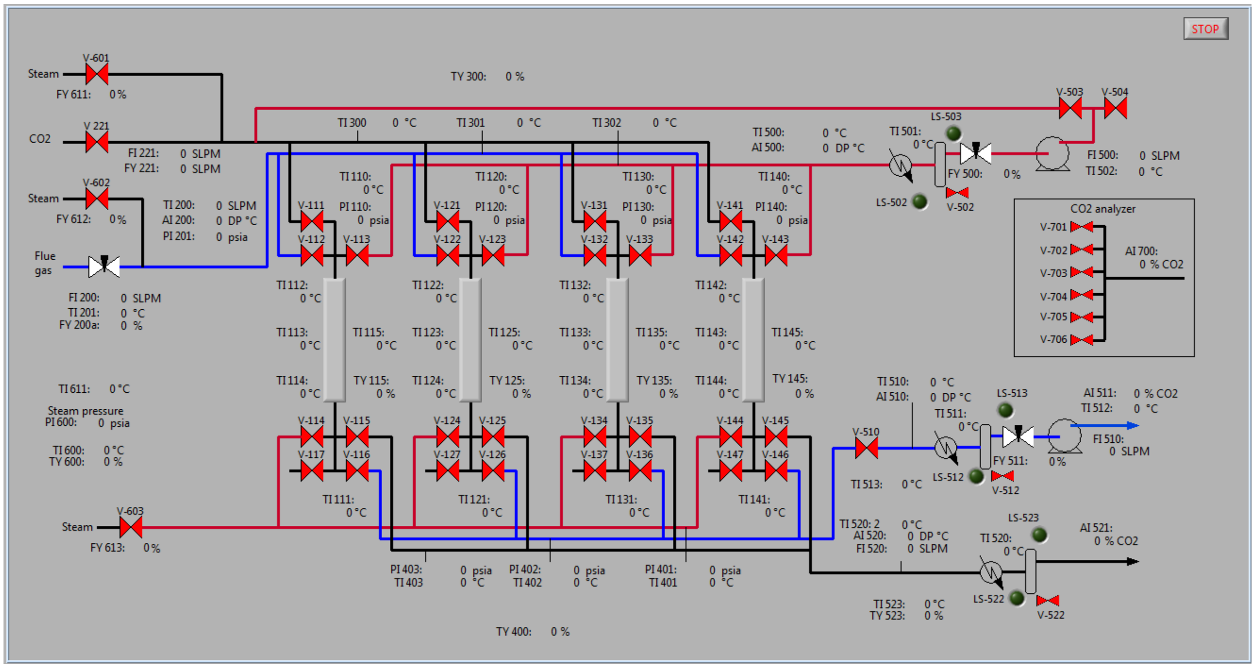

Figure 74. Screenshot of the user interface.

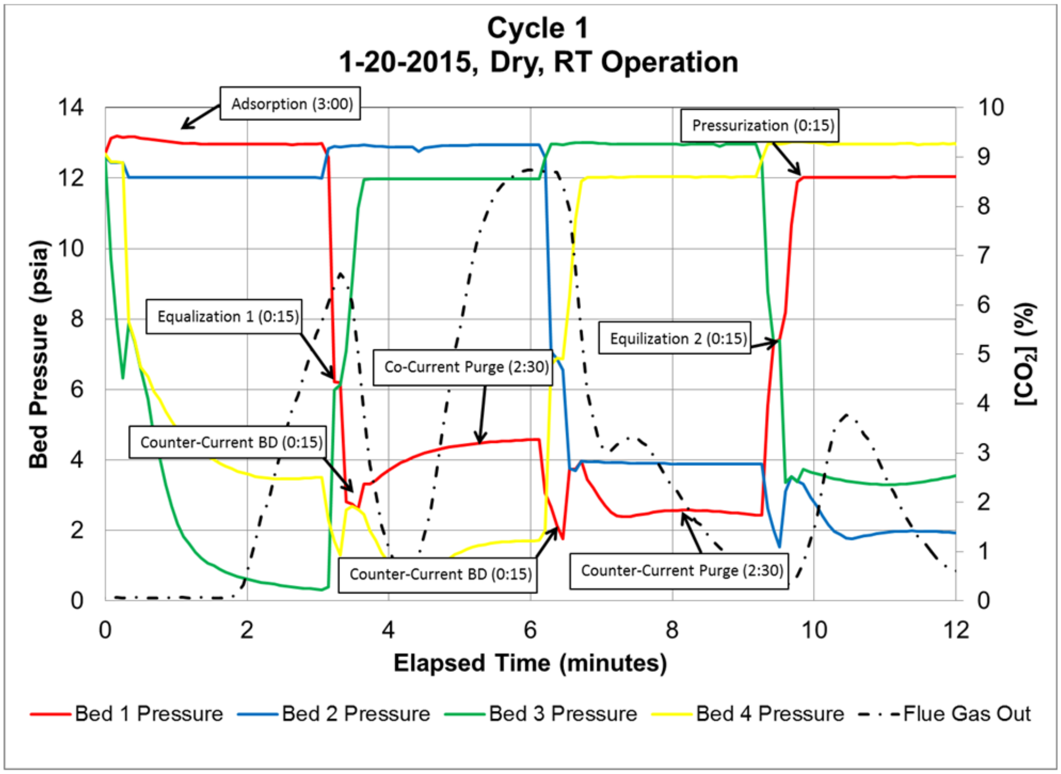

Figure 75. Vacuum swing in the 4-beds and outlet flue gas CO_2 concentration for Cycle #1.

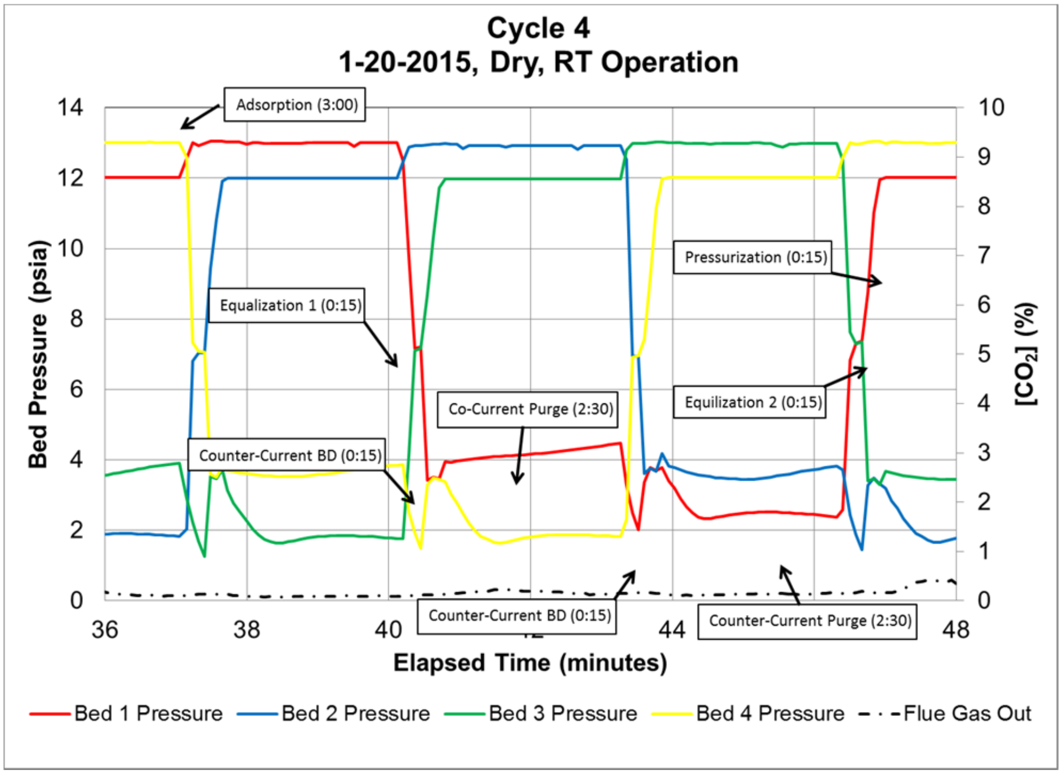

Figure 76. Vacuum swing in the 4-beds and outlet flue gas CO_2 concentration for Cycle #4.

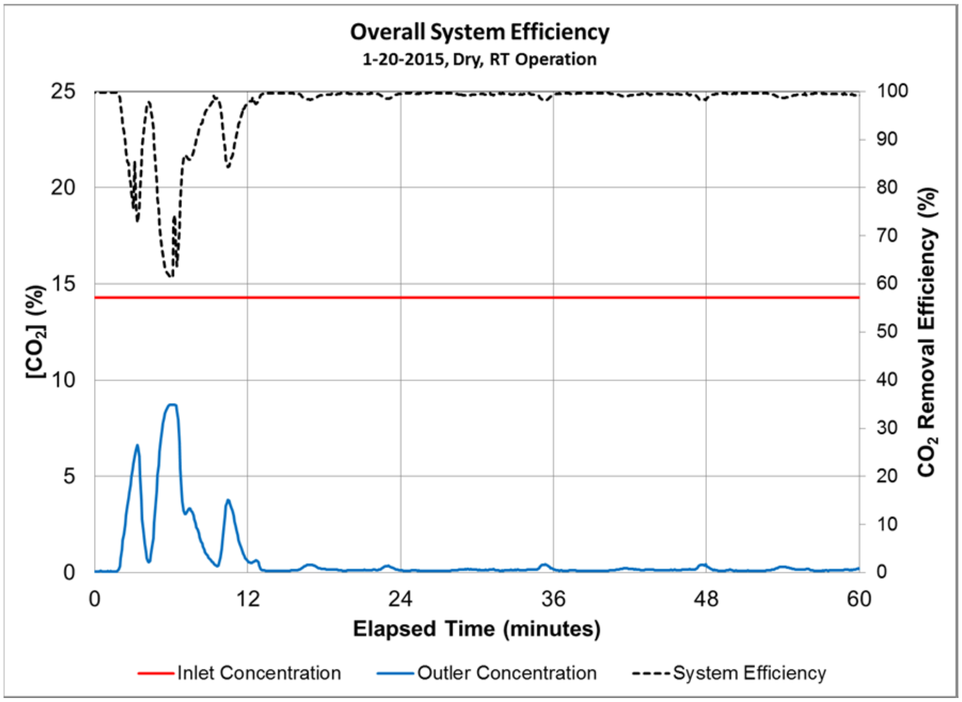

Figure 77. CO_2 removal efficiency as a function of time showing cyclic steady state.

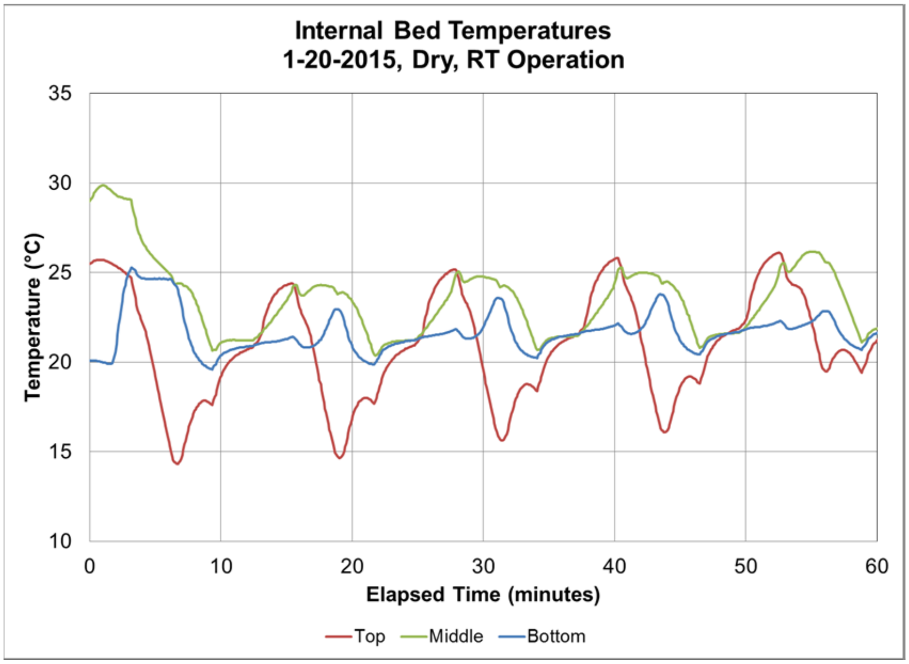

Figure 78. Bed #1 temperature as a function of time showing heat release due to heat of adsorption at different locations in the bed.

In these cycling tests the system was started as is without purging the 4-beds with N_2 to desorb any adsorbed CO_2. Figure 75 shows that the beds get saturated during adsorption step leading to CO_2 slippage on the flue gas out, but by cycle #4 as seen in Figure 76 the slippage is nearly zero as the beds have cleaned themselves up considerably. Figure 77 shows the outlet flue gas CO_2 concentration reaching a steady state with cycling and achieving more than 98% CO_2 capture. Figure 78 shows the temperature changes in bed #1 during the first 5 cycles. The temperature change is large near the top of the bed (flue gas inlet side) and it reduces as we reach the bottom of the bed (flue gas outlet side), which is expected as the total heat release is dependent on the amount of CO_2 adsorbed, which is the highest near the flue gas inlet side.

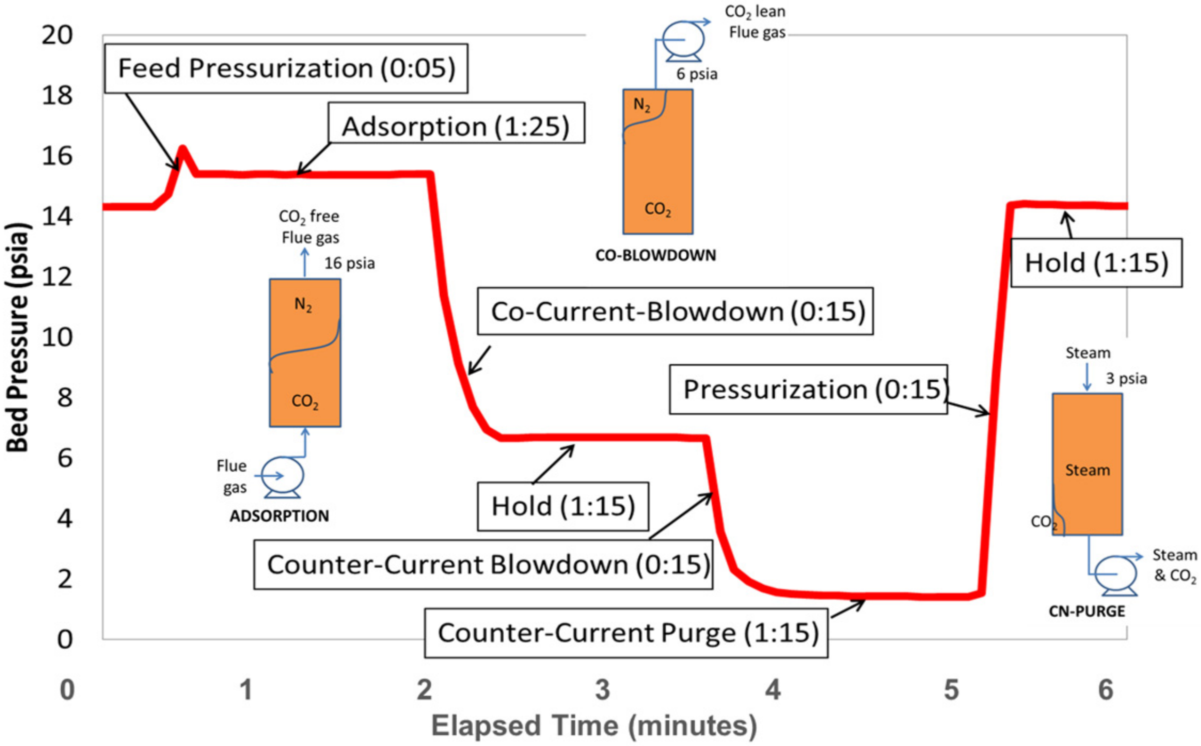

Figure 79. 4-bed vacuum swing adsorption cycle scheme with co-current blowdown and counter-current steam purge.

Next, we imlemented the steam purge during counter-current purge step. Figure 79 shows the typical pressure changes (vacuum swing) during the 4-bed VSA cycle process with stteam purge and a co-current blowdown step. Figure 80 shows a summary of the test results with the fixed bed system over 375 cycles where we optimized the adsorption step time and used a co-current blowdown step to 6 psia before the counter current blowdown and steam purge. We observed that the desorption CO_2 product purity was in excess of 95% when using this full 4-bed VSA cycle scheme. This shows that co-adsorption of nitrogen in the sorbent bed could be mitigated and the CO_2 desorption product purity can be improved to greater than 95% by using co-current blowdown step. This addresses DOE Peer Review Panel Recommendation 2 (R2) i.e., impact of co-adsorption of nitrogen needs to be evaluated on the CO_2 product purity. The use of intermediate co-current blowdown step resulted in the co-adsorbed nitrogen leaving the sorbnet beds from the adsorption product (CO_2 free flue gas out) end resulting in high CO_2 desorption product purity of 95+% on wet basis after condensation of steam in the desorption product at 35°C using cooling water.

Tests at GTI

Figure 81 shows the steady state performance of the fixed bed unit under coal derived flue gas in the presence of 400 ppm NO_x and 22 ppm SO_x. The fixed bed system achieved over 90% CO_2 capture with 95% CO_2 purity on a dry basis, this was achieved with an adsorption time of 2 min per bed i.e., a full cycle time of 8 min.

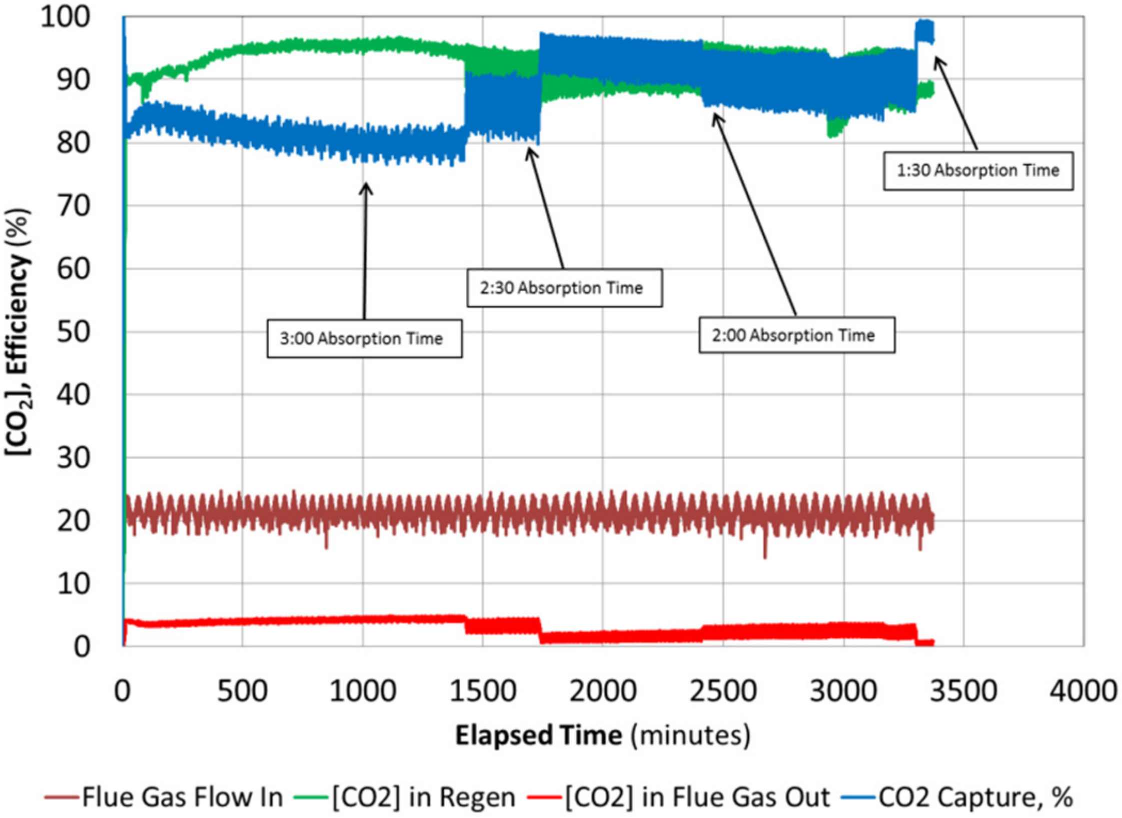

Figure 80. Results with fixed bed prototype unit at a flue gas flow rate of 1.0 scfm, CO_2 = 13.2%, P_{ads}=14 psia.

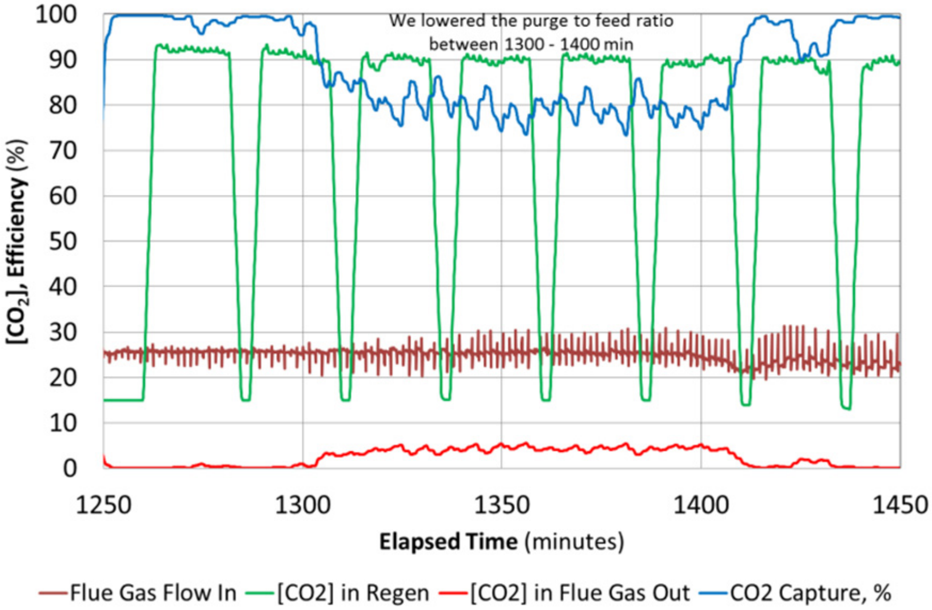

Figure 81. Results with fixed bed prototype unit at a flue gas flow rate of 1.0 scfm (wet basis), CO_2 = 13.2%, P_{ads}=14 psia under coal derived flue gas containing 22 ppm SOx and 400 ppm NOx.

Figure 82 shows 4-bed VSA system performance under Illinois #6 coal derived flue gas at GTI. The system removed 95+% CO_2 in the flue gas and the CO_2 product purity was above 90% and the sorbent maintained stable performance in the presence of 370 ppmv NOx and 50 ppmv SOx. Figure 83 shows a summary of the test results with real coal derived flue gas showing that the sorbent achieved greater than 95+CO_2 capture in these tests carried out at 1 scfm flue gas flow rate. We optimized the various operating parameters such as the adsorption step time (cycle time) and steam purge flow rate. Figure 84 shows the impact of purge steam: CO_2 ratio in the desorption product (counter-current purge step) on the system performance. A low Steam: CO_2 ratio of 0.44 still provided a high CO_2 capture efficiency of 95+%. Altogether, we tested the 4-bed VSA system for more than 1030 hours including the tests at TDA and GTI. At, GTI 4-bed VSA system was tested for more than 750 hours with stable performance achieving 90+% CO_2 capture (Figure 85).

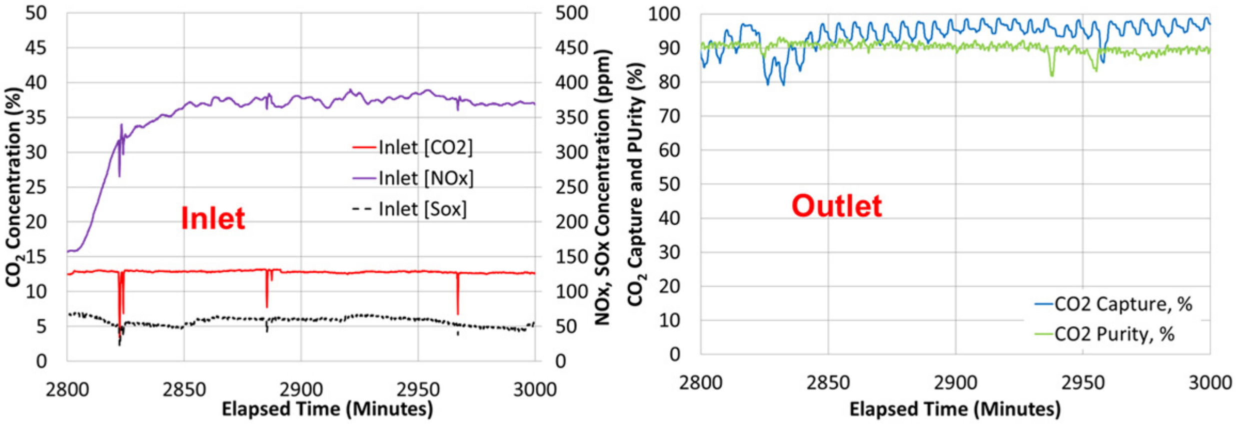

Figure 82. Results with fixed bed prototype unit at a Illinois #6 coal derived flue gas flow rate of 1.0 scfm (wet basis), CO_2 = 13.2%, P_{ads}=14 psia under coal derived flue gas containing 50 ppm SOx and 370 ppm NOx.

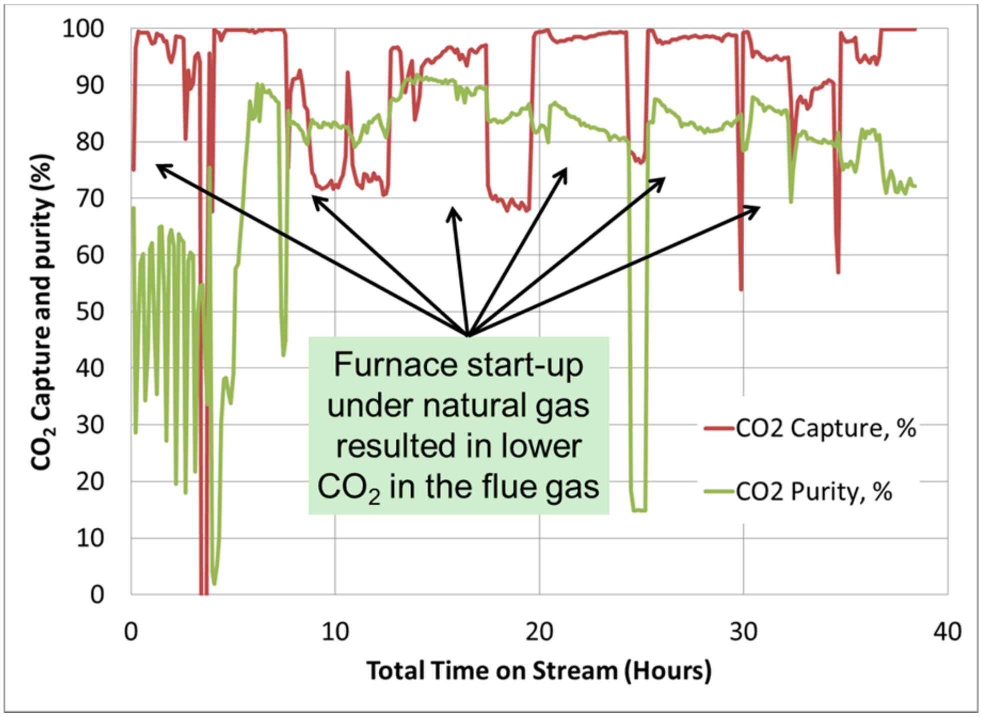
Furnace start-up under natural gas resulted in lower CO_2 in the flue gas

Figure 83. Performance summary of real coal derived flue gas tests at GTI.

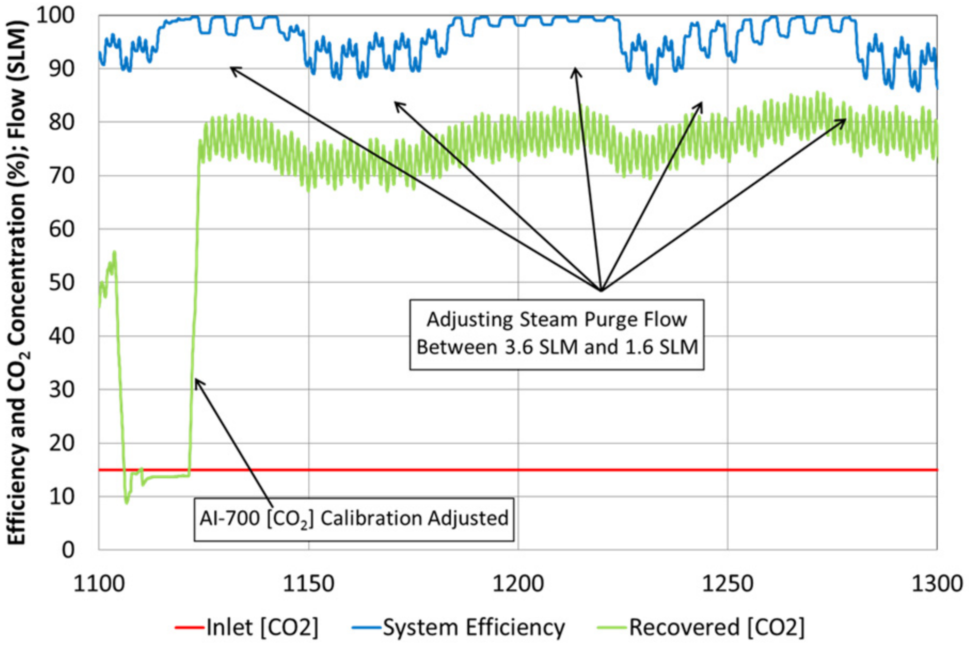

Figure 84. Optimization of Steam purge flow. Flue gas flow = 24 slpm, inlet CO_2 concentration = 15% vol., steam: CO_2 ratio varied between 0.44 to 1.

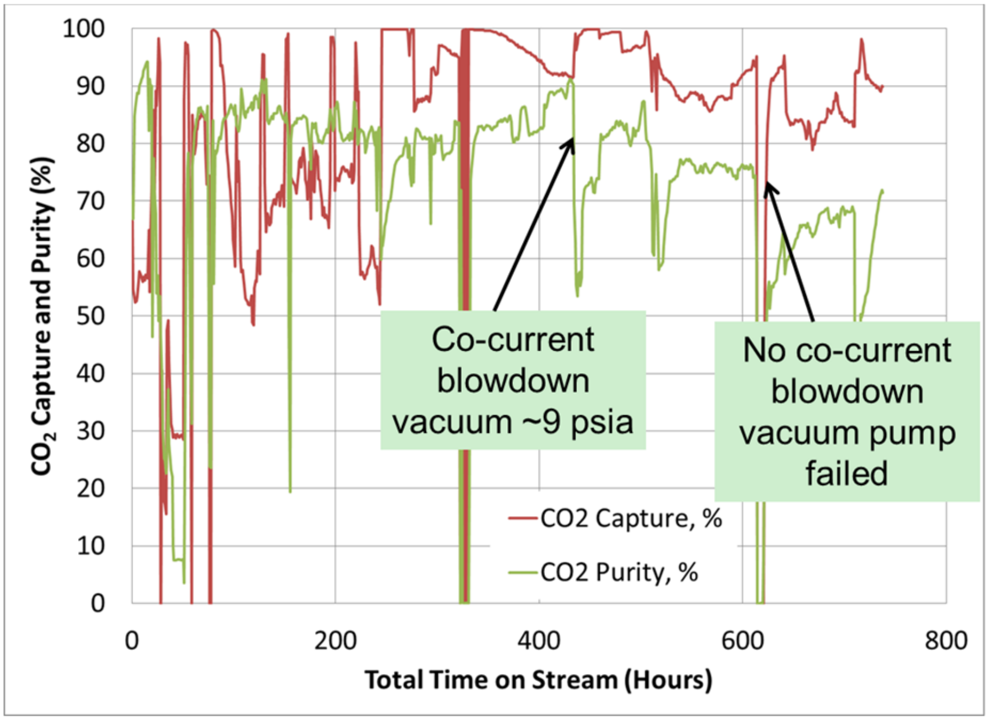

Figure 85. Performance summary of field tests at GTI.

Table 16. Summary of tests with the 4-bed VSA (fixed bed) prototype system.

Start Date	End Date	Cycle #	Coal-derived flue gas (hrs)	Simulated flue gas (hrs)	Total (hrs)
2/9/2015	2/9/2015	23	0	4.6	4.6
2/10/2015	2/11/2015	223	0	46.3	46.3
2/19/2015	2/19/2015	22	0	4.5	4.5
2/20/2015	2/20/2015	40	0	6.5	6.5
3/6/2015	3/7/2015	106	0	21.9	21.9
3/10/2015	3/11/2015	180	0	33.9	33.9
3/13/2015	3/16/2015	131	0	57.8	57.8
3/17/2015	3/17/2015	31	0	5.6	5.6
3/26/2015	3/27/2015	159	3.3	21	24.3
4/8/2015	4/10/2015	103	2.2	8.7	10.9
4/15/2015	4/17/2015	438	3	42.8	45.8
4/27/2015	5/1/2015	893	12.7	80.6	93.3
5/4/2015	5/7/2015	686	8.5	62.9	71.4
5/12/2015	5/15/2015	756	3.3	75.9	79.2
5/18/2015	5/22/2015	983	0	102.8	102.8
5/26/2015	5/29/2015	681	0	77.2	77.2
6/1/2015	6/5/2015	1159	0	102	102
6/8/2015	6/12/2015	1291	0	100.8	100.8
6/15/2015	6/19/2015	1316	0	100.4	100.4
6/22/2015	6/25/2015	574		43.7	43.7
Total		9795	33	1000	1033

Table 17. Summary of tests with the 4-bed VSA (fixed bed) prototype system at GTI.

Begin Date	End Date	Test	Flue Gas Type	P_{des}, psia	Avg. Bed T, °C	Horiba NO_X (ppmv)	Horiba SO_2 (ppmv)	Horiba CO (ppmv)	Horiba O_2 (%)
3/26	3/27	1	Coal/Sim	≈1.5	58	576.8	1.2	4.5	6.2
4/8	4/10	2	Coal/Sim	2.3-3.7	50	55.4	230.6	11.5	1.1
4/15	4/17	3	Coal/Sim	1.5–3.2	58	144.3	81.9	5.2	5.3
4/27	5/1	4	Coal/Sim	1.5-2.0	50–65	326.4	31.7	5.5	4.0
5/4	5/7	5	Coal/Sim	1.6-1.9	55	315.8	36.4	5.8	5.3
5/12	5/15	6	Coal/Sim	≈2.0	70	275.6	38.1	5.4	2.4
5/18	5/22	7	Simulated	≈2.0	70				
5/26	5/29	8	Simulated	≈2.3	70				
6/1	6/5	9	Simulated	≈3.3	70				
			Simulate						

4.12.4 CO_2 Capture from Natural Gas derived flue gas

As shown in Figure 86, in the coal derived flue gas tests at GTI, the furnace was started each day in the morning with natural gas firing and once the furnace and the downstream components reach their operating temperatures, the feed was shifted to Illinois #6 coal. TDA's 4-bed VSA system achieved more than 95% CO_2 capture with a CO_2 desorption product purity of 90% on wet basis after condensing the steam used in the purge with cooling water at 35°C. The summary of the combined results at GTI from multiple days with natural gas derived flue gas operation during start-up of the coal firing is shown in Figure 87. During these natural gas derived flue gas runs, when we used a VSA cycle scheme without co-current blowdown step the average CO_2 capture was 98+% and CO_2 purity achieved on wet basis for the desorption product (after cooling the flue gas down to 35°C) was ~60% by vol. while for a VSA cycle scheme with co-current blowdown step the average CO_2 capture was 95% and CO_2 purity achieved on wet basis for the desorption product was 85% by vol.

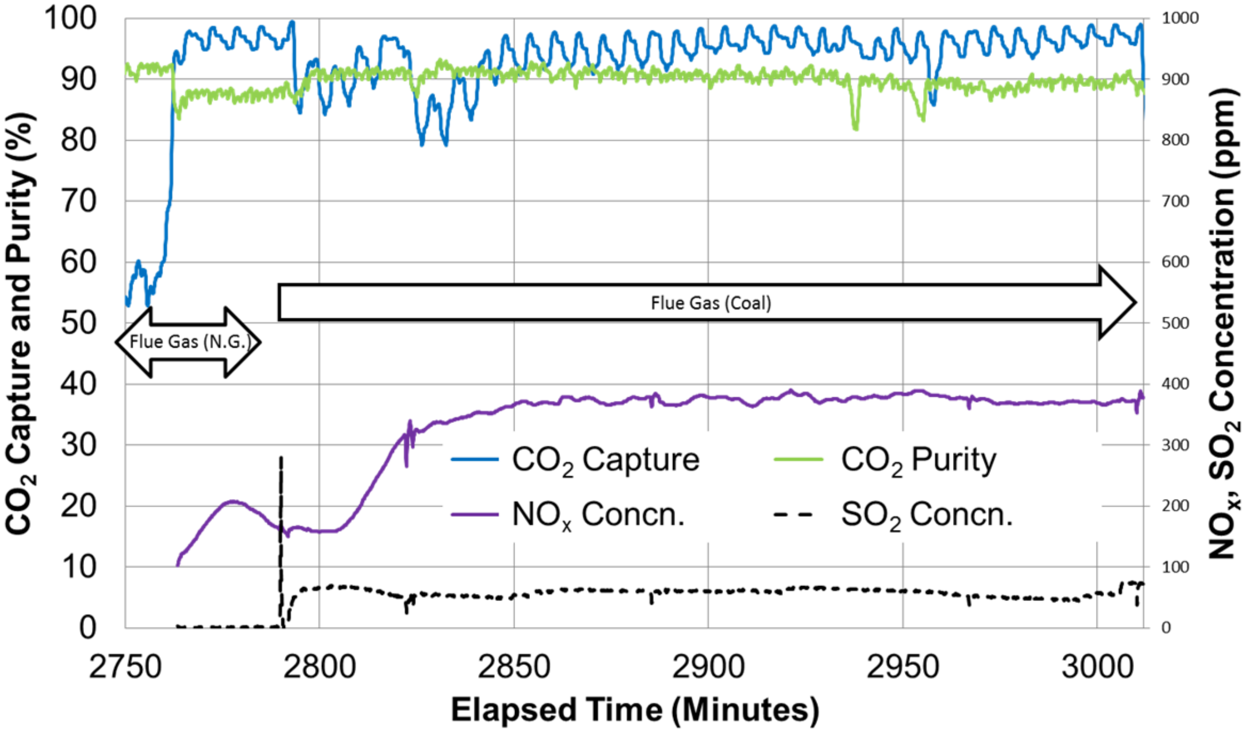

Figure 86. Results with fixed bed prototype unit at a flue gas flow rate of 1.0 scfm (wet basis), CO_2 = 13.2%, P_{ads}=14 psia under natural gas (start-up) and coal (steady state) derived flue

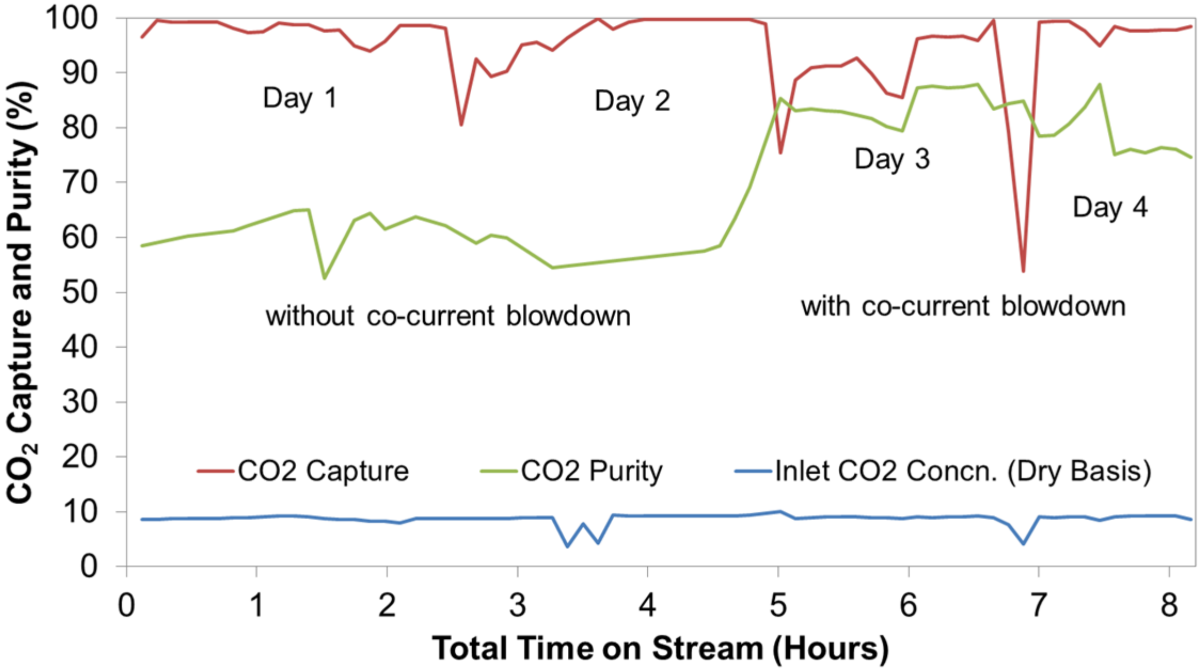

Figure 87. Summary of the tests at GTI with fixed bed prototype unit under natural gas derived flue gas flow rate of 1.0 scfm (wet basis), CO_2 = 9% (dry basis), P_{ads}=14 psia.

4.13 Task 13. System Analysis and Process Economic Evaluation

4.13.1 Advanced Packed Bed Design

Even though the fixed-bed contactors represent the simplest design and the least expensive housing option, the use of such reactors has been limited due to the potentially high pressure drop generated by these systems. Even in the rapidly cycling beds, because of the very large amounts of CO_2 to be removed, a significant inventory of sorbent must be placed into the flow path. Unfortunately, the conventional "pancake" reactor design (with very large diameter low depth beds with low aspect ratios) common for fixed-bed reactors used in similar applications will not be practical due to their large footprint and flow distribution issues. In our system, we use radially outflow reactors to house the sorbent. The reactor will resemble a traditional fixed-bed reactor, while the proper internal manifolds enable gas distribution in the radial direction allowing the flue gas to pass over a relatively thin bed of sorbent presented across the height of the reactor. The flue gas is introduced into the reactor via a common supply line from the top of the bed and is distributed into the two internal manifolds (as indicated by the arrows in Figure 88. The

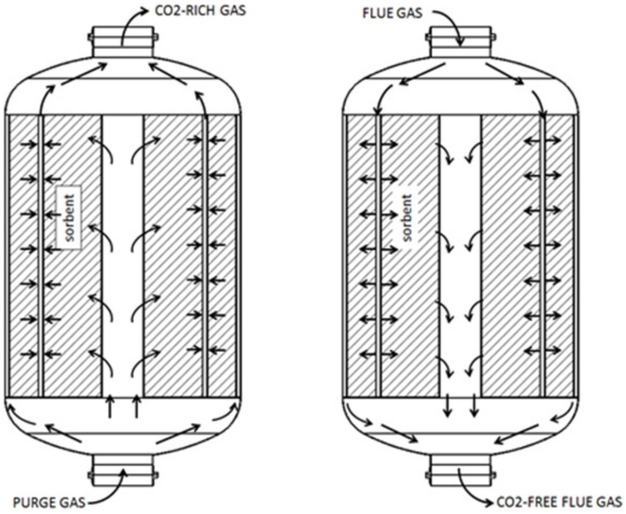

Figure 88. Radial flow full scale sorbent reactors in regeneration (left) and CO_2 adsorption (right).

CO_2 free flue gas is collected in separate internal exhaust manifolds which then merges into a single exhaust line and leaves the reactor at the top of the reactor.

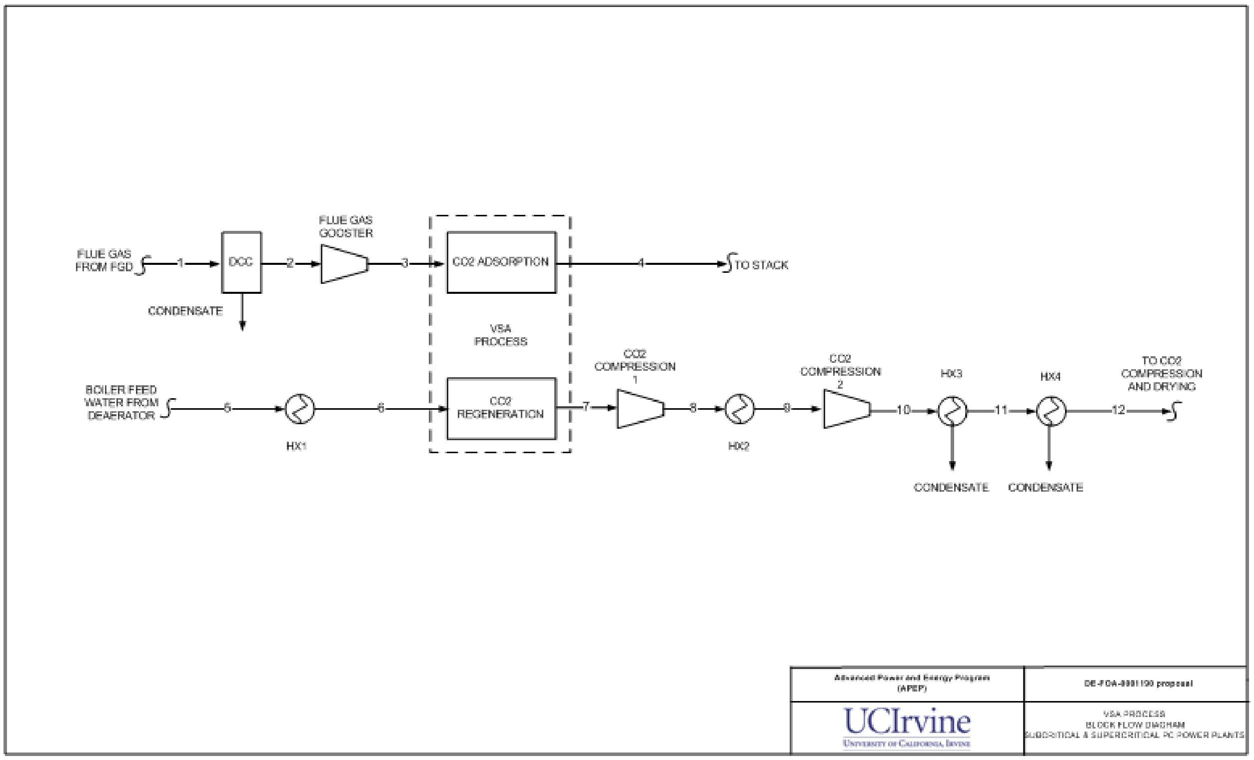

Figure 89. PFD around TDAs VSA based post combustion CO_2 capture system.

During the regeneration, pressure equalization of the beds moderates the sorbent pressure to 8.5 psia. A vacuum pump is used for further depressurization. The low pressure steam will be introduced at the bottom of the bed through the exhaust (three) manifolds where the CO_2 free flue gas has been removed. The steam also sweeps across the bed in the radial direction, but in the counter direction of the flue gas flow; the adsorbed CO_2 comes off from the surface and recovered, generating a 50% vol. CO_2/steam mixture (dry basis CO_2 purity of 95+%) at 0.18 bar at the regenerator exit after accounting for the pressure drop through the bed (the balance being ~50% vol. H_2O with some N_2 and O_2 impurities from the flue gas trapped within the sorbent pores). This off-gas from the regenerator is then compressed in a two-stage compressor to raise its pressure to 1.24 bar. The compression also raises the stream temperature to 182°C. We use this heat of compression to raise the low pressure steam (0.2 bar) used as the regenerator sweep gas. The low pressure steam is raised in two boilers following the compressors, providing 61°C saturated steam for the regeneration process. As the regeneration off-gas (mainly consisting of the released CO_2 and steam) goes through the compression and cooling steps, the water condenses and is recovered to feed back into the cycle. Following the two compressors in the regenerator, a product stream of 68.7% CO_2/steam mixture is produced at 77°C. The CO_2 is further concentrated and compressed in the compression/purification train.

Because the flue gas and the steam are at similar pressures and temperature, the transition from adsorption to regeneration (and vice versa) is very rapid, eliminating the need for multiple beds. We believe that 8 beds will be sufficient to all the transitions in a rapid cycling vacuum/concentration swing system. Based on the 2,326,545 lb/hr flue gas flow rate (the flow rate for AEP's 550MW Conesville #5 power plant), we expect only a 0.2 psid pressure drop across the bed.

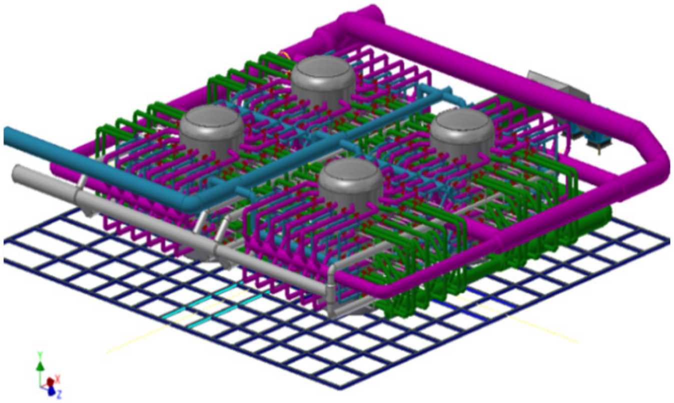

Figure 90. Stacked beds with external manifolds prepared by B&W.

Another unique advantage of the design is in the reduction in the number of flow selection valves to distribute the gases into the reactors. Combining all supply lines to the reactors into a single manifold (and distributing the gases internally in the reactor) requires only 1 valve per supply line per bed instead of 4 providing a 4X reduction in the number of valves for the operation of the system which was used in our early designs. In the initial fixed bed design carried out by B&W the gas flows during the adsorption and regeneration were distributed into "stacked" beds using external manifolds (Figure 90). This stacked bed design required 16 valves that had contributed to 25% of the overall costs. The radial outflow design represents a significant modification, substantially reducing the number of these valves per bed and hence the overall cost.

Figure 91. A commercial Round Louvre Valve.

We envision the valves used in our process to be similar to the Louvre Lock Valves that are available off-the-shelf and can be purchased at competitive costs (as little or no further design work is needed). Figure 10 shows a picture of the Louvre Damper Valves (DN 5600 mm with NICROFLEX sealing, rating T=400^{o}C, P_{diff}= 90 mbar) supplied to a DeNOx plant at the STEAG power station Herne, Germany. These valves are already designed to treat the desired gas volumes at the operating conditions of interest for similar application. We anticipate a straight forward integration into our system, providing substantial cost savings.

Like every CO_2 capture process, TDA's system also includes a section that compresses, intercools, recompresses and refrigerates the CO_2 for purification; finally recovering the liquid CO_2 so that it can be pumped to 2200 psig for sequestration. The CO_2 compression, condensation and purification train used in our process will be similar to that described by Ramezan (2007).

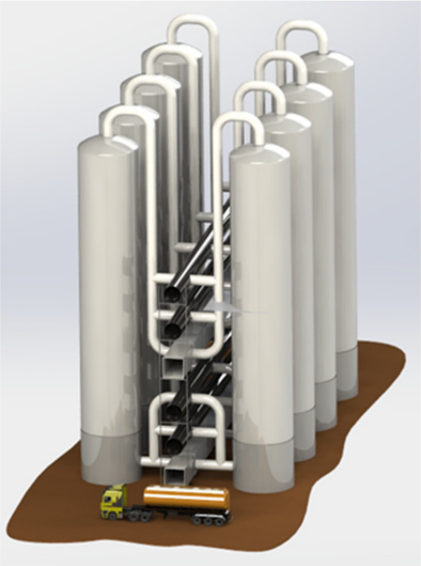

Figure 92. Full scale system.

Figure 92 shows the full scale CO_2 capture system for a 550 MW_e net power output. The system consists of 8-beds each 7.3 m (24 ft) in diameter and 33.5 m (110 ft) tall. The sorbent bulk density is 0.28 kg/L. All piping/ducting is insulated to prevent water condensation and the vessel manifolds is manufactured from 48” pipe. The inner and outer bed thicknesses are 47” and 28”, respectively (average bed thickness ~ 37.5”, which is similar to the bed length in the 4-bed field test unit). The design of the bed internals are as illustrated in Figure 88.

Impact of Sorbent Densification
We doubled the volumetric loading while retaining the gravimetric loading by increasing the bulk density of the sorbent pellets from 0.28 to 0.46 kg/L. The sorbent cost increased by $0.2 per kg increasing the initial sorbent cost by $0.5 MM (from $8.7 to $9.2 MM) while decreasing the reactor height from 110 to 72 ft (while keeping the same reactor internals), which reduced the VSA system Cost from $276 MM to $217 MM. Figure 93 shows the reduction in bed size achieved for the full scale TDA’s CO_2 capture system from increase in sorbent bulk density.

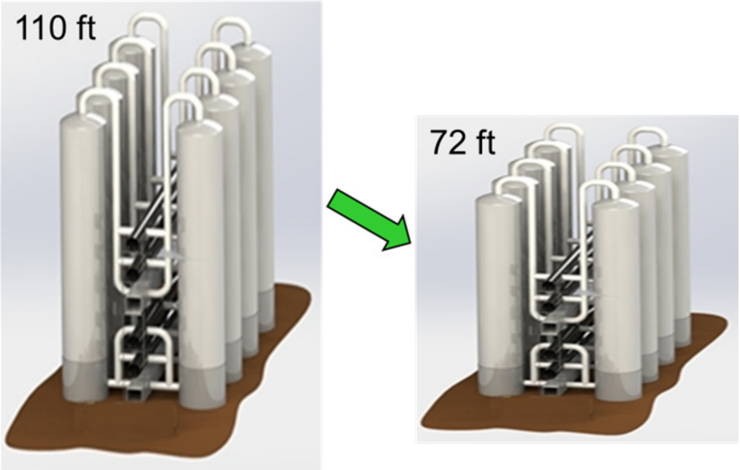

Figure 93. Full scale VSA system size using higher density sorbent.

Direct Contact Cooler
Flue gas from the wet FGD process is saturated at 58°C, which could result in condensation of water in the sorbent beds or in the lines, which are not desired. Hence, we adopted a design used by Fluor for their Econoamine Process to keep the flue gas entering the adsorbers at 58°C while the humidity is well below the saturation levels to prevent condensation. The condensation issue is inherent for all CO_2 capture processes (solvent, sorbent or membrane based) and not specific to TDA’s VSA system. No one desires to use their system as a condenser and almost all processes prefer lower temperature operation. The direct contact cooler used in TDA’s process has 5-6 MWe energy penalty (energy for water pump) and the flue gas comes out at <45°C dew point (this is significantly higher than that targeted for other sorbent based CO_2 capture systems). Table 18 summarizes the energy penalty associated with direct contact coolers against the DOE no capture cases (Case 9 and Case 11) in the DOE study (DOE/NETL-2010/1397 Rev 2a, DOE/NETL-341/082312). The direct contact cooler (DCC) uses the very same water removed from the flue gas (no net water consumption in the process).

Table 18. Energy penalty associated with the direct contact cooler used in TDA process.

	Case 9	Case 10	Subcritical	Case 11	Case 12	Supercritical
	DOE	TDA	Diff.	DOE	TDA	Diff.
Circulating Water Pump	5,250	9,053	3,803	4,730	8,147	3,417
Cooling Tower Fans	2,720	4,676	1,956	2,440	4,113	1,673
Condensate Pumps	890	1,053	163	800	882	82
Total (DCC & Steam purge)			5,922			5,172

Stand-alone Steam Generation

In TDA's CO_2 capture system, the regeneration process is a stand-alone process, which does not use steam from the power plant. This allows the steam generator to operate with the same efficiency and gross output per kg of coal used as in the no-capture cases (Case 9 and Case 11 in DOE study). We do not need very high purity steam and the steam needed in our CO_2 capture system for the purge (during CO_2 desorption) is generated from compression of the CO_2 from vacuum to 18 psia as shown in the Figure 94. The steam generated at the plant is HP steam and has a high heating value while the steam used for purge in our system is at 3 psia and has very low heating value. In the field test we showed that the steam usage can be reduced from 1 mole per mole of CO_2 to 0.44 mole per mole of CO_2 i.e., from 410,000 lb/hr to 186,500 lb/hr. It is still only a fraction of that used by amines (1,784,175 lb/hr). The steam used by TDA's VSA system is at 70°C (200°F) and 3 psia, which has very low heating value compared to that used by amines at 291°C (565°F) and 73.5 psia (Heating value of steam used by TDA's VSA system is 13 MW compared to the 141 MW for the amine based system).

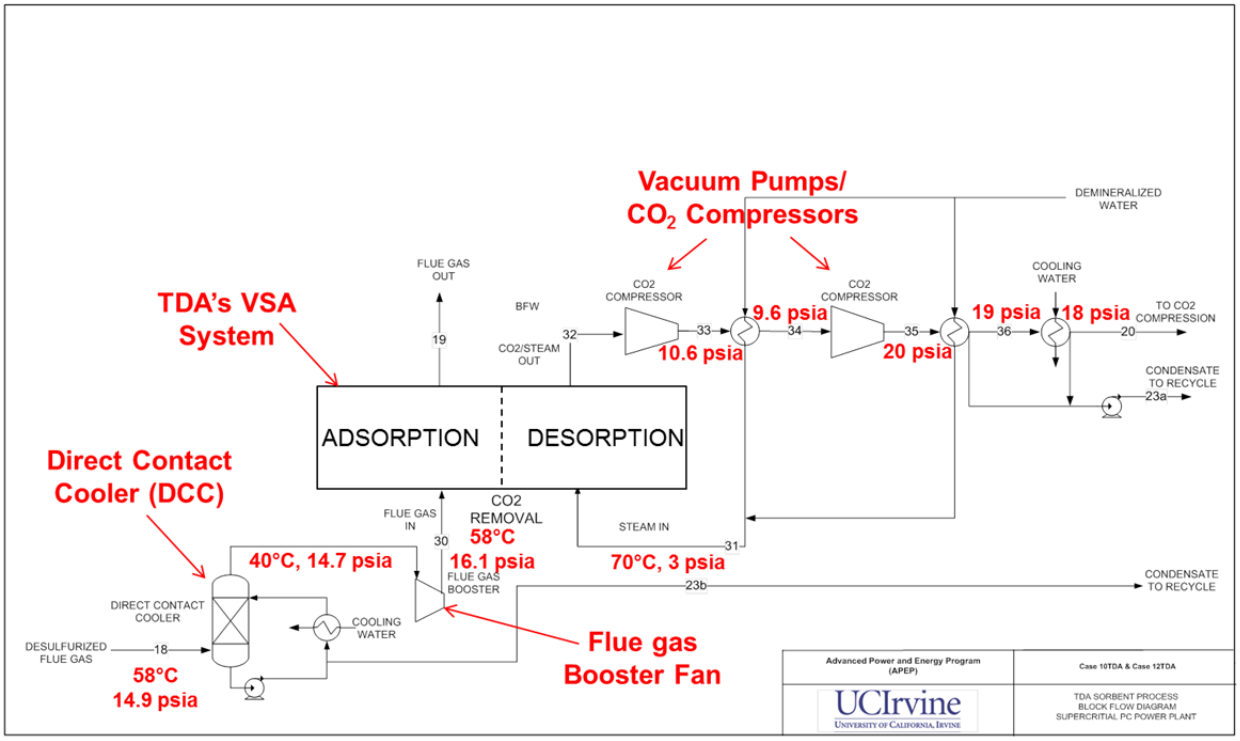

Figure 94. TDA's VSA based CO_2 capture process.

Process Improvements in BP3

In the beginning of BP3, we extended the process simulation results to include the super-critical power plants in addition to the sub-critical power plants, which was modeled in BP1 & BP2. Based on the field test results, we also reduced the amount of steam used to purge the sorbent beds under vacuum at 0.2 atm from 1 mol steam per mol CO_2 to 0.44 mol steam per mol. CO_2. We also extended the life of the sorbent beds to 2 years. We also removed the LP steam extraction and cooling water use to maintain the isothermal operation of the sorbent beds. This allows the bed to swing in temperatures as the CO_2 is adsorbed and most of the heat is stored in the solid sorbent and extracted back for desorption. The impact on the overall power plant performance from these design changes in the case of both sub-critical and super-critical power plants are shown in Table 19 and for reference DOE amine Capture Case 10 and Case 12

(DOE/NETL-2010/1397 Rev 2a, DOE/NETL-341/082312) are also included. Each case generates the same amount of electricity on a net basis, nominal 550 MW_e of net power and the amount of fuel varies in proportion to the heat rate. Table 20 and Table 21 summarize the overall plant costs and the cost of electricity (COE) for the different TDA design cases and the reference amine Cases 10 and 12.

VSA Cycle Improvements

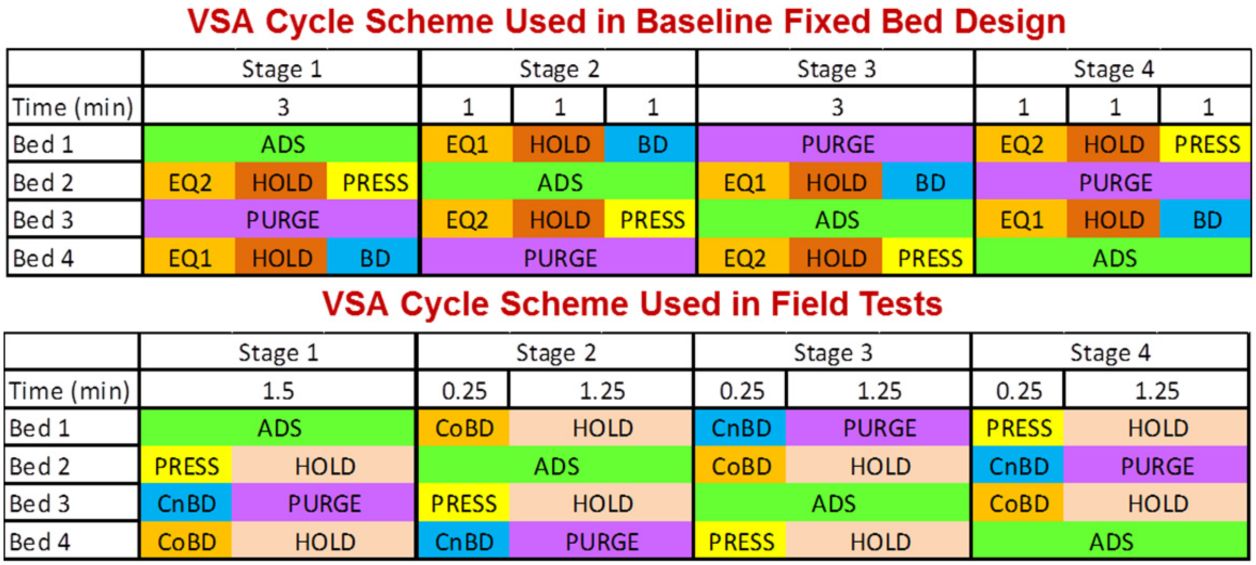

VSA Cycle Scheme Used in Baseline Fixed Bed Design

	Stage 1			Stage 2			Stage 3			Stage 4		
Time (min)	3			1	1	1	3			1	1	1
Bed 1	ADS			EQ1	HOLD	BD	PURGE			EQ2	HOLD	PRESS
Bed 2	EQ2	HOLD	PRESS	ADS			EQ1	HOLD	BD	PURGE		
Bed 3	PURGE			EQ2	HOLD	PRESS	ADS			EQ1	HOLD	BD
Bed 4	EQ1	HOLD	BD	PURGE			EQ2	HOLD	PRESS	ADS		

VSA Cycle Scheme Used in Field Tests

	Stage 1		Stage 2		Stage 3		Stage 4	
Time (min)	1.5		0.25	1.25	0.25	1.25	0.25	1.25
Bed 1	ADS		CoBD	HOLD	CnBD	PURGE	PRESS	HOLD
Bed 2	PRESS	HOLD	ADS		CoBD	HOLD	CnBD	PURGE
Bed 3	CnBD	PURGE	PRESS	HOLD	ADS		CoBD	HOLD
Bed 4	CoBD	HOLD	CnBD	PURGE	PRESS	HOLD	ADS	

Figure 95. VSA cycle comparison – Baseline fixed bed design vs those used in field tests.

The baseline VSA cycle schemes used in our fixed bed design in BP2 used a pressure equalization step as shown in Figure 95. In the field tests we observed that Co-current Blowdown (CoBD) provided the same benefits in improving the CO_2 product purity as a pressure equalization step. The use of CoBD also decouples the beds providing flexibility in VSA cycle scheduling. The cycle scheme we used in the field tests is also shown in Figure 95. The overall cycle time for the 4-bed VSA cycle scheme used in the field tests is 6 min with adsorption step time at 1.5 min and the purge time at 1.25 min. The HOLD time is about 2.5 min out of 6 min. In the baseline scheme for the fixed bed system used in system design and sizing, the HOLD time was 2 min out of 12 min. Ideally, this HOLD time needs to be completely eliminated so that we get full utilization of the sorbent beds at all times. This is now possible with the elimination of pressure equalization steps and the use of CoBD step alone decoupling the operation of the individual beds. We have discussed these advanced VSA cycle scheme without any HOLD step as part of the sensitivity analysis.

Table 19. Performance summary of BP3 from UCI’s Aspen modeling of TDA’s post combustion CO_2 capture process.

CASE NO.		10	11aa	11aa-Rev	10TDA	12	12-1VSA	12-1VSA-Rev	12TDA
CASE DEVELOPED BY		DoE	UCI	UCI	UCI	DoE	UCI	UCI	UCI
BOILER TYPE		Subcritical	Subcritical	Subcritical	Subcritical	Supercritical	Supercritical	Supercritical	Supercritical
CO2 CAPTURE TECHNOLOGY		Amine	VSA	VSA	VSA	Amine	VSA	VSA	VSA
CASE DESCRIPTION		As reported in DoE report	Fixed bed system using steam for regeneration & 1 yr sorbent life	Fixed bed system using less steam for regeneration & 2 yr sorbent life	Fixed bed system using less steam for regeneration & 2 yr sorbent life	As reported in DoE report	Fixed bed system using steam for regeneration & 1 yr sorbent life	Fixed bed system using less steam for regeneration & 2 yr sorbent life	Fixed bed system using less steam for regeneration & 2 yr sorbent life
VSA HEAT OPTION	UNITs	N/A	LP Steam & Cooling water	LP Steam & Cooling water	None	N/A	LP Steam & Cooling water	LP Steam & Cooling water	None
STEAM TURBINE POWER	Kwe	672,700	707,748	687,214	678,804	662,800	696,195	677,749	669,874
TOTAL AUXILIARY CONSUMPTION	Kwe	122,740	157,748	137,214	128,804	112,830	146,195	127,749	119,874
NET POWER OUTPUT	Kwe	549,960	550,000	550,000	550,000	549,970	550,000	550,000	550,000
AUXILIARY LOAD SUMMARY									
FEED HANDLING	Kwe	6,090	5,395	5,223	5,107	5,610	5,017	4,884	4,750
ASH HANDLING	Kwe	800	709	686	671	740	662	644	627
PRIMARY AIR FANS	Kwe	1,960	1,736	1,681	1,644	1,800	1,613	1,570	1,527
FORCED DRAFT FANS	Kwe	2,500	2,215	2,144	2,097	2,300	2,057	2,002	1,947
INDUCED DRAFT FANS	Kwe	12,080	10,702	10,360	10,131	11,120	9,945	9,681	9,415
SCR	Kwe	70	62	60	59	70	63	61	59
BAGHOUSE	Kwe	100	89	86	84	100	89	87	85
FGD	Kwe	4,470	3,956	3,830	3,745	4,110	3,672	3,575	3,476
CO2 REMOVAL UNIT	Kwe	22,400	9,459	9,157	9,402	20,600	8,785	8,552	8,733
CO2 COMPRESSION	Kwe	48,790	102,476	83,908	80,390	44,890	95,178	78,366	74,728
MISCELLANEOUS BALANCE OF PLANT	Kwe	2,000	1,772	1,715	1,677	2,000	1,789	1,741	1,693
STEAM TURBINE AUXILIARIES	Kwe	400	421	409	404	400	420	409	404
CONDENSATE PUMPS	Kwe	700	1,080	1,053	1,030	560	906	882	868
CIRCULATING WATER PUMPS	Kwe	11,190	9,493	9,053	7,429	10,100	8,551	8,147	6,751
GROUND WATER PUMPS	Kwe	1,020	809	772	694	910	728	694	609
COOLING TOWER	Kwe	5,820	4,903	4,676	1,869	5,230	4,317	4,113	1,887
TRANSFORMER LOSSES	Kwe	2,350	2,472	2,401	2,371	2,290	2,405	2,342	2,314
% NET PLANT EFFICIENCY, HHV	%	26.20	29.53	30.50	31.19	28.40	31.79	32.66	33.58
NET HEAT RATE	KJ/KWH	13,764	12,192	11,804	11,542	12,663	11,324	11,024	10,720
CHANGE IN NET HEAT RATE OVER DoE REPORT CASE	%		-11.42%	-14.24%	-16.14%		-10.57%	-12.94%	-15.34%
CONDENSER COOLING DUTY	10^6 KJ/H	2,034	2,929	2,859	3,002	1,737	2,603	2,534	2,681
CONSUMABLES									
AS-RECEIVED FEED	KG/H	278,956	247,128	239,246	233,946	256,652	229,527	223,443	217,292
LIMESTONE SORBENT FEED	KG/H	28,404	25,541	24,727	24,179	25,966	23,572	22,947	22,316
CO2 SORBENT INITIAL FEED	KG	0	3,050,522	2,953,230	2,886,991	0	2,833,263	2,758,161	2,682,026
CO2 SORBENT ANNUAL FEED	KG/YR	0	1,525,261	1,476,615	1,443,495	0	1,416,631	1,379,080	1,341,013
RAW WATER USAGE	M^3/MIN	42.5	33.7	32.1	29.7	38.1	30.3	28.9	26.8
THERMAL INPUT	KWT HHV	2,102,643	1,862,733	1,803,322	1,763,370	1,934,519	1,730,067	1,684,207	1,637,841
CARBON CAPTURED	%	90.0	90.0	90.0	90.0	90.0	90.0	90.0	90.0

Table 20. Overall plant cost comparison, 2011 installed cost ($1,000) by Unit.

CASE NO.	10	11aa	11aa-Rev	10TDA	12	12-1VSA	12-1VSA-Rev	12TDA
CASE DEVELOPED BY	DoE	UCI	UCI	UCI	DoE	UCI	UCI	UCI
BOILER TYPE	Subcritical	Subcritical	Subcritical	Subcritical	Supercritical	Supercritical	Supercritical	Supercritical
CO2 CAPTURE TECHNOLOGY	Amine	VSA	VSA	VSA	Amine	VSA	VSA	VSA
CASE DESCRIPTION	As reported in DoE report	Fixed bed system using steam for regeneration & 1 yr sorbent life	Fixed bed system using less steam for regeneration & 2 yr sorbent life	Fixed bed system using less steam for regeneration & 2 yr sorbent life	As reported in DoE report	Fixed bed system using steam for regeneration & 1 yr sorbent life	Fixed bed system using less steam for regeneration & 2 yr sorbent life	Fixed bed system using less steam for regeneration & 2 yr sorbent life
VSA HEAT OPTION	N/A	LP Steam & Cooling water	LP Steam & Cooling water	None	N/A	LP Steam & Cooling water	LP Steam & Cooling water	None
UNIT	2011 Installed Cost ($1000)							
Coal & sorbent handing, prep & feed	87,949	81,439	79,971	78,844	83,341	77,819	76,506	75,165
Feedwater & Misc. BOP Systems	119,683	108,350	107,998	104,877	123,565	124,706	110,002	108,561
PC boiler	401,917	371,239	360,517	354,986	437,215	465,975	397,546	389,960
Flue gas cleanup	208,901	182,024	177,768	184,141	196,119	122,680	168,733	174,097
CO2 removal	531,906	229,515	217,177	216,190	505,963	222,573	208,449	206,844
CO2 compression & drving	91,699	84,392	82,740	81,603	87,534	81,025	79,708	78,358
Ductwork and Stack	50,150	49,077	27,084	26,910	45,092	4,106	24,697	24,489
Steam turbine generator + auxiliaries	162,583	164,512	162,304	161,272	166,965	177,449	167,071	165,848
Cooling water system	78,552	77,506	75,292	78,618	73,311	72,917	70,591	73,861
Ash handling systems	19,116	17,862	17,541	17,322	18,252	17,145	16,889	16,627
Accessory electric plant	100,885	111,605	104,857	102,579	100,255	90,534	104,544	102,317
Instrumentation & controls	30,822	32,350	31,902	31,734	31,053	32,585	32,131	31,982
Improvement to site	18,462	18,413	18,253	18,237	18,332	18,256	18,175	18,153
Buildings & structures	75,259	74,813	74,394	74,212	72,402	71,937	71,688	71,471
Total	1,977,884	1,603,097	1,537,798	1,531,524	1,959,399	1,579,707	1,546,731	1,537,733
Total $/kW	**3,596**	**2,915**	**2,796**	**2,785**	**3,563**	**2,872**	**2,812**	**2,796**

Table 21. Cost of electricity comparison (2011 $, CCF = 0.1243).

CASE NO.	10	11aa	11aa-Rev	10TDA	12	12-1VSA	12-1VSA-Rev	12TDA
CASE DEVELOPED BY	DoE	UCI	UCI	UCI	DoE	UCI	UCI	UCI
BOILER TYPE	Subcritical	Subcritical	Subcritical	Subcritical	Supercritical	Supercritical	Supercritical	Supercritical
CO2 CAPTURE TECHNOLOGY	Amine	VSA	VSA	VSA	Amine	VSA	VSA	VSA
CASE DESCRIPTION	As reported in DoE report	Fixed bed system using steam for regeneration & 1 yr sorbent life	Fixed bed system using less steam for regeneration & 2 yr sorbent life	Fixed bed system using less steam for regeneration & 2 yr sorbent life	As reported in DoE report	Fixed bed system using steam for regeneration & 1 yr sorbent life	Fixed bed system using less steam for regeneration & 2 yr sorbent life	Fixed bed system using less steam for regeneration & 2 yr sorbent life
VSA REGENERATION OPTION	N/A	LP Steam & Cooling water	LP Steam & Cooling water	None	N/A	LP Steam & Cooling water	LP Steam & Cooling water	None
Net power, MW	549.96	550.00	550.00	550.00	549.97	550.00	550.00	550
Capacity factor (CF), %	85	85	85	85	85	85	85	85
Total plant cost (TPC), $	1,977,885,000	1,603,096,678	1,537,798,012	1,531,523,511	1,959,399,000	1,579,707,379	1,546,731,268	1,537,732,572
6 month labor cost	12,549,000	11,036,528	10,761,803	10,736,685	12,556,000	10,942,703	10,797,564	10,761,541
1 month maintenance materials	1,867,000	1,592,369	1,524,342	1,518,123	1,869,000	1,569,137	1,533,197	1,524,277
1 month non-fuel consumables	3,202,000	3,367,757	2,937,779	2,809,515	2,931,000	3,021,291	2,709,637	2,602,476
1 month waste disposal	547,000	484,199	468,756	458,371	503,000	449,714	437,791	425,738
25% of 1 month fuel cost at 100% CF	3,850,000	3,410,458	3,301,683	3,228,534	3,542,000	3,167,561	3,083,597	2,998,705
2% of TPC	39,558,000	32,061,934	30,755,960	30,630,470	39,188,000	31,594,148	30,934,625	30,754,651
60 day supply of fuel & consumables at 100% CF	36,379,000	33,553,165	31,846,707	31,016,521	33,451,000	30,953,165	29,675,888	28,794,667
0.5% of TPC (spare parts)	9,889,000	8,015,483	7,688,990	7,657,618	9,797,000	7,898,537	7,733,656	7,688,663
Initial catalyst & chemicals cost, $	4,187,000	11,285,950	9,685,278	9,464,486	3,784,000	10,489,000	9,046,568	8,796,827
Land	900,000	900,000	900,000	900,000	900,000	900,000	900,000	900,000
Other owners's costs	296,683,000	240,464,502	230,669,702	229,728,527	293,910,000	236,956,107	232,009,690	230,659,886
Financing costs	53,403,000	43,283,610	41,520,546	41,351,135	52,904,000	42,652,099	41,761,744	41,518,779
Total overnight cost (TOC), $	2,440,898,000	1,992,552,633	1,909,859,558	1,901,023,496	2,414,734,000	1,960,300,839	1,917,355,227	1,905,158,783
Fixed operating cost for initial year of operation (OCF), $	64,655,855	54,134,989	52,279,566	52,103,841	64,137,607	53,479,553	52,529,753	52,277,734
Annual feed cost at above CF for initial year (OCV1), $	157,063,965	139,146,704	134,708,668	131,724,206	144,504,012	129,236,490	125,810,772	122,347,171
Other annual variable operating cost at above CF for initial year (OCV2), $	57,280,930	55,532,119	50,294,947	48,817,287	54,089,231	51,409,441	47,742,381	46,435,415
Annual CO2 transporting, storing, and monitoring cost at above CF for initial year (OCV3), $	44,266,973	38,755,789	37,518,464	36,677,067	40,909,815	35,994,374	35,040,258	34,072,930
1st year cost of electricity (COE) w/o CO2 TS&M, $/MWh	**142.0**	**121.2**	**115.9**	**114.5**	**137.3**	**116.7**	**113.4**	**111.8**
1st year cost of electricity (COE), $/MWh	**152.9**	**130.7**	**125.1**	**123.5**	**147.3**	**125.5**	**122.0**	**120.1**
Cost of CO2 Capture, $/tonne CO2 compared to amine CO2 capture		-23.41	-30.32	-32.77		-24.82	-29.58	-32.66
Cost of CO2 Capture, $/tonne CO2 compared to non CO2 capture	65.29	51.17	46.72	46.04	66.39	50.64	47.93	47.06

4.13.2 Process Modeling Summary

Process Design Basis and Methodology

The process design is based on a nominal 550 MW (net) PC plant for this post combustion capture study. The basis for this design is identical to that used for Case 10 and Case 12 of the BBS with post-combustion capture, and include the following:

1) Feed coal analysis
2) Site characteristics and ambient conditions
3) Boiler performance
4) Steam cycle conditions
5) Environmental controls and performance
6) Balance of plant subsystems

The design basis for CO_2 capture and compression are summarized in Table 22:

Table 22. Design Basis for CO_2 Capture and Compression

CO_2 Removal	Greater than 90% of carbon in feed coal
CO_2 Purity	Satisfy 'Conceptual Design Limits' for Enhanced Oil Recovery as listed in Exhibit 2-1 of the NETL QGESS titled "*CO_2 Impurity Design Parameters.*"
CO_2 Delivery Pressure	2,215 psia
CO_2 Transport & Storage Cost	\$10/tonne CO_2

The system boundaries for the plant are defined by the following:

1) Delivered coal entering the power plant, through high-pressure, high-purity CO_2 stream crossing the plant boundary.
2) Combustion air intake from the ambient.
3) Flue gas to stack inclusive of stack.
4) Net electricity conditioned and sent to electric grid.
5) Raw make-up water.
6) Waste streams generated by the power plant, including the CO_2 capture system, are adequately treated on-site prior to disposal either by landfill or other commercial disposal options.

The following property packages are used within the framework of Aspen Plus®:

- PR-BM (Peng-Robinson equation of state with Boston-Mathias modifications) for high pressure streams
- IDEAL (Ideal gas law) for low pressure gas or vapor streams
- STEAM-TA (ASME 1967 Steam Table Corrections) for the water and steam.

Process Descriptions

Figure 96 depicts the overall block flow diagram for Case 10TDA and Case 12TDA, the subcritical and supercritical PC power plants integrated with TDA's sorption process for the capture of CO_2 while Figure 97 depicts the process flow diagram for TDA's sorption process for these two cases. The flue gas leaving the FGD unit is cooled in a direct contact cooler with water and then boosted in pressure using a booster fan before it enters TDA's vacuum swing adsorption (VSA) unit. The CO_2 regenerated along with the accompanying steam is compressed while steam required for the regeneration is generated using the heat of compression. The CO_2 stream is then cooled against cooling water before it is compressed to the final pressure in an intercooled compressor. The stream data for the Case10TDA and Case12TDA are presented in Table 23 through Table 26.

Results and Discussion
Table 27 summarizes the overall plant performance for the reference amine capture Case 10 and Case 12, and the TDA sorption based capture Case 10TDA and Case 12TDA. Each case generates the same amount of electricity on a net basis, nominal 550 MW of net power and the amount of fuel varies in proportion to the heat rate. It may be seen that the heat rate on an HHV basis for Case 10TDA with the TDA sorption process is significantly lower than Case 10, reduced from 13,764 kJ/kWh for the reference amine Case 10 to 11,542 kJ/kWh for Case 10TDA or by as much as 16%. The heat rate on an HHV basis for Case 12TDA with the TDA sorption process is reduced from 12,663 kJ/kWh for the reference amine Case 12 to 10,720 kJ/kWh for Case 12TDA or again by as much as 15%. Table 28 summarizes the air emissions for Case 10TDA and Case 12TDA.

Table 29 shows the water balance for Case 10 and Case 12 while Table 30 shows the water balance for Case 10TDA and Case 12TDA. Water demand is the total amount of water required for a given process. The internal recycle is the fraction of the water recovered within the process, primarily as condensate, and re-used while the difference between demand and recycle is raw water withdrawal which has to be removed from the ground or diverted from a surface-water source for use in the plant. Half of its supply is assumed to be provided by a potable water source while the remainder from groundwater. Water consumption is the portion of the raw water withdrawn that is evaporated, transpired, incorporated into products or otherwise not returned to the water source from which it was withdrawn. Thus, water consumption represents the net impact of the process on the water source. Process water discharge includes blowdown from the cooling towers and the demineralizer used in the preparation of BFW. Raw water usage includes makeup to cooling towers, FGD process, that required by the CO_2 capture process (e.g., fraction of the steam used in the regeneration step that is carried away with the flue gas), and the demineralizers. The water usage is significantly lower for the TDA sorption based cases; for Case 10TDA, it is about 29% lower than the corresponding amine based Case 10, and for Case 12TDA, it is again about 29% lower than the corresponding amine based Case 12. These reductions primarily are due to lower heat rates; less heat being rejected via the cooling towers and requiring less makeup water.

Table 31 and Table 32 summarize the overall plant costs and cost of electricity for the reference amine Case 10 and Case 12, and the two TDA sorption based capture cases. The cost of electricity (COE) was calculated using a capital charge factor (CCF) of 0.1243 and a capacity factor (CF) of 85% for all cases, while using \$10/tonne of CO_2 as its TS&M cost (per DoE guidelines) for the CO_2 capture cases. This entire TS&M cost was treated as a variable cost but in reality a certain fraction of it would be a fixed cost. The CO_2 avoided costs are also presented in Table 8. The cost estimation methodology including size adjustment (scaling) of non-research units was done using the NETL Quality Guidelines for Energy System Studies reports listed under References and Bibliography.

It may be seen that the plant cost for Case 10TDA at \$2,785/kW is as much as 23% lower than that for Case 10 at \$3,596/kW, while the plant cost for Case 12TDA at \$2,796/kW is about 22% lower than that for Case 12 at \$3,563/kW. The 1st year levelized cost of electricity inclusive of the CO_2 TS&M costs for Case 10TDA is reduced by 19% over Case 10 while for Case 12TDA it is again reduced by about 19% over Case 12. The 1st year levelized CO_2 avoided cost for Case 10TDA at \$54.5/tonne is lower than that for Case 10 by about \$41/tonne while for Case 12TDA at \$55.3/tonne is lower than that for Case 12 by again about \$41/tonne. The 1st year levelized CO_2 capture cost for Case 10TDA at \$46.0/tonne is lower than that for Case 10 by about \$19/tonne while for Case 12TDA at \$47.1/tonne is lower than that for Case 12 by about \$19/tonne.

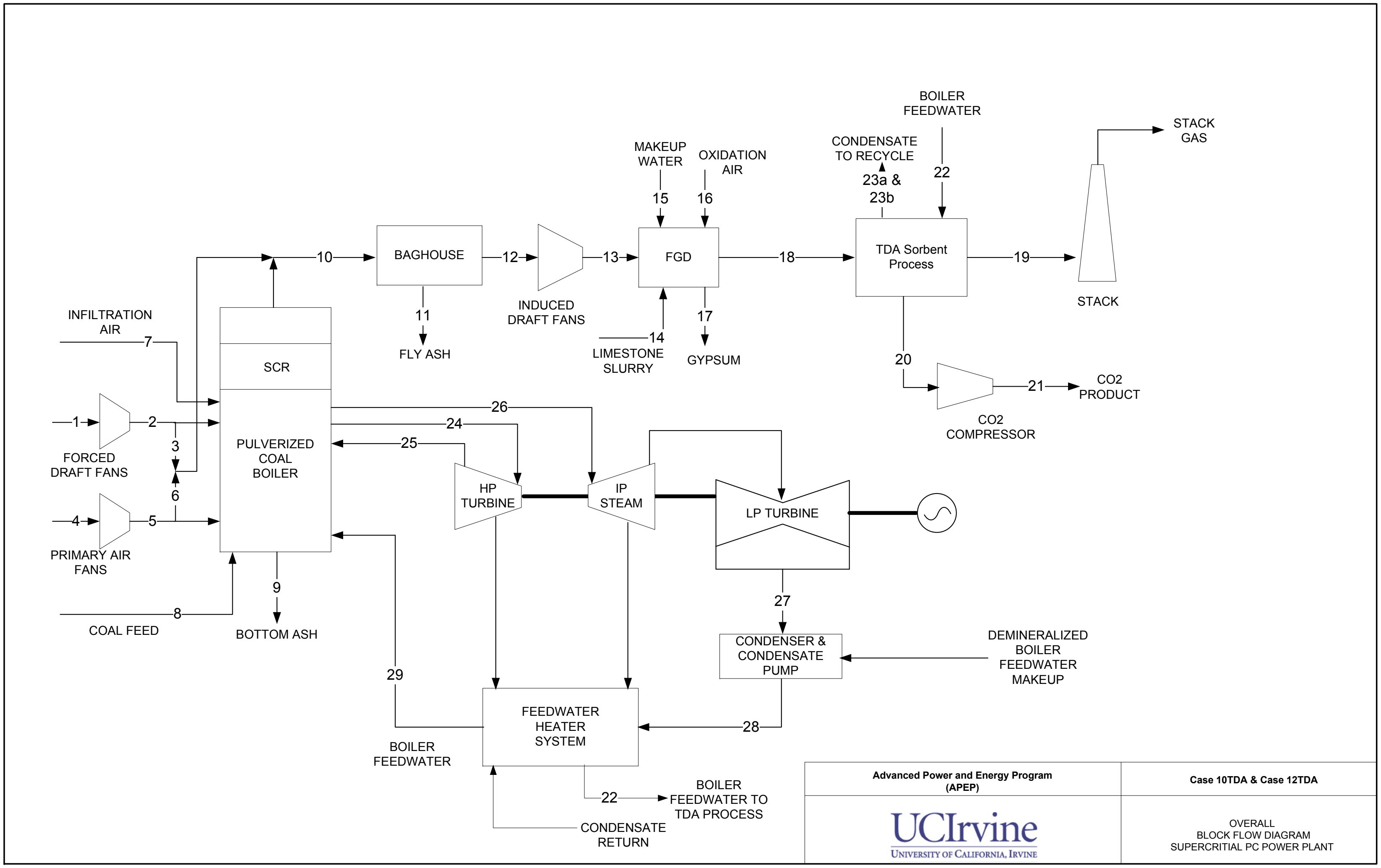

Figure 96. Block flow diagram for Case 10TDA and Case 12TDA.

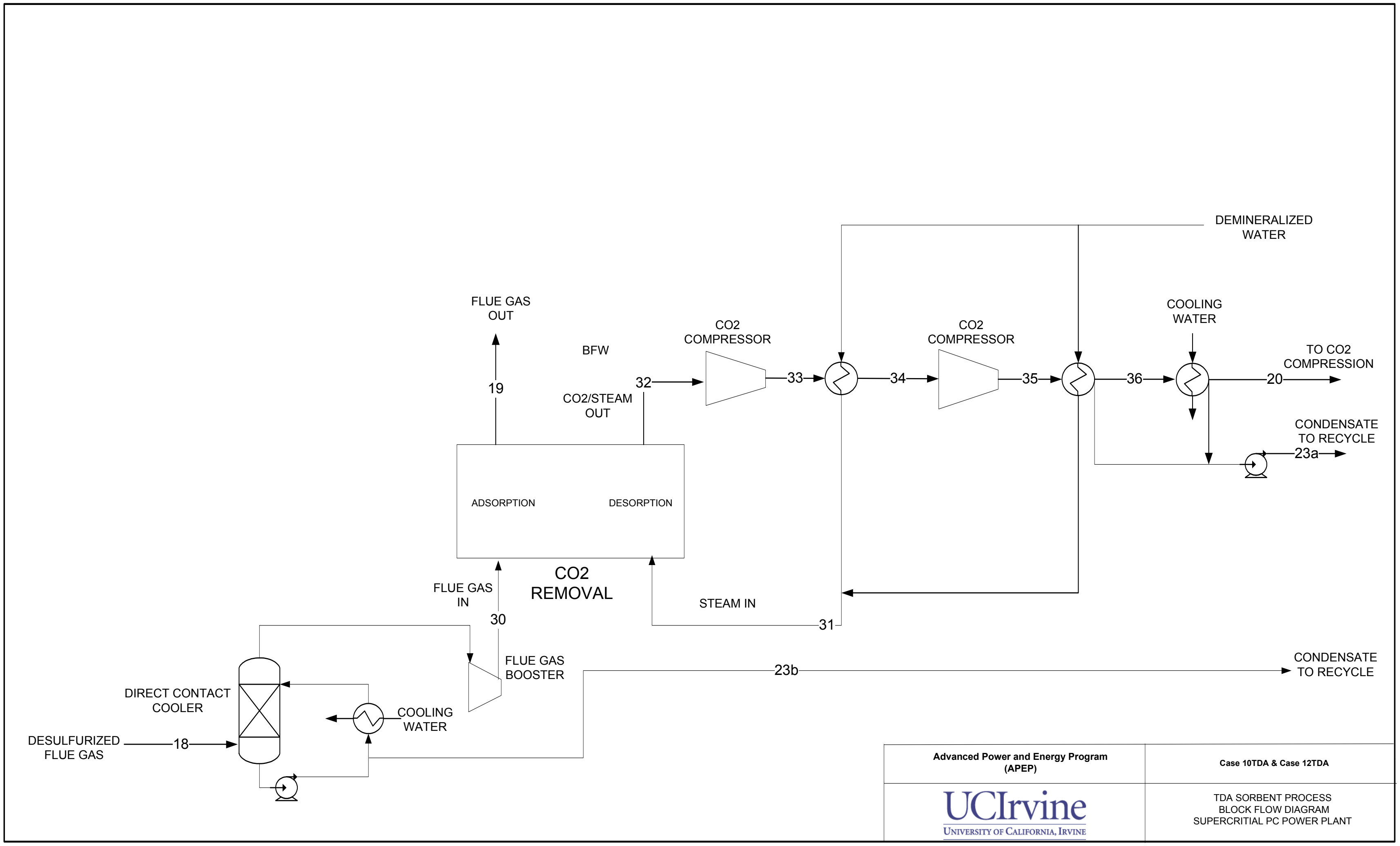

Figure 97. Case10TDA and Case12TDA process flow diagrams.

Table 23. Case 10TDA Stream data – Part A. (see Table 28 for trace pollutants).

Stream number	1+7	2	3	4	5	6	8	9	10	11	12	13	14	15	16	17	18
Temperature C	15	19	19	15	26	26	15		169		169	182	15	15	181	58	58
Pressure bar	1.01	1.05	1.05	1.01	1.11	1.11	1.01	1.01	0.99	0.99	0.98	1.06	1	1	3.1	1	1.03
Mass Flow kg/hr (Solid)							234,542	4,549	18,194	18,194			21,832	-	-	33,747	
Vapor Frac (w/o Solids)	1.00	1.00	1.00	1.00	1.00	1.00			1.00		1.00	1.00	0.00	0.00	1.00	0.00	1.00
Mole Flow kmol/hr (w/o Solids)	62,146	62,146	1,849	19,091	19,091	2,619	-	-	85,920	-	85,920	85,920	2,846	11,338	820	210	94,964
Mass Flow kg/hr (w/o Solids)	1,792,893	1,792,893	53,349	550,758	550,758	75,547	-	-	2,555,449	-	2,555,449	2,555,449	51,267	204,261	23,785	3,782	2,709,312
Enthalpy kJ/kg (w/o Solid)	-105.04	-101.11	-101.11	-105.04	-94.39	-94.39			-2505.50		-2505.50	-2491.80	-	-16007.27	98.38	-	-3274.50
Density kg/m3 (w/o Solid)	1.22	1.25	1.25	1.22	1.29	1.29			0.80		0.79	0.83	-	1003.10	2.40	-	1.06
Molecular Weight (w/o Solid)	28.85	28.85	28.85	28.85	28.85	28.85	18.02		29.74		29.74	29.74	-	18.02	29.03	-	28.53
Mole Frac (w/o Solids)																	
O2	0.2076	0.2076	0.2076	0.2076	0.2076	0.2076	0.0000	0.0000	0.0247	0.0000	0.0247	0.0247	0.0000	0.0000	0.2300	0.0000	0.0223
N2	0.7719	0.7719	0.7719	0.7719	0.7719	0.7719	0.0000	0.0000	0.7310	0.0000	0.7310	0.7310	0.0000	0.0000	0.7506	0.0000	0.6614
AR	0.0094	0.0094	0.0094	0.0094	0.0094	0.0094	0.0000	0.0000	0.0089	0.0000	0.0089	0.0089	0.0000	0.0000	0.0128	0.0000	0.0080
H2	0.0000	0.0000	0.0000	0.0000	0.0000	0.0000	0.0000	0.0000	0.0000	0.0000	0.0000	0.0000	0.0000	0.0000	0.0000	0.0000	0.0000
CO	0.0000	0.0000	0.0000	0.0000	0.0000	0.0000	0.0000	0.0000	0.0000	0.0000	0.0000	0.0000	0.0000	0.0000	0.0000	0.0000	0.0000
CO2	0.0003	0.0003	0.0003	0.0003	0.0003	0.0003	0.0000	0.0000	0.1452	0.0000	0.1452	0.1452	0.0000	0.0000	0.0005	0.0004	0.1313
H2O	0.0108	0.0108	0.0108	0.0108	0.0108	0.0108	0.0000	0.0000	0.0880	0.0000	0.0880	0.0880	1.0000	1.0000	0.0062	0.9996	0.1769
CH4	0.0000	0.0000	0.0000	0.0000	0.0000	0.0000	0.0000	0.0000	0.0000	0.0000	0.0000	0.0000	0.0000	0.0000	0.0000	0.0000	0.0000
SO2	0.0000	0.0000	0.0000	0.0000	0.0000	0.0000	0.0000	0.0000	0.0021	0.0000	0.0021	0.0021	0.0000	0.0000	0.0000	0.0000	0.0000
C2H6	0.0000	0.0000	0.0000	0.0000	0.0000	0.0000	0.0000	0.0000	0.0000	0.0000	0.0000	0.0000	0.0000	0.0000	0.0000	0.0000	0.0000
C3H8	0.0000	0.0000	0.0000	0.0000	0.0000	0.0000	0.0000	0.0000	0.0000	0.0000	0.0000	0.0000	0.0000	0.0000	0.0000	0.0000	0.0000
C4H10-01	0.0000	0.0000	0.0000	0.0000	0.0000	0.0000	0.0000	0.0000	0.0000	0.0000	0.0000	0.0000	0.0000	0.0000	0.0000	0.0000	0.0000
TOTAL	1.0000	1.0000	1.0000	1.0000	1.0000	1.0000	0.0000	0.0000	0.9999	0.0000	0.9999	0.9999	1.0000	1.0000	1.0001	1.0000	1.0000

The enthalpy reference state for a compound is that of the constituent elements in their standard states at 25°C and 1.01 bar.

Table 24. Case 10TDA Stream data – Part B. (see Table 28 for trace pollutants).

Stream number	19	20	21	22	23a	23b	24	25	26	27	28	29	30	31	32	33	34	35	36
Temperature C	70	27	35	150	56	47	566	363	568	39	39	251	40	70	50	176	79	154	100
Pressure bar	1.10	1.24	152.68	4.83	5.86	5.86	166.51	42.78	38.99	0.07	17.24	213.77	1.11	0.21	0.21	0.73	0.66	1.38	1.31
Mass Flow kg/hr (Solid)																			
Vapor Frac (w/o Solids)	1.00	1.00	1.00	0.00	0.00	0.00	1.00	1.00	1.00	0.92	0.00	0.00	1.00	1.00	1.00	1.00	1.00	1.00	1.00
Mole Flow kmol/hr (w/o Solids)	70,101	11,225	11,225	4,938	4,934	13,641	109,722	100,975	101,657	69,387	90,723	111,002	81,323	4,938	16,159	16,159	16,159	16,159	14,167
Mass Flow kg/hr (w/o Solids)	1,969,709	493,929	493,929	88,951	88,882	245,743	1,976,671	1,819,108	1,831,384	1,250,025	1,634,405	1,999,725	2,463,568	88,951	582,812	582,812	582,812	582,812	546,931
Enthalpy kJ/kg (w/o Solid)	-590.11	-8941.80	-9175.40	-15338.00	-15735.00	-15862.00	-12495.00	-12850.00	-12378.00	-13598.00	-15806.00	-14879.00	-2286.50	-13343.00	-9600.20	-9465.00	-9570.20	-9489.60	-9304.20
Density kg/m3 (w/o Solid)	1.08	2.21	794.65	916.49	985.33	835.92	47.62	15.74	10.31	0.05	993.43	816.30	1.29	0.13	0.28	0.71	0.82	1.40	1.64
Molecular Weight (w/o Solid)	28.10	44.00	44.00	18.02	18.02	18.02	18.02	18.02	18.02	18.02	18.02	18.02	30.29	18.02	36.07	36.07	36.07	36.07	38.60
Mole Frac (w/o Solids)																			
O2	0.0303	0.0000	0.0000	0.0000	0.0000	0.0000	0.0000	0.0000	0.0000	0.0000	0.0000	0.0000	0.0261	0.0000	0.0000	0.0000	0.0000	0.0000	0.0000
N2	0.8960	0.0000	0.0000	0.0000	0.0000	0.0000	0.0000	0.0000	0.0000	0.0000	0.0000	0.0000	0.7723	0.0000	0.0000	0.0000	0.0000	0.0000	0.0000
AR	0.0109	0.0000	0.0000	0.0000	0.0000	0.0000	0.0000	0.0000	0.0000	0.0000	0.0000	0.0000	0.0094	0.0000	0.0000	0.0000	0.0000	0.0000	0.0000
H2	0.0000	0.0000	0.0000	0.0000	0.0000	0.0000	0.0000	0.0000	0.0000	0.0000	0.0000	0.0000	0.0000	0.0000	0.0000	0.0000	0.0000	0.0000	0.0000
CO	0.0000	0.0000	0.0000	0.0000	0.0000	0.0000	0.0000	0.0000	0.0000	0.0000	0.0000	0.0000	0.0000	0.0000	0.0000	0.0000	0.0000	0.0000	0.0000
CO2	0.0178	0.9997	0.9997	0.0000	0.0000	0.0000	0.0000	0.0000	0.0000	0.0000	0.0000	0.0000	0.1533	0.0000	0.6944	0.6944	0.6944	0.6944	0.7921
H2O	0.0451	0.0003	0.0003	1.0000	1.0000	1.0000	1.0000	1.0000	1.0000	1.0000	1.0000	1.0000	0.0388	1.0000	0.3056	0.3056	0.3056	0.3056	0.2079
CH4	0.0000	0.0000	0.0000	0.0000	0.0000	0.0000	0.0000	0.0000	0.0000	0.0000	0.0000	0.0000	0.0000	0.0000	0.0000	0.0000	0.0000	0.0000	0.0000
SO2	0.0000	0.0000	0.0000	0.0000	0.0000	0.0000	0.0000	0.0000	0.0000	0.0000	0.0000	0.0000	0.0000	0.0000	0.0000	0.0000	0.0000	0.0000	0.0000
C2H6	0.0000	0.0000	0.0000	0.0000	0.0000	0.0000	0.0000	0.0000	0.0000	0.0000	0.0000	0.0000	0.0000	0.0000	0.0000	0.0000	0.0000	0.0000	0.0000
C3H8	0.0000	0.0000	0.0000	0.0000	0.0000	0.0000	0.0000	0.0000	0.0000	0.0000	0.0000	0.0000	0.0000	0.0000	0.0000	0.0000	0.0000	0.0000	0.0000
C4H10-01	0.0000	0.0000	0.0000	0.0000	0.0000	0.0000	0.0000	0.0000	0.0000	0.0000	0.0000	0.0000	0.0000	0.0000	0.0000	0.0000	0.0000	0.0000	0.0000
TOTAL	1.0000	1.0000	1.0000	1.0000	1.0000	1.0000	1.0000	1.0000	1.0000	1.0000	1.0000	1.0000	1.0000	1.0000	1.0000	1.0000	1.0000	1.0000	1.0000

The enthalpy reference state for a compound is that of the constituent elements in their standard states at 25°C and 1.01 bar.

Table 25. Case 12TDA Stream data – Part A. (see Table 28 for trace pollutants).

Stream number	1+7	2	3	4	5	6	8	9	10	11	12	13	14	15	16	17	18
Temperature C	15	19	19	15	26	26	15		169		169	182	15	15	181	58	58
Pressure bar	1.01	1.05	1.05	1.01	1.11	1.11	1.01	1.01	0.99	0.99	0.98	1.06	1	1	3.1	1	1.03
Mass Flow kg/hr (Solid)							214,621	4,162	16,649	16,649			21,714	-	-	33,565	
Vapor Frac (w/o Solids)	1.00	1.00	1.00	1.00	1.00	1.00			1.00		1.00	1.00	0.00	0.00	1.00	0.00	1.00
Mole Flow kmol/hr (w/o Solids)	56,865	56,865	1,692	17,468	17,468	2,397	-	-	78,619	-	78,619	78,619	2,831	11,277	815	209	86,909
Mass Flow kg/hr (w/o Solids)	1,640,538	1,640,538	48,822	503,956	503,956	69,143	-	-	2,338,299	-	2,338,299	2,338,299	50,989	203,155	23,656	3,761	2,479,898
Enthalpy kJ/kg (w/o Solid)	-105.04	-101.11	-101.11	-105.04	-94.39	-94.39			-2505.60		-2505.60	-2491.90	-	-16007.27	98.38	-	-3274.10
Density kg/m3 (w/o Solid)	1.22	1.25	1.25	1.22	1.29	1.29			0.80		0.79	0.83	-	1003.10	2.40	-	1.06
Molecular Weight (w/o Solid)	28.85	28.85	28.85	28.85	28.85	28.85	18.02		29.74		29.74	29.74	-	18.02	29.03	-	28.53
Mole Frac (w/o Solids)																	
O2	0.2076	0.2076	0.2076	0.2076	0.2076	0.2076	0.0000	0.0000	0.0247	0.0000	0.0247	0.0247	0.0000	0.0000	0.2300	0.0000	0.0223
N2	0.7719	0.7719	0.7719	0.7719	0.7719	0.7719	0.0000	0.0000	0.7310	0.0000	0.7310	0.7310	0.0000	0.0000	0.7506	0.0000	0.6613
AR	0.0094	0.0094	0.0094	0.0094	0.0094	0.0094	0.0000	0.0000	0.0089	0.0000	0.0089	0.0089	0.0000	0.0000	0.0128	0.0000	0.0080
H2	0.0000	0.0000	0.0000	0.0000	0.0000	0.0000	0.0000	0.0000	0.0000	0.0000	0.0000	0.0000	0.0000	0.0000	0.0000	0.0000	0.0000
CO	0.0000	0.0000	0.0000	0.0000	0.0000	0.0000	0.0000	0.0000	0.0000	0.0000	0.0000	0.0000	0.0000	0.0000	0.0000	0.0000	0.0000
CO2	0.0003	0.0003	0.0003	0.0003	0.0003	0.0003	0.0000	0.0000	0.1452	0.0000	0.1452	0.1452	0.0000	0.0000	0.0005	0.0004	0.1313
H2O	0.0108	0.0108	0.0108	0.0108	0.0108	0.0108	0.0000	0.0000	0.0880	0.0000	0.0880	0.0880	1.0000	1.0000	0.0062	0.9996	0.1769
CH4	0.0000	0.0000	0.0000	0.0000	0.0000	0.0000	0.0000	0.0000	0.0000	0.0000	0.0000	0.0000	0.0000	0.0000	0.0000	0.0000	0.0000
SO2	0.0000	0.0000	0.0000	0.0000	0.0000	0.0000	0.0000	0.0000	0.0021	0.0000	0.0021	0.0021	0.0000	0.0000	0.0000	0.0000	0.0000
C2H6	0.0000	0.0000	0.0000	0.0000	0.0000	0.0000	0.0000	0.0000	0.0000	0.0000	0.0000	0.0000	0.0000	0.0000	0.0000	0.0000	0.0000
C3H8	0.0000	0.0000	0.0000	0.0000	0.0000	0.0000	0.0000	0.0000	0.0000	0.0000	0.0000	0.0000	0.0000	0.0000	0.0000	0.0000	0.0000
C4H10-01	0.0000	0.0000	0.0000	0.0000	0.0000	0.0000	0.0000	0.0000	0.0000	0.0000	0.0000	0.0000	0.0000	0.0000	0.0000	0.0000	0.0000
TOTAL	1.0000	1.0000	1.0000	1.0000	1.0000	1.0000	0.0000	0.0000	0.9999	0.0000	0.9999	0.9999	1.0000	1.0000	1.0001	1.0000	0.9999

The enthalpy reference state for a compound is that of the constituent elements in their standard states at 25°C and 1.01 bar.

Table 26. Case 12TDA Stream data – Part B. (see Table 28 for trace pollutants).

Stream number	19	20	21	22	23a	23b	24	25	26	27	28	29	30	31	32	33	34	35	36
Temperature C	70	27	35	151	56	47	593	354	593	39	39	287	40	70	50	176	79	154	100
Pressure bar	1.10	1.24	152.68	4.83	5.86	5.86	242.33	49.01	45.22	0.07	17.24	288.55	1.11	0.21	0.21	0.73	0.66	1.38	1.31
Mass Flow kg/hr (Solid)																			
Vapor Frac (w/o Solids)	1.00	1.00	1.00	0.00	0.00	0.00	1.00	1.00	1.00	0.91	0.00	0.00	1.00	1.00	1.00	1.00	1.00	1.00	1.00
Mole Flow kmol/hr (w/o Solids)	64,146	10,274	10,274	4,519	4,516	12,492	105,868	86,391	86,391	58,464	75,316	105,868	74,417	4,519	14,790	14,790	14,790	14,790	12,968
Mass Flow kg/hr (w/o Solids)	1,802,742	452,069	452,069	81,413	81,350	225,057	1,907,238	1,556,354	1,556,354	1,053,243	1,356,846	1,907,238	2,254,751	81,412	533,419	533,419	533,419	533,419	500,607
Enthalpy kJ/kg (w/o Solid)	-589.19	-8941.80	-9175.40	-15337.00	-15735.00	-15862.00	-12490.00	-12888.00	-12318.00	-13604.00	-15806.00	-14708.00	-2285.80	-13343.00	-9600.20	-9465.00	-9570.20	-9489.60	-9304.50
Density kg/m3 (w/o Solid)	1.08	2.21	794.65	916.31	985.35	835.94	69.11	18.66	11.57	0.05	993.43	771.21	1.29	0.13	0.28	0.71	0.82	1.40	1.64
Molecular Weight (w/o Solid)	28.10	44.00	44.00	18.02	18.02	18.02	18.02	18.02	18.02	18.02	18.02	18.02	30.30	18.02	36.07	36.07	36.07	36.07	38.60
Mole Frac (w/o Solids)																			
O2	0.0303	0.0000	0.0000	0.0000	0.0000	0.0000	0.0000	0.0000	0.0000	0.0000	0.0000	0.0000	0.0261	0.0000	0.0000	0.0000	0.0000	0.0000	0.0000
N2	0.8960	0.0000	0.0000	0.0000	0.0000	0.0000	0.0000	0.0000	0.0000	0.0000	0.0000	0.0000	0.7723	0.0000	0.0000	0.0000	0.0000	0.0000	0.0000
AR	0.0109	0.0000	0.0000	0.0000	0.0000	0.0000	0.0000	0.0000	0.0000	0.0000	0.0000	0.0000	0.0094	0.0000	0.0000	0.0000	0.0000	0.0000	0.0000
H2	0.0000	0.0000	0.0000	0.0000	0.0000	0.0000	0.0000	0.0000	0.0000	0.0000	0.0000	0.0000	0.0000	0.0000	0.0000	0.0000	0.0000	0.0000	0.0000
CO	0.0000	0.0000	0.0000	0.0000	0.0000	0.0000	0.0000	0.0000	0.0000	0.0000	0.0000	0.0000	0.0000	0.0000	0.0000	0.0000	0.0000	0.0000	0.0000
CO2	0.0178	0.9997	0.9997	0.0000	0.0000	0.0000	0.0000	0.0000	0.0000	0.0000	0.0000	0.0000	0.1533	0.0000	0.6944	0.6944	0.6944	0.6944	0.7920
H2O	0.0450	0.0003	0.0003	1.0000	1.0000	1.0000	1.0000	1.0000	1.0000	1.0000	1.0000	1.0000	0.0388	1.0000	0.3056	0.3056	0.3056	0.3056	0.2080
CH4	0.0000	0.0000	0.0000	0.0000	0.0000	0.0000	0.0000	0.0000	0.0000	0.0000	0.0000	0.0000	0.0000	0.0000	0.0000	0.0000	0.0000	0.0000	0.0000
SO2	0.0000	0.0000	0.0000	0.0000	0.0000	0.0000	0.0000	0.0000	0.0000	0.0000	0.0000	0.0000	0.0000	0.0000	0.0000	0.0000	0.0000	0.0000	0.0000
C2H6	0.0000	0.0000	0.0000	0.0000	0.0000	0.0000	0.0000	0.0000	0.0000	0.0000	0.0000	0.0000	0.0000	0.0000	0.0000	0.0000	0.0000	0.0000	0.0000
C3H8	0.0000	0.0000	0.0000	0.0000	0.0000	0.0000	0.0000	0.0000	0.0000	0.0000	0.0000	0.0000	0.0000	0.0000	0.0000	0.0000	0.0000	0.0000	0.0000
C4H10-01	0.0000	0.0000	0.0000	0.0000	0.0000	0.0000	0.0000	0.0000	0.0000	0.0000	0.0000	0.0000	0.0000	0.0000	0.0000	0.0000	0.0000	0.0000	0.0000
TOTAL	0.9999	1.0000	1.0000	1.0000	1.0000	1.0000	1.0000	1.0000	1.0000	1.0000	1.0000	1.0000	0.9999	1.0000	1.0000	1.0000	1.0000	1.0000	1.0000

The enthalpy reference state for a compound is that of the constituent elements in their standard states at 25°C and 1.01 bar.

Table 27. Overall plant performance comparison.

CASE NO.		**10**	**10TDA**	**12**	**12TDA**
STEAM CYCLE		Subcritical		Supercritical	
CO_2 CAPTURE TECHNOLOGY		Amine	VSA	Amine	VSA
STEAM TURBINE POWER	Kwe	672,700	678,804	662,800	669,874
TOTAL AUXILIARY CONSUMPTION	Kwe	122,740	128,804	112,830	119,874
NET POWER OUTPUT	Kwe	549,960	550,000	549,970	550,000
AUXILIARY LOAD SUMMARY					
FEED HANDLING	Kwe	6,090	5,107	5,610	4,750
ASH HANDLING	Kwe	800	671	740	627
PRIMARY AIR FANS	Kwe	1,960	1,644	1,800	1,527
FORCED DRAFT FANS	Kwe	2,500	2,097	2,300	1,947
INDUCED DRAFT FANS	Kwe	12,080	10,131	11,120	9,415
SCR	Kwe	70	59	70	59
BAGHOUSE	Kwe	100	84	100	85
FGD	Kwe	4,470	3,745	4,110	3,476
CO2 REMOVAL UNIT	Kwe	22,400	9,402	20,600	8,733
CO2 COMPRESSION	Kwe	48,790	80,390	44,890	74,728
MISCELLANEOUS BALANCE OF PLANT	Kwe	2,000	1,677	2,000	1,693
STEAM TURBINE AUXILIARIES	Kwe	400	404	400	404
CONDENSATE PUMPS	Kwe	700	1,030	560	868
CIRCULATING WATER PUMPS	Kwe	11,190	7,429	10,100	6,751
GROUND WATER PUMPS	Kwe	1,020	694	910	609
COOLING TOWER	Kwe	5,820	1,869	5,230	1,887
TRANSFORMER LOSSES	Kwe	2,350	2,371	2,290	2,314
% NET PLANT EFFICIENCY, HHV	%	26.20	31.19	28.40	33.58
NET HEAT RATE	KJ/KWH	13,764	11,542	12,663	10,720
REDUCTION IN NET HEAT RATE OVER AMINE CASE	**%**	**-**	**16**	**-**	**15**
CONDENSER COOLING DUTY	10^6 KJ/H	2,034	3,002	1,737	2,681
CONSUMABLES					
AS-RECEIVED FEED	KG/H	278,956	233,946	256,652	217,292
LIMESTONE SORBENT FEED	KG/H	28,404	24,179	25,966	22,316
CO2 SORBENT INITIAL FEED	KG	0	2,886,991	0	2,682,026
CO2 SORBENT ANNUAL FEED	KG/YR	0	1,443,495	0	1,341,013

Table 28. Air emissions.

	kg/GJ	lb/10^6 Btu	Tonne/year 85% CF	Ton/year 85% CF	kg/MWh	lb/MWh
Case 10TDA						
SO_2 [1]	0.037	0.086	3,156	3,480	0.346	0.763
NO_x [1]	0.030	0.070	2,559	2,821	0.281	0.619
Particulates [1]	0.006	0.014	512	564	0.056	0.124
Hg [1]	4.91E-07	1.14E-06	0.042	0.046	4.59E-06	1.01E-05
CO_2 [1]	8.7	20.3	746,195	822,680	82	180
CO_2 [2]					101	223
Case 12TDA						
SO_2 [1]	0.037	0.086	2,932	3,233	0.326	0.718
NO_x [1]	0.030	0.070	2,377	2,621	0.264	0.582
Particulates [1]	0.006	0.014	475	524	0.053	0.116
Hg [1]	4.91E-07	1.14E-06	0.039	0.043	4.32E-06	9.53E-06
CO_2 [1]	8.7	20.3	693,357	764,426	77	170
CO_2 [2]					94	207

[1] emissions based on gross power instead of net power

[2] CO_2 emissions based on net power instead of gross power

Table 29. DOE cases 10 and 12 water balances.

Case 10					
Water Use	Water Demand, m^3/min (gpm)	Internal Recycle, m^3/min (gpm)	Raw Water Withdrawal, m^3/min (gpm)	Process Water Discharge, m^3/min (gpm)	Raw Water Consumption, m^3/min (gpm)
Econamine	0.2 (39)	0.0 (0)	0.2 (39)	0.0 (0)	0.2 (39)
FGD Makeup	5.5 (1,460)	0.0 (0)	5.5 (1,460)	0.0 (0)	5.5 (1,460)
BFW Makeup	0.4 (104)	0.0 (0)	0.4 (104)	0.0 (0)	0.4 (104)
Cooling Tower	43.8 (11,580)	7.4 (1,959)	36.4 (9,621)	9.9 (2,604)	26.6 (7,017)
Total	49.9 (13,182)	7.4 (1,959)	42.5 (11,224)	9.9 (2,604)	32.6 (8,620)
Case 12					
Econamine	0.1 (36)	0.0 (0)	0.1 (36)	0.00 (0)	0.1 (36)
FGD Makeup	5.1 (1,340)	0.0 (0)	5.1 (1,340)	0.00 (0)	5.1 (1,340)
BFW Makeup	0.0 (0)	0.0 (0)	0.0 (0)	0.00 (0)	0.0 (0)

Table 30. TDA VSA case water balances.

	Water Demand		Internal Recycle		Raw Water Withdrawal		Process Water Discharge		Raw Water Consumption	
Water Use	m^3/min	gpm	m^3/min	gpm	m^3/min	gpm	m^3/min	gpm	m^3/min	gpm
Case 10TDA										
FGD Makeup	4.6	1,224	0.0	0	4.6	1,224	0.0	0	4.6	1,224
BFW Makeup	1.9	498	1.5	390	0.4	108	0.1	20	0.3	88
Cooling Tower	29.1	7,690	4.4	1,167	24.7	6,523	6.5	1,729	18.1	4,794
Total	35.6	9,413	5.9	1,557	29.7	7,855	6.6	1,749	23.1	6,106
Case 12TDA										
FGD	4.3	1,13	0.0	0	4.3	1,13	0.0	0	4.3	1,134

Table 31. Overall plant cost comparison - 2011 installed cost ($1,000) by Unit.

CASE NO.	**10**	**10TDA**	**12**	**12TDA**
STEAM CYCLE	Subcritical		Supercritical	
CO_2 CAPTURE TECHNOLOGY	Amine	VSA	Amine	VSA
Coal & sorbent handing, prep & feed	87,949	78,844	83,341	75,165
Feedwater & Misc. BOP Systems	119,683	104,877	123,565	108,561
PC boiler	401,917	354,986	437,215	389,960
Flue gas cleanup	208,901	184,141	196,119	174,097
CO2 removal	531,906	216,190	505,963	206,844
CO2 compression & drying	91,699	81,603	87,534	78,358
Ductwork and Stack	50,150	26,910	45,092	24,489
Steam turbine generator + auxiliaries	162,583	161,272	166,965	165,848
Cooling water system	78,552	78,618	73,311	73,861
Ash handling systems	19,116	17,322	18,252	16,627
Accessory electric plant	100,885	102,579	100,255	102,317
Instrumentation & controls	30,822	31,734	31,053	31,982
Improvement to site	18,462	18,237	18,332	18,153
Buildings & structures	75,259	74,212	72,402	71,471
Total	1,977,884	1,531,524	1,959,399	1,537,733

Table 32. Cost of electricity comparison (2011 $, CCF = 0.1243).

CASE NO.	**10**	**10TDA**	**12**	**12TDA**
STEAM CYCLE	Subcritical		Supercritical	
CO_2 CAPTURE TECHNOLOGY	Amine	VSA	Amine	VSA
Net power, MW	550	550	550	550
Capacity factor (CF), %	85	85	85	85
Total plant cost (TPC)	1,977,885,000	1,531,523,511	1,959,399,000	1,537,732,572
6 month labor cost	12,549,000	10,736,685	12,556,000	10,761,541
1 month maintenance materials	1,867,000	1,518,123	1,869,000	1,524,277
1 month non-fuel consumables	3,202,000	2,809,515	2,931,000	2,602,476
1 month waste disposal	547,000	458,371	503,000	425,738
25% of 1 month coal cost at 100% CF	3,850,000	3,228,534	3,542,000	2,998,705
2% of TPC	39,558,000	30,630,470	39,188,000	30,754,651
60 day supply of fuel & consumables at 100% CF	36,379,000	31,016,521	33,451,000	28,794,667
0.5% of TPC (spare parts)	9,889,000	7,657,618	9,797,000	7,688,663
Initial catalyst & chemicals cost	4,187,000	9,464,486	3,784,000	8,796,827
Land	900,000	900,000	900,000	900,000
Other owner's costs	296,683,000	229,728,527	293,910,000	230,659,886
Financing costs	53,403,000	41,351,135	52,904,000	41,518,779
Total overnight cost (TOC)	2,440,898,000	1,901,023,496	2,414,734,000	1,905,158,783
Fixed operating cost for initial year of operation (OCF)	64,655,855	52,103,841	64,137,607	52,277,734
Annual fuel cost for initial year (OCV1) at above CF	157,063,965	131,724,206	144,504,012	122,347,171
Other annual variable operating cost for initial year (OCV2) at above CF	57,280,930	48,817,287	54,089,231	46,435,415
Annual CO2 TS&M cost for initial year (OCV3) at above CF	44,266,973	36,677,067	40,909,815	34,072,930
1st year cost of electricity (COE) w/o CO_2 TS&M, $/MWh	142.0	114.5	137.3	111.8
1st year cost of electricity (COE)[1], $/MWh	**152.9**	**123.5**	**147.3**	**120.1**

---

[1] Compared to like technology.

4.13.3 Sensitivity Analysis

Life of Sorbent

The sensitivity of the 1st year levelized cost of electricity inclusive of the CO_2 TS&M costs to TDA's CO_2 sorbent life is presented in Table 9. The cost of electricity decreases slightly as the sorbent life is increased from 2 years to 5 years reducing the Cost of CO_2 capture by about $0.8 per tonne of CO_2.

Table 33. Sensitivity of COE and cost of CO_2 capture to CO_2 sorbent life.

CASE	**10TDA**			**12TDA**		
SORBENT LIFE, YEARS	2	4	5	2	4	5
1st year cost of electricity (COE) w/o CO2 TS&M, $/MWh	114.5	113.9	113.8	111.8	111.3	111.2
1st year cost of electricity (COE), $/MWh	123.5	122.9	122.8	120.1	119.6	119.5
1st year CO_2 avoided cost[2], $/tonne	54.5	53.7	53.6	55.3	54.5	54.4
1st year CO_2 capture cost[2], $/tonne	46.0	45.4	45.2	47.1	46.4	46.3

VSA Cycle time

The optimized VSA cycle scheme provides full utilization of the sorbent bed with no HOLD time. It also allows us to reduce the overall cycle time from 12 min (baseline design) to 6 min (field tests) to 4.5 min (full-scale). In the optimized VSA cycle scheme is shown in Figure 98. In this improved VSA cycle scheme the flow is directed to multiple beds, which also provides improved gas-solid contact time and reduced pressure drop.

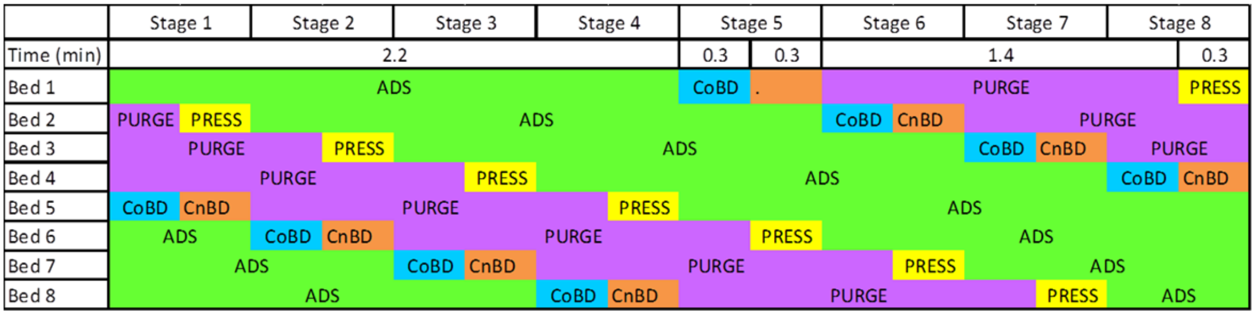

<table>
<tr><th></th><th colspan="2">Stage 1</th><th colspan="2">Stage 2</th><th colspan="2">Stage 3</th><th colspan="2">Stage 4</th><th colspan="2">Stage 5</th><th colspan="2">Stage 6</th><th colspan="2">Stage 7</th><th colspan="2">Stage 8</th></tr>
<tr><td>Time (min)</td><td colspan="8">2.2</td><td>0.3</td><td>0.3</td><td colspan="5">1.4</td><td>0.3</td></tr>
<tr><td>Bed 1</td><td colspan="8">ADS</td><td>CoBD</td><td>.</td><td colspan="5">PURGE</td><td>PRESS</td></tr>
<tr><td>Bed 2</td><td>PURGE</td><td>PRESS</td><td colspan="8">ADS</td><td>CoBD</td><td>CnBD</td><td colspan="4">PURGE</td></tr>
<tr><td>Bed 3</td><td colspan="3">PURGE</td><td>PRESS</td><td colspan="8">ADS</td><td>CoBD</td><td>CnBD</td><td colspan="2">PURGE</td></tr>
<tr><td>Bed 4</td><td colspan="5">PURGE</td><td>PRESS</td><td colspan="8">ADS</td><td>CoBD</td><td>CnBD</td></tr>
<tr><td>Bed 5</td><td>CoBD</td><td>CnBD</td><td colspan="5">PURGE</td><td>PRESS</td><td colspan="8">ADS</td></tr>
<tr><td>Bed 6</td><td colspan="2">ADS</td><td>CoBD</td><td>CnBD</td><td colspan="5">PURGE</td><td>PRESS</td><td colspan="6">ADS</td></tr>
<tr><td>Bed 7</td><td colspan="4">ADS</td><td>CoBD</td><td>CnBD</td><td colspan="5">PURGE</td><td>PRESS</td><td colspan="4">ADS</td></tr>
<tr><td>Bed 8</td><td colspan="6">ADS</td><td>CoBD</td><td>CnBD</td><td colspan="5">PURGE</td><td>PRESS</td><td colspan="2">ADS</td></tr>
</table>

4- bed PSA Cycle Steps:

Step 1	Adsorption at 16 psia (ADS)
Step 2	Cocurrent Blowdown to 6-8 psia (CoBD)
Step 3	Countercurrent Blowdown to 3-4.5 psia (CnBD)
Step 4	Steam Purge at 3-4.5 psia (PURGE)
Step 5	Pressurization with CO2 free product/air to 14.7 psia (PRESS)

Figure 98. Optimized VSA cycle scheme for the full scale 8-bed VSA system.

Table 34 shows the impact of cycle time on the initial sorbent cost and the 8-bed VSA system cost. Figure 99 shows the impact of the cycle time on the size of the VSA system, which

---

[2] Compared to like technology.

reduces from 72 ft tall to 36 ft tall and 27 ft tall as the cycle time is reduced from 12 min to 6 min and 4.5 min. Table 35 summarizes the impact of cycle time on the COE and cost of CO_2 capture. As the cycle time is reduced from 12 min to 6 min and 4.5 min, the cost of CO_2 capture is reduced by about \$4.3 and \$4.4 per tonne of CO_2 for sub-critical and super-critical power plants, respectively. This shows that cycle time has a very large impact on COE and Cost of CO_2 capture.

Table 34. Impact of VSA cycle time on initial sorbent and VSA system costs.

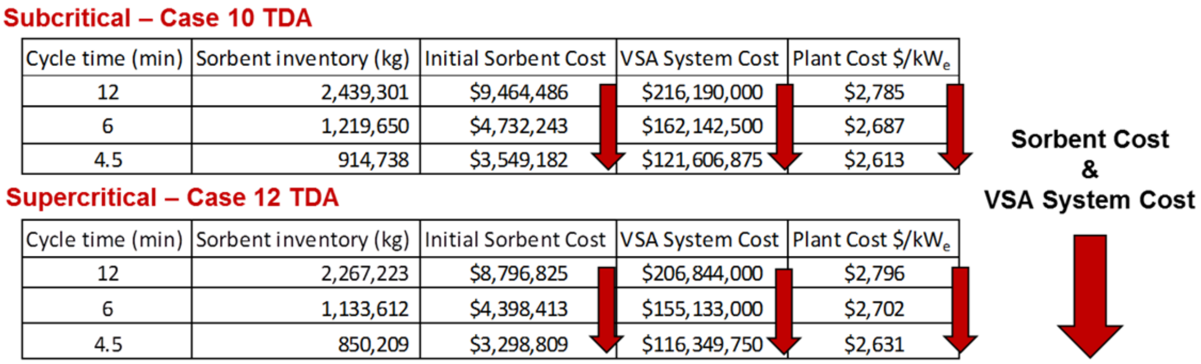

Subcritical – Case 10 TDA

Cycle time (min)	Sorbent inventory (kg)	Initial Sorbent Cost	VSA System Cost	Plant Cost $/kW$_e$
12	2,439,301	$9,464,486	$216,190,000	$2,785
6	1,219,650	$4,732,243	$162,142,500	$2,687
4.5	914,738	$3,549,182	$121,606,875	$2,613

Supercritical – Case 12 TDA

Cycle time (min)	Sorbent inventory (kg)	Initial Sorbent Cost	VSA System Cost	Plant Cost $/kW$_e$
12	2,267,223	$8,796,825	$206,844,000	$2,796
6	1,133,612	$4,398,413	$155,133,000	$2,702
4.5	850,209	$3,298,809	$116,349,750	$2,631

Sorbent Cost & VSA System Cost

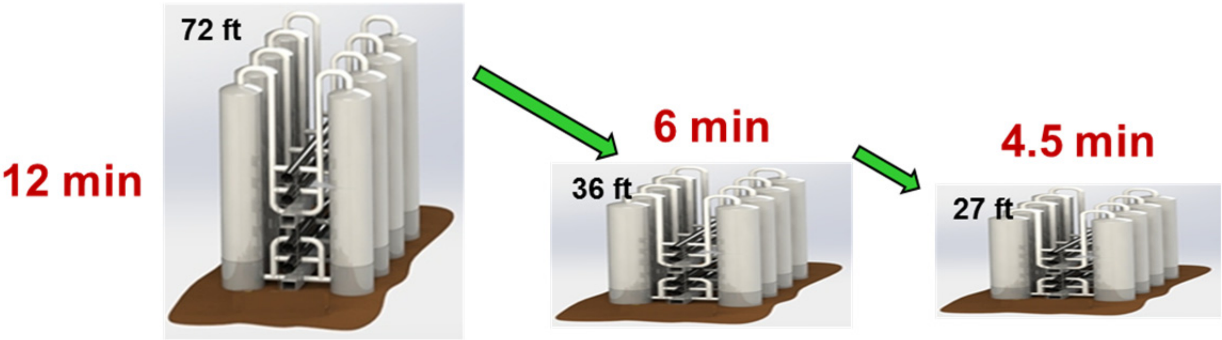

Figure 99. Impact of cycle time on VSA system size.

Table 35. Sensitivity of COE and cost of CO_2 capture to VSA cycle time.

	Subcritical Case 10TDA			Supercritical Case 12TDA		
Cycle time (min)	COE ($/MWh)	CO2 ($/tonne)	eff.	COE ($/MWh)	CO2 ($/tonne)	eff.
12	123.5	46.0	31.19	120.1	47.1	33.58
6	121.1	43.3	31.19	117.9	44.4	33.58
4.5	119.6	41.7	31.19	116.5	42.7	33.58

Desorption Pressure (Vacuum)

Instead of carrying out desorption at 3 psia using a relatively small steam purge, we could desorb at higher pressures using more steam. This is accomplished by maintaining the same steam purge velocity in both cases. When carrying out desorption at higher pressures say 4.5 psia instead of 3 psia, there is a larger loss associated with increased steam use while there is a gain in power consumed by vacuum pumps that led to a net efficiency improvements for the overall power plant. Most importantly when carrying out desorption at higher pressures such as 4.5 psia, there are commercial vacuum pumps that are now more available. Table 36 summarizes the net energy consumption by TDA's VSA system at different desorption

Table 36. Energy penalty associated with CO_2 capture as a function of desorption pressure.

	Case 10 - TDA				Case 12- TDA				Case 10 - DO	Case 12 - DO
	3.0 psi	4.5 psi	6.0 psi	7.5 psi	3.0 psi	4.5 psi	6.0 psi	7.5 psi	Amines	
	Subcritical	Subcritical	Subcritical	Subcritical	Supercritical	Subcritical	Subcritical	Subcritical	Subcritical	Supercritical
Feed HHV, kW	1,763,370	1,763,370	1,763,370	1,763,370	1,637,841	1,637,841	1,637,841	1,637,841	2,102,643	1,934,519
CO2 flow, kmol/hr	12,618	12,618	12,618	12,618	11,721	11,720	11,720	11,720	15,046	13,844
90% capture	11,357	11,357	11,357	11,357	10,549	10,548	10,548	10,548	13,542	12,460
Steam flow, kmol/hr	4,997	7,495	9,994	12,492	4,641	6,962	9,283	11,604	48,632	44,922
Actual steam flow, m^3/h	548,800	548,800	548,800	548,800	509,765	509,765	509,765	509,765	218,008	201,376
T, F	200	200	200	200	200	200	200	200	565	565
P, psia	3	4.5	6	7.5	3	4.5	6	7.5	74	74
H, Btu/lbm	1148.75	1148.4125	1147.98	1147.5	1148.75	1148.4125	1147.98	1147.5	1,313	1,313
Steam heat value, kW_{th}	13,764	20,640	27,510	34,373	12,785	19,172	25,553	31,928	153,060	141,384
Steam heat value, kW_e	5,363	8,041	10,718	13,392	5,299	7,947	10,592	13,234	59,632	58,604
Vacuum pump power, kW_e	34,336	26,870	22,073	18,615	32,552	25,475	20,929	17,651	-	-
Total power loss, kW_e	39,699	34,912	32,791	32,007	37,851	33,422	31,521	30,885	59,632	58,604

pressures compared against those of the amines based system. The heating value of the steam used in the CO_2 capture process is converted to electric energy using a conversion efficiency of 38.96% and 41.45% for subcritical and supercritical power plants, respectively. We observed that the net power consumption for CO_2 capture reduces as we increase the desorption pressure. However, the benefits diminish in value as we go to desorption pressures above 4.5 psia. Table 37 shows the sensitivity of COE and cost of CO_2 capture to desorption pressure. The sensitivity analysis shown in the Table 37 does not take the improvements in cycle optimization etc. into account (uses the base case for comparison). At a desorption pressure of 4.5 psia the cost of CO_2 capture is reduced by $1.0 and $0.6 per tonne CO_2 for subcritical and supercritical power plants, respectively.

Table 37. Sensitivity of COE and cost of CO_2 capture to desorption pressure.

	Subcritical Case 10TDA			Supercritical Case 12TDA		
Vacuum level (psia)	COE ($/MWh)	CO2 ($/tonne)	eff.	COE ($/MWh)	CO2 ($/tonne)	eff.
3	123.5	46.0	31.19	120.1	47.1	33.58
4.5	122.1	45.0	31.55	119.4	46.5	33.81
6	121.4	44.4	31.74	118.7	45.9	34.01
7.5	121.0	44.2	31.82	118.3	45.6	34.10

Coal Price

In the latest DOE update to their study on baseline fossil energy power plants (DOE/NETL-341/082312), they had updated the cost basis to 2011 $ from 2007 $. The fuel costs were updated to June 2011 values according to the Quality Guidelines for Energy System Studies, "Fuel Prices for Selected Feedstocks in NETL Studies." The June 2011 fuel costs were $2.94/MMBtu ($68.6/ton) for Illinois No. 6 bituminous coal. Table 38 (adapted from Exhibit 4-1 from the DOE study) summarizes the changes to the fuel cost from June 2007 to June 2011, which is significant almost 80% increase in fuel cost. If we look at the trend for the fuel cost particularly, Illinois No. 6 bituminous coal over the past five years, we see that June 2011 costs is not a presentative number rather one of the high points in the historical coal price data as seen in the data obtained from EIA website (Figure 100). Hence, we carried out a sensitivity analysis of COE and cost of CO2 capture to coal price. We used the current coal price of $32.75/ton and applied a 20% margin to it to get $39.3/ton, which was used in this sensitivity analysis. Table 39 summarizes the impact of coal price on the COE and cost of CO_2 capture. We observed that when updated to the current coal price, the cost of CO_2 capture is reduced by

$2.5 and $2.3 for subcritical and supercritical power plants, respectively. The sensitivity analysis shown in the Table 40 does not take the improvements in cycle optimization etc. into account (uses the base case for comparison).

Table 38. Comparison fuel cost 2007 $ and 2011 $ basis.

	June 2007 Cost Basis	June 2011 Cost Basis
Illinois No. 6 Coal, $/MMBtu	1.64	2.94
Illinois No. 6 Coal, $/ton	38.18	68.60

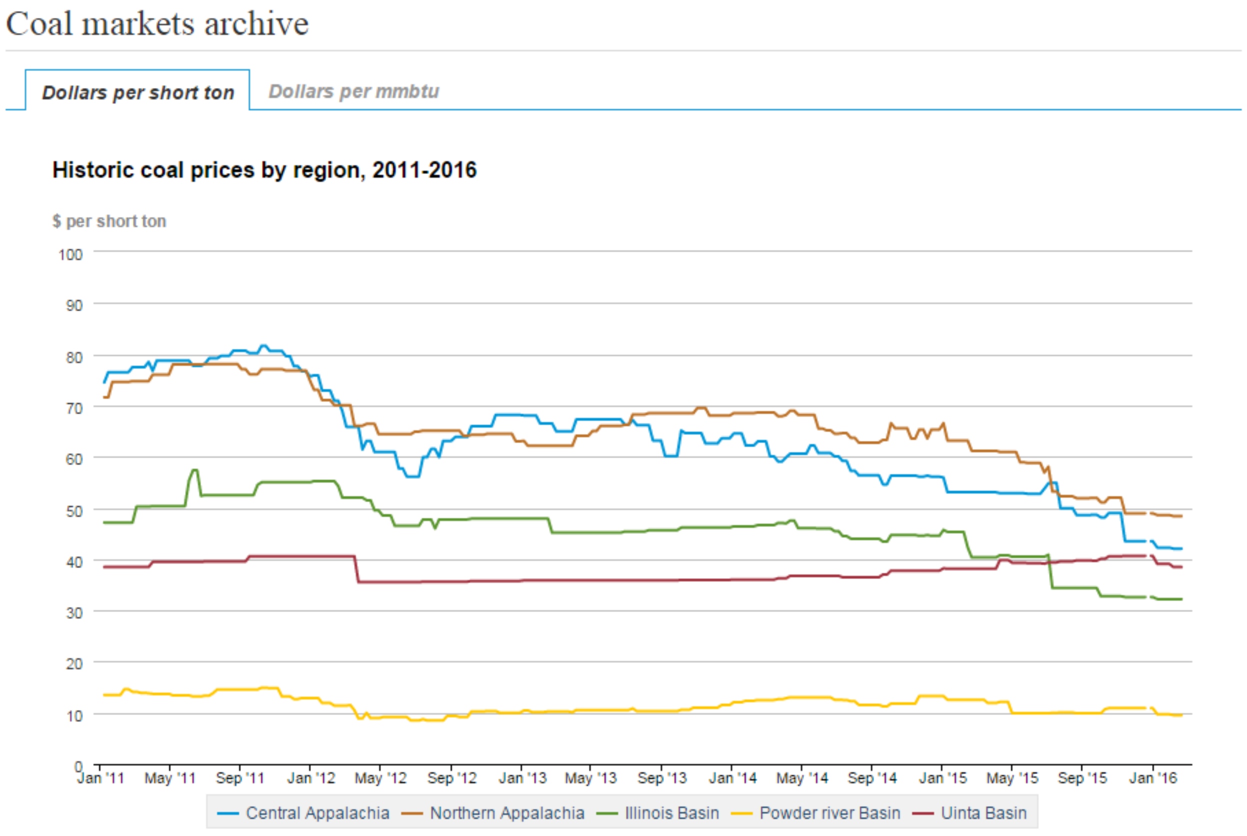

Source: SNL Energy

Figure 100. Historical coal price over the past 5 years.

Table 39. Sensitivity of COE and cost of CO_2 capture to coal price.

	Subcritical Case 10 Amines			Supercritical Case 12 Amines		
Coal Price ($/ton)	COE ($/MWh)	CO2 ($/tonne)	eff.	COE ($/MWh)	CO2 ($/tonne)	eff.
68.6	153.03	65.46	26.20	147.44	66.56	28.40
39.3	136.21	60.81	26.20	131.96	62.22	28.40
	Subcritical Case 10TDA			Supercritical Case 12TDA		
Coal Price ($/ton)	COE ($/MWh)	CO2 ($/tonne)	eff.	COE ($/MWh)	CO2 ($/tonne)	eff.
68.6	123.5	46.0	31.19	120.1	47.1	33.58
39.3	109.4	43.5	31.19	107.1	44.8	33.58

Cost Analysis of Optimized Conditions

When combining the benefits of short cycle time, cycle optimization and regeneration under higher vacuum, the cost of CO_2 captured is lowered to $38.90 and $39.71 per tonne for subcritical and supercritical PC power plants. The COE is 40.6% and 40.3% lower than those for corresponding sub and supercritical power plants equipped with amine based CO_2 capture systems. When the coal price is updated to current price ($39.3/ton) the cost of CO2 capture is well below the $40 target ($36.47 and $37.41 per tonne) for both the sub-critical and super-critical power plants. This shows that there is potential for TDA technology to meet or even be lower than the DOE target $40 per tonne based 2011 $. Further improvements are possible by carrying out regenerations at even higher vacuum levels than 4.5 psia used in these optimized design.

Table 40. COE and cost of CO_2 capture under optimized conditions.

	4.5 min Cycle time, 4.5 psia vacuum, $68.6/ton Coal price		4.5 min Cycle time, 4.5 psia vacuum, $39.3/ton Coal price	
	Subcritical	Supercritical	Subcritical	Supercritical
	Case 10 TDA	Case 12 TDA	Case 10 TDA	Case 12 TDA
COE ($/MWh)	$116.71	$113.76	$102.76	$100.72
CO2 ($/tonne)	$38.90	$39.71	$36.47	$37.41
eff.	31.55	33.81	31.55	33.81

4.13.4 System Analysis Summary

In collaboration with the Advanced Power and Energy Program of the UCI, TDA completed the process design using Aspen Plus^{TM} simulation software. The analysis provided a thorough comparison against a current state-of-the-art amine based CO_2 capture system integrated with both sub-critical and super-critical coal-fired power plants. In the simulation work, UCI strictly followed the guidelines and assumptions established by DOE/NETL for assessing the economic viability of competing CO_2 capture technologies. First, the accuracy of the Aspen Model was verified by checking the simulation results against the DOE/NETL analysis (Case 10 and Case 12 in the updated DOE/NETL report DOE/NETL-2010/1397 Rev. 2a). The results of the UCI's Aspen model simulating the amines based CO_2 capture case was found in close agreement with the DOE/NETL results (Table 41).

The analysis explored several design options; the moving bed system, axial flow "stacked" fixed beds with external manifolds, radial flow fixed beds with internal manifolds, using LP steam from steam turbine cycle for purge and LP steam generated from CO_2 compression. We decided to use the steam generated from CO_2 compression to eliminate any changes to the ST cycle. In this final summary we incorporated the lower steam consumption of Steam: CO_2 ratio of 0.44 in the steam purge step as shown in our tests at GTI using coal derived flue gas and also used a VSA cycle time of 4.5 min and desorption pressure of 4.5 psia. TDA's post combustion CO_2 capture system integrated with a sub-critical and super-critical pulverized coal fired power plant achieves a net plant efficiency of 31.55% and 33.81% on HHV basis; these are significantly higher than that can be achieved by amines based CO_2 capture system (26.2% and 28.4%). The water consumption in the plant on a net kW basis is also lower for TDA's process (29.7 and 26.8 m^3/min for TDA Case 10 and case 12 vs 42.5 and 38.1 m^3/min for amines Case 10 and

Case 12), preserving a valuable resource). The capital expense for the plant was estimated following the DOE/NETL cost guidelines (e.g. higher contingencies were applied for unproven technologies such as the VSA unit). The total cost for the sub-critical and super-critical coal fired plants integrated with TDA's process is estimated as \$2,583/kW$_e$ and \$2,613/kW$_e$, respectively. These are 28.2% and 26.7% lower than those of the corresponding amine based cases.

Table 41. Comparison of TDA's VSA based CO_2 capture system against amine based CO_2 capture system integrated with a super-critical power plant (550 MW$_e$ net plant output).

Power plant Type	**Sub-critical PC Plant**		**Supercritical PC Plant**	
CO_2 Capture Technology	**Amines**	**TDA- VSA**	**Amines**	**TDA - VSA**
Case ID	**Case 10 DOE**	**Case 10 TDA**	**Case 12 DOE**	**Case 12 TDA**
Gross Power Generated, kWe	672,700	669,778	662,800	661,828
Auxiliary Load, kWe	122,740	119,778	112,830	111,828
Net Power, kWe	549,960	550,000	549,970	550,000
Net Plant Efficiency, % HHV	**26.20**	**31.55**	**28.40**	**33.81**
Coal Feed Rate, kg/h	278,956	231,261	256,652	215,810
Total Plant Cost, \$/kWe	3,596	2,583	3,563	2,613
COE without CO_2 TS&M, \$/MWh	142.22	107.86	137.45	105.99
COE with CO_2 TS&M, \$/MWh	**153.03**	**116.71**	**147.44**	**113.76**
Cost of CO_2 Captured, \$/tonne	**65.46**	**38.90**	**66.56**	**39.71**

The levelized cost of electricity including the TS&M costs for CO_2 is calculated as \$116.71/MWh and \$113.76/MWh for TDA system integrated with sub-critical and super-critical pulverized coal fired power plants; much lower than the \$153.03/MWhand \$147.44/MWh calculated for the corresponding amine based systems. The cost of CO_2 captured for TDA's VSA based system is \$38.90 and \$39.71 per tonne compared to \$65.46 and \$66.56 per tonne for amine based system on 2011 \$ basis, providing 40% lower cost of CO_2 captured. In this analysis we have used a sorbent life of 4 years. If a longer sorbent life can be maintained (which is not unreasonable for fixed bed commercial PSA systems), this would bring the cost of CO_2 captured lower by \$0.05 per tonne (e.g., \$38.85 and \$39.66 per tonne at 5 years sorbent replacement).

These system analysis results suggest that TDA's VSA-based post-combustion capture technology can substantially improve the power plant's thermal performance while achieving near zero emissions, including greater than 90% carbon capture. The higher net plant efficiency and lower capital and operating costs results in a substantial reduction in the cost of carbon capture and cost of electricity for the power plant equipped with TDA's technology.

4.14 Task 14. Preliminary Environmental Health & Safety (EH&S) Assessment

As part of this DOE funded program, an Environmental, Health & Safety Assessment was performed by our partner Babcock & Wilcox (B&W) on the pulverized coal-fired power plant utilizing the TDA solid-sorbent process and all system waste streams. Results from this study are provided to DOE in a Topical report. The toxicological, ecological, and regulatory compliance for each waste stream was evaluated and discussed in that report. B&W concluded that further testing is still required on the ultimate fate of trace metals such as mercury and arsenic with the spent solid-sorbent and that there are no additional EH&S concerns with the TDA solid-sorbent over a current pulverized coal-fired power plant.

5. Conclusions and Recommendations

In this project we developed a new post combustion carbon capture technology based on a vacuum swing adsorption system that uses a steam purge and demonstrated its technical feasibility and economic viability in laboratory-scale tests and tests in actual coal derived flue gas. We also carried out a detailed process design and analysis of the new system as part of both sub-critical and super-critical pulverized coal fired power plants. The new technology uses a low cost, high capacity adsorbent that selectively removes CO_2 in the presence of moisture at the flue gas temperature without a need for significant cooling of the flue gas or moisture removal. The sorbent is based on a TDA mesoporous carbon that consists of surface functionalized groups that remove CO_2 via physical adsorption. The high surface area and favorable porosity of the sorbent also provides a unique platform to introduce additional functionality, such as active groups to remove trace metals (e.g., Hg, As).

In collaboration with the Advanced Power and Energy Program of the University of California, Irvine (UCI), TDA developed system simulation models using Aspen Plus^{TM} simulation software to assess the economic viability of TDA's VSA-based post-combustion carbon capture technology. The levelized cost of electricity including the TS&M costs for CO_2 is calculated as \$116.71/MWh and \$113.76/MWh for TDA system integrated with sub-critical and super-critical pulverized coal fired power plants; much lower than the \$153.03/MWhand \$147.44/MWh calculated for the corresponding amine based systems. The cost of CO_2 captured for TDA's VSA based system is \$38.90 and \$39.71 per tonne compared to \$65.46 and \$66.56 per tonne for amine based system on 2011 \$ basis, providing 40% lower cost of CO_2 captured. In this analysis we have used a sorbent life of 4 years. If a longer sorbent life can be maintained (which is not unreasonable for fixed bed commercial PSA systems), this would lower the cost of CO_2 captured by \$0.05 per tonne (e.g., to \$38.85 and \$39.66 per tonne at 5 years sorbent replacement).

These system analysis results suggest that TDA's VSA-based post-combustion capture technology can substantially improve the power plant's thermal performance while achieving near zero emissions, including greater than 90% carbon capture. The higher net plant efficiency and lower capital and operating costs results in a substantial reduction in the cost of carbon capture and cost of electricity for the power plant equipped with TDA's technology.

5.1 Recommendations for Future Work

The results of the DE-FE0007580 project suggest that TDA's VSA-based post-combustion carbon capture technology merits further research and development. It is recommended that the performance of a fully-equipped system should be demonstrated at larger-scale (e.g., 1 MW) using actual flue gas for a longer duration (6 to 12 months). The system should contain all critical components (including all VSA reactors, accumulators etc.) to fully demonstrate the cycle sequence, enabling the demonstration of product CO_2 purity and recovery. The demonstration duration should be long enough to allow over 72,000 cycles (with a 4.5 min full cycle time this corresponds to 7.5 months of testing) under optimum operating conditions. The selected next demonstration scale should be large enough to require sorbent production in large quantities (at the recommended 1 MW demonstration 8 m^3 of sorbent will be needed). A more detailed system simulation and cost analysis is also recommended, including design work and accurate quotes from the suppliers of the major process equipment (e.g., vacuum pumps, steam turbines and boilers). Successful completion of this recommended work will provide the basis for the new technology to be employed in potential commercial pilot-scale demonstrations (50-100 MW scale).

6. References

DOE/NETL-2007/1281 (2007) “Cost and Performance Baseline for Fossil Energy Plants Volume 1: Bituminous Coal and Natural Gas to Electricity,” Revision 1, August 2007.

DOE/NETL-2010/1397 (2010) “Cost and Performance Baseline for Fossil Energy Plants Volume 1: Bituminous Coal and Natural Gas to Electricity,” Revision 2, November 2010.

DOE/NETL-2010/1397 (2013) “Cost and Performance Baseline for Fossil Energy Plants Volume 1: Bituminous Coal and Natural Gas to Electricity,” Revision 2a, September 2013.

DOE/NETL-341/082312 (2012) “Updated Costs (June 2011 Basis) for Selected Bituminous Baseline Cases,” August 2012

Farooq, S.; Rathor, M. N.; Hidajat, K. A. (1993) “A predictive model for a kinetically controlled pressure swing adsorption process,” Chem. Eng. Sci., Vol. 48, Pg. 4129-4141.

Jayaraman, A. (2004) “New Nano-structured sorbent materials for gas separation, purification and storage,” Ph.D. Dissertation, Universioty of Michigan, Chapter 2, Pg.

Guío-Pérez, D.C., T. Pröll, and H. Hofbauer, Solids residence time distribution in the secondary reactor of a dual circulating fluidized bed system. Chemical Engineering Science, 2013. 104(0): p. 269-284.

Knight, A., et al., CO_2 sorbent attrition testing for fluidized bed systems. Powder Technology, 2014. 266(0): p. 412-423.

Porrazzo, R., G. White, and R. Ocone, Aspen Plus simulations of fluidised beds for chemical looping combustion. Fuel, 2014. 136(0): p. 46-56.

Ridha, F.N., et al., Post-combustion CO_2 capture by formic acid-modified CaO-based sorbents. International Journal of Greenhouse Gas Control, 2013. 16(0): p. 21-28.

Sun, L. M.; Le Quere, P.; LeVan, M. D. (1996) “Numerical simulation of diffusion-limited PSA process models by finite difference methods,” Chem. Eng. Sci., Vol. 51(24),Pg. 5341-5352.

Tonks, Bill (2007). “CBM/CMM/AMM/VAM Mitigation, Past-Present-Future” presented at 1st Annual US EPA CMOP CMM Conference St. Louis, MO 25-27 September, 2007.

Attachment 1. Moving and Circulating Fluidized Bed Literature

Rank	Author	Document Title	Publication Date	Source Type	Volume	Issue	Page	Abstract
1	M.M. Hossain, K.E. Sedor, H.I. De Lasa	Coâ€"Ni/Al2O3 oxygen carrier for fluidized bed chemical-looping combustion: Desorption kinetics and metalâ€"support interaction	(1 Oct 2007)	Chemical Engineering Science	62	18	5464-5472	This study was aimed at developing a suitable oxygen carrier for fluidized bed chemical-looping combustion (CLC) processes. To this end a Co promoted Coâ€"Ni/Al2O3 carrier material was synthesized and evaluated. The reactivity of the solid carrier material was assessed by investigating the energetics and kinetics of metalâ€"support interaction using temperature programmed H2 desorption technique. The estimated activation of energy of hydrogen desorption for Coâ€"Ni/Al2O3 was found to be less than that of unpromoted Ni/Al2O3 samples. This result suggested that doping the fluidizable oxygen carrier with Co decreases the metal-support interaction and the binding energies between the metals and the H2 molecules, with this playing a significant role to increase the activity of such material. The reactivity and stability of the prepared oxygen carrier particles, under repeated reduction/oxidation cycles, was established in a CREC riser simulator using CH4 and air for the reduction and oxidation cycles, respectively. Over multiple CLC cycles, the Coâ€"Ni/Al2O3 particles displayed excellent reactivity and stability with minimum changes in metal dispersion and crystallite size. Thus, it is concluded that Co might promote the performance of Coâ€"Ni/Al2O3 particles by reducing the metalâ€"support interactions, as assessed using temperature programmed H2 desorption. This reduced interaction has a favorable effect on the oxygen carrier reactivity during the oxidation and reduction reactions.
2	H.R. Kim, D. Wang, L. Zeng, S. Bayham, A. Tong, E. Chung, M.V. Kathe, S. Luo, O. Mcgiveron, A. Wang, Z. Sun, D. Chen, L.S. Fan	Coal direct chemical looping combustion process: Design and operation of a 25-kWth sub-pilot unit	(1 Jun 2013)	Fuel	108	null	370-384	The Coal-Direct Chemical Looping (CDCL) process using iron-based oxygen carriers has been developed as a coal conversion process with in situ CO2 capture. The CDCL system cycles oxygen carriers between two reactors, a reducer reactor and a combustor reactor, in order to convert coal for electric power generation. The reducer reactor features a unique design of a gasâ€"solid counter-current moving bed configuration to achieve the reduction of Fe2O3 particles to a mixture of Fe and FeO while converting the coal into CO2 and steam. The combustor reactor is a fluidized bed that oxidizes the reduced particles back to Fe2O3 with air. The oxidation of iron is an exothermic reaction and the heat can be recovered for electricity generation. In the riser, the particles are pneumatically transported back to the reducer. An integrated 25-kWth CDCL sub-pilot plant has been constructed and demonstrated, which is the first integrated chemical looping demonstration unit for the direct conversion of solid fuel with a circulating moving bed system. The design and operation experience of the 25kWth CDCL sub-pilot unit are reported in this paper. Specifically, the design criteria and operation conditions of the CDCL reactor system are first discussed which is followed by the construction of the sub-pilot unit. The tests with metallurgical coke and sub-bituminous coal resulted in 81% and 97% carbon conversions, respectively. Both tests yielded CO2 purity greater than 99%, indicating the complete oxidation of volatile gases in the moving bed reducer. The gas analyses from the combustor outlet demonstrated a proper regeneration of oxygen carriers. A low CO2 concentration in the combustor also confirms that there was no unconverted carbon transfer to the combustor and hence eliminated the need for an additional carbon separation device such as a carbon stripper. The demonstration results from the sub-pilot system substantiate the process concept of the CDCL, which is capable of processing coal continuously with reactor in situ CO2 capture and the cyclic usage of oxygen carriers.
3	M.R. Quddus, M.M. Hossain, H.I. De Lasa	Ni based oxygen carrier over Î³-Al2O3 for chemical looping combustion: Effect of preparation method on metal support interaction	(1 Jul 2013)	Catalysis Today	210	null	124-134	This study deals with the development of a Ni based oxygen carrier (OC) over La-modified and Co-doped Î³-Al2O3 suitable for a fluidized bed chemical-looping combustion (CLC) process. La is found to stabilize the bulk phase transformation of Î³-Al2O3 whereas Co minimizes the formation of irreducible bulk nickel aluminate. Apart from these beneficial effects, the reducibility and the structural properties of the prepared OCs are found to be modified by the different preparation methods used. The N2 adsorption isotherm shows that Î³-Al2O3 retains its structural integrity in only one preparation method. Reducibility as determined by consecutive temperature programmed reduction and oxidation techniques resembles the chemical properties of Î´- and Î¸-Al2O3 for the other two preparation methods. However, no bulk phase change is detected for the three OCs using XRD. This suggests that the observed changes occur mainly at the molecularly thin surface layers of the OCs which display structural properties (geometric, electronic, coordination) significantly different from those of the bulk. The prepared OCs are also tested under CLC operating condition of the Chemical Reactor Engineering Center (CREC) fluidized Riser Simulator, using multiple reduction/oxidation cycles. Reactivity results obtained show expected reducibility, oxygen carrying capacity and stability with the three different preparation techniques.

4	S. Bhavsar, B. Tackett, G. Veser	Evaluation of iron- and manganese-based mono- and mixed-metallic oxygen carriers for chemical looping combustion	(15 Nov 2014)	Fuel	136	null	268-279	Chemical looping combustion (CLC) is an emerging technology for clean combustion of fossil fuels with inherent CO2 capture. In the present work, we investigate the use of iron and manganese based mixed oxides (MnxFe1â�′xâ€“CeO2) supported on CeO2 as oxygen carriers in CLC. The low cost and low toxicity of iron and manganese make them interesting candidates for CLC, but both mono-metallic carriers suffer from issues of low reactivity, and manganese is additionally prone to form undesired spinel structures with typical oxide supports. Mono- and bimetallic oxygen carriers were synthesized across the entire spectrum of compositions from pure Mn to pure Fe (with x=0, 0.1, 0.33, 0.5, 0.8, 0.9, 1), characterized, and tested in thermogravimetric and fixed-bed reactor studies using H2 and CH4 as fuels. We find that the use of ceria as support results in stable operation for all compositions of the metal phase, including pure Mn. Bimetallic carriers with high Fe content, which contain a FeMnO3 phase, exhibit an unusual, reversible de-alloying/re-alloying behavior during cyclic redox operation, which precludes any synergistic effects between the two metals and results in slowed reduction kinetics. However, Mn-rich carriers show a pronounced increase in carrier reactivity and selectivity for total oxidation of methane due to the addition of small amounts of Fe, indicating the promise of appropriately designed FeMn carriers as low-cost, environmentally benign oxygen carrier materials for chemical looping combustion.
5	Z. Huang, F. He, Y. Feng, K. Zhao, A. Zheng, S. Chang, H. Li	Synthesis gas production through biomass direct chemical looping conversion with natural hematite as an oxygen carrier	(1 Jul 2013)	Bioresource Technology	140	null	138-145	Biomass direct chemical looping (BDCL) conversion with natural hematite as an oxygen carrier was conducted in a fluidized bed reactor under argon atmosphere focusing on investigation the cyclic performance of oxygen carrier. The presence of oxygen carrier can evidently promote the biomass conversion. The gas yield and carbon conversion increased from 0.75Nm3/kg and 62.23% of biomass pyrolysis to 1.06Nm3/kg and 87.63% of BDCL, respectively. The components of the gas product in BDCL were close to those in biomass pyrolysis as the cyclic number increased. The gas yield and carbon conversion decreased from 1.06Nm3/kg and 87.63% at 1st cycle to 0.93Nm3/kg and 77.18% at 20th cycle, respectively, due to the attrition and structural changes of oxygen carrier. X-ray diffraction (XRD) analysis showed that the reduction extent of oxygen carrier increased with the cycles. Scanning electron microscope (SEM) and pore structural analysis displayed that agglomeration was observed with the cycles.
6	D.C. GuÃ-o-PÃ©rez, T. PrÃ¶ll, H. Hofbauer	Solids residence time distribution in the secondary reactor of a dual circulating fluidized bed system	(18 Dec 2013)	Chemical Engineering Science	104	null	269-284	Highlightsâ€¢Residence time of the particles in the fuel reactor of a CLC unit is investigated.â€¢Residence time distribution of particles is measured in a cold flow model.â€¢A ferromagnetic tracer and inductance sensors are used.â€¢A model is successfully adjusted to the experimental data for diverse conditions.â€¢Effects of circulation rate, fluidization velocity and inventory are investigated.
7	K.E. Sedor, M.M. Hossain, H.I. De Lasa	Reactivity and stability of Ni/Al2O3 oxygen carrier for chemical-looping combustion (CLC)	(1 Jun 2008)	Chemical Engineering Science	63	11	2994-3007	Chemical-looping combustion (CLC) is a technology that reduces the carbon dioxide emissions from fossil fuel power stations. A nickel supported on Î±-alumina oxygen carrier is investigated in this study, for use in a CLC process. Oxygen carriers with various nickel loadings on alumina are prepared according to the incipient wetness technique. The reactivity and stability of the prepared oxygen carrier samples, during repeated reductionâ€“oxidation cycles, is demonstrated using temperature programmed reduction and oxidation. Pulse chemisorption results show that the dispersion and active crystallite diameter of the nickel particles remain constant over multiple reductionâ€“oxidation cycles, indicating that no agglomeration occurs up to a nickel loading of 20wt% supported on alumina. The stability and reactivity of the oxygen carriers, under industrial relevant conditions, are also investigated using the CREC fluidized bed riser simulator. It is observed that a 20wt% nickel supported on alumina oxygen carrier is stable under industrial relevant fluidized bed reaction conditions, converting 76% of methane to carbon dioxide and water vapor, the combustion products. The metal support interaction is assessed by H2 temperature programmed desorption, which shows that the metal-support interaction decreases as more nickel is loaded onto the alumina support.
8	M.M. Hossain, D. Lopez, J. Herrera, H.I. De Lasa	Nickel on lanthanum-modified Î³-Al2O3 oxygen carrier for CLC: Reactivity and stability	(15 May 2009)	Catalysis Today	143	1	179-186	This study deals with the development of a lanthanum-modified Ni/La-Î³-Al2O3 oxygen carrier suitable for a fluidized bed chemical-looping combustion (CLC) process. BET specific surface area analysis shows that the addition of La favors the thermal stability of Î³-Al2O3 by preventing phase transformation. Temperature programmed characterization shows that the presence of La enhances the reducibility of the oxygen carrier by influencing the metalâ€“support interactions helping the formation of reducible nickel species. Reactive characterization of the prepared oxygen carriers in a Chemical Reactor Engineering Center (CREC) fluidized Riser Simulator, using multiple reduction/oxidation cycles, demonstrates that the Ni/La-Î³-Al2O3 particles display excellent reactivity and stability. The addition of La in the Ni/La-Î³-Al2O3 influences the state of the surface minimizing the formation of nickel aluminate. It is argued that the addition of La also inhibits metal particle agglomeration by maintaining consistent metal dispersion during the cyclic oxidation/reduction processes.

9	C. Dueso, M.T. Izquierdo, F. GarcÃ-a-Labiano, L.F. De Diego, A. Abad, P. GayÃ¡n, J. AdÃ¡nez	Effect of H2S on the behaviour of an impregnated NiO-based oxygen-carrier for chemical-looping combustion (CLC)	(25 Sep 2012)	Applied Catalysis B: Environmental	126	null	186-199	Gaseous fuels for chemical-looping combustion (CLC) process may contain sulphur-compounds which could affect the oxygen-carrier behaviour, especially if NiO is used as active phase. In this work, several samples of a NiO-based oxygen-carrier prepared by impregnation (18wt.%) on Î±-Al2O3, so-called NiO18-Î±Al, were extracted from a CLC unit after continuous operation with CH4 containing 500vppm of H2S and characterized subsequently. Part of the sulphur fed to the system was release as SO2 in the air-reactor during the CLC experiments while the rest remained in the solid particles. Ni3S2 was found in the oxygen-carrier extracted from the fuel-reactor, although small amounts of NiSO4 were also detected. On the contrary, NiSO4 was the main sulphur compound in the oxygen-carrier from the air-reactor while a low concentration of Ni3S2 was present. Despite the accumulated sulphur and the oxygen transport capacity loss during the operation, the oxygen-carrier was capable of recovering the initial reactivity for the CH4 combustion after some time without H2S feeding to the CLC system. In addition, a study about the possible regeneration of the oxygen-carrier in the air-reactor working at different temperatures and oxygen concentrations was performed. Independently of the operating conditions, part of the sulphur remained in the solid and total regeneration was not possible. The analysis of the NiO18-Î±Al oxygen-carrier after the CLC operation using TPR and XPS techniques revealed that sulphur reacted preferably with free NiO instead of NiAl2O4. Although Ni3S2 was the majority sulphide in the fuel-reactor, minor amounts of other sulphides such as NiS were detected. Sulphur was preferably concentrated in the outer surface of the particles. Taking into account all these results, a previous desulphuration process of the fuel would be necessary when NiO-based oxygen-carriers are used in a CLC system.
10	H. Gu, L. Shen, J. Xiao, S. Zhang, T. Song, D. Chen	Iron ore as oxygen carrier improved with potassium for chemical looping combustion of anthracite coal	(1 Jul 2012)	Combustion and Flame	159	7	2480-2490	Chemical looping combustion (CLC) is an innovative combustion technology with inherent separation of CO2 without energy penalty. When solid fuel is applied in CLC, the gasification of solid fuel is the rate-limiting process for in situ gasification of coal and reduction of oxygen carrier. The K2CO3-decorated iron ore after calcinations was used as oxygen carrier in CLC of anthracite coal, and potassium ferrites were formed during the calcinations process. The experiments were performed in a laboratory fluidized bed reactor with steam as a gasification medium. Effects of reaction temperature, K2CO3 loading in iron ore and cycle on the gas concentration, carbon conversion, gasification rate and yields of carbonaceous gases were investigated. The carbon gasification was accelerated during the fast reaction stage between 860Â°C and 920Â°C, and the waterâ€“gas shift reaction was significantly enhanced in a wider temperature range of 800Â°C to 920Â°C. With the K2CO3 loading in iron ore increasing from 0% to 20% at 920Â°C, the carbon conversion was accelerated in the fast reaction stage, and the fast reaction stage became shorter. The yield of CO2 reached a maximum of 94.4% and the yield of CO reached a minimum of 3.4% when use the iron ore loaded with 6% K2CO3. SEM analysis showed that the K2CO3-decorating in iron ore would cause a sintering on the particle surface of oxygen carrier, and the K2CO3 loading in iron ore should not be too high. Cycle experiments indicate that the K2CO3-decorated iron ore has a relative stable catalytic effect in the CLC process.
11	L. Nalbandian, A. Evdou, V. Zaspalis	La1â⍰xSrxMyFe1â⍰yO3â⍰Î´ perovskites as oxygen-carrier materials for chemical-looping reforming	(1 Jun 2011)	International Journal of Hydrogen Energy	36	11	6657-6670	The use of perovskites with the general formula La1â⍰xSrxMyFe1â⍰yO3 (MÂ =Â Ni, Co, Cr, Cu) as oxygen carriers for syngas generation from methane by Chemical Looping Reforming is investigated in the present work. The experimental study concerns the oxidation of a fuel, using the oxygen from a solid oxygen carrier, instead of oxygen from air. Subsequent oxidation of the reduced solid is performed either with gaseous oxygen or with water. In the latter case additional hydrogen is produced, which is very pure and therefore appropriate to be used in fuel cell applications. The performance of the candidate materials is ranked by taking into account the hydrogen and carbon monoxide yields during the fuel oxidation step as well as the amount of oxygen per mole solid (Î´) that can be delivered reversibly to the fuel. The effect of the materials composition and of NiO addition is examined. The best performance was obtained with the La0.7Sr0.3Cr0.1Fe0.9O3 sample mixed with 5% NiO. The H2 yield was up to 90%.

12	W.C. Yang	Particuology and climate change	(1 Dec 2010)	Particuology	8	6	507-513	The global concern over the greenhouse gas emissions and its effect on global warming and climate change has focused attention on the necessity of carbon dioxide capture and sequestration. There are many processes proposed to capture carbon either before or after combustion and these processes invariably involve investigation and application of traditional particuology. The solids employed are of different sizes, densities, morphologies, and strengths. Their handling, transportation, recirculation, and reactor applications are the essence of â€˜particuologyâ€™. Particuology can play an important and vital role in achieving cost-effective removal of carbon and minimize emissions of greenhouse gases. In this paper, the existing and developing carbon capture processes are briefly reviewed and the opportunities for application of particuology are identified. The review was not intended to be exhaustive. It is only in sufficient detail to make connection between particuology and climate change. For immediate and future challenges of reducing global warming and carbon capture and sequestration, innovative reactor design and application of particuology is imperative. Expertise and innovation in particuology can greatly enhance the speed of development of those technologies and help to achieve cost-effective implementation. Particuology is indeed intimately related to the climate change and global warming.
13	E. Ksepko	Perovskite-type Sr(Mn1â�’xNix)O3 materials and their chemical-looping oxygen transfer properties	(15 May 2014)	International Journal of Hydrogen Energy	39	15	8126-8137	Highlightsâ€¢Sr(Mn1â�’xNix)O3 perovskites were synthesized and characterized.â€¢The reactivity of the perovskites for CLC of hydrogen was evaluated.â€¢Perovskites showed stable CLC performance with excellent reactivity.
14	P. Erri, A. Varma	Solution combustion synthesized oxygen carriers for chemical looping combustion	(1 Oct 2007)	Chemical Engineering Science	62	18	5682-5687	Chemical looping combustion is an attractive method for CO2 capture in power plants, while maintaining high energy efficiency. The cyclic nature of the process, however, places significant demands on the redox and mechanical characteristics of the oxygen carrier. In this work, NiO/NiAl2O4 and (NiO)1-y(MgO)y/Ni(1-x)MgxAl2O4 were synthesized by solution combustion and investigated in two forms: porous extruded and dense pressed pellets. The pressed oxygen carriers of both compositions exhibited excellent stability during thermogravimetric analysis at temperatures 800â€“1200â�˜C with cycling of oxidizing/reducing gases while, due to sintering effects, the extruded pellets showed deteriorating performance. The addition of magnesium to the structure decreased reduction of the spinel, thus stabilizing the support. Attrition tests revealed superior performance of the (NiO)0.21(MgO)0.79/Ni0.62Mg0.38Al2O4, exceeding that of commercially available sintered iron oxide reference.
15	H. Tian, Q. Guo	Thermodynamic investigation into carbon deposition and sulfur evolution in a Ca-based chemical-looping combustion system	(1 Sep 2011)	Chemical Engineering Research and Design	89	9	1524-1532	Chemical-looping combustion is a promising technology that concentrates CO2 and separates it during combustion. In this study, both the carbon deposition and sulfur evolution in the reduction of a calcium sulfate (CaSO4) oxygen carrier with a typical syngas were investigated using thermodynamic simulations. The effects of reaction temperature, operating pressure and the oxygen ratio number (defined in this paper) on the amount of deposited carbon and released sulfurous gases are discussed. A reaction temperature from 750 to 950Â°C, an operating pressure from 1 to 15bars and an oxygen ratio number between 0.4 and 0.8 were determined to be the most favorable operating conditions. In addition, the amounts of released sulfurous gases were found to be largely dependent on the partial pressures of H2 and CO based on the thermo-gravimetric analyzer (TGA) tests. When the partial pressure of H2 or CO was above 40kPa, the release of sulfurous gases could be prevented in the reaction between CaSO4 and syngas, even if the reaction temperature was as high as 1000Â°C. The XRD profiles of the products also demonstrated that the mole fraction of CaS in the products increased gradually with an increasing partial pressure of H2 or CO, until the products were almost pure CaS.
16	A. Knight, N. Ellis, J.R. Grace, C.J. Lim	CO2 sorbent attrition testing for fluidized bed systems	(1 Nov 2014)	Powder Technology	266	null	412-423	Highlightsâ€¢Attrition testing of potential CO2 sorbents is conducted in an ASTM testing unit.â€¢Attrition analyzed from time-varying particle size distributions and SEM imaging.â€¢Cement-bound lime pellets are highly sensitive to humidity and CaOH formation.â€¢Silica-coated limestone pellets have high resistance to attrition at 500Â°C.â€¢A modified Gwyn-relationship describes fragmentation effects for tested particles.

17	M. Virginie, J. AdÃ¡nez, C. Courson, L.F. De Diego, F. GarcÃ-a-Labiano, D. Niznansky, A. Kiennemann, P. GayÃ¡n, A. Abad	Effect of Feâ€“olivine on the tar content during biomass gasification in a dual fluidized bed	(13 Jun 2012)	Applied Catalysis B: Environmental	121	null	214-222	The Fe/olivine catalyst effectiveness regarding tar primary reduction during biomass gasification in dual fluidized beds has been investigated. The use of Fe/olivine instead olivine leads to an important decrease in the amount of produced tar, which was reduced by up to 65% at 850Â°C, naphthalene being the most stable molecule. It has been found that Fe/olivine materials have a double effect on tar destruction. On the one hand, they act as a catalyst for tar and hydrocarbon reforming. On the other hand, they can act as an oxygen carrier that transfers oxygen from the combustor to the gasifier, and part of the oxygen is used to burn volatile compounds. The catalyst was fairly stable because the result was confirmed during 48h of continuous operation. The Fe/olivine material characterization (X-ray diffraction, MÃ¶ssbauer spectroscopy, temperature programmed reduction and oxidation, etc.) revealed that the catalyst structure was maintained despite the large number of oxidizingâ€“reducing cycles. The carbon that formed on the catalyst surface was low and easily oxidized in the combustion zone. Therefore, the inexpensive and non-toxic Fe/olivine catalyst is a material suitable for use as primary catalyst in a fluidized bed gasification of biomass.
18	S. Cheah, K.R. Gaston, Y.O. Parent, M.W. Jarvis, T.B. Vinzant, K.M. Smith, N.E. Thornburg, M.R. Nimlos, K.A. Magrini-Bair	Nickel cerium olivine catalyst for catalytic gasification of biomass	(2 May 2013)	Applied Catalysis B: Environmental	134	null	34-45	A nickel cerium modified olivine was used as a fluidized bed material in a biomass gasifier and the impact of the modification on biomass conversion, product gas composition, and tar speciation at different temperatures of oak gasification was measured. The experiments were conducted in the pyrolysis mode, without additional input of steam or oxygen (e.g., from air) into the system. In both plain and modified olivine, carbon- and hydrogen-based yields in light gases produced increased as temperature increased from 600 to 800Â°C. Using modified olivine resulted in significant improvement in carbon- and hydrogen-based yields and substantial reduction in tars and methane. With modified olivine, the biochar produced at 800Â°C was 40% less than that with plain olivine. Characterization of the fresh and post-reaction catalyst showed that a fraction of the NiO was reduced in situ in the gasifier by the syngas. In addition, the catalyst was also contributing oxygen to the environment inside the gasifier in a chemical-looping like mode, resulting in less char and coke formation than that of gasification of biomass without an additional oxygen source. Statistical analysis of molecular beam mass spectrometry data provided detailed tar speciation information under different gasification conditions. At both 650 and 800Â°C, the modified olivine was effective in producing more syngas either through conversion of hydrocarbon rich tars into syngas or blocking the pathway for hydrocarbon rich tar formation. However, the impact of the modified olivine in converting oxygenates (that are primarily derived from deconstruction of biomass) into deoxygenated compounds was probably minimal.
19	F.N. Ridha, V. Manovic, Y. Wu, A. Macchi, E.J. Anthony	Post-combustion CO2 capture by formic acid-modified CaO-based sorbents	(1 Aug 2013)	International Journal of Greenhouse Gas Control	16	null	21-28	The performance of CaO-based sorbents modified with formic acid in both its liquid and vapor phase has been investigated for high-temperature post-combustion CO2 capture in calcium-looping cycles. The treatment of limestone with aqueous solutions containing 10 or 30vol% formic acid was found to promote crystal growth. By contrast, higher acid concentrations produced smaller crystals. However, all sorbents modified by acid solutions had almost identical reductions of 44% and 46% in surface area and pore volume (determined by N2 adsorption), respectively, relative to the parent material. Despite the low porosity, limestone (fine powder) treated with 10% acid solution displayed the highest CO2 capture capacity in the first cycle with a capture of 0.6g CO2/g sorbent compared to 0.49g/g for untreated powder material. By 20 cycles, the modified sorbent still captured 67.4% more CO2 than the natural sorbent captured under similar conditions. Relatively low concentration formic acid solution improved the CO2 capture capacity of CaO-based sorbents better than treatment with acid vapor due to the limited acidification achieved by vapor phase treatment.

20	J.M. Valverde, P.E. Sanchez-Jimenez, L.A. Perez-Maqueda	Calcium-looping for post-combustion CO2 capture. On the adverse effect of sorbent regeneration under CO2	(1 Aug 2014)	Applied Energy	126	null	161-171	The multicyclic carbonation/calcination (c/c) of CaO solid particles at high temperature is at the basis of the recently emerged Calcium-looping (CaL) technology, which has been shown to be potentially suitable for achieving high and sustainable post-combustion CO2 capture efficiency. Despite the success of pilot plant projects at the MWth scale, a matter of concern for scaling-up the CaL technology to a commercial level (to the GWth scale) is that the CaO carbonation reactivity can be recovered only partially when the sorbent is regenerated by calcination at high temperatures (around 950Â°C) as required by the CO2 high concentration in the calciner. In order to reactivate the sorbent, a novel CaL concept has been proposed wherein a recarbonator reactor operated at high temperature/high CO2 concentration leads to further carbonation of the solids before entering into the calciner for regeneration. Multicyclic thermogravimetric analysis (TGA) tests demonstrate the feasibility of recarbonation to reactivate the sorbent regenerated at high calcination temperatures yet at unrealistically low CO2 partial pressure mainly because of technical limitations concerning low heating/cooling rates. We report results from multicyclic c/c and carbonation/recarbonation/calcination (c/r/c) TGA tests at high heating/coling rates and in which the sorbent is regenerated in a dry atmosphere at high CO2 partial pressure. It is shown that at these conditions there is a drastic drop of CaO conversion to a very small residual value in just a few cycles. Moreover, the introduction of a recarbonation stage has actually an adverse effect. Arguably, CaCO3 decomposition in a CO2 rich atmosphere is ruled by CO2 dynamic adsorption/desorption in reactive CaO (111) surfaces as suggested by theoretical studies, which would preclude the growth of the regenerated CaO crystal structure along these reactive surfaces, and this effect would be intensified by recarbonation. Nevertheless, the presence of H2O in the calciner, which is also adsorbed/desorbed dynamically in CaO reactive planes, would shield CO2 adsorption/desorption thus mitigating the deeply detrimental effect of CO2 on the carbonation reactivity of the regenerated CaO structure. Oxy-combustion, which produces a significant amount of H2O, is currently used in pilot-scale plants to raise the temperature in the calciner. Auxiliary techniques are being explored to help heating the partially carbonated solids since oxyxombustion represents an important penalty to the CaL technology. Our study suggests that steam injection would be necessary in a dry calciner environment to avoid a sharp loss of CaO conversion if the sorbent is regenerated at high CO2 partial pressure.
21	A. Cabello, P. GayÃ¡n, F. GarcÃ-a-Labiano, L.F. De Diego, A. Abad, M.T. Izquierdo, J. AdÃ¡nez	Relevance of the catalytic activity on the performance of a NiO/CaAl2O4 oxygen carrier in a CLC process	(5 Apr 2014)	Applied Catalysis B: Environmental	147	null	980-987	This paper presents a detailed investigation related to the physical and chemical changes underwent by a low Ni content oxygen carrier during 90h of continuous operation in a CLC plant [1]. The oxygen carrier reached a combustion efficiency of 99% with a metallic Ni inventory of 17kg/MWth, which was the lowest value found in literature for any kind of Ni-based oxygen carrier. The present study was carried out in order to find the reasons by which this material exhibited a different combustion behavior in relation to other Ni-based oxygen carriers. Fresh and after-used particles were characterized by several techniques. XRD, TPR-TPO and XPS techniques proved that the use of CaAl2O4 as oxygen carrier support avoided the formation of NiAl2O4, which is a less reactive Ni-based compound than NiO and always formed in other Ni-based materials. The fact that all the NiO impregnated was found as free NiO in the oxygen carrier particles implied that this material maintained a high reactivity after 90h of continuous CLC operation. The results obtained in the batch fluidized bed reactor have revealed the great relevance of the catalytic activity of the metallic Ni on the global fuel gas combustion process. The low Ni content present in this material makes necessary the use of very high reduction solid conversion to have enough metallic Ni in the fuel reactor to catalyze the CH4 reforming reaction, and therefore to obtain high combustion efficiencies. This result will become very relevant for the design of a CLC unit using this Ni-based material as oxygen carrier.

22	J. Pecho, T.J. Schildhauer, M. Sturzenegger, S. Biollaz, A. Wokaun	Reactive bed materials for improved biomass gasification in a circulating fluidised bed reactor	(1 May 2008)	Chemical Engineering Science	63	9	2465-2476	Reactive bed materials for the optimisation of the biomass gasification in a fast internally circulating fluidised bed (FICB) reactor system were tested under sulphur-free (S-free) and H2S enriched conditions in a micro-scale fluidised bed reactor. In the experiments, the bed materials (natural olivine, (FexMg1-x)2SiO4, perovskite-type oxides, Ba0.3Sr0.7Fe0.9Mn0.1O3-Î´ and La0.65Sr0.35Cr0.5Mn0.5O3-Î´, Gd0.1Ce0.9O2 and a natural calcite, CaCO3) were examined under realistic redox-cycling conditions to study their oxygen capacity and release, their catalytic activity towards toluene reforming as well as their mechanical and chemical stability.It was found that the synthesised materials outperform the natural materials as reactive bed materials for the FICFB process under S-free atmosphere. Gd0.1Ce0.9O2 has better catalytic properties, perovskites show a higher oxygen storage capacity. However, in the presence of H2S, the perovskite loose their oxygen capacity, while calcite can form a sulphide/sulphate cycle which allows for significant oxygen capacity. Additionally, the catalytic activity goes up. Therefore, under real conditions, the two natural materials, calcite and to a lower extent olivine, have clear advantages with respect to price, catalytic activity and oxygen capacity.
23	B. Sreenivasulu, D.V. Gayatri, I. Sreedhar, K.V. Raghavan	A journey into the process and engineering aspects of carbon capture technologies	(1 Jan 2015)	Renewable and Sustainable Energy Reviews	41	null	1324-1350	Atmospheric warming due to greenhouse gases has become a serious global concern. Extensive efforts are being made to combat this phenomenon through Carbon Capture as carbon dioxide is its major contributor. In this work, a comprehensive review has been made on various Carbon Capture methodologies including adsorption, absorption, membrane separation, Chemical Looping Combustion, cryogenic separation with focus on their process chemistry, critical process parameters, contactor configurations, kinetics, thermodynamics, process development and scale-up. The challenges at the research and development stages have also been identified so as to provide the future directions for research.
24	E.S. Rubin, H. Mantripragada, A. Marks, P. Versteeg, J. Kitchin	The outlook for improved carbon capture technology	(1 Oct 2012)	Progress in Energy and Combustion Science	38	5	630-671	Carbon capture and storage (CCS) is widely seen as a critical technology for reducing atmospheric emissions of carbon dioxide (CO2) from power plants and other large industrial facilities, which are major sources of greenhouse gas emissions linked to global climate change. However, the high cost and energy requirements of current CO2 capture processes are major barriers to their use. This paper assesses the outlook for improved, lower-cost technologies for each of the three major approaches to CO2 capture, namely, post-combustion, pre-combustion and oxy-combustion capture. The advantages and limitations of each of method are discussed, along with the current status of projects and processes at various stages in the development cycle. We then review a variety of â€œroadmapsâ€ developed by governmental and private-sector organizations to project the commercial roll-out and deployment of advanced capture technologies. For perspective, we also review recent experience with R&D programs to develop lower-cost technologies for SO2 and NOx capture at coal-fired power plants. For perspective on projected cost reductions for CO2 capture we further review past experience in cost trends for SO2 and NOx capture systems. The key insight for improved carbon capture technology is that achieving significant cost reductions will require not only a vigorous and sustained level of research and development (R&D), but also a substantial level of commercial deployment, which, in turn, requires a significant market for CO2 capture technologies. At present such a market does not yet exist. While various incentive programs can accelerate the development and deployment of improved CO2 capture systems, government actions that significantly limit CO2 emissions to the atmosphere ultimately are needed to realize substantial and sustained reductions in the future cost of CO2 capture.
25	H. Tian, Q. Guo, X. Yue, Y. Liu	Investigation into sulfur release in reductive decomposition of calcium sulfate oxygen carrier by hydrogen and carbon monoxide	(1 Nov 2010)	Fuel Processing Technology	91	11	1640-1649	Chemical looping combustion (CLC) is a promising technology with the inherent property of separating CO2 from flue gas. For calcium sulfate (CaSO4) oxygen carrier, the inhibition of the produced sulfurous gases in the reduction of CaSO4, including sulfur dioxide (SO2), hydrogen sulfide (H2S) and carbonyl sulfide (COS), is the key for a CLC system. In this paper, the sensitivities of reacting temperature, oxygen ratio number (defined in this paper) and the mole fraction of both carbon monoxide (CO) and hydrogen(H2) in the syngas to the sum of the amounts of released SO2, H2S and COS are discussed respectively. Thermo-gravimetric analysis (TGA) tests demonstrated that the amount of the produced sulfurous gases is greatly dependent on the partial pressure of H2 or CO in the reduction of CaSO4. When the partial pressure of H2 or CO is higher than 40kPa, the production of sulfurous gases, indicating the deterioration of the recyclability of CaSO4, can be prevented completely even if the reacting temperature is as high as 1000Â°C. A new kind of CaSO4/CaCO3 oxygen carrier is prepared using a mechanical mixing method. The addition of CaCO3 nanoparticles largely improves the recyclability of the oxygen carrier in comparison with the fresh CaSO4 oxygen carrier, without CaCO3 nanoparticles, in a multi-cycle TGA test.

26	Y. Shen, K. Yoshikawa	Recent progresses in catalytic tar elimination during biomass gasification or pyrolysisâ€”A review	(1 May 2013)	Renewable and Sustainable Energy Reviews	21	null	371-392	Biomass gasification is an interesting technology in the future development of a worldwide sustainable energy system, which can help to decrease our current dependence on fossil fuels. Biomass gasification is a thermal process where solid fuel is converted into a useful gas using several gasifying agents such as air, and steam. The producer gas has a great number of applications. The most important is being combustion for power and heat generation as well as raw gas for production of fuels or chemicals. This review mainly presents the recent progresses on tar elimination during the biomass gasification. Then, novel non-catalytic absorption and adsorption methods of tar removal under ambient temperature conducted by our laboratory members were also explained. In our opinion, the tar removal can be conducted by combination of catalytic reforming in the gasifier and oil materials adsorption in the scrubber. Furthermore, the tar catalytic reforming is a most significant step during biomass gasification or pyrolysis. Thus, the development of reasonable catalysts for tar elimination has been faced with a significant challenge in current society.
27	Y. Cheng, C. Wu, J. Zhu, F. Wei, Y. Jin	Downer reactor: From fundamental study to industrial application	(21 Apr 2008)	Powder Technology	183	3	364-384	Graphical AbstractThis paper is to give a comprehensive review on the development of fundamental researches on downer reactors as well as the particular industrial demonstrations for the fluid catalytic cracking (FCC) of heavy oils and the coal pyrolysis in the thermal plasma.
28	X. Zhang, X. Song, Z. Sun, P. Li, J. Yu	Density functional theory study on the mechanism of calcium sulfate reductive decomposition by methane	(1 Aug 2013)	Fuel	110	null	204-211	Fossil fuel combustion system is one of the major sources of carbon dioxide (CO2) emissions, which is considered to be the main greenhouse gas contribution to the global warming. Chemical looping combustion (CLC) is a promising combustion technology with inherent separation of CO2. Calcium sulfate (CaSO4) can be used as a new oxygen carrier in this system. In CLC, CaSO4 is reduced to calcium sulfide (CaS) in the fuel reactor firstly. Then CaS is oxygenated to CaSO4 back in the air reactor. The decomposition of CaSO4 is usually accompanied by some side reactions, and the products depended on the experimental conditions. In this paper, the decomposition mechanism of CaSO4 reduced by methane (CH4) was investigated in the frame of density functional theory (DFT). In the calculation, the exchangeâ€“correlation term was approximated by Perdewâ€“Wang (PW91) equation, a function within the generalized gradient approximation (GGA) family. To understand the interaction between CH4 and CaSO4, the reaction pathways and TSs of CaSO4 decomposition were investigated and identified. The calculated results showed that, in the interaction of CaSO4 and CH4, electrons were transferred from sp3 hybrid orbital to O p state and S s state when CH4 was activated. CH bond and SO bond were activated and stretched with the electron transfer, which resulted in the dissociation of SO bond finally. The objective product CaS could be obtained with the reductive decomposition of CaSO4 by CH4. A probably mechanism was proposed, that is, the reaction process of CaSO4 and CH4 is CH4+CaSO4â†’CH3OH+CaSO3â†’CH2OOH+CaSO2Hâ†’HCHO+H2O+CaSO2â†’HCOOH+H2O+CaSOâ†’2H2O+CO2+CaS.
29	B. Christian Enger, R. LÃ¸deng, A. Holmen	A review of catalytic partial oxidation of methane to synthesis gas with emphasis on reaction mechanisms over transition metal catalysts	(31 Aug 2008)	Applied Catalysis A, General	346	1	27-Jan	Catalytic partial oxidation of methane has been reviewed with an emphasis on the reaction mechanisms over transition metal catalysts. The thermodynamics and aspects related to heat and mass transport is also evaluated, and an extensive table on research contributions to methane partial oxidation over transition metal catalysts in the literature is provided.Presented are both theoretical and experimental evidence pointing to inherent differences in the reaction mechanism over transition metals. These differences are related to methane dissociation, binding site preferences, the stability of OH surface species, surface residence times of active species and contributions from lattice oxygen atoms and support species.Methane dissociation requires a reduced metal surface, but at elevated temperatures oxides of active species may be reduced by direct interaction with methane or from the reaction with H, H2, C or CO.The comparison of elementary reaction steps on Pt and Rh illustrates that a key factor to produce hydrogen as a primary product is a high activation energy barrier to the formation of OH. Another essential property for the formation of H2 and CO as primary products is a low surface coverage of intermediates, such that the probability of Oâ€“H, OHâ€“H and COâ€“O interactions are reduced.The local concentrations of reactants and products change rapidly through the catalyst bed. This influences the reaction mechanisms, but the product composition is typically close to equilibrated at the bed exit temperature.

30	T. Kuramochi, A. RamÃrez, W. Turkenburg, A. Faaij	Techno-economic prospects for CO2 capture from distributed energy systems	(1 Mar 2013)	Renewable and Sustainable Energy Reviews	19	null	328-347	CO2 emissions from distributed energy systems are expected to become increasingly significant, accounting for about 20% for current global energy-related CO2 emissions in 2030. This article reviews, assesses and compares the techno-economic performance of CO2 capture from distributed energy systems taking into account differences in timeframe, fuel type and energy plant type. The analysis includes the energy plant, CO2 capture and compression, and distributed transport between the capture site and a trunk pipeline. Key parameters, e.g., capacity factor, energy prices and interest rate, were normalized for the performance comparison.The findings of this study indicate that in the short-mid term (around 2020â€“2025), the energy penalty for CO2 capture ranges between 23% and 30% for coal-fired plants and 10â€“28% for natural gas-fired plants. Costs are between 30 and 140â‚¬/tCO2 avoided for plant scales larger than 100MWLHV (fuel input) and 50â€“150â‚¬/tCO2 avoided for 10â€“100MWLHV. In the long-term (2030 and beyond), the energy penalty for CO2 capture might reduce to between 4% and 9% and the costs to around 10â€“90â‚¬/tCO2 avoided for plant scales larger than 100MWLHV, 25â€“100â‚¬/tCO2 avoided for 10â€“100MWLHV and 35â€“150â‚¬/tCO2 avoided for 10MWLHV or smaller.CO2 compression and distributed transport costs are significant. For a distance of 30km, 10â‚¬/tCO2 transported was calculated for scales below 500tCO2/day and more than 50â‚¬/tCO2 transported for scales below 5tCO2/day (equivalent to 1MWLHV natural gas). CO2 compression is responsible for the largest share of these costs.CO2 capture from distributed energy systems is not prohibitively expensive and has a significant cost reduction potential in the long term. Distributed CO2 emission sources should also be considered for CCS, adding to the economies of scale of CO2 transport and storage, and optimizing the deployment of CCS.
31	D. Meier, B. Van De Beld, A.V. Bridgwater, D.C. Elliott, A. Oasmaa, F. Preto	State-of-the-art of fast pyrolysis in IEA bioenergy member countries	(1 Apr 2013)	Renewable and Sustainable Energy Reviews	20	null	619-641	Fast pyrolysis of biomass is becoming increasingly important in some member countries of the International Energy Agency (IEA). Six countries have joined the IEA Task 34 of the Bioenergy Activity: Canada, Finland, Germany, Netherlands, UK, and USA. The National Task Leaders give an overview of the current activities in their countries both on research, pilot and demonstration level.
32	J.C.M. Pires, F.G. Martins, M.C.M. Alvim-Ferraz, M. SimÃµes	Recent developments on carbon capture and storage: An overview	(1 Sep 2011)	Chemical Engineering Research and Design	89	9	1446-1460	The Intergovernmental Panel on Climate Change assumes the warming of the climate system, associating the increase of global average temperature to the observed increase of the anthropogenic greenhouse gas (GHG) concentrations in the atmosphere. Carbon dioxide (CO2) is considered the most important GHG, due to the dependence of world economies on fossil fuels, since their combustion processes are the most important sources of this gas. CO2 concentrations are increasing in the last decades mainly due to the increase of anthropogenic emissions. The processes involving CO2 capture and storage is gaining attention on the scientific community as an alternative for decreasing CO2 emission, reducing its concentration in ambient air. However, several technological, economical and environmental issues as well as safety problems remain to be solved, such as the following needs: increase of CO2 capture efficiency, reduction of process costs, and verification of environmental sustainability of CO2 storage. This paper aims to review the recent developments (from 2006 until now) on the carbon capture and storage (CCS) methodologies. Special attention was focused on the basic findings achieved in CCS operational projects.
33	M.S. Yim, F. Caron	Life cycle and management of carbon-14 from nuclear power generation	(1 Jan 2006)	Progress in Nuclear Energy	48	1	Feb-36	With its long half-life (5730 years) and high mobility in the environment, 14C is a radionuclide of considerable interest in nuclear power production. Carbon-14 is present in virtually all parts of nuclear reactor primary system and has a high production rate. It is released to the environment through gaseous and liquid discharges and though the disposal of solid radioactive waste. This paper summarizes existing scientific understanding of 14C issues surrounding nuclear power production. Two main purposes of the paper are: (1) To provide the basic/up-to-date understanding of the life cycle of 14C, starting from its production in reactors, to eventually its transport and its potential incorporation in natural cycles; (2) To present the technical issues in current 14C waste management. The emphasis of the paper is on Light Water Reactors (LWRs, which include Pressured Water Reactors-PWRs, and Boiling Water Reactors-BWRs) and Heavy Water Reactors (HWRs-CANDU type reactors). Major issues with 14C in HTGR are also addressed.

34	S. Chen, W. Xiang, D. Wang, Z. Xue	Incorporating IGCC and CaO sorption-enhanced process for power generation with CO2 capture	(1 Jul 2012)	Applied Energy	95	null	285-294	Integrated gasification combined cycle (IGCC) is a power generation technology to convert solid fuels into electricity. IGCC with CCS is regarded as a promising option to mitigate CO2 emission. In this paper, the CaO sorption-enhanced process is incorporated downstream with coal gasification to produce a hydrogen-rich stream for electricity production and CO2 separation. A WGS-absorber substitutes the high- and low-temperature waterâ€“gas shift reactors and desulfurization units in conventional IGCCâ€“CCS to produce a hydrogen-rich stream, which is sent onto a gas turbine. CaO is used as the sorbent to enhance hydrogen production and for CO2 capture. Regeneration of CaO is completed via calcination in a regenerator vessel. The IGCC with CaO sorption-enhanced process is modeled and simulated using Aspen Plus software. Two commercial available gasification technologies, Shell and Texaco, are integrated with the sorption-enhanced process. The results showed IGCC with CaO sorption-enhanced process has a satisfactory system performance. Even though the net electricity efficiency is not as high as expected, just around 30â€“33%, the system has a high CO2 capture efficiency â�¼97% and low pollutant emissions. Moreover, compared with conventional IGCCâ€“CCS, the schematic diagram of the IGCCâ€“CCS process is simplified. Parameters that affect the plant performance are analyzed in the sensitive analysis, including WGS-absorber temperature, H2O/CO ratio, pressure, etc. Some challenges to the system are also discussed.
35	H. TaÅŸkin, C. Kubat, Ã–. Uygun, S. Arslankaya	FUZZYFCC: Fuzzy logic control of a fluid catalytic cracking unit (FCCU) to improve dynamic performance	(15 Apr 2006)	Computers and Chemical Engineering	30	5	850-863	In this paper, fuzzy logic control of a fluid catalytic cracking unit (FCCU) is proposed. Fluid catalytic cracking (FCC) process is a unit that converts heavy distillates like gas oil or residues to gasoline and middle distillates using cracking catalyst. About 45% of worldwide gasoline production comes from FCC processes and its ancillary units. Since a typical FCC unit can process a large amount of the feedstock into more valuable products, the overall economic benefits of a refining could be considerably increased if proper control and optimization strategies are implemented. FCC processes are known to be very difficult to model and control because of the large process scale, complicated hydro-dynamics and complex kinetics of both cracking and coke burning reactions. One of the more heavily investigated terms of nonlinear control, in the field of â€œintelligent controlâ€, is that due to fuzzy logic controllers (FLCs). FLCs have been successfully applied to a stream of difficult, nonlinear dynamical process such as FCC. Here, with an application to a Turkish refinery FCC unit of FLC fuzzy results obtained using Matlab-Fuzzy Logic Toolbox version 6.5 were found to be acceptable. The paper indicates how fuzzy logic control (FLC), as a promising control technique, would be effectively used for improved process control of FCC in refinery process industry.
36	G.F. Naterer, S. Suppiah, L. Stolberg, M. Lewis, M. Ferrandon, Z. Wang, I. Dincer, K. Gabriel, M.A. Rosen, E. Secnik, E.B. Easton, L. Trevani, I. Pioro, P. Tremaine, S. Lvov, J. Jiang, G. Rizvi, B.M. Ikeda, L. Lu, M. Kaye, W.R. Smith, J. Mostaghimi, P. Spekkens, M. Fowler, J. Avsec	Clean hydrogen production with the Cuâ€“Cl cycle â€“ Progress of international consortium, I: Experimental unit operations	(1 Dec 2011)	International Journal of Hydrogen Energy	36	24	15472-15485	Highlightsâ–º Recent advances are presented for the thermochemical copperâ€“chlorine (Cuâ€“Cl) cycle of hydrogen production. â–º This first of two companion papers reports on unit operation experiments and system integration of the Cuâ€“Cl cycle. â–º Hydrogen production with Canadaâ€™s Generation IV nuclear reactor (SCWR; Super-Critical Water Reactor) is discussed.

37	R. Ramachandran, G.P. Rangaiah, S. Lakshminarayanan	Data analysis, modeling and control performance enhancement of an industrial fluid catalytic cracking unit	(1 Apr 2007)	Chemical Engineering Science	62	7	1958-1973	Considerable fluctuations were observed in the riser temperature of one of the fluid catalytic cracking (FCC) unit of a Southeast Asian refinery. This undesired occurrence has an adverse effect on the performance of the process unit. In the present study, several statistical tools are developed and then used, for the first time, for analyzing routine operating data in order to characterize the dynamics of the riser temperature and other critical variables that may be affecting the riser temperature. Subsequently, a first-principles-based dynamic model of the FCC unit is implemented to closely simulate the FCC unit under investigation. The model is validated by predicting the measured operating data of the FCC unit. This facilitated an in-depth study of the FCC unit, leading to the identification of several strategies for improving the control loop performance of the riser temperature.
38	G.F. Naterer, S. Suppiah, L. Stolberg, M. Lewis, Z. Wang, V. Daggupati, K. Gabriel, I. Dincer, M.A. Rosen, P. Spekkens, S.N. Lvov, M. Fowler, P. Tremaine, J. Mostaghimi, E.B. Easton, L. Trevani, G. Rizvi, B.M. Ikeda, M.H. Kaye, L. Lu, I. Pioro, W.R. Smith, E. Secnik, J. Jiang, J. Avsec	Canadaâ€™s program on nuclear hydrogen production and the thermochemical Cuâ€"Cl cycle	(1 Oct 2010)	International Journal of Hydrogen Energy	35	20	10905-10926	This paper presents an overview of the status of Canadaâ€™s program on nuclear hydrogen production and the thermochemical copperâ€"chlorine (Cuâ€"Cl) cycle. Enabling technologies for the Cuâ€"Cl cycle are being developed by a Canadian consortium, as part of the Generation IV International Forum (GIF) for hydrogen production with the next generation of nuclear reactors. Particular emphasis in this paper is given to hydrogen production with Canadaâ€™s Super-Critical Water Reactor, SCWR. Recent advances towards an integrated lab-scale Cuâ€"Cl cycle are discussed, including experimentation, modeling, simulation, advanced materials, thermochemistry, safety, reliability and economics. In addition, electrolysis during off-peak hours, and the processes of integrating hydrogen plants with Canadaâ€™s nuclear plants are presented.
39	G.F. Naterer, S. Suppiah, L. Stolberg, M. Lewis, Z. Wang, I. Dincer, M.A. Rosen, K. Gabriel, E. Secnik, E.B. Easton, I. Pioro, S. Lvov, J. Jiang, J. Mostaghimi, B.M. Ikeda, G. Rizvi, L. Lu, A. Odukoya, P. Spekkens, M. Fowler, J. Avsec	Progress of international hydrogen production network for the thermochemical Cuâ€"Cl cycle	(24 Jan 2013)	International Journal of Hydrogen Energy	38	2	740-759	Highlightsâ–º Recent advances by an international team on the Cuâ€"Cl cycle of hydrogen production. â–º Nuclear hydrogen production initiative within the Generation IV International Forum (GIF). â–º Linkage with Canada's Generation IV reactor, SCWR (Super-Critical Water Reactor). â–º Progress on unit operation experiments, corrosion resistant materials and system integration.